THE ROLE OF THE FUNGAL CELL WALL IN HOST-FUNGAL INTERACTIONS

EDITED BY: Vishukumar Aimanianda, Jagadeesh Bayry and Laura Alcazar-Fuoli
PUBLISHED IN: Frontiers in Cellular and Infection Microbiology

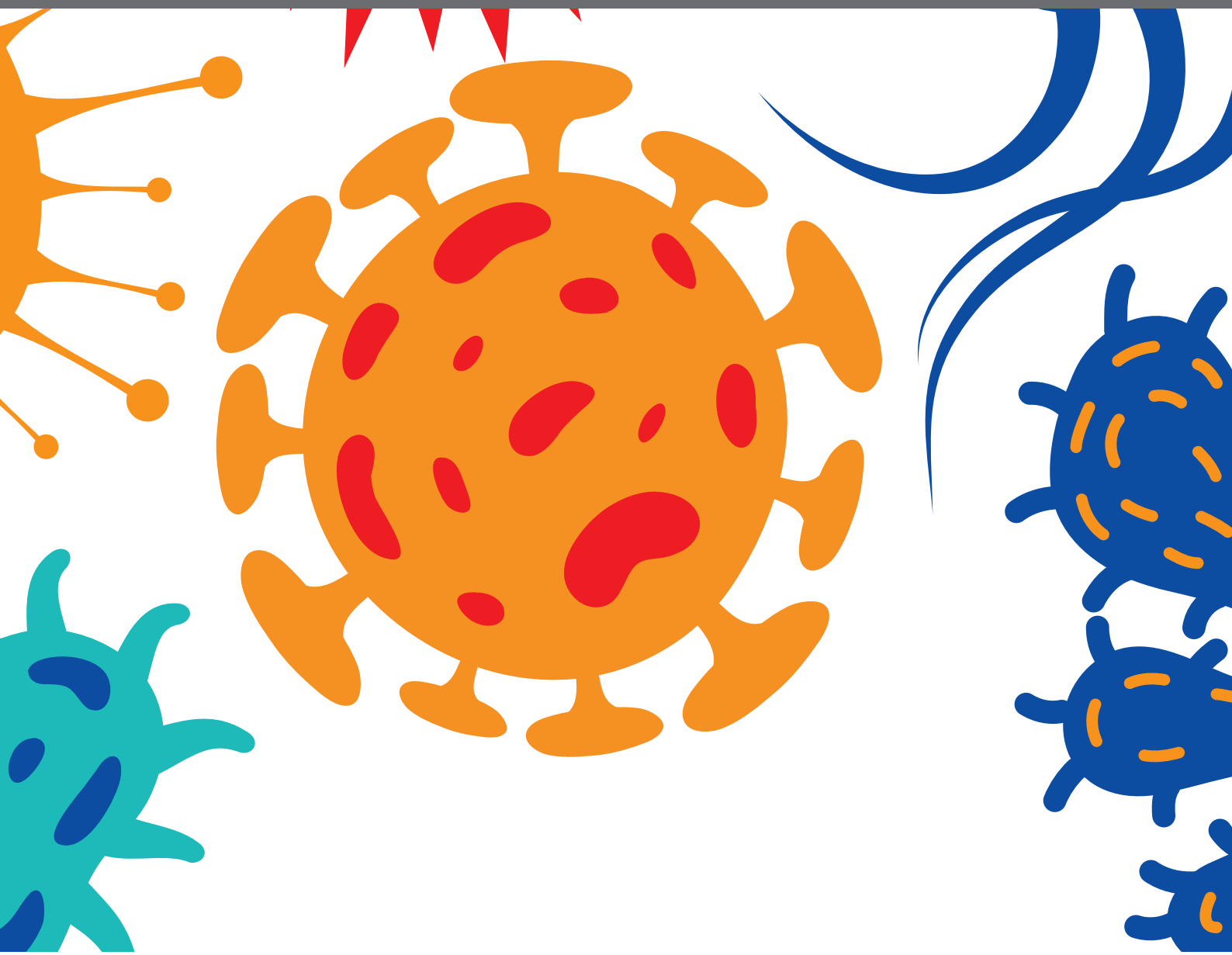

frontiers Research Topics

frontiers

ISSN 1664-8714
ISBN 978-2-88966-020-9
DOI 10.3389/978-2-88966-020-9

About Frontiers

Frontiers is more than just an open-access publisher of scholarly articles: it is a pioneering approach to the world of academia, radically improving the way scholarly research is managed. The grand vision of Frontiers is a world where all people have an equal opportunity to seek, share and generate knowledge. Frontiers provides immediate and permanent online open access to all its publications, but this alone is not enough to realize our grand goals.

Frontiers Journal Series

The Frontiers Journal Series is a multi-tier and interdisciplinary set of open-access, online journals, promising a paradigm shift from the current review, selection and dissemination processes in academic publishing. All Frontiers journals are driven by researchers for researchers; therefore, they constitute a service to the scholarly community. At the same time, the Frontiers Journal Series operates on a revolutionary invention, the tiered publishing system, initially addressing specific communities of scholars, and gradually climbing up to broader public understanding, thus serving the interests of the lay society, too.

Dedication to Quality

Each Frontiers article is a landmark of the highest quality, thanks to genuinely collaborative interactions between authors and review editors, who include some of the world's best academicians. Research must be certified by peers before entering a stream of knowledge that may eventually reach the public - and shape society; therefore, Frontiers only applies the most rigorous and unbiased reviews.
Frontiers revolutionizes research publishing by freely delivering the most outstanding research, evaluated with no bias from both the academic and social point of view. By applying the most advanced information technologies, Frontiers is catapulting scholarly publishing into a new generation.

What are Frontiers Research Topics?

Frontiers Research Topics are very popular trademarks of the Frontiers Journals Series: they are collections of at least ten articles, all centered on a particular subject. With their unique mix of varied contributions from Original Research to Review Articles, Frontiers Research Topics unify the most influential researchers, the latest key findings and historical advances in a hot research area! Find out more on how to host your own Frontiers Research Topic or contribute to one as an author by contacting the Frontiers Editorial Office: researchtopics@frontiersin.org

THE ROLE OF THE FUNGAL CELL WALL IN HOST-FUNGAL INTERACTIONS

Topic Editors:
Vishukumar Aimanianda, Institut Pasteur, France
Jagadeesh Bayry, Institut National de la Santé et de la Recherche Médicale (INSERM), France
Laura Alcazar-Fuoli, Instituto de Salud Carlos III (ISCIII), Spain

Citation: Aimanianda, V., Bayry, J., Alcazar-Fuoli, L., eds. (2020). The Role of the Fungal Cell Wall in Host-Fungal Interactions. Lausanne: Frontiers Media SA. doi: 10.3389/978-2-88966-020-9

Table of Contents

frontiers in Cellular and Infection Microbiology

EDITORIAL
published: 29 July 2020
doi: 10.3389/fcimb.2020.00392

Editorial: The Role of the Fungal Cell Wall in Host-Fungal Interactions

Laura Alcazar-Fuoli[1,2], *Jagadeesh Bayry*[3] *and Vishukumar Aimanianda*[4*]

[1] *Mycology Reference Laboratory, National Centre for Microbiology, Instituto de Salud Carlos III, Madrid, Spain,* [2] *Spanish Network for Research in Infectious Diseases, Instituto de Salud Carlos III, Madrid, Spain,* [3] *Institut National de la Santé et de la Recherche Médicale, Centre de Recherché des Cordeliers, Sorbonne Université, Université de Paris, Paris, France,* [4] *Institut Pasteur, Molecular Mycology Unit, CNRS, UMR2000, Paris, France*

Keywords: fungal cell-wall, biosynthesis, remodeling, host-fungal interaction, antifungals

Editorial on the Research Topic

The Role of the Fungal Cell Wall in Host-Fungal Interactions

By providing mechanical strength and protection from the ever-changing hostile environment, the cell-wall (CW) forms an essential structure of fungal cells. Concerning host-pathogen interaction, the CW is the first fungal structure to interact with the host. It is a dynamic organelle with complex composition, varying between fungal species, morphotypes, and growth conditions, which poses difficulties in deciphering its role during host-fungal interactions. Therefore, new strategies to understand CW-organization are needed to improve the management of fungal infections. While CW-directed antifungals show good/acceptable efficacy, their clinical application is limited to echinocandins that inhibit biosynthesis of β-(1,3)-glucan, a major component in the fungal CW. Echinocandins are used for salvage therapy against invasive fungal infections (IFI) owing to their toxicity, paradoxical effect at higher doses, and due to the emergence of fungal resistance against echinocandins. This demands a necessity to discover alternative CW-targets and to develop new antifungals. On the other hand, in spite of medical advances, diagnostic-delay is attributed to be one of the reasons for increasing mortality due to IFI. Although circulating CW-antigens have been proven to be diagnostic biomarkers, the existing protocols suffer from specificity and sensitivity issues, requiring new tools overcoming these drawbacks. In our focused topic, the nine articles collected highlight recent developments regarding the fungal CW in these research areas.

A protective immune response relies on recognition of fungal-pathogens by pattern recognition molecules of the host immune-system. The review by Madan and Kishore summarizes the host immune surveillance role of the Surfactant Protein D (SP-D), a pattern-recognition receptor, in recognizing and eliminating human fungal pathogens. The CW-ligands interacting with SP-D, mechanism of interactions and immunomodulatory effects thereby are discussed. Fungicidal or fungistatic affect exerted by, and therapeutic potentials of SP-D upon external administration in murine models of allergic and invasive mycoses are highlighted.

Fungal-keratitis is a superficial infection mainly due to the species of *Aspergillus* and *Fusarium*; although not life-threatening, this infection greatly affects the quality of life. In the research article by Mohammed et al. local activation of alternative complement pathway, a humoral immune defense mechanism of the host during early stage of corneal-infection by *A. flavus*, has been demonstrated. They have also identified the negative regulators of complement activation, capable of interacting with *A. flavus,* demonstrating a parallel immune evasion mechanism associated with this fungus during corneal-infection.

Being an extracellular phenomenon, the fungal CW-biogenesis relies on a coordinated function of several glycosyltransferases; among them, β-(1,3)-glycosyltransferases of the GH75 family (CAZyme) play essential roles. The brief research-report by Degani and Popolo describes the role

OPEN ACCESS

Edited and reviewed by:
Joseph Heitman,
Duke University, United States

***Correspondence:**
Vishukumar Aimanianda
vkumar@pasteur.fr

Specialty section:
This article was submitted to Fungal Pathogenesis, a section of the journal Frontiers in Cellular and Infection Microbiology

Received: *20 May 2020*
Accepted: *25 June 2020*
Published: *29 July 2020*

Citation:
Alcazar-Fuoli L, Bayry J and Aimanianda V (2020) Editorial: The Role of the Fungal Cell Wall in Host-Fungal Interactions. Front. Cell. Infect. Microbiol. 10:392. doi: 10.3389/fcimb.2020.00392

of Phr1p, a β-(1,3)-glycosyltransferases, in maintaining *Candida albicans* CW integrity, by acting cooperatively with a chitin synthase, Chs1p. Further, Phr1p-GFP construct allowed them to localize Phr1p in the septum of *C. albicans* undergoing cytokinesis, suggesting the utility of fluorescent protein tagging in fungal CW-biogenesis.

Chitin, although not a major component, maintains fungal CW-integrity upon cross-linking with β-glucans. Leroy et al. investigated the role of *C. albicans* CW-chitin released into the bloodstream during candidemia on platelets activity, as platelets are important during innate immune response. They observed that the chitin purified from *C. albicans* reduces adhesion of platelet to this fungus as well as neutrophils, thereby promoting fungal escape from immune cells. Pre-treatment of platelets with chitin resulted in their reduced aggregation by reducing intracellular Ca^{+2}-influx and P-selectin expression in platelets, thus affecting platelet-leukocyte interaction and neutrophil recruitment to the sites of infection. This brings new insight into the pathobiological role of fungal CW-chitin. In some pathogenic fungi, chitosan, the deacetylated derivative of chitin also plays a role in virulence. However, Mouyna et al. demonstrate that although there are seven putative chitin deacetylases (Cda; converting chitin to chitosan) in *Aspergillus fumigatus*, an airborne pathogen, the chitosan level in *A. fumigatus* conidia (infective propagules) is very low. Further, deletion of all seven-Cda did not alter the growth and virulence, suggesting a non-essential role of CW-chitosan in the *A. fumigatus* biology/pathobiology. On the other hand, galactosaminogalactan, a heteropolysaccharide in the CW of *A. fumigatus*, produced during germination, exerts anti-inflammatory property upon inducing IL-1Ra by peripheral blood mononuclear cells. However, therapeutic application of this polymer is limited due to its acid-soluble nature. The research by Gressler et al. demonstrate that the oligosaccharides of galactosaminogalactan with 13–20 monosaccharide-units rich in de-*N*-acetylated galactosamine are water-soluble, capable of inducing IL-1Ra and can rescue inflammatory damage in colitis mouse model, suggesting the potential of CW-oligosaccharides as glycodrugs.

Infecting capacity and antifungal susceptibility varies across various species of *Candida*. Walker and Munro observed that caspofungin (an echinocandin) treatment results in reorganization of the CW in most *Candida* species (except *C. glabrata* and *C. parapsilosis*), exposing chitin and β-(1,3)-glucan (polysaccharides in the inner CW) that inhibited *Candida* uptake by macrophages, decreasing their TNF-α production. This study demonstrates drug-induced modifications in the CWs of *Candida* species, affecting their interaction with immune cells.

IFI occur mainly during immunosuppressed condition, immunomodulators are therefore receiving attention as antifungal therapy. In this context, Paulovičová et al. generated biotinylated manno-oligosaccharides that mimic CW-mannan of *Candida*, studied their immunomodulatory potential *in vitro*, which was dependent on the chain-lengths and linkage patterns of these oligoconjugates, thus suggesting their capacity as anti-*Candida* vaccines.

Galactomannan detection for the diagnosis of invasive aspergillosis suffers from false-positivity, due to cross-reactivity of the monoclonal antibodies (mAb) used, recognizing bacterial antigenic determinants. Using *A. parasiticus* CW-fragments as the immunogen, Schubert et al. developed AP3, a mouse mAb that specifically recognizes β-(1,5)-galactofuranose with a minimum length of tetramer, a structure common among many *Aspergillus* species. Owing to the higher epitope-specificity of AP3, its efficient application in invasive aspergillosis diagnosis has been envisaged.

Altogether, this themed article collection adds to our current knowledge on tools to study fungal CW-organization, immunomodulatory role of CW during host-fungal interaction, synthetic derivatives of CW in immunotherapies and CW-directed mAb in the diagnosis of fungal disease.

AUTHOR CONTRIBUTIONS

VA drafted the manuscript. All authors contributed to the revision and approved the submitted version.

ACKNOWLEDGMENTS

We thank all the contributors to this research-topic.

Conflict of Interest: The authors declare that the research was conducted in the absence of any commercial or financial relationships that could be construed as a potential conflict of interest.

frontiers in Cellular and Infection Microbiology

ORIGINAL RESEARCH
published: 16 July 2019
doi: 10.3389/fcimb.2019.00234

Monoclonal Antibody AP3 Binds Galactomannan Antigens Displayed by the Pathogens *Aspergillus flavus*, *A. fumigatus*, and *A. parasiticus*

Max Schubert[1†], *Sheng Xue*[2†], *Frank Ebel*[3], *Annegret Vaggelas*[3], *Vadim B. Krylov*[4], *Nikolay E. Nifantiev*[4], *Ivana Chudobová*[1], *Stefan Schillberg*[1,5*] *and Greta Nölke*[1]

[1] *Department of Plant Biotechnology, Fraunhofer Institute for Molecular Biology and Applied Ecology IME, Aachen, Germany,* [2] *Institute for Translational Medicine, College of Medicine, Qingdao University, Qingdao, China,* [3] *Faculty of Veterinary Medicine, Institute for Infectious Diseases and Zoonoses, Ludwig-Maximilians-University Munich, Munich, Germany,* [4] *N.D. Zelinsky Institute of Organic Chemistry, Russian Academy of Sciences, Moscow, Russia,* [5] *Institute for Phytopathology, Justus Liebig University Giessen, Giessen, Germany*

OPEN ACCESS

Edited by:
Laura Alcazar-Fuoli, Carlos III Health Institute, Spain

Reviewed by:
Michael S. Price, Liberty University, United States
Georgios Chamilos, University of Crete, Greece

****Correspondence:***
Stefan Schillberg
stefan.schillberg@ime.fraunhofer.de

† These authors have contributed equally to this work and are first authors

Specialty section:
This article was submitted to Fungal Pathogenesis, a section of the journal Frontiers in Cellular and Infection Microbiology

Received: *12 March 2019*
Accepted: *14 June 2019*
Published: *16 July 2019*

Citation:
Schubert M, Xue S, Ebel F, Vaggelas A, Krylov VB, Nifantiev NE, Chudobová I, Schillberg S and Nölke G (2019) Monoclonal Antibody AP3 Binds Galactomannan Antigens Displayed by the Pathogens Aspergillus flavus, A. fumigatus, and A. parasiticus. Front. Cell. Infect. Microbiol. 9:234. doi: 10.3389/fcimb.2019.00234

Aspergillus fumigatus and *A. flavus* are the fungal pathogens responsible for most cases of invasive aspergillosis (IA). Early detection of the circulating antigen galactomannan (GM) in serum allows the prompt application of effective antifungal therapy, thus improving the survival rate of IA patients. However, the use of monoclonal antibodies (mAbs) for the diagnosis of IA is often associated with false positives due to cross-reaction with bacterial polysaccharides. More specific antibodies are therefore needed. Here we describe the characterization of the *Aspergillus*-specific mAb AP3 (IgG1κ), including the precise identification of its corresponding antigen. The antibody was generated using *A. parasiticus* cell wall fragments and was shown to bind several *Aspergillus* species. Immunofluorescence microscopy revealed that AP3 binds a cell wall antigen, but immunoprecipitation and enzyme-linked immunosorbent assays showed that the antigen is also secreted into the culture medium. The inability of AP3 to bind the *A. fumigatus* galactofuranose (Gal*f*)-deficient mutant Δ*glfA* confirmed that Gal*f* residues are part of the epitope. Several lines of evidence strongly indicated that AP3 recognizes the Gal*f* residues of *O*-linked glycans on *Aspergillus* proteins. Glycoarray analysis revealed that AP3 recognizes oligo-[β-D-Gal*f*-1,5] sequences containing four or more residues with longer chains more efficiently. We also showed that AP3 captures GM in serum, suggesting it may be useful as a diagnostic tool for patients with IA.

Keywords: *Aspergillus* antigen, detection assay, epitope identification, galactofuranose, glycobiology

INTRODUCTION

The genus *Aspergillus* comprises 339 filamentous fungi that are ubiquitous in nature and have many potential applications in biotechnology, but some species also pose a risk to human and animal health (Samson et al., 2014). *A. niger* and *A. oryzae* are widely used for fermentation in the food industry and for the production of hydrolytic enzymes (Biesebeke and Record, 2008). In contrast, *A. fumigatus* and *A. flavus* are major pathogens responsible for allergic bronchopulmonary aspergillosis (ABPA), chronic pulmonary aspergillosis (CPA) and invasive aspergillosis (IA), which

can be fatal in immunocompromised patients, such as carriers of human immunodeficiency virus, or patients receiving transplants of allogeneic stem cells or solid organs (Singh and Paterson, 2005; Krishnan et al., 2009). The early detection of biomarkers elicited by invasive *Aspergillus* species is necessary to achieve effective antifungal therapy outcomes (Hedayati et al., 2007; Walsh et al., 2008).

A. flavus is responsible for 15–20% of reported IA cases (Perfect et al., 2001; Krishnan et al., 2009). Furthermore, *A. flavus* and *A. parasiticus* also infect plants, where they produce highly carcinogenic secondary metabolites known as aflatoxins, particularly when they grow on oil-rich staple crops under field and storage conditions (Villers, 2014). These aflatoxins are stable during food processing, and contaminated food must be discarded causing significant economic losses amounting to billions of US$ in the US alone (Robens and Cardwell, 2003).

Antibodies against different *Aspergillus* antigens have been used to track infections by staining the fungal cell wall (Ste-Marie et al., 1990; Hao et al., 2008; Kumar and Shukla, 2015; Schubert et al., 2018). Other *Aspergillus*-specific antibodies have been used to detect allergens (Kurup and Banerjee, 2000) and disease-related biomarkers (Thornton, 2010) released by pathogenic strains, and to detect aflatoxin contamination in agricultural products (Wacoo et al., 2014). Fungal-type galactomannan (GM) is a heat-stable heteropolysaccharide and a major component of *Aspergillus* cell walls. It comprises a linear mannan core and short, branched β-1,5-linked galactofuranose (Gal*f*) chains (Latge et al., 1994). Antibodies that recognize GM, the main biomarker of IA, are commercially available (Thornton, 2010). Most *Aspergillus*-specific antibodies are generated using undefined preparations, such as crude extracts, so the precise antigens are often unknown. This makes it difficult to characterize the antibodies in detail and limits their commercial applications. We have generated monoclonal antibodies (mAbs) against several different intracellular and extracellular antigens of aflatoxigenic *A. flavus* and *A. parasiticus* using crude cell wall antigen preparations (Schubert et al., 2018). Here we describe the generation and antigen-specific characterization of mAb AP3, its potential suitability for the rapid serological detection of IA, and possible further commercial applications.

MATERIALS AND METHODS

Fungal Strains

Pure cultures of *A. flavus, A. parasiticus, A. nidulans, A. niger, Fusarium oxysporum, F. culmorum, Phytophthora nicotianae, Rhizoctonia solani, Pythium ultimum, Botrytis cinerea, Cercospora nicotianae, Thielaviopsis basicola*, and *Penicillium chrysogenum* were obtained from the German Collection of Microorganisms and Cell Cultures (DSMZ, Braunschweig, Germany) and maintained on potato dextrose agar (PDA; Carl Roth, Karlsruhe, Germany), tomato agar (25% (v/v) tomato juice, 3 g/l $CaCO_3$, 15 g/l agar) or liquid potato dextrose broth medium (PDB; Carl Roth). The wild-type *A. fumigatus* strain D141 (Reichard et al., 1990) and Gal*f*-deficient mutant Δ*glfA* were cultivated as previously described (Schmalhorst et al., 2008). The *F. oxysporum* strain DSM 62316 used for immunofluorescence analysis and enzyme-linked immunosorbent assay (ELISA) experiments was cultivated and prepared as previously reported (Wiedemann et al., 2016).

Preparation of Fungal Antigens

Cell Wall Fragments and Cell Wall Proteins

Aspergillus conidia were isolated and used to inoculate liquid cultures in PDB or Czapek Dox medium. For all other fungi, an overgrown agar slice was used to inoculate liquid cultures based on the media and cultivation conditions recommended by the DSMZ. Harvested mycelia were disrupted under liquid nitrogen using a mortar and pestle to obtain cell wall fragments (CWFs) and were washed three times in 1 M NaCl to remove cytosolic antigens (Pitarch et al., 2008).

CWFs representing each fungal species listed above were resuspended in deionized water, lyophilized and weighed. Cell wall-associated proteins (CWPs) were extracted from *A. flavus* (AF-CWPs) and *A. parasiticus* CWFs (AP-CWPs) using a reducing extraction buffer (50 mM Tris-HCl pH 8.0, 0.1 M EDTA, 2% (w/v) SDS, 10 mM DTT) and resuspended in 1× phosphate-buffered saline (PBS; 137 mM NaCl, 2.7 mM KCl, 8.1 mM Na_2HPO_4, 1.5 mM KH_2PO_4, pH 7.4) as previously described (Prados-Rosales et al., 2009).

Preparation of Extracellular Aspergillus Antigens and GM Supernatants

Extracellular *Aspergillus* antigens secreted during growth were prepared by inoculating 400 ml Czapek Dox medium with 10^6 *A. flavus* conidia/ml and removing the mycelia after 7 days of growth at 28°C by filtering through three layers of Miracloth (Merck, Darmstadt, Germany). The supernatant was then precipitated in 2.5 volumes of ethanol overnight at 4°C, and the pellet was collected by centrifugation (3,000 g, 10 min, 4°C). The precipitate was washed three times with ethanol and resuspended in water, then freeze-dried and stored at −20°C. The protein content was determined using the Roti-Quant Bradford assay (Carl Roth). Supernatants from the *A. fumigatus* Δ*glfA* mutant, and GM-containing supernatants from *A. fumigatus* strain D141 (SD-Asp) and *F. oxysporum* strain DSM 62316, were prepared as previously described (Wiedemann et al., 2016).

Antibody Generation and Purification

Five 6-weeks-old female BALB/c mice (veterinary license: 9.93.2.10.54.07.044) were intraperitoneally immunized with 150 μg *A. parasiticus* CWFs in a total volume of 100 μl prepared with Gerbu Adjuvant MM (Gerbu Biotechnik, Heidelberg, Germany), and subsequent boosts were carried out at 2-weeks intervals. Five days after the final boost (boost six), B-lymphocytes were isolated from spleens and fused to myeloma cells (SP2/mIL6). The resulting hybridoma cells were cultivated

Abbreviations: 2DE, two-dimensional gel electrophoresis; ABPA, allergic bronchopulmonary aspergillosis; AF-CWP, *A. flavus* cell wall protein; CPA, chronic pulmonary aspergillosis; CWF, cell wall fragment; CWP, cell wall protein; DAS-ELISA, double antibody sandwich-ELISA; ELISA, enzyme-linked immunosorbent assay; Gal*f*, galactofuranose; GM, galactomannan; GPI, glycosylphosphatidylinositol; IA, invasive aspergillosis; Ig, immunoglobulin; mAb, monoclonal antibody; SD-Asp, *A. fumigatus* spent culture media.

in Gibco RPMI GlutaMAX medium (Thermo Fisher Scientific, Waltham, MA, USA) and the supernatants of cells producing *Aspergillus*-specific antibodies were screened by ELISA using a goat anti-mouse Fc antibody for the selection of IgG antibodies. Positive hybridoma cells were singularized by limiting dilution, and monitored using the Cellavista imaging system (Roche, Basel, Switzerland). Stable cell line AP3 (producing mAb AP3) was maintained for long-time storage by cryopreservation in liquid nitrogen. The isotype of this cell line was determined using a mouse immunoglobulin isotyping kit (BD Biosciences, San Jose, CA, USA). The cells were transferred to serum-free H5000 medium (PAN-Biotech, Aidenbach, Germany) and incubated continuously for up to 2 months at 37°C in a 5% CO_2 atmosphere in a CELLine bioreactor flask CL1000 (Sigma-Aldrich, St. Louis, MO, USA).

The AP3 antibody was purified by passing the hybridoma supernatant through MEP HyperCel resin (Pall, Port Washington, NY, USA) using the ÄKTAexplorer 10 fast protein liquid chromatography (FPLC) system (GE Healthcare, Munich, Germany). The purified antibody was dialyzed against PBS, supplemented with 0.02% (w/v) NaN_3 and stored at 4°C. Biotinylated mAb AP3 was prepared using the EZ-Link biotinylation kit (Thermo Fisher Scientific) according to the manufacturer's instructions.

Recombinant Protein Production

The cDNA coding for the *A. flavus* mycelial catalase (XP_002380889.1) was synthesized with codon optimization for *Escherichia coli* and transferred to the bacterial expression vector pET-22b(+) (Novagen, Darmstadt, Germany), providing sequences for an N-terminal signal peptide (targeting the periplasmic space) and a C-terminal His_6 tag (for affinity purification and detection). The construct was introduced into competent *E. coli* BL21(DE3) cells (New England Biolabs, Frankfurt am Main, Germany) and a positive clone of *A. flavus* mycelial catalase was selected for production and purification by Ni-NTA affinity chromatography, according to the manufacturer's instructions (Novagen).

One-Dimensional Electrophoresis (1DE) and Immunoblot

AF-CWPs and precipitated extracellular *Aspergillus* antigens were boiled in 5× reducing SDS loading buffer (62.5 mM Tris-HCl pH 6.8, 10% (v/v) 2-mercaptoethanol, 4% (w/v) SDS, 30% (w/v) glycerol, 0.05% (w/v) bromophenol blue), and separated by discontinuous SDS-PAGE using a 12% (w/v) polyacrylamide separating gel. Proteins were visualized using Coomassie Brilliant Blue (Fairbanks et al., 1971). The separated proteins were transferred to 0.45-µm nitrocellulose membranes by electroblotting, and free binding sites were blocked with 3% (w/v) milk powder in PBS containing 0.05% (v/v) Tween-20 (PBS-T). After each step, the membrane was washed with PBS-T. Proteins were detected with the purified mAb AP3 (2 µg/ml) and an alkaline phosphatase (AP)-labeled goat anti-mouse Fc (GAM^{AP} Fc, 160 ng/ml) (Jackson Immunoresearch Laboratories, West Grove, PA, USA). After washing in PBS-T and equilibrating in AP buffer (100 mM Tris-HCl pH 9.6, 100 mM NaCl, 5 mM $MgCl_2$), the signal was detected by incubating in AP buffer containing nitro-blue tetrazolium and 5-bromo-4-chloro-3-indolylphosphate (NBT/BCIP) diluted 1:100.

Two-Dimensional Electrophoresis (2DE), Immunoblot and Mass Spectrometry

Aspergillus spores were germinated in Czapek Dox medium (28°C, 16 h). Young *A. flavus* mycelia were ground to a fine powder under liquid nitrogen, and the proteins were precipitated by adding 1.8 ml ice-cold acetone containing 0.7% (v/v) 2-mercaptoethanol. The samples were incubated at −20°C for at least 1 h and then centrifuged (13,000 g, 20 min, 4°C). The pellets were resuspended in ice-cold acetone plus 0.7% (v/v) 2-mercaptoethanol followed by incubation and centrifugation as above. After the second centrifugation step, the pellets were washed twice in ice-cold acetone without 2-mercaptoethanol, dried at room temperature, and stored at −20°C. The proteins in the pellets were resolubilized overnight at room temperature in isoelectric focusing buffer (7 M urea, 2 M thiourea, 2% (w/v) CHAPS, 30 mM Tris-HCl pH 8.8), and the mixture was centrifuged as above to remove debris. The protein content of the supernatant was quantified using the 2D quant kit (GE Healthcare), and two 100-µg CWP aliquots were labeled with 200 pmol Cy3 (GE Healthcare) according to the manufacturer's instructions.

Gel electrophoresis was carried out as previously described (Horn et al., 2013). Two 2D gels were prepared under the same conditions—the first one was used for immunoblot analysis as described above, the second one as a preparative gel for the identification of proteins by mass spectrometry. After protein separation, both gels were scanned using the Ettan DIGE Imager (GE Healthcare) with the filter for Cy3 to localize all protein spots and to enable matching. Fungal proteins recognized by mAb AP3 were detected by first probing with AP3 (400 ng/ml) followed by a goat anti-mouse Cy5-labeled antibody (120 ng/ml). The membrane was then scanned twice using the Cy3 and Cy5 filters to reveal the positions of proteins bound by the AP3 antibody. The images were processed with DeCyder v7.0 (GE Healthcare). Spots of interest were marked on the preparative gel followed by blind picking. The proteins in gel spots were alkylated and digested with trypsin (Promega, Mannheim, Germany) before identification by mass spectrometry as previously described (Spiegel et al., 2015). The raw data files were evaluated using the NCBI *A. flavus* reference database (12,587 sequences; 5,779,766 residues).

Immunofluorescence Microscopy

Round glass coverslips were washed in 70% (v/v) ethanol, coated with 0.1% (v/v) poly-L-lysine and air dried. The coverslips were then washed in deionized water and deposited in 12-well cell culture plates, which were blocked with 3% (w/v) milk powder in PBS-T. Germinated *A. flavus* and *A. parasiticus* conidia (overnight incubation in RPMI medium at 37°C) were added to the wells, and the plates were centrifuged (2,000 g, 15 min, room temperature) to deposit the germlings onto the coverslips. For direct staining, mAb AP3 (2 µg/ml) was added to the wells and incubated for 2 h at room temperature.

After washing with PBS-T, AP3 binding to conidia and short hyphae was detected by adding 1.5 μg/ml $GAM^{Dylight}$ 594 H+L (Jackson ImmunoResearch Laboratories) and incubating for 1 h at room temperature. The round coverslips were then placed upside down on a slide and sealed with nail polish to prevent desiccation. Samples were analyzed with a Leica DMR fluorescence microscope (Leica Microsystems, Wetzlar, Germany) using excitation/emission maxima of 592/617 nm. *A. fumigatus* D141, Δ*glfA* and *P. chrysogenum* were detected with mAb AP3 and suitable Cy3-labeled secondary antibodies (Jackson ImmunoResearch Laboratories). Images were captured using a Leica SP-5 confocal laser scanning microscope (Leica Microsystems) as previously described (Wiedemann et al., 2016).

Periodate Oxidation

Extracellular *Aspergillus* antigens and CWPs from *A. flavus* were immobilized on ELISA plates (40 μg/well) and treated with 200 μl sodium *meta*-periodate buffer (20 mM $NaIO_4$ in 50 mM sodium acetate buffer, pH 4.5) for 16 h in darkness at 4°C. The periodate oxidation of the SD-Asp antigen was carried out as previously described (Thornton, 2008). The binding of mAb AP3 (400 ng/ml) to the antigen after periodate treatment was measured by ELISA as described below. Untreated *Aspergillus* antigens were used as a positive control and PBS as a negative control.

Digestion of *Aspergillus* Antigens

Extracellular *Aspergillus* antigens and *A. flavus* CWPs (40 μg) were dissolved in 50 mM ammonium bicarbonate buffer supplemented with 1.5 μg trypsin protease (Promega). The solution was then incubated at 37°C overnight and the antigen (20 μg) was separated by SDS-PAGE using a 12% (w/v) polyacrylamide separating gel. The binding of AP3 to the protease-treated antigens was analyzed by immunoblot as described above.

ELISA

Quantification of mAb AP3

The concentration of AP3 was determined by sandwich ELISA using an IgG1 standard (Rasche et al., 2011) to generate a calibration curve. A high-binding microtiter plate (Greiner Bio-One, Frickenhausen, Germany) was coated with 300 ng/ml goat-Fab anti-mouse Fab in PBS (Jackson ImmunoResearch Laboratories) overnight at 4°C. After each step, the plates were washed with 200 μl PBS-T. After blocking with 200 μl 3% (w/v) skimmed milk in PBS-T for 1 h, several dilutions of AP3 (0.4–100 ng/ml) were loaded onto the ELISA plate adjacent to the calibration curve of the standard IgG1. Binding was detected by adding 160 ng/ml horseradish peroxidase (HRP)-labeled goat anti-mouse Fc antibody (Jackson ImmunoResearch Laboratories) and 2,2′-azino-*bis*(3-ethylbenzthiazoline-6-sulfonic acid) (ABTS) as the substrate. After 30 min incubation at room temperature, the absorbance was determined by spectrophotometry at 405 nm. After each incubation step, the microtiter plate was washed three times with PBS-T. All measurements were taken in triplicate.

Reactivity of mAb AP3 to Fungal Antigens

The specificity of mAb AP3 binding was measured by direct ELISA with CWFs. The prepared CWFs were used to coat high-binding microtiter plates (150 μg/ml in water) overnight at 37°C. After blocking as described above, several concentrations of AP3 (0.002–2 μg/ml) were applied as the primary antibody, followed by detection as described above. The effect of periodate oxidation was evaluated by coating high-binding microtiter plates with periodate-treated *A. flavus* CWPs (2 μg) and GM standard SD-Asp (1:100), and using untreated *Aspergillus* antigens as a control. After blocking as described above, purified AP3 (400 ng/ml) was applied as the primary antibody, followed by detection as described above.

Double antibody sandwich ELISA (DAS-ELISA) was carried out to detect CWPs and extracellular antigens secreted by *A. flavus*. High-binding microtiter plates were coated with mAb AP3 (400 ng/ml) overnight at 4°C. After blocking with 2% (w/v) biotin-free bovine serum albumin (BSA; Carl Roth), 100-μl aliquots of serially-diluted *A. flavus* antigens (0.005–25 μg/ml) were applied for 1 h and detected using biotinylated mAb AP3 (600 ng/ml) and AP-labeled streptavidin (200 ng/ml) (Jackson ImmunoResearch Laboratories), followed by detection as described above.

To analyze *Aspergillus* supernatants by direct-coating ELISA, the culture supernatants from *A. fumigatus* wild-type D141 (SD-Asp, 1:10–1:100) and Δ*glfA* (1:10) were coated onto high-binding microtiter plates for 1 h at room temperature. After blocking as described above, purified AP3 (400 ng/ml) or the GM-specific antibody IgM L10-1 (Heesemann et al., 2011) and the IgM AB135-8 (Wiedemann et al., 2016), which recognizes a novel Gal*f*-containing antigen, were applied as primary antibodies, followed by detection using a secondary HRP-labeled goat anti-mouse IgG or goat anti-mouse IgM. The signal was developed by incubating in ABTS for 20 min and detected by measuring the absorbance at 405 nm. Measurements were taken in triplicate.

Sandwich ELISA was used to detect the presence of GM in serum. Purified AP3 (400 ng/ml), L10-1, or AB135-8, were coated onto a high-binding microtiter plate at 4°C overnight. After blocking as described above, 100 μl GM-positive serum from the Platelia *Aspergillus* enzymatic immunoassay (EIA) kit (Bio-Rad, Hercules, CA, USA) was diluted 1:5,000 or 1:100,000, applied for 1 h and developed using the Gal*f*-specific EB-A2 conjugate and the detection reagents provided in the kit. The reaction was stopped after 30 min and the absorbance was measured at 450 nm. Measurements were taken in triplicate.

To investigate the cooperation of L10-1 and AP3 as capture and detection antibodies in a sandwich ELISA, purified AP3 or L10-1 (each 900 ng/ml) were coated onto a high-binding microtiter plate at 4°C overnight. After blocking as described above, serially-diluted CWPs or extracellular antigens (1:320–1:20,480) from *A. flavus* were applied for 1 h, and bound antigens were detected using the corresponding detection antibody: AP3 or L10-1 (each 900 ng/ml). Binding was detected using a secondary HRP-labeled goat anti-mouse IgG or goat anti-mouse IgM. Absorbance was measured at 405 nm after 40 min incubation in ABTS substrate. Measurements were taken in triplicate.

Glycoarray

The carbohydrate specificity of mAb AP3 was determined using a thematic glycoarray as previously described (Krylov et al., 2018b; Matveev et al., 2018). To 96-well streptavidin-coated plates (Pierce, Waltham, MA, USA), we added 20 pmol/well of the biotin-tagged oligosaccharides 1–13 (Argunov et al., 2015, 2016; Krylov et al., 2018a) in 100 µl PBS containing 0.05% (v/v) Tween-20 and 0.1% (w/v) BSA. The plates were then incubated for 2 h at 37°C before adding mAb AP3 serially diluted in the same buffer (1000, 250, 50 and 10 ng/ml) and incubating for another 1 h at 37°C. After washing, we added a rabbit anti-mouse IgG HRP conjugate (Imtek, Moscow, Russia) and incubated for 1 h at 37°C. After washing three times, color development was initiated by adding 100 µl TMB monocomponent substrate for 15 min and stopped by adding 50 µl 1 M sulfuric acid. Absorbance was measured at 450 nm using a MultiSkan GO plate reader (Thermo Fisher Scientific). Measurements were carried out twice in triplicate, and results are presented as means ± SD.

Statistical Analysis

Significant differences between the antigen-binding and control treatments in ELISAs and glycoarray experiments were determined by one way analysis of variance (ANOVA) followed by *post-hoc* Bonferroni testing using Excel software (Microsoft, Redmond, Washington, USA). Significant differences in antigen binding between ELISA experiments were confirmed by Student's *t*-test, with the significance threshold set at $p < 0.05$.

RESULTS

Characterization of the *Aspergillus*-Specific mAb AP3

Following the immunization of mice with *A. parasiticus* cell wall fragments (CWFs), seven hybridoma clones producing *Aspergillus*-specific IgG antibodies were selected by ELISA. The hybridoma clone that showed the strongest reactivity against *A. parasiticus* CWFs was selected for further analysis, and the corresponding mAb (AP3) was assigned to isotype IgG1 and κ. Because CWFs and extracted cell wall proteins (CWPs) comprise a mixture of antigens of different sizes and chemical compositions, the precise antigen bound by AP3 was initially unknown.

First we analyzed the ability of AP3 to bind to *A. flavus* CWPs by immunoblot. The CWPs were separated by SDS-PAGE (**Figure 1A**) and the proteins were transferred to a membrane and probed with AP3. The antibody bound to multiple undefined bands with molecular masses exceeding 35 kDa and was particularly reactive against *A. flavus* proteins with molecular masses exceeding 70 kDa (**Figures 1B**, **3A**). This provided the first evidence that the epitope recognized by AP3 is shared by multiple glycoproteins.

The reactivity of AP3 against *Aspergillus* antigen preparations and its cross-reactivity with other fungal plant pathogens was also tested by ELISA. The antibody bound to CWFs prepared from *A. flavus*, *A. parasiticus*, *A. nidulans* and *A. niger* (**Figure 1C**; **Table 1**), as well as CWPs extracted from *A. flavus* and *A. parasiticus*, but not to other fungal preparations (**Table 1**). This probably reflects the ability of AP3 to detect an epitope that is conserved in the genus *Aspergillus* but absent in the other fungal genera tested in this experiment (**Table 1**).

Immunofluorescence microscopy showed that the antigen recognized by AP3 is located on the *Aspergillus* cell surface (**Figure 2**), particularly the hyphal walls and tips of the germination tubes in *A. parasiticus* (**Figure 2A**), *A. flavus* (**Figure 2B**), and *A. fumigatus* (**Supplemental Figures 1A,B**) compared to control samples (**Figures 2C,D**; **Supplemental Figures 1E,F**).

We next investigated the ability of mAb AP3 to bind extracellular antigens precipitated from the *A. flavus* culture supernatant (**Figure 3B**) and *A. fumigatus* spent culture medium (SD-Asp) (**Supplemental Figure 2A**) by immunoblot and ELISA. Compared to the protein-rich cell wall fraction (**Figure 3A**), the extracellular fraction contained mainly GM and small amounts of protein, hence no distinct protein band was observed in the Coomassie-stained gel (**Figure 3B**). The low protein content of the extracellular fraction was also confirmed by Bradford assay (data not shown). However, more sensitive immunoblot analysis revealed multiple undefined bands with molecular masses exceeding 70 kDa (**Figure 3B**), indicating that glycoantigens sharing the epitope recognized by AP3 are also present in the culture supernatant. The strong binding observed by direct-coating ELISA (**Figure 3C**; **Supplemental Figure 2A**) confirmed that the antigens detected by AP3 are present in both the culture supernatant and the *Aspergillus* cell wall.

Identification of the AP3 Antigen

The *Aspergillus* glycoproteins recognized by AP3 were identified by 2DE and mass spectrometry. The separation of young *A. flavus* CWPs by 2DE (**Figure 4**) revealed a wide range of protein spots with different molecular masses and pI values. However, only a small number of these proteins were detected by immunoblot with mAb AP3 as the probe (**Figures 4C,D**).

MS/MS analysis revealed five unique proteins in nine spots, indicating that some of the identified proteins were present in multiple spots, possibly due to different forms of post-translational modification (**Table 2**). Matching the protein sequences against the *A. flavus* NRRL3357 database identified *A. flavus* mycelial catalase, Hsp70, Hsp90, an amidase family protein, and a cell wall glucanase (**Table 2**). However, these proteins do not share any peptides or sequence similarities. *In silico* analysis revealed that the detected proteins have numerous acceptor sites for *N*-linked and/or *O*-linked glycosylation (**Table 2**). We therefore tested whether protein glycosylation might be necessary for antigen recognition by mAb AP3. The gene encoding the *A. flavus* mycelial catalase (XP_002380889.1) was produced in *E. coli* BL21 (DE3) cells. Immunoblot analysis revealed that mAb AP3 failed to detect the bacterial recombinant protein, whereas a histidine-specific antibody detected a distinct band with the expected molecular mass of *A. flavus* mycelial catalase (110 kDa) (**Supplemental Figure 3**). Because *E. coli* does not synthesize eukaryotic-type *N*-linked and *O*-linked glycans, the inability of AP3 to recognize the non-glycosylated mycelial catalase suggests that it binds a carbohydrate epitope present on certain *Aspergillus* glycoproteins or associated with the

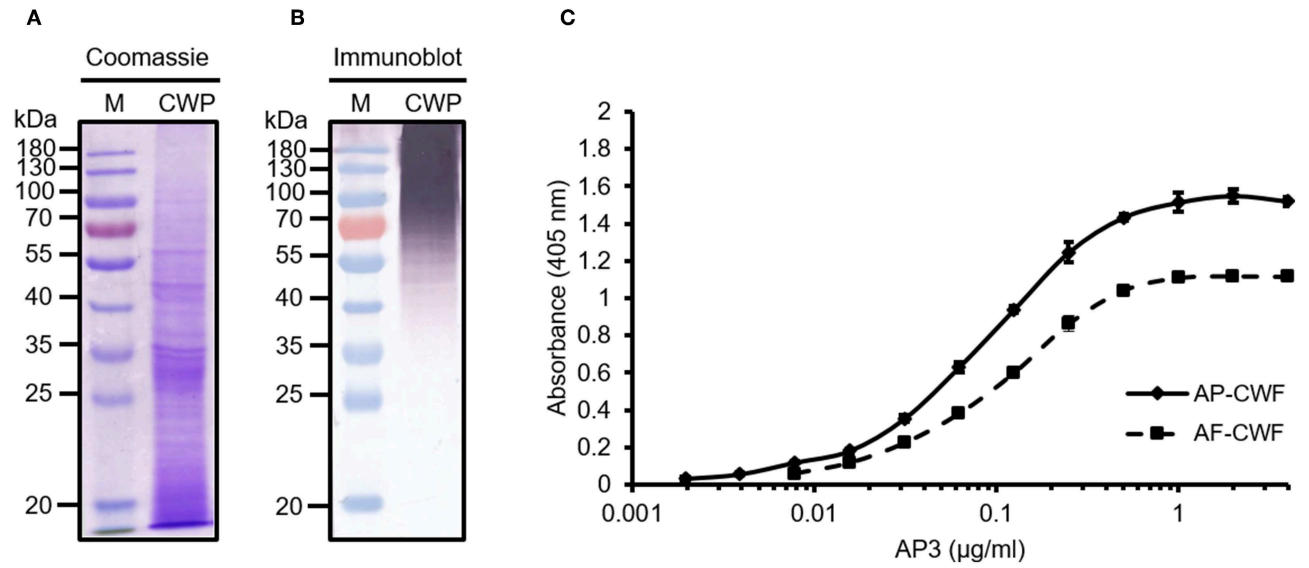

FIGURE 1 | Analysis of *A. flavus* cell wall proteins (CWPs) and the specific detection of cell wall fragments (CWFs) by ELISA using mAb AP3. Extracted CWPs were separated by SDS-PAGE and stained with **(A)** Coomassie Brilliant Blue or **(B)** transferred to a nitrocellulose membrane. Immunoblot detection was carried out using 200 µl culture supernatant from monoclonal hybridoma cell line AP3 and GAM^{AP} Fc (120 ng/ml) followed by visualization using NBT/BCIP. M: Pre-stained protein marker (Fermentas). **(C)** For the ELISA, 150 µg/ml CWFs from *A. flavus* (AF-CWF) and *A. parasiticus* (AP-CWF) were coated onto a microtiter plate. After blocking free binding sites with 3% (w/v) skimmed milk, bound antigens were detected using purified mAb AP3 (0.008–4 µg/ml) and an HRP-labeled goat anti-mouse Fc antibody (160 ng/ml). Absorbance was measured in triplicate after 15 min substrate incubation.

TABLE 1 | Cross-reactivity of mAb AP3 against CWFs from different fungal pathogens measured by ELISA.

Species	Source	Binding of mAb AP3
Aspergillus flavus Link:Fries	DSMZ 818	+++
Aspergillus parasiticus Speare	DSMZ 1300	+++
Aspergillus nidulans (Eidam) Winter	DSMZ 820	++
Aspergillus niger van Tieghem	IME	+
Fusarium oxysporum f. sp. *nicotianae*	IME	–
Fusarium culmorum W. G. Smith	IME	–
Phytophthora nicotianae	DSMZ 1828	–
Rhizoctonia solani Kühn	IME	–
Pythium ultimum Trow	DSMZ 62987	–
Botrytis cinerea Persoon:Fries	IME	–
Cercospora nicotianae	IME	–
Thielaviopsis basicola	IME	–

CWFs (150 µg/ml in water) were coated overnight at 37°C. After blocking free binding sites with 3% (w/v) skimmed milk, the bound antigen was detected using purified mAb AP3 (400 ng/ml). Antibody binding to fungal CWFs was confirmed by the addition of GAM^{HRP} Fc (1:5,000). Absorption at 405 nm was measured after 30 min incubation with the substrate ABTS. Cross-reactivity was determined based on the extinction levels after subtracting the background signal. DSMZ, German Collection of Microorganisms and Cell Cultures, Leibniz Institute, Braunschweig, Germany; IME, Fraunhofer IME, Aachen, Germany; –, $OD_{405\ nm} < 0.1$; +, $OD_{405\ nm} = 0.50–0.99$; ++, $OD_{405\ nm} = 1.00–1.49$; +++, $OD_{405\ nm} > 1.5$.

Aspergillus glycosylation pattern, as indicated by the immunoblot data (**Figures 1B**, **3**).

To determine whether AP3 recognizes a carbohydrate or a protein epitope, the CWPs and extracellular secreted antigens were treated with protease or periodate, to remove the protein component and to oxidize the glycans, respectively (**Figure 3**). No differences in immunoblot profiles were observed when we compared untreated controls with *A. flavus* CWPs (**Figure 3A**) and extracellular antigens (**Figure 3B**) digested with trypsin. This might reflect the location of trypsin cleavage sites toward the N-terminus of the target protein, resulting in minor mass changes, or proteolytic stability caused by the presence of glycans around the peptide backbone of the amino acids adjacent to the glycosylation site, thus preventing the contact between the glycoprotein surface and the protease active site (Sola and Gribenow, 2009). The epitope recognized by AP3 was found to be periodate sensitive ($p < 0.05$) and therefore most likely a carbohydrate (**Figure 3C**). Our results therefore demonstrate that AP3 recognizes an *Aspergillus* glycoantigen rather than a peptide or protein epitope. Furthermore, the smear-like staining observed for the extracellular fraction in the immunoblot suggests that most of the AP3 antigens are fragments of cell wall carbohydrate polymers.

Taken together, our data suggested that AP3 recognizes a major carbohydrate of the *Aspergillus* cell wall, which is homogenously distributed on the hyphal surface, found in a speckled pattern on swollen conidia, and not present on the surface of resting conidia. This pattern resembles that of GM (Heesemann et al., 2011) and we therefore tested the Gal*f*-deficient *A. fumigatus* mutant Δ*glfA* (Schmalhorst et al., 2008). Immunofluorescence microscopy revealed that the hyphae of the parental *A. fumigatus* strain D141 were completely stained (**Supplemental Figure 4A**), but AP3 did not bind to the Δ*glfA* mutant (**Supplemental Figures 1C,D**), indicating that Gal*f*

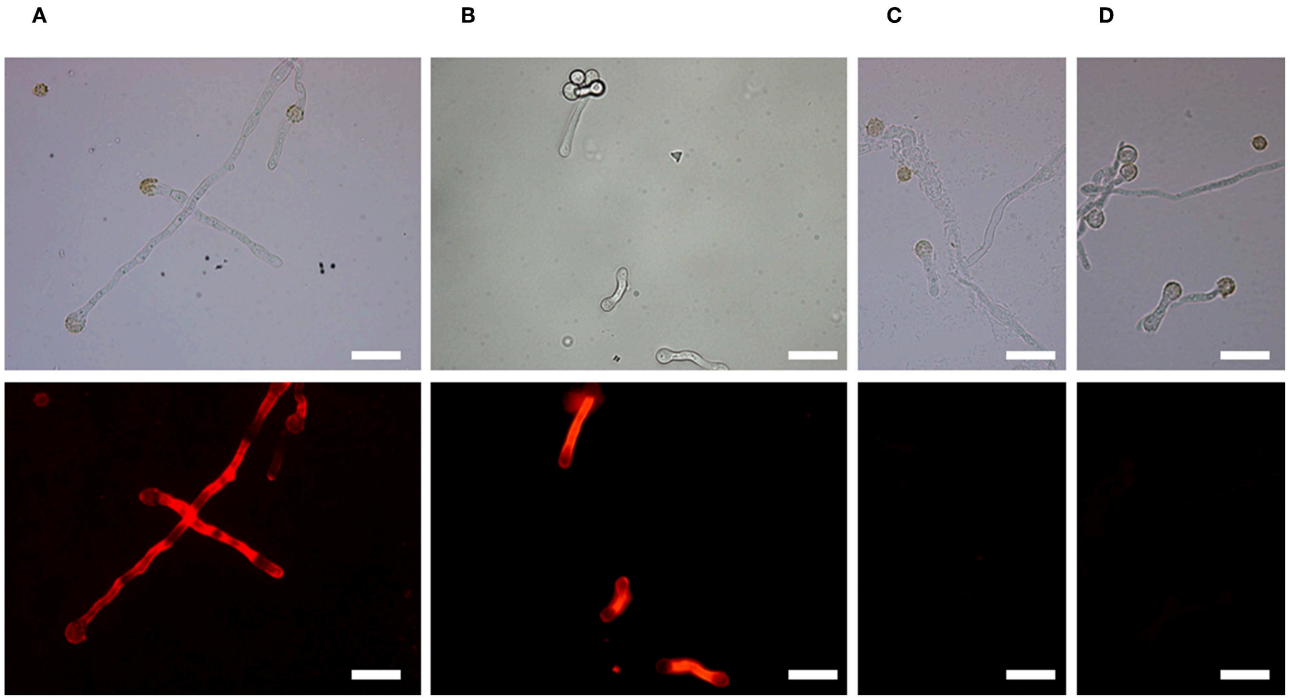

FIGURE 2 | Binding of mAb AP3 to *A. parasiticus* and *A. flavus* revealed by immunofluorescence microscopy. **(A)** *A. parasiticus*. **(B)** *A. flavus*. **(C)** *A. parasiticus* control. **(D)** *A. flavus* control. Mycelia were immobilized on glass coverslips and incubated with 200 µl hybridoma supernatant containing 25 µg/ml mAb AP3 or (Rasche et al., 2011; unrelated control). The binding of AP3 to its antigen was verified using GAM^{Dylight} 594 H + L (1.5 µg/ml). Antibody–antigen complexes were visualized under a Leica DMR fluorescence microscope. For comparison, light microscope images are shown above the immunofluorescence images. Scale bar = 50 µm.

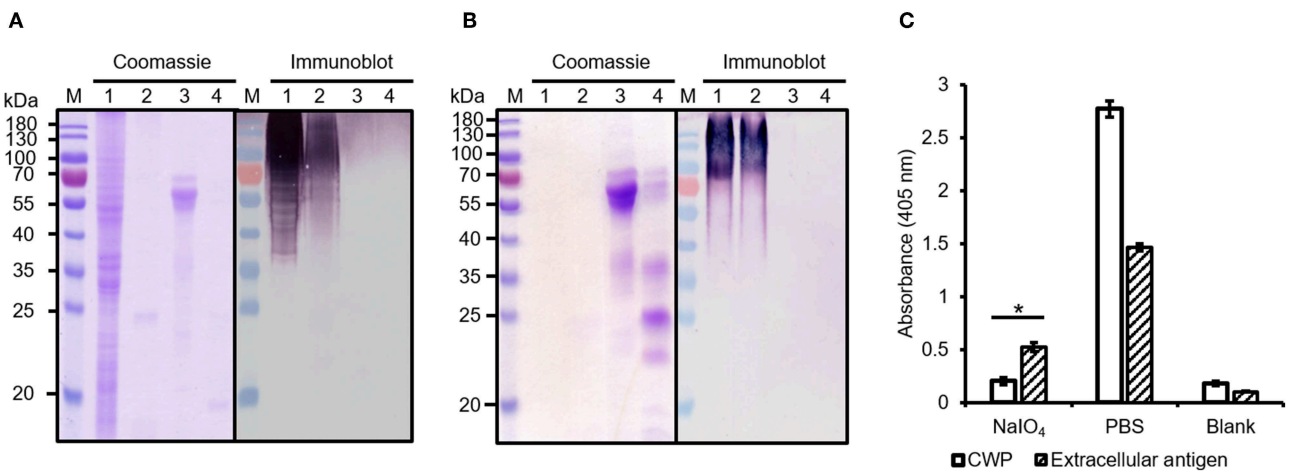

FIGURE 3 | Analysis of protease-treated and periodate-treated *Aspergillus* antigens. **(A)** Cell wall proteins and **(B)** extracellular secreted antigens of *A. flavus* were extracted and digested with trypsin. Fractions were separated by SDS-PAGE and stained with Coomassie Brilliant Blue. Proteins transferred to a nitrocellulose membrane were detected with a purified mAb AP3 (400 ng/ml) and an AP-labeled goat anti-mouse antibody (120 ng/ml) followed by NBT/BCIP substrate incubation. M: Protein marker (Fermentas); Lane 1: sample without trypsin treatment; 2: sample with trypsin; 3: control protein fetuin without trypsin treatment; 4: control protein fetuin with trypsin. **(C)** Prepared *A. flavus* cell wall proteins (CWPs) and extracellular antigens (40 µg/well) were coated onto a microtiter plate and oxidized with periodate (80 mM). Untreated preparations were used as controls. After blocking free binding sites with 3% (w/v) skimmed milk, bound antigens were detected with mAb AP3 (400 ng/ml) and an HRP-labeled goat anti-mouse Fc antibody (120 ng/ml). Absorbance was measured in triplicate after 20 min substrate incubation. Values represents means ± SD ($n = 3$) for treated ($NaIO_4$), untreated (PBS), and control (Blank). An asterisk denotes a statistically significant reduction in antigen binding between treated and untreated samples (CWF and extracellular antigen, $p < 0.05$).

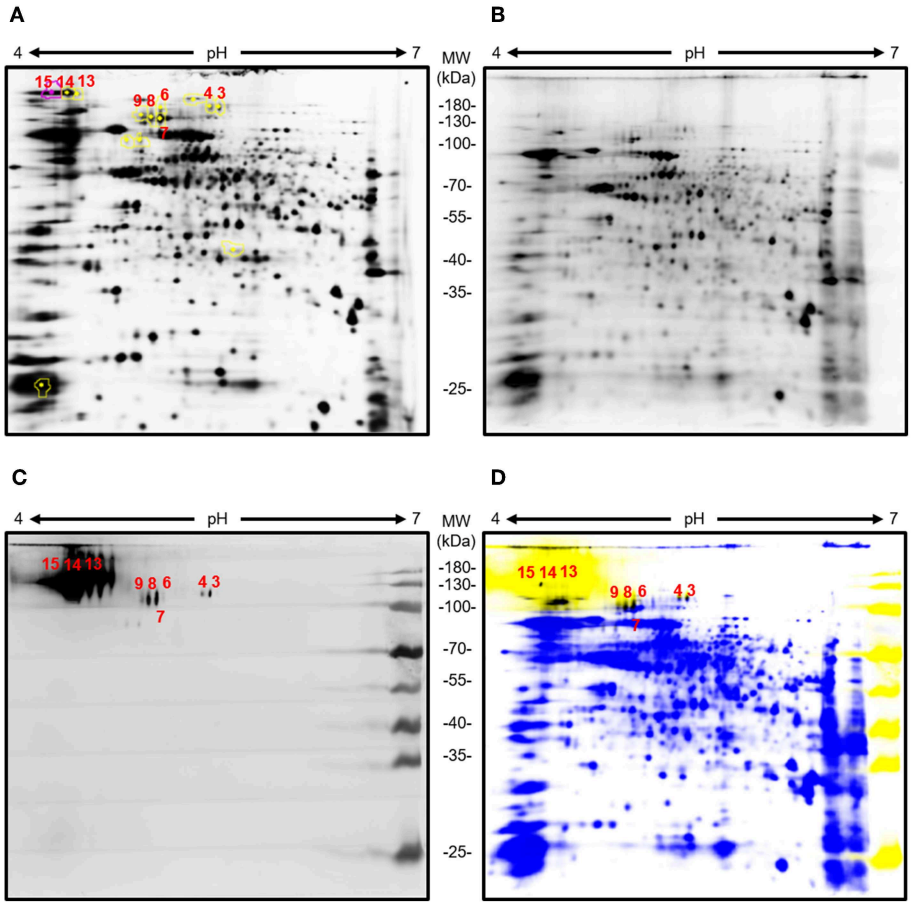

FIGURE 4 | Analysis of young *A. flavus* mycelia cell wall proteins by 2DE and immunoblot with AP3 as the detection antibody. Total *Aspergillus* mycelia and CWPs (100 μg) were labeled with Cy3 and separated in the first dimension on a 7-cm pH 4–7 immobilized pH gradient strip followed by separation in the second dimension by 12.5% (v/v) SDS-PAGE. Separated *Aspergillus* CWPs were transferred onto a nitrocellulose membrane. Immunoblot detection was carried out using purified mAb AP3 (400 ng/ml) and a goat anti-mouse Cy5-labeled antibody (120 ng/ml). Gels and membranes were scanned with an Ettan DIGE Imager equipped with appropriate filters for Cy3 and Cy5, and images were processed with DeCyder software v7.0. **(A)** Cy3 labeled 2D gel of young *A. flavus* proteins. **(B)** Cy3-labeled total CWPs blotted onto a membrane. **(C)** CWPs specifically detected by mAb AP3 visualized using a Cy5-labeled antibody. **(D)** Overlay of Cy3-labeled total CWPs (blue) and AP3-recognized CWPs (yellow). Shared protein spots are highlighted in black. Numbers indicate protein spots selected for analysis by mass spectrometry.

residues are part of the epitope. Moreover, the double-staining of *A. fumigatus* hyphae with AP3 (IgG) and the GM-specific antibody L10-1 (IgM) demonstrated that the staining patterns of both antibodies are similar (**Supplemental Figure 4**). This prompted us to analyze *Penicillium chrysogenum*, a non-pathogenic mold known to produce GM. AP3 decorated the hyphal surface of *P. chrysogenum* and additional material bound to the glass surface in close proximity to the hyphae (**Supplemental Figures 5A,B**). This staining pattern suggests that AP3 recognizes structurally identical GM antigens that are present on the surface of this fungus and partially released into the surrounding medium. We performed additional tests on culture supernatants derived from the *A. fumigatus* wild-type strain D141 and Δ*glfA* mutant for further characterization of AP3 by ELISA (**Figure 5**). Supernatants diluted 1:10 in PBS were coated onto the ELISA plate and probed with AP3, the GM-specific IgM L10-1, and AB135-8, an IgM that recognizes a Gal*f* antigen found prominently in the *Fusarium* cell wall but present in only limited amounts in the *Aspergillus* cell wall (Wiedemann et al., 2016). All three antibodies recognized their antigen in the culture supernatant of the wild-type strain, but not in the supernatant of the Δ*glfA* mutant (**Figure 5**). Similar results were observed for AP3 and L10-1 at a dilution of 1:100 (**Supplemental Figure 2A**).

Antibody-Based GM Detection and Specificity of mAb AP3

We next investigated whether AP3 and L10-1 (Heesemann et al., 2011) can cooperate to bind the soluble fungal-type GM of *A. fumigatus* (SD-Asp) (**Supplemental Figure 2B**), *A. flavus* extracellular antigens, and *A. flavus* cell wall proteins (AF-CWPs) (**Supplemental Figures 2C,D**). We therefore carried out a sandwich ELISA in which AP3 was the capture reagent and L10-1 the detection reagent or vice versa, and the detection reagent was in turn bound by an HRP-labeled anti-mouse isotype-specific secondary antibody. As shown in **Supplemental Figures 2B,D**, L10 detected all tested Gal*f*-containing antigens that were captured by AP3. Similarly, AP3 recognized CWPs immobilized

TABLE 2 | List of *Aspergillus* proteins detected by mAb AP3.

Spot no.	Short name	Protein	NCBI reference sequence	MW (kDa)	pI[a]	Score[b]	Peptides[c]	Sequence coverage (%)	Signal peptide[d]	*N*-glycan acceptor sites[e]	*O*-glycan acceptor sites[f]	Cellular localization	Function[g]
3	Catalase	Mycelial catalase cat1	XP_002380889.1	79.8	5.34	398	18 (13)	21	Yes	4	24	Extracellular (cell wall)	Cell protection (Paris et al., 2003)
4						373	14 (9)	17					
6	Hsp70	Hsp70 chaperone Hsp88	XP_002381416.1	79.8	5.02	680	32 (23)	34	No	3	3	Intracellular	Protein folding (Teutschbein et al., 2010)
8						331	16 (10)	19					
7	Hsp90	Molecular chaperone and allergen Mod-E/Hsp90/Hsp1	XP_002382894.1	79.6	4.97	405	13 (10)	20	No	4	8	Intracellular (cytosolic, cell wall)	Protein folding (Lamoth et al., 2012, 2014, 2016)
9	Amidase	Amidase family protein	XP_002377652.1	60.7	5.22	276	11 (7)	22	Yes	7	9	Extracellular	Unknown
13	Glucanase	Cell wall glucanase (Scw11), putative	XP_002372749.1	61.8	4.63	155	6 (4)	10	Yes	0	122	Extracellular (cell wall)	Cell wall remodeling (Mouyna et al., 2013)
14						262	10 (6)	15					
15						187	8 (5)	11					

Protein spots were identified by Tandem mass spectrometry and protein sequences were analyzed in silico using the A. flavus NRRL3357 reference database.

[a]*Predicted Mw and pI by ExPASy Compute pI/Mw tool.*

[b]*Protein score in Mascot Search.*

[c]*Number of total identified peptides/unique peptides.*

[d]*Predicted signal peptide (ProP 1.0).*

[e]*Predicted N-glycosylation sites (NetNGlyc1.0).*

[f]*Predicted O-glycosylation sites (NetOGlyc4.0).*

[g]*Reference.*

FIGURE 5 | Detection of *A. fumigatus* D141 GM and Δ*glfA* supernatant by ELISA. Culture supernatants from *A. fumigatus* Δ*glfA* and wild-type D141 strains were coated (1:10) onto a microtiter plate. GM was detected using 400 ng/ml purified mAb AP3 or 400 ng/ml of the IgMs L10-1 and AB135-8, which recognize distinct Gal*f*-dependent antigens, followed by isotype-specific antibodies labeled with HRP. Data are means ± SD ($n = 3$). An asterisk denotes a statistically significant difference in antigen binding between the D141 and Δ*glfA* strain ($p < 0.005$).

on the solid phase by L10-1. However, the extracellular antigens of *A. flavus* were not captured by L10-1 antigens (**Figure 2C**). Given the diverse structures of Gal*f*-antigens in *Aspergillus* species, these results provide further evidence that AP3 recognizes a defined Gal*f* epitope that may differ slightly from that recognized by L10-1. Moreover, these findings suggest that mAb AP3 detects a Gal*f* epitope that is present less frequently in extracellular *Aspergillus* antigens compared to CWPs from *A. flavus*.

GM is the most important immunological biomarker of invasive aspergillosis (IA). Therefore, the ability of AP3 to detect *Aspergillus* GM in serum was compared to the Gal*f*-specific IgM L10-1 (**Figure 6**). In a sandwich ELISA format, AP3, and L10-1 were coated onto the ELISA plate. After incubation with the positive control serum, the wells were incubated with HRP-labeled EB-A2 (a Gal*f*-specific IgM antibody) according to the procedure of the Platelia *Aspergillus* EIA. As shown in **Figure 6**, AP3 generated significantly ($p < 0.05$) stronger signals than L10-1, which demonstrates the potential of AP3 as a candidate diagnostic antibody for IA.

The epitope specificity of mAb AP3 was investigated using a library of 13 synthetic oligosaccharides representing distinct fragments of *Aspergillus* GM (Argunov et al., 2015, 2016; Krylov et al., 2018a), differing in length and in the nature of the linkages between monosaccharide residues (**Figure 7A**). AP3 showed the highest affinity ($p < 0.05$) for heptamer **13**, which contains a hexameric block of β-1,5-linked Gal*f* residues (**Figure 7B**), and lower affinity for pentamers **10** and **11**, containing four β-1,5-Gal*f*

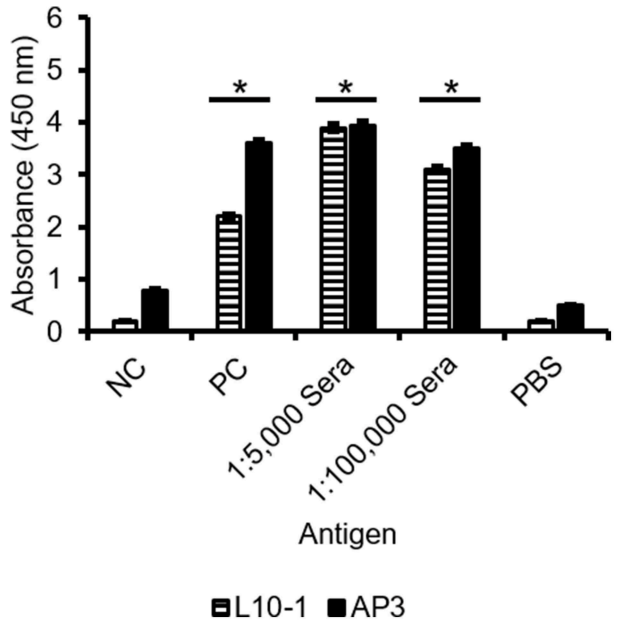

FIGURE 6 | Detection of GM in sera by sandwich ELISA using GM-specific antibodies. Microtiter plates were coated with 400 ng/ml purified mAb AP3 and L10-1. After blocking free binding sites with 3% (w/v) skimmed milk, sera diluted 1:5,000 or 1:100,000 were applied and detected using the EB-A2 conjugate. The signal was measured in triplicate at 450 nm after 20 min substrate incubation (ABTS). PC: *Aspergillus*-positive control serum from the Platelia *Aspergillus* EIA. NC: negative control serum from the Platelia *Aspergillus* EIA. PBS: negative control. An asterisk denotes a statistically significant difference in antigen binding relative to the NC control serum ($p < 0.005$).

units linked to a terminal Man*p* residue via β-1,6 or β-1,3 bonds. There was no affinity for pentamer **12** with β-1,6 linkages between Gal*f* residues, representing structures recently discovered in *A. fumigatus* GM (Kudoh et al., 2015; Krylov et al., 2018a), nor for trimer **6**, comprising three β-1,5-Gal*f* units. Taken together, these data indicate show that AP3 binds specifically to a tetramer of β-1,5-Gal*f* units present in *Aspergillus* GM and Gal*f*-containing *Aspergillus* glycoproteins. The binding of AP3 to *P. chrysogenum* indicates the presence of an identical structure in this species (**Supplemental Figure 5**).

DISCUSSION

Identification of the Epitope Recognized by mAb AP3

The fungal cell wall is a complex and dynamic structure that provides protection and mediates interactions with the environment. Detailed investigations of the composition and biosynthesis of the *A. fumigatus* cell wall have identified carbohydrates, such as chitin, glucans, and GM as major structural components. The cell wall is adorned with CWPs that can be attached to the plasma membrane by glycosylphosphatidylinositol (GPI) anchors or linked to glucan structures, thus facilitating the wall's structural organization (Bernard and Latgé, 2001; Bruneau et al., 2001).

In this study, we report the generation of mAb AP3 using *A. parasiticus* CWFs comprising a complex mixture of different antigens, and the characterization of its antigen specificity. The diversity, abundance and accessibility of potential antigens makes it challenging to identify the precise epitope (Schubert et al., 2018). The proteome and metabolome of *Aspergillus* spp. are highly dependent on the growth conditions, particularly stress-induced changes which are known to affect protein expression, cell wall composition, the production of secondary metabolites (Imanaka et al., 2010; Champer et al., 2016), and the abundance, chain length and composition of GM (Kudoh et al., 2015). The identification the epitope recognized by AP3 is also hampered by our use of different *Aspergillus* strains and cultivation conditions in different laboratory environments.

Despite the challenges described above, the specificity of mAb AP3 was confirmed in well-controlled replicate experiments using different *Aspergillus* strains and antigen compositions, leading to the successful localization and identification of the epitope. Indirect detection methods, such as ELISAs and deglycosylation assays indicated that AP3 detects substantial parts of a glycoantigen which is secreted into the culture medium, bound to the cell surface, and located on *Aspergillus* proteins. Importantly, immunofluorescence microscopy using the *Aspergillus* Δ*glfA* mutant strain, which is unable to synthesize Gal*f* residues (Schmalhorst et al., 2008), indicated that the epitope recognized by AP3 contains Gal*f* as a key constituent.

The *Aspergillus* proteins recognized by the antibody AP3 were identified by a combination of 2DE and mass spectrometry. Although we cannot be certain which of the proteins identified in the same spot was recognized by AP3, MS/MS analysis revealed that the antibody bound up to five distinct *Aspergillus* proteins that did not share any amino acid sequence similarity but carried multiple acceptor sites for *N*-linked and/or *O*-linked glycans, suggesting they are heavily glycosylated. The abundant glycosylation may explain the detection of these proteins in 2D gels at a higher molecular weights (>70 kDa) than expected. With the exception of Hsp70 and Hsp90, these glycoproteins carry a signal peptide causing them to be localized either in the cell wall (such as cell wall glucanase and amidase) or extracellular space (such as the mycelial catalase Cat1). Although Hsp90 is normally a cytosolic protein, it can travel to the fungal cell wall and regulate cell wall integrity (Lamoth et al., 2016). The lack of *N*-glycan acceptor sites and the very high number of potential *O*-glycosylation sites (122) in the cell wall glucanase, together with the strong fluorescence signal in the immunoblot (spots 13, 14, and 15) (**Figure 4C**), suggests that the AP3 antibody binds mainly to Gal*f* residues attached to *O*-linked glycan chains. Accordingly, the treatment of extracellular *Aspergillus* antigen and *A. flavus* CWPs with PNGase F did not affect the binding of mAb AP3, confirming that the signal was not associated with individual β-1,2-linked or α-1,2-linked Gal*f* residues attached to *N*-linked glycans and that AP3 binding was probably restricted to either β-1,5-linked or β-1,6-linked *O*-glycans and fungal-type GM (Komachi et al., 2013).

Finally, the direct glycoarray which uses 13 synthetic Gal*f* oligosaccharides resolved the linkage and length of the Gal*f* epitope detected by mAb AP3. These results provide a clear

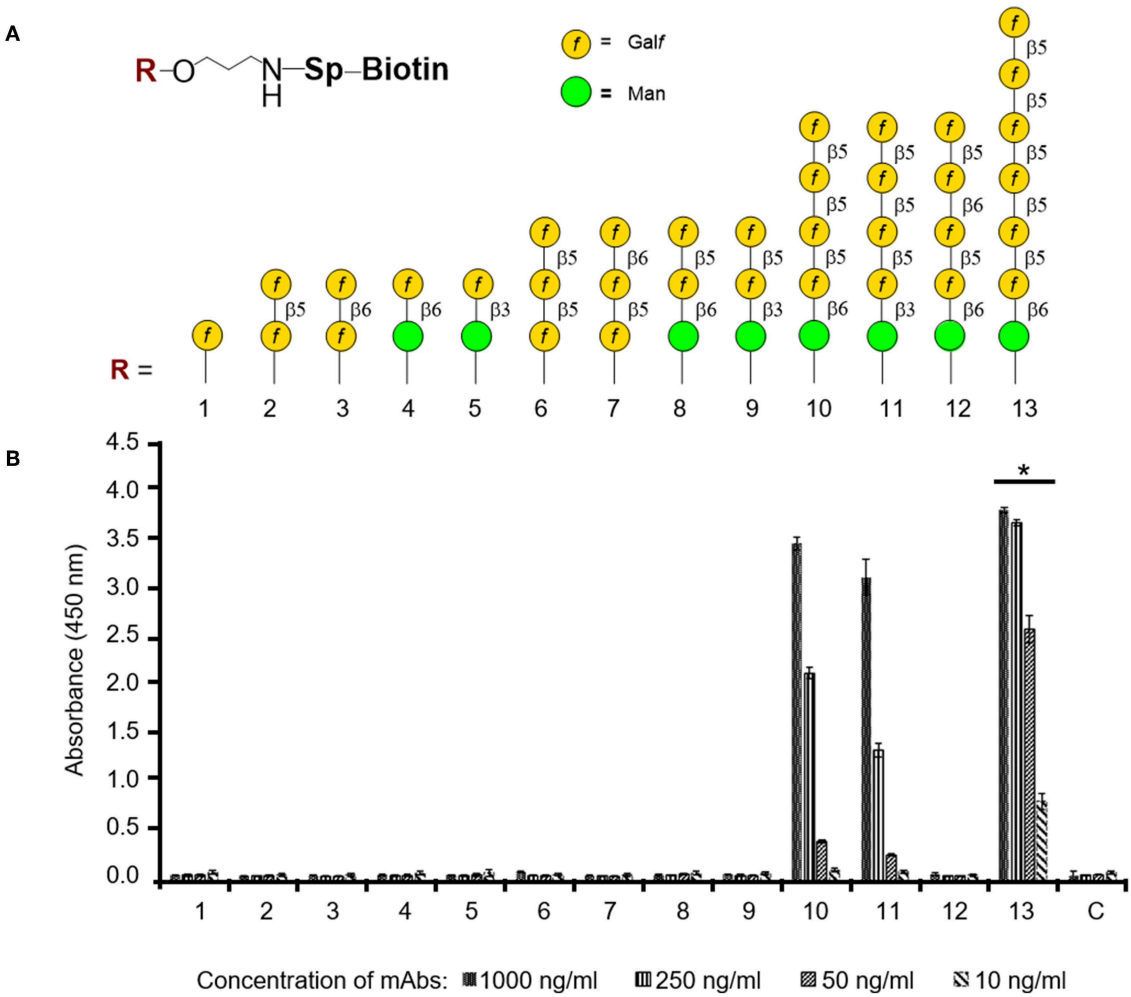

FIGURE 7 | ELISA to determine the oligosaccharide specificity of mAb AP3. **(A)** Composition of thematic glycoarray oligosaccharide ligands representing key structural elements of GM. The carbohydrate sequences are represented as previously reported (Varki et al., 2009). **(B)** Carbohydrate specificity of antibody AP3. Biotin-tagged oligosaccharides 1–13 were applied to a streptavidin-coated microtiter plate and detected with mAb AP3 (1,000, 250, 50, and 10 ng/ml) and anti-mouse IgG HRP conjugate followed by TMB substrate incubation. All measurements were taken twice in triplicate. Asterisk denotes the statistically significant difference in binding between AP3 and heptamer 13 compared to pentamers 10 and 11 ($p < 0.05$).

line of evidence that the Gal*f* pattern recognized by AP3 is characterized by a β-1,5-Gal*f* tetramer, whereas shorter oligosaccharides including a β-1,5-Gal*f* trimer are not detected. Interestingly, the replacement of the third β-1,5 Gal*f* unit with β-1,6 Gal*f* in the tetramer (oligosaccharide 12) destroys the antigen entirely. Therefore, the specificity of mAb AP3 is restricted to Gal*f*-containing structures in *Aspergillus* fungal-type GM and *O*-linked glycans ([β-D-Gal*f*-1,5]$_4$), whereas *N*-glycans containing Gal*f* (α-1,2 Gal*f*) and Gal*f*-containing glycosphingolipids (β-1,2 and or β-1,6 Gal*f*) are not detected (Latge, 2009; Tefsen et al., 2012).

Specificity of mAb AP3 Compared to Other Gal*f*-Specific Antibodies

Carbohydrates, such as GM and abundant immunodominant glycoproteins, often provide excellent biomarkers for fungal diseases because they are conserved among related species of fungi (Thornton and Wills, 2015). For example, *A. flavus* and *A. fumigatus* galactomannoproteins are recommended as biomarkers for the serological diagnosis of IA (Chan et al., 2002; Woo et al., 2003; Chong et al., 2004). Consequently, several GM-specific antibodies have already been developed for IA diagnostics, but thus far most of these antibodies belong to the IgM subclass (Thornton, 2010).

The IgM EB-A2 (Stynen et al., 1992) is the best-characterized Gal*f*-specific antibody used for the diagnosis of IA and has been regarded as the gold standard for more than 20 years. It is supplied as part of Bio-Rad's commercial Platelia *Aspergillus* EIA kit, which has been validated in several clinical studies and is approved by the FDA (Pfeiffer et al., 2006). Early epitope characterization studies suggested that EB-E2 recognized a tetramer of at least four β-1,5-linked Gal*f* moieties in *Aspergillus* GM, present in the cell wall and in glycoproteins (Stynen et al., 1992; Kudoh et al., 2015). However, a glycoarray was recently

used to reinvestigate the oligosaccharide specificity of EB-A2, revealing that it also detects dimers and trimers with β-1,6 linkages (Krylov et al., 2019). This could explain the observed cross-reactivity between EB-A2 and non-*Aspergillus* fungi, contaminating GM in β-lactam antibiotics and foodstuffs, the cancer prodrug cyclophosphamide, and several other bacterial antigens, such as *Cryptococcus* galactoxylomannan (Dalle et al., 2005), which can generate false-positive results (Viscoli et al., 2004; Aubry et al., 2006; Zandijk et al., 2008).

Both EB-A2 and AP3 can also bind *Penicillium* spp., reflecting the presence of identical Gal*f* epitopes in these species (Unkefer and Gander, 1979). Cross-reactivity has also been reported between EB-A2 and *Fusarium* GM (Tortorano et al., 2012). Interestingly, we observed no cross-reactivity between AP3 and *F. oxysporum* Gal*f*-containing antigen preparations, which comprise β-1,6-linked β-D-Gal*f* residues with multiple side chains (Chen et al., 2015). This suggests that AP3 has a greater specificity for *Aspergillus* GM than EB-A2. AP3 was unable to detect lipoteichoic acid (LTA), a bacterial membrane polysaccharide substituted with β-1,5-linked D-Gal*f* residues (data not shown). We cannot exclude the possibility that AP3 binds to other fungi and bacteria, as well as cross-reacting antigens, such as LTA from *Bifidobacter* spp., but the specificity of AP3 for longer Gal*f* chains may reduce the likelihood of cross-reaction to other epitopes.

More recently, two novel Gal*f*-specific antibodies have been generated by immunizing mice with the synthetic pentasaccharide β-D-Gal*f*-1,5-[β-D-Gal*f*-1,5]$_3$-α-D-Man*p*: mAb 7B8, which specifically recognizes the Gal*f* trimer, and mAb 8G4, which mainly detects the parental Gal*f* tetramer (Matveev et al., 2018). These are IgG antibodies like AP3 and they likewise detect defined Gal*f* epitopes located on the *Aspergillus* cell wall and glycoproteins as well as the secreted GM of several *Aspergillus* species. Neither 7B8 nor 8G4 react with *Bifidobacterium longum* and show less cross reactivity than EB-A2 (Mennink-Kersten et al., 2005). In contrast to AP3, 7B5, and 8G4 also recognize a shorter Gal*f* trimer ([β-D-Gal*f*-1,5]$_3$) and a Gal*f*-dimer with a β-1,6 Gal*f* linkage (Matveev et al., 2018).

Potential Applications of mAb AP3

In this study, we tested for the first time the potential of different Gal*f*-specific antibodies (EB-A2, L10-1, and AP3) to cooperate in the detection of Gal*f*-containing structures on AF-CWPs and *Aspergillus* GM. Interestingly, AP3 was unable to detect *Aspergillus* GM/EPS when used as the capture or detection reagent in a DAS-ELISA, whereas AF-CWPs were detected (data not shown). This is remarkable because detailed analysis of the EB-A2 antigen showed that GM contains more than 10 Gal*f* epitopes, making it possible to develop a DAS-ELISA with the GM-specific antibody acting as both the capture and detection antibodies (Stynen et al., 1992). AP3 can cooperate with L-10 and EB-A2 to detect AF-CWP and *Aspergillus* GM. However, *Aspergillus* GM could be not detected by an AP3 capture reagent with L10-1 as the detection antibody, although the reciprocal configuration was successful. The epitope detected by L10-1 has yet to be identified, so it is possible that L10-1 blocks the epitope detected by AP3 in this setup.

The glycosylation profiles of the proteins identified by 2DE were not analyzed in detail, but we speculate that the Gal*f*-epitope detected by AP3 is probably less abundant in secreted GM than CWPs, given that several such epitopes are accessible on the CWPs of *A. flavus*. The limited number of proteins specifically detected by AP3 in 2DE experiments, and the differential recognition of Gal*f*-containing epitopes by ELISA, suggest that the epitope is present on a limited number of Gal*f*-containing proteins and differs in this respect from the epitope recognized by L10-1 and EB-A2, thus making this antibody valuable for the detection of *Aspergillus* spp.

The unique ability of AP3 to bind Gal*f* oligosaccharides comprising four or more residues with β-1,5-linkages makes this antibody an ideal candidate for the detection of *Aspergillus* GM with higher sensitivity and specificity than current diagnostic reagents. It could also be used to monitor the distribution of long-chain Gal*f* oligosaccharides on fungal cell walls in combination with antibodies that recognize shorter oligosaccharide chains. Further studies are needed to validate the potential of AP3 and different Gal*f*-specific antibodies as a platform for the rapid analysis of galactofuranosylation and to distinguish between Gal*f*-containing structures on glycoproteins and fungal-type GM.

Compared to GM-specific and Gal*f*-specific IgMs, the greater stability and specificity of affinity-matured IgG antibodies, such as AP3, 7B8, and 8G4 may allow the development of novel detection assays for *Aspergillus* infections. Accordingly, the specificity of mAb AP3 for long-chain β-1,5 Gal*f* and its successful detection of GM in human serum demonstrates its value as a diagnostic tool. Although further evaluation of the AP3 sandwich assay is necessary with a larger number of patients, we have demonstrated the potential of AP3 for the rapid and sensitive diagnosis of IA.

In addition, the greater stability and reactivity of AP3 compared to IgM-based reagents could be advantageous in applications that involve the molecular imaging of *Aspergillus* infections *in vivo* (Rolle et al., 2016). The development of an IgG-based reagent could also provide therapeutic benefits (Di Mambro et al., 2019). For example, a β-glucan-specific IgG2b subtype antibody protected mice against infections with *Candida albicans*, whereas the corresponding IgM with an identical complementarity determining region did not (Torosantucci et al., 2009). The Gal*f*-specific IgM L10-1 did not confer a protective effect during an *A. fumigatus* infection (Heesemann et al., 2011). The recognition of *A. fumigatus* hyphae by the Fcγ receptor was shown to be necessary for opsonization (Gazendam et al., 2016). More recently, a humanized IgG targeting the *Crf* cell wall transglycosylase of *A. fumigatus* reduced the fungal burden in a neutropenic rat model (Chauvin et al., 2019). Therefore, mAb AP3 could also be developed as a therapeutic modality to recruit phagocytes to extracellular *Aspergillus* germ tubes, thus curing *Aspergillus* infections.

CONCLUSION

AP3 is an IgG that recognizes *Aspergillus* Gal*f*-containing epitopes of four or more residues. It was generated by the immunization of mice with *A. parasiticus* CWFs and the subsequent production of hybridoma lines. The epitope detected by mAb AP3 is present in fungal-type GM and *O*-linked glycans on several *Aspergillus* glycoproteins. The carbohydrate specificity of AP3 was assessed using a thematic glycoarray comprising a series of synthetic oligosaccharide ligands structurally related to *Aspergillus* GM. Our data suggest that AP3 recognizes a β-1,5 Gal*f* tetramer that differs from the epitopes recognized by other GM/Gal*f*-specific mAbs. However, AP3 can also cooperate with other Gal*f*-specific mAbs to identify secreted GM and cell wall-associated glycoproteins in *Aspergillus* detection assays. In this context, AP3 could be developed as a valuable tool for *Aspergillus* cell wall and protein glycosylation studies, to screen crops for *Aspergillus* infection, and to diagnose IA with a lower risk of false positives.

DATA AVAILABILITY

The raw data supporting the conclusions of this manuscript will be made available by the authors, without undue reservation, to any qualified researcher.

ETHICS STATEMENT

All animal experiments were approved by the Landesamt für Natur, Umwelt und Verbraucherschutz Nordrhein-Westfalen (LANUV), reference number 8.87.-51.05.30.10.077. All animals received humane care according to the requirements of the German Tierschutzgesetz, §8 Abs. 1 and the Guide for the Care and Use of Laboratory Animals published by the National Institutes of Health.

AUTHOR CONTRIBUTIONS

MS, SS, GN, NN, and FE contributed to the conception and design of the study. MS, SX, AV, IC, VK, and NN performed the research and analyzed data. MS, SX, and AV helped with microscopy and ELISA experiments. IC and SX contributed with the 2DE experiments and mass spectrometry. VK and NN performed the glycoarray analysis. NN, FE, GN, and SS acquired funding. MS, SX, and NN prepared the original draft. All authors contributed to manuscript revision, read, and approved the submitted version.

FUNDING

This work was funded by the Sino-German (CSC-DAAD) Postdoc Scholarship Program, Russian Science Foundation (grant 19-73-30017), and BMBF grant no. FKZ 031A284A, FKZ 50739422, and FKZ 54364828.

ACKNOWLEDGMENTS

We would like to thank Denise Herwartz, Katrin Hauten, and Dr. Nicole Raven for the production and maintenance of the hybridoma cell line AP3 and Dr. Stefan Rasche for the purification of mAb AP3. We were grateful to Marcel Houdelet, Matthias Berens, and Tannaz Goodarzi for the production of recombinant *Aspergillus* catalase and the testing of mAb AP3, Dr. Françoise Routier for the Δ*glfA* mutant, and Dr. Richard M. Twyman for editorial assistance.

SUPPLEMENTARY MATERIAL

The Supplementary Material for this article can be found online at: https://www.frontiersin.org/articles/10.3389/fcimb.2019.00234/full#supplementary-material

REFERENCES

Argunov, D. A., Krylov, V. B., and Nifantiev, N. E. (2015). Convergent synthesis of isomeric heterosaccharides related to the fragments of galactomannan from *Aspergillus fumigatus*. *Org. Biomol. Chem*. 13, 3255–3267. doi: 10.1039/c4ob02634a

Argunov, D. A., Krylov, V. B., and Nifantiev, N. E. (2016). The use of pyranoside-into-furanoside rearrangement and controlled o(5) –> o(6) benzoyl migration as the basis of a synthetic strategy to assemble (1–>5)- and (1–>6)-linked galactofuranosyl chains. *Org. Lett*. 18, 5504–5507. doi: 10.1021/acs.orglett.6b02735

Aubry, A., Porcher, R., Bottero, J., Touratier, S., Leblanc, T., Brethon, B., et al. (2006). Occurrence and kinetics of false-positive *Aspergillus* galactomannan test results following treatment with β-lactam antibiotics in patients with hematological disorders. *J. Clin. Microbiol*. 44, 389–394. doi: 10.1128/JCM.44.2.389-394.2006

Bernard, M., and Latgé, J.-P. (2001). *Aspergillus fumigatus* cell wall: composition and biosynthesis. *Med. Mycol*. 39, 9–17. doi: 10.1080/mmy.39.1.9.17

Biesebeke, R. T., and Record, E. (2008). Scientific advances with *Aspergillus* species that are used for food and biotech applications. *Microbes Environ*. 23, 177–181. doi: 10.1264/jsme2.23.177

Bruneau, J. M., Magnin, T., Tagat, E., Legrand, R., Bernard, M., Diaquin, M., et al. (2001). Proteome analysis of *Aspergillus fumigatus* identifies glycosylphosphatidylinositol-anchored proteins associated to the cell wall biosynthesis. *Electrophoresis* 22, 2812–2823. doi: 10.1002/1522-2683(200108)22:13<2812::aid-elps2812>3.0.co;2-q

Champer, J., Ito, J. I., Clemons, K. V., Stevens, D. A., and Kalkum, M. (2016). Proteomic analysis of pathogenic fungi reveals highly expressed conserved cell wall proteins. *J. Fungi* 2:6. doi: 10.3390/jof2010006

Chan, C. M., Woo, P. C., Leung, A. S., Lau, S. K., Che, X. Y., Cao, L., et al. (2002). Detection of antibodies specific to an antigenic cell wall galactomannoprotein for serodiagnosis of *Aspergillus fumigatus* aspergillosis. *J. Clin. Microbiol*. 40, 2041–2045. doi: 10.1128/JCM.40.6.2041-2045.2002

Chauvin, D., Hust, M., Schütte, M., Chesnay, A., Parent, C., Moreira, G. M. S. G., et al. (2019). Targeting *Aspergillus fumigatus* crf transglycosylases with neutralizing antibody is relevant but not sufficient to erase fungal burden in a neutropenic rat model. *Front. Microbiol*. 10:600. doi: 10.3389/fmicb.2019.00600

Chen, Y. L., Mao, W. J., Tao, H. W., Zhu, W. M., Yan, M. X., Liu, X., et al. (2015). Preparation and characterization of a novel extracellular polysaccharide with antioxidant activity, from the mangrove-associated fungus *Fusarium oxysporum*. *Mar. Biotechnol*. 17, 219–228. doi: 10.1007/s10126-015-9611-6

Chong, K. T., Woo, P. C., Lau, S. K., Huang, Y., and Yuen, K. Y. (2004). AFMP2 encodes a novel immunogenic protein of the antigenic mannoprotein superfamily in *Aspergillus fumigatus*. *J. Clin. Microbiol*. 42, 2287–2291. doi: 10.1128/JCM.42.5.2287-2291.2004

Dalle, F., Charles, P. E., Blanc, K., Caillot, D., Chavanet, P., Dromer, F., et al. (2005). *Cryptococcus neoformans* galactoxylomannan contains an epitope(s) that is cross-reactive with *Aspergillus* galactomannan. *J. Clin. Microbiol.* 43, 2929–2931. doi: 10.1128/jcm.43.6.2929-2931.2005

Di Mambro, T., Guerriero, I., Aurisicchio, L., Magnani, M., and Marra, E. (2019). The yin and yang of current antifungal therapeutic strategies: how can we harness our natural defenses? *Front. Pharmacol.* 10:80. doi: 10.3389/fphar.2019.00080

Fairbanks, G., Steck, T. L., and Wallach, D. F. H. (1971). Electrophoretic analysis of the major polypeptides of the human erythrocyte membrane. *Biochemistry* 10, 2606–2617. doi: 10.1021/bi00789a030

Gazendam, R. P., Van Hamme, J. L., Tool, A. T., Hoogenboezem, M., Van Den Berg, J. M., Prins, J. M., et al. (2016). Human neutrophils use different mechanisms to kill *Aspergillus fumigatus* conidia and hyphae: evidence from phagocyte defects. *J. Immunol.* 196, 1272–1283. doi: 10.4049/jimmunol.1501811

Hao, W., Pan, Y.-X., Ding, Y.-Q., Xiao, S., Yin, K., Wang, Y.-D., et al. (2008). Well-characterized monoclonal antibodies against cell wall antigen of *Aspergillus* species improve immunoassay specificity and sensitivity. *Clin. Vaccine Immunol.* 15, 194–202. doi: 10.1128/CVI.00362-07

Hedayati, M. T., Pasqualotto, A. C., Warn, P. A., Bowyer, P., and Denning, D. W. (2007). *Aspergillus flavus*: human pathogen, allergen and mycotoxin producer. *Microbiology* 153, 1677–1692. doi: 10.1099/mic.0.2007/007641-0

Heesemann, L., Kotz, A., Echtenacher, B., Broniszewska, M., Routier, F., Hoffmann, P., et al. (2011). Studies on galactofuranose-containing glycostructures of the pathogenic mold *Aspergillus fumigatus*. *Int. J. Med. Microbiol.* 301, 523–530. doi: 10.1016/j.ijmm.2011.02.003

Horn, R., Chudobova, I., Hansel, U., Herwartz, D., Koskull-Doring, P., and Schillberg, S. (2013). Simultaneous treatment with tebuconazole and abscisic acid induces drought and salinity stress tolerance in *Arabidopsis thaliana* by maintaining key plastid protein levels. *J. Proteome. Res.* 12, 1266–1281. doi: 10.1021/pr300931u

Imanaka, H., Tanaka, S., Feng, B., Imamura, K., and Nakanishi, K. (2010). Cultivation characteristics and gene expression profiles of *Aspergillus oryzae* by membrane-surface liquid culture, shaking-flask culture, and agar-plate culture. *J. Biosci. Bioeng.* 109, 267–273. doi: 10.1016/j.jbiosc.2009.09.004

Komachi, Y., Hatakeyama, S., Motomatsu, H., Futagami, T., Kizjakina, K., Sobrado, P., et al. (2013). GfsA encodes a novel galactofuranosyltransferase involved in biosynthesis of galactofuranose antigen of *O*-glycan in *Aspergillus nidulans* and *Aspergillus fumigatus*. *Mol. Microbiol.* 90, 1054–1073. doi: 10.1111/mmi.12416

Krishnan, S., Manavathu, E. K., and Chandrasekar, P. H. (2009). *Aspergillus flavus*: an emerging non-fumigatus *Aspergillus* species of significance. *Mycoses* 52, 206–222. doi: 10.1111/j.1439-0507.2008.01642.x

Krylov, V. B., Argunov, D. A., Solovev, A. S., Petruk, M. I., Gerbst, A. G., Dmitrenok, A. S., et al. (2018a). Synthesis of oligosaccharides related to galactomannans from *Aspergillus fumigatus* and their NMR spectral data. *Org. Biomol. Chem.* 16, 1188–1199. doi: 10.1039/c7ob02734f

Krylov, V. B., Petruk, M. I., Grigoryev, I. V., Lebedin, Y. S., Glushko, N. I., Khaldeeva, E. V., et al. (2018b). Study of the carbohydrate specificity of antibodies against *Aspergillus fumigatus* using the library of synthetic mycoantigens. *Russ. J. Bioorg. Chem.* 44, 80–89. doi: 10.1134/s1068162017060073

Krylov, V. B., Solovev, A. S., Argunov, D. A., Latgé, J.-P., and Nifantiev, N. E. (2019). Reinvestigation of carbohydrate specificity of EB-A2 monoclonal antibody used in the immune detection of *Aspergillus fumigatus* galactomannan. *Heliyon* 5:e01173. doi: 10.1016/j.heliyon.2019.e01173

Kudoh, A., Okawa, Y., and Shibata, N. (2015). Significant structural change in both *O*- and *N*-linked carbohydrate moieties of the antigenic galactomannan from *Aspergillus fumigatus* grown under different culture conditions. *Glycobiology* 25, 74–87. doi: 10.1093/glycob/cwu091

Kumar, A., and Shukla, P. K. (2015). A monoclonal antibody against glycoproteins of *Aspergillus fumigatus* shows anti-adhesive potential. *Microb. Pathog.* 79, 24–30. doi: 10.1016/j.micpath.2015.01.003

Kurup, V. P., and Banerjee, B. (2000). Fungal allergens and peptide epitopes. *Peptides* 21, 589–599. doi: 10.1016/S0196-9781(00)00181-9

Lamoth, F., Juvvadi, P. R., Fortwendel, J. R., and Steinbach, W. J. (2012). Heat shock protein 90 is required for conidiation and cell wall integrity in *Aspergillus fumigatus*. *Eukaryot. Cell.* 11, 1324–1332. doi: 10.1128/EC.00032-12

Lamoth, F., Juvvadi, P. R., Gehrke, C., Asfaw, Y. G., and Steinbach, W. J. (2014). Transcriptional activation of heat shock protein 90 mediated via a proximal promoter region as trigger of caspofungin resistance in *Aspergillus fumigatus*. *J. Infect. Dis.* 209, 473–481. doi: 10.1093/infdis/jit530

Lamoth, F., Juvvadi, P. R., and Steinbach, W. J. (2016). Heat shock protein 90 (Hsp90): a novel antifungal target against *Aspergillus fumigatus*. *Crit. Rev. Microbiol.* 42, 310–321. doi: 10.3109/1040841x.2014.947239

Latge, J. P. (2009). Galactofuranose containing molecules in *Aspergillus fumigatus*. *Med. Mycol.* 47, S104–S109. doi: 10.1080/13693780802258832

Latge, J. P., Kobayashi, H., Debeaupuis, J. P., Diaquin, M., Sarfati, J., Wieruszeski, J. M., et al. (1994). Chemical and immunological characterization of the extracellular galactomannan of *Aspergillus fumigatus*. *Infect. Immun.* 62, 5424–5433.

Matveev, A. L., Krylov, V. B., Emelyanova, L. A., Solovev, A. S., Khlusevich, Y. A., Baykov, I. K., et al. (2018). Novel mouse monoclonal antibodies specifically recognize *Aspergillus fumigatus* galactomannan. *PLoS ONE* 13:e0193938. doi: 10.1371/journal.pone.0193938

Mennink-Kersten, M. A., Ruegebrink, D., Klont, R. R., Warris, A., Gavini, F., Op den Camp, H. J., et al. (2005). Bifidobacterial lipoglycan as a new cause for false-positive platelia *Aspergillus* enzyme-linked immunosorbent assay reactivity. *J. Clin. Microbiol.* 43, 3925–3931. doi: 10.1128/jcm.43.8.3925-3931.2005

Mouyna, I., Hartl, L., and Latgé, J.-P. (2013). β-1,3-glucan modifying enzymes in *Aspergillus fumigatus*. *Front. Microbiol.* 4:81. doi: 10.3389/fmicb.2013.00081

Paris, S., Wysong, D., Debeaupuis, J.-P., Shibuya, K., Philippe, B., Diamond, R. D., et al. (2003). Catalases of *Aspergillus fumigatus*. *Infect. Immun.* 71, 3551–3562. doi: 10.1128/IAI.71.6.3551-3562.2003

Perfect, J. R., Cox, G. M., Lee, J. Y., Kauffman, C. A., De Repentigny, L., Chapman, S. W., et al. (2001). The impact of culture isolation of *Aspergillus* species: a hospital-based survey of aspergillosis. *Clin. Infect. Dis.* 33, 1824–1833. doi: 10.1086/323900

Pfeiffer, C. D., Fine, J. P., and Safdar, N. (2006). Diagnosis of invasive aspergillosis using a galactomannan assay: a meta-analysis. *Clin. Infect. Dis.* 42, 1417–1727. doi: 10.1086/503427

Pitarch, A., Nombela, C., and Gil, C. (2008). Cell wall fractionation for yeast and fungal proteomics. *Methods Mol. Biol.* 425, 217–239. doi: 10.1007/978-1-60327-210-0_19

Prados-Rosales, R., Luque-Garcia, J. L., Martinez-Lopez, R., Gil, C., and Di Pietro, A. (2009). The *Fusarium oxysporum* cell wall proteome under adhesion-inducing conditions. *Proteomics* 9, 4755–4769. doi: 10.1002/pmic.200800950

Rasche, S., Martin, A., Holzem, A., Fischer, R., Schinkel, H., and Schillberg, S. (2011). One-step protein purification: use of a novel epitope tag for highly efficient detection and purification of recombinant proteins. *Open Biotechnol. J.* 5, 1–6. doi: 10.2174/1874070701105010001

Reichard, U., Buttner, S., Eiffert, H., Staib, F., and Rüchel, R. (1990). Purification and characterisation of an extracellular serine proteinase from *Aspergillus fumigatus* and its detection in tissue. *J. Med. Microbiol.* 33, 243–251.

Robens, J., and Cardwell, K. (2003). The costs of mycotoxin management to the USA: management of aflatoxins in the United States. *Toxin Rev.* 22, 139–152. doi: 10.1081/TXR-120024089

Rolle, A.-M., Hasenberg, M., Thornton, C. R., Solouk-Saran, D., Männ, L., Weski, J., et al. (2016). ImmunoPET/MR imaging allows specific detection of *Aspergillus fumigatus* lung infection *in vivo*. *Proc. Natl Acad. Sci. U.S.A.* 113, E1026–E1033. doi: 10.1073/pnas.1518836113

Samson, R. A., Visagie, C. M., Houbraken, J., Hong, S. B., Hubka, V., Klaassen, C. H. W., et al. (2014). Phylogeny, identification and nomenclature of the genus *Aspergillus*. *Stud. Mycol.* 78, 141–173. doi: 10.1016/j.simyco.2014.07.004

Schmalhorst, P. S., Krappmann, S., Vervecken, W., Rohde, M., Muller, M., Braus, G. H., et al. (2008). Contribution of galactofuranose to the virulence of the opportunistic pathogen *Aspergillus fumigatus*. *Eukaryot. Cell* 7, 1268–1277. doi: 10.1128/ec.00109-08

Schubert, M., Spiegel, H., Schillberg, S., and Nölke, G. (2018). *Aspergillus*-specific antibodies–targets and applications. *Biotechnol. Adv.* 36, 1167–1184. doi: 10.1016/j.biotechadv.2018.03.016

Singh, N., and Paterson, D. L. (2005). *Aspergillus* infections in transplant recipients. *Clin. Microbiol. Rev.* 18, 44–69. doi: 10.1128/cmr.18.1.44-69.2005

Sola, R. J., and Gribenow, K. (2009). Effects of glycosylation on the stability of protein pharmaceuticals. *J. Pharm. Sci.* 98, 1223–1245. doi: 10.1002/jps.21504

Spiegel, H., Schinkel, H., Kastilan, R., Dahm, P., Boes, A., Scheuermayer, M., et al. (2015). Optimization of a multi-stage, multi-subunit malaria vaccine candidate for the production in *Pichia pastoris* by the identification and removal of protease cleavage sites. *Biotechnol. Bioeng.* 112, 659–667. doi: 10.1002/bit.25481

Ste-Marie, L., Senechal, S., Boushira, M., Garzon, S., Strykowski, H., Pedneault, L., et al. (1990). Production and characterization of monoclonal antibodies to cell wall antigens of *Aspergillus fumigatus*. *Infect. Immun*. 58, 2105–2114.

Stynen, D., Sarfati, J., Goris, A., Prévost, M. C., Lesourd, M., Kamphuis, H., et al. (1992). Rat monoclonal antibodies against *Aspergillus* galactomannan. *Infect. Immun*. 60, 2237–2245.

Tefsen, B., Ram, A. F., Van Die, I., and Routier, F. H. (2012). Galactofuranose in eukaryotes: aspects of biosynthesis and functional impact. *Glycobiology* 22, 456–469. doi: 10.1093/glycob/cwr144

Teutschbein, J., Albrecht, D., Potsch, M., Guthke, R., Aimanianda, V., Clavaud, C., et al. (2010). Proteome profiling and functional classification of intracellular proteins from conidia of the human-pathogenic mold *Aspergillus fumigatus*. *J. Proteome Res*. 9, 3427–3442. doi: 10.1021/pr9010684

Thornton, C. R. (2008). Development of an immunochromatographic lateral-flow device for rapid serodiagnosis of invasive aspergillosis. *Clin. Vaccine Immunol*. 15, 1095–1105. doi: 10.1128/CVI.00068-08

Thornton, C. R. (2010). Detection of invasive aspergillosis. *Adv. Appl. Microbiol*. 70, 187–216. doi: 10.1016/S0065-2164(10)70006-X

Thornton, C. R., and Wills, O. E. (2015). Immunodetection of fungal and oomycete pathogens: established and emerging threats to human health, animal welfare and global food security. *Crit. Rev. Microbiol*. 41, 27–51. doi: 10.3109/1040841x.2013.788995

Torosantucci, A., Chiani, P., Bromuro, C., De Bernardis, F., Palma, A. S., Liu, Y., et al. (2009). Protection by anti-beta-glucan antibodies is associated with restricted beta-1,3 glucan binding specificity and inhibition of fungal growth and adherence. *PLoS ONE* 4:e5392. doi: 10.1371/journal.pone.0005392

Tortorano, A. M., Esposto, M. C., Prigitano, A., Grancini, A., Ossi, C., Cavanna, C., et al. (2012). Cross-reactivity of *Fusarium* spp. in the *Aspergillus* galactomannan enzyme-linked immunosorbent assay. *J. Clin. Microbiol*. 50, 1051–1053. doi: 10.1128/JCM.05946-11

Unkefer, C. J., and Gander, J. E. (1979). The 5-O-β-D-galactofuranosyl-containing glycopeptide from *Penicillium charlesii*. Carbon 13 nuclear magnetic resonance studies. *J. Biol. Chem*. 254, 12131–12135.

Varki, A., Cummings, R. D., Esko, J. D., Freeze, H. H., Stanley, P., Bertozzi, C. R., et al. (2009). *Essentials of Glycobiology*. Cold Spring Harbor, NY: Cold Spring Harbor Laboratory Press.

Villers, P. (2014). Aflatoxins and safe storage. *Front. Microbiol* 5:158. doi: 10.3389/fmicb.2014.00158

Viscoli, C., Machetti, M., Cappellano, P., Bucci, B., Bruzzi, P., Van Lint, M. T., et al. (2004). False-positive galactomannan Platelia *Aspergillus* test results for patients receiving piperacillin-tazobactam. *Clin. Infect. Dis*. 38, 913–916. doi: 10.1086/382224

Wacoo, A. P., Wendiro, D., Vuzi, P. C., and Hawumba, J. F. (2014). Methods for detection of aflatoxins in agricultural food crops. *J. Appl. Chem*. 2014, 1–15. doi: 10.1155/2014/706291

Walsh, T. J., Anaissie, E. J., Denning, D. W., Herbrecht, R., Kontoyiannis, D. P., Marr, K. A., et al. (2008). Treatment of aspergillosis: clinical practice guidelines of the infectious diseases society of America. *Clin. Infect. Dis*. 46, 327–360. doi: 10.1086/525258

Wiedemann, A., Kakoschke, T. K., Speth, C., Rambach, G., Ensinger, C., Jensen, H. E., et al. (2016). Distinct galactofuranose antigens in the cell wall and culture supernatants as a means to differentiate *Fusarium* from *Aspergillus* species. *Int. J. Med. Microbiol.* 306, 381–390. doi: 10.1016/j.ijmm.2016.05.002

Woo, P. C., Chong, K. T., Leung, A. S., Wong, S. S., Lau, S. K., and Yuen, K. Y. (2003). AFLMP1 encodes an antigenic cel wall protein in *Aspergillus flavus*. *J. Clin. Microbiol*. 41, 845–850. doi: 10.1128/JCM.41.2.845-850.2003

Zandijk, E., Mewis, A., Magerman, K., and Cartuyvels, R. (2008). False-positive results by the Platelia *Aspergillus* galactomannan antigen test for patients treated with amoxicillin-clavulanate. *Clin. Vaccine Immunol*. 15, 1132–1133. doi: 10.1128/cvi.00022-08

Conflict of Interest Statement: The authors declare that the research was conducted in the absence of any commercial or financial relationships that could be construed as a potential conflict of interest.

frontiers in Cellular and Infection Microbiology

ORIGINAL RESEARCH
published: 06 November 2019
doi: 10.3389/fcimb.2019.00365

Definition of the Anti-inflammatory Oligosaccharides Derived From the Galactosaminogalactan (GAG) From *Aspergillus fumigatus*

Markus Gressler[1], Christoph Heddergott[1], Inés C. N'Go[1], Giorgia Renga[2], Vasilis Oikonomou[2], Silvia Moretti[2], Bernadette Coddeville[3], Joana Gaifem[4,5], Ricardo Silvestre[4,5], Luigina Romani[2], Jean-Paul Latgé[1] and Thierry Fontaine[1]**

[1] Unité des Aspergillus, Institut Pasteur, Paris, France, [2] Department of Experimental Medicine, Università degli Studi di Perugia, Perugia, Italy, [3] Unité de Glycobiologie Structurale et Fonctionnelle (UGSF) UMR 8576 CNRS, Université de Lille, Lille, France, [4] Life and Health Sciences Research Institute (ICVS), School of Medicine, University of Minho, Braga, Portugal, [5] ICVS/3B's-PT Government Associate Laboratory, Braga, Portugal

OPEN ACCESS

Edited by:
Laura Alcazar-Fuoli,
Carlos III Health Institute, Spain

Reviewed by:
Jatin Mahesh Vyas,
Massachusetts General Hospital and Harvard Medical School, United States
Hee-Soo Park,
Kyungpook National University, South Korea

***Correspondence:**
Jean-Paul Latgé
jean-paul.latge@pasteur.fr
Thierry Fontaine
thierry.fontaine@pasteur.fr

Specialty section:
This article was submitted to Fungal Pathogenesis, a section of the journal Frontiers in Cellular and Infection Microbiology

Received: 26 August 2019
Accepted: 08 October 2019
Published: 06 November 2019

Citation:
Gressler M, Heddergott C, N'Go IC, Renga G, Oikonomou V, Moretti S, Coddeville B, Gaifem J, Silvestre R, Romani L, Latgé J-P and Fontaine T (2019) Definition of the Anti-inflammatory Oligosaccharides Derived From the Galactosaminogalactan (GAG) From Aspergillus fumigatus. Front. Cell. Infect. Microbiol. 9:365. doi: 10.3389/fcimb.2019.00365

Galactosaminogalactan (GAG) is an insoluble aminosugar polymer produced by *Aspergillus fumigatus* and has anti-inflammatory properties. Here, the minimum glycosidic sequences required for the induction of IL-1Ra by peripheral blood mononuclear cells (PBMCs) was investigated. Using chemical degradation of native GAG to isolate soluble oligomers, we have found that the de-*N*-acetylation of galactosamine residues and the size of oligomer are critical for the *in vitro* immune response. A minimal oligomer size of 20 galactosamine residues is required for the anti-inflammatory response but the presence of galactose residues is not necessary. In a Dextran sulfate induced colitis mouse model, a fraction of de-*N*-acetylated oligomers of $13 < dp < 20$ rescue inflammatory damage like the native GAG polymer in an IL-1Ra dependent pathway. Our results demonstrate the therapeutic suitability of water-soluble GAG oligosaccharides in IL-1 mediated hyper-inflammatory diseases and suggest that α-1,4-galactosamine oligomers chemically synthesized could represent new anti-inflammatory glycodrugs.

Keywords: galactosaminogalactan, *Aspergillus fumigatus*, IL-Ra, anti-inflammatory response, glycodrug

INTRODUCTION

The galactosaminogalactan (GAG) is a polysaccharide produced by the human fungal pathogen, *Aspergillus fumigatus* which is a major virulence factor for this fungal species. GAG mediates the adherence of mycelium to abiotic or host-cell surfaces within biofilm and protects the fungus against host-cell damages (Gravelat et al., 2013; Beaussart et al., 2015; Lee et al., 2015). In mouse model of aspergillosis, *intra-nasally* administration of GAG promotes fungal infection and directly affects the innate immune response resulting in an inhibition of the protective T-helper (Th) 1 and regulatory T cells (Treg) as well as a promotion of Th2 responses (Fontaine et al., 2011). In addition, GAG induces apoptosis in neutrophils (Robinet et al., 2014). GAG did not induce any of the proinflammatory cytokines TNFα, IL-6, IL-8, IFNγ, IL-17, and IL-9 neither the anti-inflammatory cytokine IL-10 (Gresnigt et al., 2014). However, GAG reduced the production of Th cytokines IL-17, IL-22, and IFNγ in *Aspergillus* stimulated PBMCs. Most importantly, GAG inhibits the IL-1 bioactivity by the induction of the production of high amounts of IL-1 receptor

antagonist (IL-1Ra) (Gresnigt et al., 2014). The capacity of GAG to induce IL-1Ra is responsible for its potent anti-inflammatory properties favoring *Aspergillus* infections (Gresnigt et al., 2014). The anti-inflammatory potential of GAG has been also shown in experimental dextran sodium sulfate (DSS)-induced colitis in mice with chronic granulomatous disease (CGD). The intraperitoneal administration of GAG resulted in the improvement of clinical signs of colitis and of inflammatory lesions in both wild-type and CGD mice. The effects of GAG on CGD colitis were similar to those of IL-1Ra administration (Gresnigt et al., 2014), making it a potent alternative to tackle chronic inflammatory diseases.

GAG is a linear heterogeneous high molecular weight polymer with an average size of 100 kDa and it is composed of α-1,4-linked galactopyranose (Gal*p*), α-1,4-linked galactosamine ($GalNH_2$), and α-1,4-linked N-acetylgalactosamine (GalNAc) residues. Monosaccharides are randomly distributed along the chain (Fontaine et al., 2011; Lee et al., 2016). Due to the heterogeneity of the molecule and the absence of clear repeating unit, the oligosaccharides responsible for the immunological functions of GAG are unknown. It has been only shown that the deacetylation of the GAG is essential for the adherence and the virulence of the fungus (Lee et al., 2016). However, the degree of acetylation and the size of the oligosaccharide responsible for the anti-inflammatory properties of GAG were unknown to date. For this purpose, we have isolated water-soluble oligomers that are inducers of IL-1Ra and shown that long water-soluble de-*N*-acetylated galactosamine oligomers of $13 < DP < 20$ rescue inflammatory damage similarly as the GAG polymer in an IL-1Ra dependent pathway.

MATERIALS AND METHODS

Cultivation and GAG Purification

A. fumigatus strain Dal (CBS144-89) was cultivated on malt-agar tubes for 3 days at 37°C. Conidia were collected with 4 ml 0.05% tween20 and vortexing of the tube. The conidia suspension was stored up to 3 weeks at 4°C.

GAG isolation and purification was carried out as previously described (Fontaine et al., 2011). Briefly, 100 ml Brian medium was inoculated with a final concentration of 5×10^5 conidia per ml in 150 ml Erlenmeyer flasks. After cultivation for 3 days at 37°C and 170 rpm, the pooled supernatant of 20 cultures was collected by filtration and was adjusted to pH 3 by addition of 100 µl 12 M HCl per 100 ml supernatant. Two volumes of precooled ethanol (4°C) were added and GAG was precipitated for 3 h at 4°C. The precipitate was collected by centrifugation for 20 min at 5,000 g at 4°C and subsequently washed twice with 1/10 of the culture volume of 100 mM NaCl for 1 h under agitation (100 rpm). GAG was dialyzed against tap water and twice against purified water (24 h each) and finally lyophilized to dryness and stored at ambient temperature.

Chemical Modification of Polysaccharides

De-*N*-Acetylation of Polysaccharides

GAG was suspended in 3 ml of 10 mM HCl at a final concentration of 3.33 mg/ml by sonication in plastic tubes. The de-*N*-acetylation was started by addition of 3.4 ml 18.8 M NaOH and the mixture was incubated at 100°C for up to 4–5 h. The tubes were vortexed every hour. The reaction was stopped on ice and neutralization with 12 M HCl. The mixture was buffered by 20 mM Tris, pH 7. De-*N*-acetylated GAGs (dGAG) were dialyzed against tap water and twice against dH_20 (24 h each) and finally lyophilized to dryness and stored at ambient temperature.

Acetylation of Oligosaccharides

The acetylation procedure described by Lavertu et al. (2012) was modified as following: 0.5 mg dGAG oligosaccharides (F-I and F-III) were lyophilized to dryness and were solved in 25 µl of 400 mM acetic acid and 100 µl CH_3OH. The mixture was preincubated for 1 h at ambient temperature under agitation at 300 rpm. Acetylation was initiated by addition 3 µl acetic anhydride. After 1 h of incubation, solvents were evaporated in a desiccator overnight. The samples were desalted by repeated dissolution with 500 µl water (4 times) followed by evaporation to dryness. Samples were solved in 500 µl water and finally stored at −20°C.

Production of GAG Oligosaccharides

De-*N*-acetylated GAG (dGAG) was hydrolyzed by 2 M HCl at 100°C for 1.5, 3, and 4.5 h. Preliminary assays showed that 1.5 and 3 h were optimal for generating oligosaccharides of different sizes (DP 3–26). HCl was immediately evaporated after hydrolysis by drying the oligosaccharide mixture overnight under vacuum in presence of NaOH pellets. Soluble oligosaccharides were dissolved in 1 ml of 150 mM ammonium acetate, pH 4.5 and unsolved particles were removed by centrifugation (3 min, 17,000 g). The oligosaccharides were subjected to size exclusion chromatography (SEC) on a Superdex 30 column (GE Healthcare, 10 × 750 mm) equilibrated with 150 mM ammonium acetate, pH 4.5 as described (Hamer et al., 2015). The oligosaccharides were separated at a flow rate of 0.5 ml/min and detected by the Gilson 132 RI detector. The osamine amount of each fraction was determined by 3-methyl-2-benzothiazolinon hydrazone hydrochloride hydrate assay (MBTH, see below). In total eight 8 ml-fractions were obtained by pooling four 2 ml-fractions per gel permeation assays and were named as F-I to F-VIII (**Figure S1**). The fractions were desalted by lyophilization for 2–3 days, addition of 1 ml water and subsequent second lyophilization overnight in a Savant speed vac concentrator. The samples were resolved in 400 µl water and stored at −20°C.

Analytical Procedures

MBTH Assay

De-*N*-acetylated osamines were detected and quantified by the MBTH assay (Plassard et al., 1982). The procedure was carried out in a 96 well plate (Sarstedt): 40 µl sample (containing up to 200 µg osamines/ml) were mixed with 40 µl 5 % $KHSO_4$ (Sigma Aldrich). The samples were reduced by addition of 40 µl 5% $NaNO_2$ (Sigma Aldrich) for 60 min at 50°C, whereby 40 µl 5% NaCl were used as negative control. After neutralization with 40 µl 12.5% $NH_4SO_2NH_2$ (Sigma Aldrich) (ambient temperature, 30 rpm, 10 min), 40 µl 0.5% 3-Methyl-2-benzothiazolinon hydrazine hydrochloride hydrate (Sigma Aldrich) was added.

The covered plate was incubated at 37°C for 30 min. Finally, 40 µl 0.5% $FeCl_3$ was added and the absorption at $\lambda = 650$ nm was measured by the Tecan infinite M200Pro ELISA plate reader, while $\lambda = 800$ nm served as a reference wavelength. A calibration curve of a serial dilution of D-galactosamine (GalN) served as reference. To quantify the total amount of osamine or the degree of acetylation (DA), a hydrolysis step was performed prior the MBTH assay. Samples were totally hydrolyzed by 4 M HCl at 100°C for 4 h and subsequently dried overnight in a desiccator.

Acetate Assay

The DA was also estimated by the enzymatic acetate assay. Samples (220 µl) were totally hydrolyzed by addition of 100 µl 12 M HCl (100°C, 4 h). Then, 100 µl were used for the osamine detection by MBTH assay as described above and another 100 µl were used for the acetate assay. After neutralization by addition of 75 µl 7 M NaOH and 75 µl 2 M MOPS (pH 7.5), samples were subjected to the Acetate Colorimetric Assay (Sigma-Aldrich) according the manufacturer's protocol. The absorption at $\lambda = 450$ nm was measured by the Tecan infinite M200Pro ELISA plate reader, while $\lambda = 700$ nm served as a reference wavelength. The acetate content in the hydrolyzed samples was determined by a calibration curve of 0.25–1.5 mM acetate standard solution.

Monosaccharide Identification and Quantification by Gas Chromatography

Samples (100 µg) were hydrolyzed in 500 µl 8 M HCl for hexosamine analysis or 4 M TFA for hexose analysis. *Meso*-inositol (4 µg) was used as internal standard and 50 µg Gal, GalNAc, and GlcNAc as external standards. After hydrolysis, reduction with BH_4Na and acetylation samples were analyzed by GC on a Perichrom PR2100 instrument with a flame ionization detector using a capillary column (30 m × 0.32 mm) filled with a DB-1 (SGE) as described previously (Fontaine et al., 2011).

Enzymatic Degradation of GAG Fractions

Production of a Recombinant Endo-α-1,4-Galactosaminidase

For the enzymatic degradation of GAG, a poly-GalN hydrolase of *Pseudomonas sp.* (Tamura et al., 1988), here named GAGnase, was produced in *Escherichia coli*. Prior to the total synthesis of the gene, the DNA sequence was codon-optimized for expression in *E. coli*. In addition, a histidine tag was added to the carboxyl terminus to facilitate subsequent purification (**Figure S2**). The gene was cloned into the pET28a (+) expression vector and transformed into the *E. coli* BL21 Gold expression strain. A culture in the exponential growth phase was induced with 1 mM IPTG (final concentration), followed by production for 4 h at 30°C. The protein could be found in the culture supernatant (it contains a signal of bacterial secretion), the cytoplasm and in the inclusion bodies. The enzyme present in the supernatant was purified using ProBond™ Nickel-chelating agarose beads (ThermoFisher) (ratio 0.5 ml beads/50 ml supernatant) (**Figure S2**). The final preparation was kept in a 20 mM HEPES buffer pH 7.4, 137 mM NaCl and stored in aliquots at −20°C.

Enzymatic Degradation of Oligosaccharides

The enzymatic hydrolysis of GAG was carried out as previously described (Tamura et al., 1992). In brief, 5 mg/ml GAG/dGAG or 1 mg/ml GAG oligosaccharides were dissolved in 50 mM NaAc, pH 6.0. The reaction (100 µl scale) was started by addition of 2 µg/ml GAGnase and further incubated for 2 h at 37°C. The GAGnase was quickly heat-inactivated (100°C, 5 min) and the degradation efficiency was estimated by the sugar reducing end assay using the PABA as reagent (Lever, 1972).

MALDI-TOF Mass Spectrometry

MALDI-TOF spectra were analyzed in reflectron positive mode using a 4800 TOF/TOF spectrometer (Applied Biosystems, Framingham, MA, USA) equipped with a pulsed nitrogen laser (337 nm and frequency of 200 Hz). An average of 5,000 shots per spot was used for MS data acquisition. Samples were prepared by mixing directly on the target 0.5 µl of oligosaccharide solution in water (10–50 pmol) with 0.5 µl of 2,5-dihydroxybenzoic acid matrix solution (10 mg/ml in CH_3OH/H_2O, 50:50, V/V). The samples were dried at room temperature.

Isolation of Peripheral Blood Mononuclear Cells (PBMC)

Blood samples from healthy donors were obtained from Etablissement Français du Sang Saint-Louis (Paris, France) with written informed consent as per the guidelines provided by the Institutional Ethics Committee, Institut Pasteur (convention 12/EFS/023). Human blood sample from healthy patients was diluted 1:1 with PBS (Gibco). In a 50 ml falcon tube, 15 ml of lymphocytes separation medium (Eurobio) were slowly overlaid by 30 ml of the blood dilution. The cells were separated by centrifugation at ambient temperature (20 min, 1800 rpm). The upper phase (buffer and plasma) was discarded and the PBMCs (2–5 ml) were collected. The cells were washed by addition of 40 ml PBS and subsequent centrifugation at ambient temperature (10 min, 1,500 rpm). The wash step was repeated (30 ml PBS; 10 min, 1200 rpm). The cells were finally suspended in 10–20 ml RPMI 1640 + Glutamax-I (Gibco) and counted in a hemocytometer (c-Chip DHC-M01; Digital Bio). The cells were finally diluted to a concentration of 1×10^7 cells/ml in RPMI and stored on ice.

Detection of Interleukin Production in PBMCs by Enzyme-Linked Immunosorbent Assay (ELISA)

PMBCs were seeded in a final concentration of 5×10^5 cells in 200 µl RPMI 1640 + Glutamax-I supplemented with 10% human serum in a U-shape 96 well plate. Native and de-*N*-acetylated GAGs were tested in a final concentration 0.5, 1, and 5 µg/ml (according to the MBTH assay). All de-*N*-acetylated and per-*N*-acetylated oligosaccharides have been tested in a final concentration of 1, 5, 10, and 25 µg/ml. Lipopolysaccharides (LPS) from *E. coli* (10 ng/ml; SIGMA) served as positive control. The cells were stimulated by GAGs, oligosaccharides or LPS for 24 h at 37°C, 5% CO_2. The plates were centrifuged at ambient temperature (200 g, 3 min) and the supernatants were collected.

Supernatants were stored at −20°C upon use. Experiments were carried out with five different batches of GAG and GAG-oligosaccharides with a minimum of four blood donors. The detection of IL-1Ra in the supernatants was carried out using the DuoSet ELISA Kits (R&D Systems) according to the manufacturers' protocol. The supernatants were tested in a final dilution of 1:33. The absorption at $\lambda = 450$ nm was measured by the Tecan infinite M200Pro ELISA plate reader, while $\lambda = 570$ nm served as a reference wavelength. In order to take variable donor-dependent cytokine levels into account, induction by GAG and GAG oligosaccharides were calculated as ratios to induction by LPS: Cytokine levels induced by 10 ng/ml LPS were set to 100% in each biological replicate and cytokine levels by GAG or GAG oligosaccharides were estimated accordingly.

Detection of Cytotoxicity by Lactate Dehydrogenase (LDH) Assay

Putative cytotoxicity of GAGs and GAG oligosaccharide was estimated as LDH release from PBMCs. PMBCs were seeded in a final concentration of 5×10^5 cells in 200 µl RPMI 1640 + Glutamax-I supplemented with 10% human serum in a U-shape 96 well plate. GAGs and oligosaccharides were tested in a final concentration 1.0 and 5.0 µg/ml (amount according to MBTH assay of hydrolyzed samples). Lipopolysaccharides (LPS) from *E. coli* (10 ng/ml; SIGMA) served as negative control. Totally lysed cells TritonX100 served as positive control and reference. All supernatants were 1:5 diluted in PBS + 1% BSA (positive control 1:20) and LDH assay was carried out by the LDH Cytotoxicity Detection Kit (Roche) according to the manufacturer's protocol. None of these oligosaccharides were toxic to PBMCs (**Figure S3**), showing that IL-1Ra secretion was not associated to cell apoptosis or necrosis.

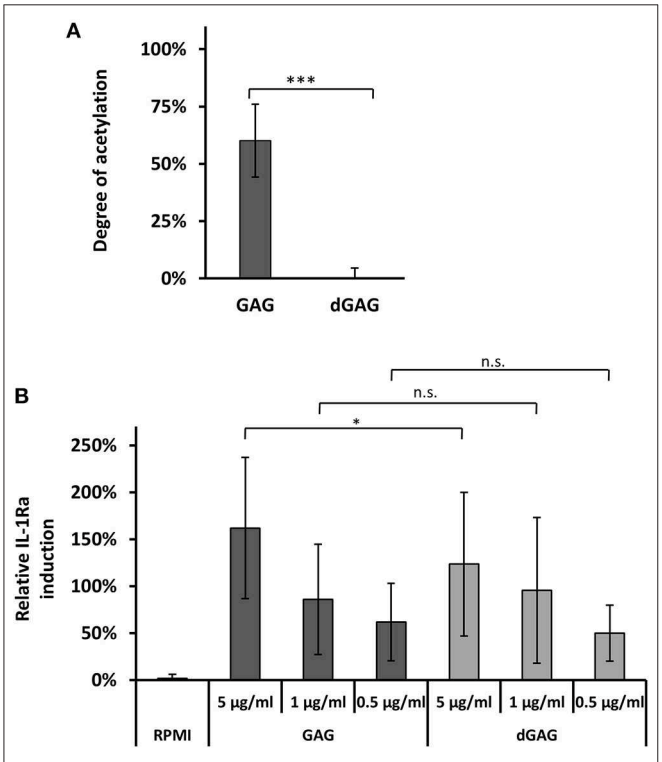

FIGURE 1 | De-*N*-acetylation of GAG. Degree of acetylation (DA) of GAGs **(A)**. DA was determined by an acetate assay (GAG, native polymer; dGAG, de-N-acetylated) **(B)**. *In vitro* IL-1Ra secretion in PBMC supernatants in presence of GAG. LPS (10 ng/ml) served as external standard and were set to 100% in each biological replicate. Statistical analysis by WMW test in comparison to GAG: ns, non significative; $^*p < 0.05$; $^{***}p < 0.001$.

GAG and Oligo-GAG Application in DSS-Treated Mice

DSS (Dextran sulfate sodium, 2.5% wt/vol, 36,000–50,000 kDa; MP Biomedicals) was administered in drinking water *ad libitum* for 7 days. Fresh solution was replaced on day 3. Mice were injected intraperitoneally with 1 mg/kg of GAG samples for 7 consecutive days after DSS treatment. Weight loss, stool consistency, and fecal blood were recorded daily. Upon necropsy, tissues were collected for histology and cytokine analysis. Colonic sections were stained with hematoxylin/eosin. Colitis disease activity index was calculated daily for each mouse based on weight loss, occult blood, and stool consistency. A score of 1–4 was given for each parameter as in McNamee et al. (2011) To evaluate cytokine production, colons, opened longitudinally and washed in complete medium with antibiotics, were cultured at 37°C for 24 h in RPMI and 5% FBS. The supernatants were collected for ELISA and the remaining colonic explant tissue was homogenized and used for protein quantification (Quant-iT Protein Assay Kit, Life Technologies). The concentration of secreted cytokines in the supernatant was subsequently normalized to total tissue protein and expressed as picogram of cytokine per microgram of tissue. TNF-α, IL-1β, IL-17A, IL-17F, IL-10, and IL-1Ra were measured in culture supernatants of 24 h cultures using commercially available ELISAs (R&D systems) according to the protocols supplied by the manufacturer.

STATISTICAL ANALYSIS

All experiments were performed with at least five different batches of GAG and oligosaccharides and a minimum of four blood donors. All statistics of *in vitro* experiments were carried out with a two-tailed unpaired Wilcoxon–Mann–Whitney Test by the free-of-charge software EDISON-WMW (Marx et al., 2016). Statistical analyses from *in vivo* experiments (**Figure 5**) were performed with one- or two-way ANOVA. Data, from one experiment using 10 mice/group, were expressed as mean ± SD and were analyzed in triplicate using GraphPad Prism Software. *P* values are indicated by asterisk as follows: $^*p < 0.05$; $^{**}p < 0.01$; $^{***}p < 0.001$.

ETHICAL STATEMENT

Murine experiments were performed according to the Italian Approved Animal Welfare Authorization 360/2015-PR and Legislative degree 26/2014 regarding the animal license obtained by the Italian Ministry of Health lasting for five years(2015-2020).

RESULTS

Soluble Long α-1,4-Galactosamine Oligomers (DP > 20) From GAG Induce IL-1Ra on PBMCs

Whole GAG fractions, isolated from Brian culture supernatant of *A. fumigatus*, were composed of galactose, galactosamine, and *N*-acetylgalactosamine residues. A degree of acetylation (DA) of galactosamine was determined to be 66 ± 7%, which is in agreement with previous observations (Lee et al., 2016). To further investigate the impact of the DA on IL-1Ra induction, the GAG polymer was de-*N*-acetylated by a harsh alkali treatment (4 h, 100°C, 10 M NaOH) (No and Meyers, 1989) to produce a fully de-*N*-acetylated GAG (dGAG). GC analysis of monosaccharide revealed that the galactose content in native GAG (%Gal 8.3 ± 0.2%) was slightly reduced in dGAG (2.3 ± 2.0%) (**Figure S1**). Both native GAG and dGAG induced IL-1Ra in a concentration dependent manner to similar extent (**Figure 1**). To produce and isolate soluble oligosaccharides of different size, dGAG was hydrolyzed in 2 M HCl for 1.5, 3, or 4.5 h at 100°C. After the removal of acid by under vacuum, water-soluble oligomers were recovered by centrifugation and separated by size exclusion chromatography (SEC) on a Superdex 30 column (**Figure S1**). While 1.5 h hydrolysis mainly resulted in the production of larger oligosaccharides, 3 and 4.5 h hydrolysis times induced the release of small-size oligosaccharides. Resulting of pooled oligomer fractions from the three hydrolysates (fractions I-VIII) were analyzed by MALDI-MS and GC (**Figures S1, S4** and **Figure 2A**). Fractions V till VII contained oligosaccharides till DP10 with the presence of GalN and Gal residues and traces of glucose. Fractions II to IV were characterized by higher MW oligosaccharides till DP26 containing only GalN residues (**Figure 2A** and **Figure S4**). Fraction I, composed also exclusively of GalN residues did not give any ion peak by MALDI-TOF showing that this fraction contained larger oligosaccharides (dp > 26). All these 8 fractions were tested as putative IL-1Ra inducers (**Figure 2B**). Oligomers of dp < 13 (Fractions IV to VIII) did not induce IL-1Ra expression at the tested concentrations. A moderate activation was observed for fraction III (13 < dp < 20) at the concentration

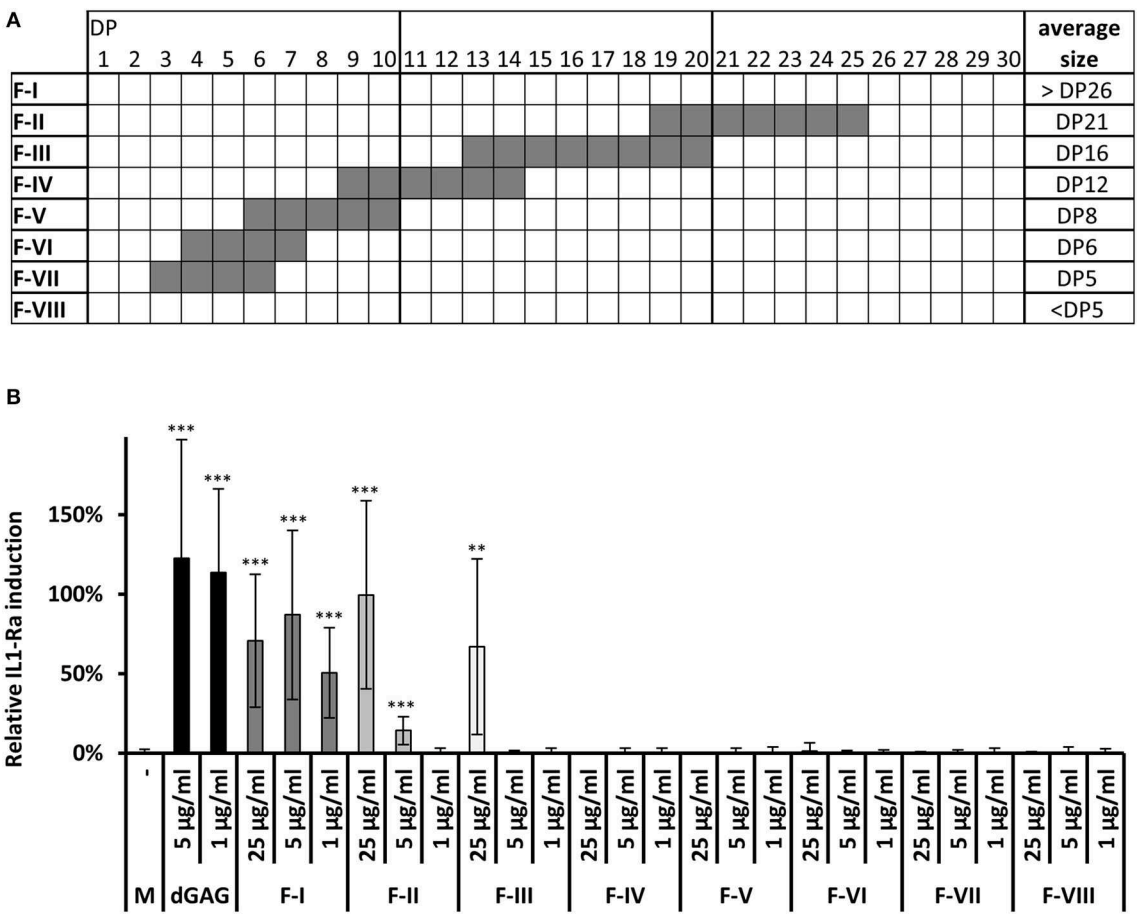

FIGURE 2 | Chemical analysis and IL-1Ra inducing activity of oligosaccharides generated by acid hydrolysis of dGAG. **(A)** Summerized MALDI-TOF MS analysis of fractions I-VIII. (DP, degree of polymerization; for detailed MS spectra see **Figure S2**). **(B)** IL-1Ra production by dGAG oligosaccharides. dGAG oligosaccharides fractions I-VIII were tested at 25, 5, and 1 µg/ml. dGAG (5 and 1 µg/ml) served as positive control. LPS (10 ng/ml) served as external standard and were set to 100% in each biological replicate. Wilcoxon-Mann-Whitney Test: $^{**}p < 0.01$; $^{***}p < 0.001$ (compared to control, M).

of 25 μg/ml, but not at lower concentration (5 and 1 μg/ml). Fractions I and II stimulated IL-1Ra production at 1 and 5 μg/ml, showing that galactose-free, de-*N*-acetylated oligosaccharides are potential inducers. Fraction I induced IL-1Ra production at a similar extend as the GAG native polymer showing that larger were the soluble GalN oligosaccharides better was the production of IL-1Ra.

Fractions I and II were subjected to an enzymatic degradation with a recombinant endo-α-1,4-polygalactosaminidase (GAGnase) from *Pseudomonas sp.* (see material and methods for the production of the recombinant enzyme and **Figure S2**), which specially hydrolyzed α-1,4-linked GalN polymers to release GalN oligomers of DP 2 and 3, but does not use poly-*N*-acetyl-galactosamine or other polysaccharides as substrate (Tamura et al., 1988, 1992). Fractions I and II were degraded by the recombinant GAGnase as determined by the release of reducing ends (**Figure 3A**). Moreover, the hydrolyzed fractions lost their ability to induce IL-1Ra secretion in PBMCs, showing that only long α-1,4-GalN oligomers are inducers (**Figure 3B**). The GAGnase protein neither activates nor inhibits IL-1Ra expression at the desired concentration (**Figure 3C**).

Deacetylation of Galactosamine Oligomers Is Essential to Induce the Production of IL-1Ra

To test the impact of acetylation of GAG-oligosaccharides on PBMC stimulation, GalN oligomers (fraction I to III) were *N*-acetylated by acetic anhydride. After the acetylation procedure, the per-*N*-acetylation and the absence of degradation by GAGnase were confirmed by acetate assays (**Figure 4A**) and MALDI-TOF-MS (**Figure S5**). A water-insoluble material was observed in fractions I and II and but not in fraction III, showing a decrease of solubility for the larger *N*-acetylated oligomers. Most importantly, per-*N*-acetylated fractions I and II have lost their capability to induce IL-1Ra (**Figure 4B**). A slight induction of IL-1Ra was seen with the insoluble re-*N*-acetylated fraction I which may be due to the presence of insoluble particles which can induce unspecifically cytokine production (Becker et al., 2016). Taking together, our data provided evidence that soluble large GalN oligomers specifically triggered the IL-1Ra induction *in vitro*.

Soluble Long De-*N*-Acetylated GAG Oligomers Ameliorate Colitis in Dextran Sulfate Sodium (DSS)-Treated Mice

To test the *in vivo* immunosuppressive potential of GAG derivates, oligomers were tested in the experimental dextran sulfate sodium (DSS)-induced colitis model in C57BL/6 mice (Gresnigt et al., 2014). DSS treated mice lost over 25% body weight, showed a reduced survival, an elevated DAI (disease activity index) and colonic injury observed by macroscopic imaging. Fractions I (>dp26) and III (13 < dp < 20) as well as their *N*-acetylated counterparts have been injected to DSS-treated mice (**Figure 5**). Intraperitoneal injections of both versions of F-I led to ameliorating the clinical signs of colitis by increasing

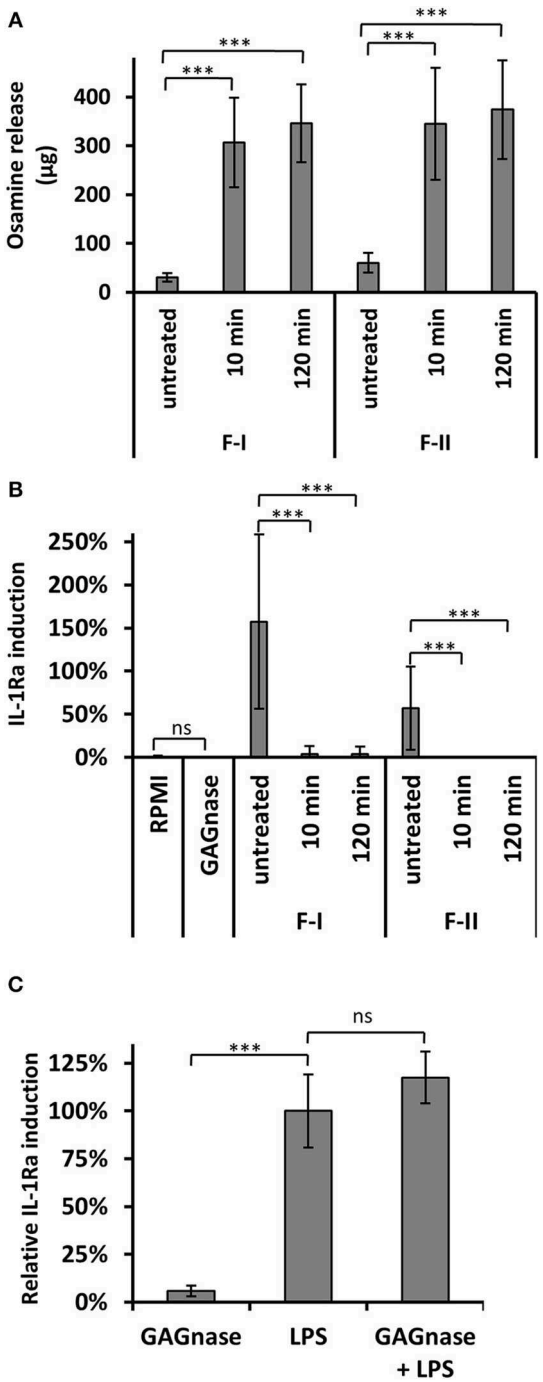

FIGURE 3 | IL-1Ra stimulation by GAG oligomers is abolished by GAGnase. **(A)** Fraction F-I and F-II are degraded by GAGnase. Fractions I and II (500 μg/ml) were enzymatically hydrolyzed by GAGnase (2 μg/ml) for 10 or 120 min or were kept in acetate buffer for 120 min (untreated). The degradation was followed by PABA assay to quantify sugar reducing end. **(B)** Induction of IL1-Ra expression in PBMCs by GAGnase treated fractions. **(C)** IL-1Ra induction of PBMCs in presence of GAGnase (20 ng/μl). GAGnase neither activate nor inhibit induction. LPS (10 ng/ml) served as reference control and were set to 100% in each biological replicate. bars indicate the SD, WMW Test: ***$p < 0.001$; ns, not significant (compared to control samples).

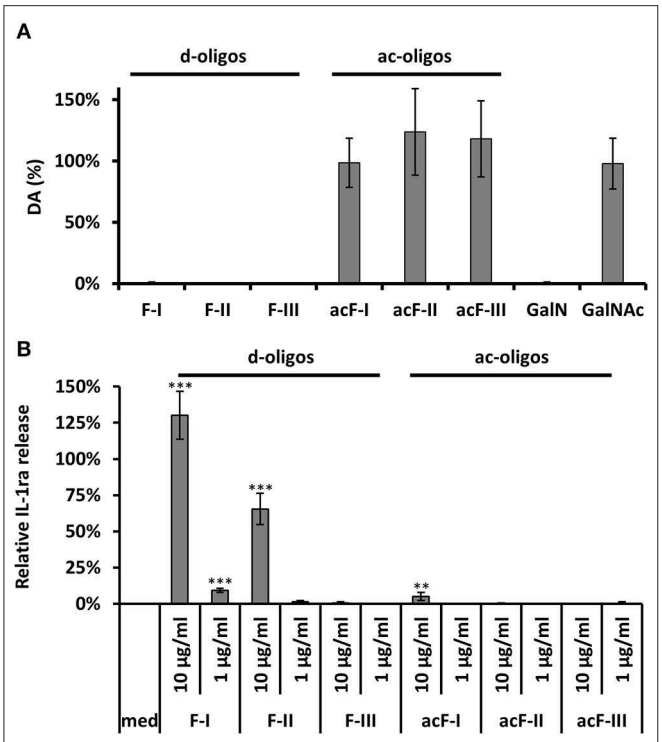

FIGURE 4 | *N*-acetylation of de-*N*-acetylated GAG oligosaccharides and its impact on the IL-1Ra production. **(A)** Determination of the degree of acetylation (DA) by acetate assay of de-*N*-acetylated and acetylated fractions I, II and III. GalN and GalNAc served as positive and negative controls. **(B)** *In vitro* IL-1Ra production by de-*N*-acetylated and acetylated GAG fractions I, II, and III (10 and 1 μg/ml). LPS (10 ng/ml) served as positive control. WMW Test: $^{**}p < 0.01$, $^{***}p < 0.001$.

animal survival, reducing weight loss and DAI (**Figure 5A**), colon size and histological alterations showing the amelioration of colonic injury (**Figure 5**). Cytokine profile, such as a decrease of IL-17A and IL-17F and increase of IL-1Ra, showed that the deacetylated version (F-I) rescued DSS treated mice in a similar way as the whole GAG polymer. In addition, F-I also promoted IL-10, a cytokine known to be protective in colitis because IL-10-deficient mice spontaneously develop enterocolitis and colon cancer (Wang et al., 2015). The per-*N*-acetylated fraction I (acF-I) did not induce IL-1Ra, suggesting that *N*-acetylated F-I has a beneficial effect through an IL-1Ra independent pathway. Acetylated and de-*N*-acetylated smaller oligosaccharides (acF-III and F-III) showed opposite effects *in vivo*. IP injection of F-III rescued the mice from death and the weight loss, ameliorated DAI and strongly reduced inflammatory lesions (**Figure 5**). At the cytokine level, F-III induced a similar pattern of cytokine secretion as F-I with a decrease of pro-inflammatory cytokine and increase of anti-inflammatory interleukins such as IL-10 and IL-1Ra (**Figure 5D**). Since F-III was a poor IL-1Ra inducer *in vitro* (**Figure 2B**), our data suggested that the size of GalN oligomers was less crucial *in vivo* than *in vitro*. In contrast, the administration of the acetylated counterpart, acF-III, did not rescue the inflammation where all colitis characteristics (death, loss of weight, DAI, colon analysis, cytokine pattern) were similar to those of DSS control mice (**Figure 5**). Even worse, acF-III administration increase pro-inflammatory cytokines such as TNFα, IL-1β, and IL-17 (**Figure 5**).

Taken together, data from **Figure 5**, two colitis rescue profiles were observed with GAG oligomers. De-*N*-acetylated oligomers (average dp of 16 or larger) rescued DSS-treated mice with a significant reduction of inflammatory cells infiltration, muscle thickening and amelioration of colonic structure. This effect is concomitant to the induction of IL-1Ra secretion as also observed *in vitro*. In contrast, insoluble acetylated oligomers of dp > 26 rescued DSS-treated mice in a IL-1Ra-independent mode of action. In summary, water-soluble poly-galactosamine oligosaccharides are promising candidates for alternative treatments of IL-1Ra-dependent diseases.

DISCUSSION

IL-1-mediated inflammation has been established in a broad spectrum of diseases, ranging from rare autoinflammatory diseases to common conditions such as gout and rheumatoid arthritis, type 2 diabetes, atherosclerosis, and acute myocardial infarction (Cavalli and Dinarello, 2018). The search for potent IL-1 blockers to treat major inflammatory diseases has turned into a very active field, which addresses several therapeutic approaches (Finckh and Gabay, 2008; Gabay et al., 2010). Among them, prevention of binding of active IL-1 on its cell surface receptors by use of the recombinant form of IL-1Ra (Anakinra) offers an ideal option as it has been used in several diseases (Dinarello et al., 2012). Due to its anti-inflammatory potential, GAG produced by *A. fumigatus* opens the way to novel innovative strategies to control IL-1 signaling and to design new anti-inflammatory drugs (Gresnigt et al., 2014). Here, to investigate the minimum oligosaccharide sequences derived from GAG able to induce anti-inflammatory response, partial chemical hydrolysis allowed isolating soluble active oligomers. From our data, galactose is not required for the bio-activity of GAG, in contrast, de-*N*-acetylated GalN residues were essential to induce the secretion of IL-1Ra both *in vitro* and *in vivo*. The size of oligomers plays a critical function where a minimum size of 13 (and better >19) α-1,4-GalN residues were required to be active *in vitro*. *In vivo* experiments have confirmed the *in vitro* data and are able to rescue inflammatory damage in a colitis model. Interestingly, the poor *in vitro* inducer F-III has a similar *in vivo* beneficial effect than larger oligomers, suggesting that the dose/size effect of GalN oligomers is different *in vitro* and *in vivo*. The chemical synthesis of defined GalN oligomers and *in vivo* kinetic studies will be helpful to investigate the optimal size and the delivery of such molecule *in vivo*.

The question of the chemical specificity of the IL-1Ra inducers by cell wall polysaccharides is now fundamental. Cell wall chitin and β-glucans are also IL-1Ra inducers (Poutsiaka et al., 1993; Smeekens et al., 2015; Becker et al., 2016). β-glucan structures remain essential to the IL-1Ra induction since soluble forms are not inducers (Poutsiaka et al., 1993). This result is in agreement with our data indicating the differential immunological effect of soluble and insoluble polysaccharide

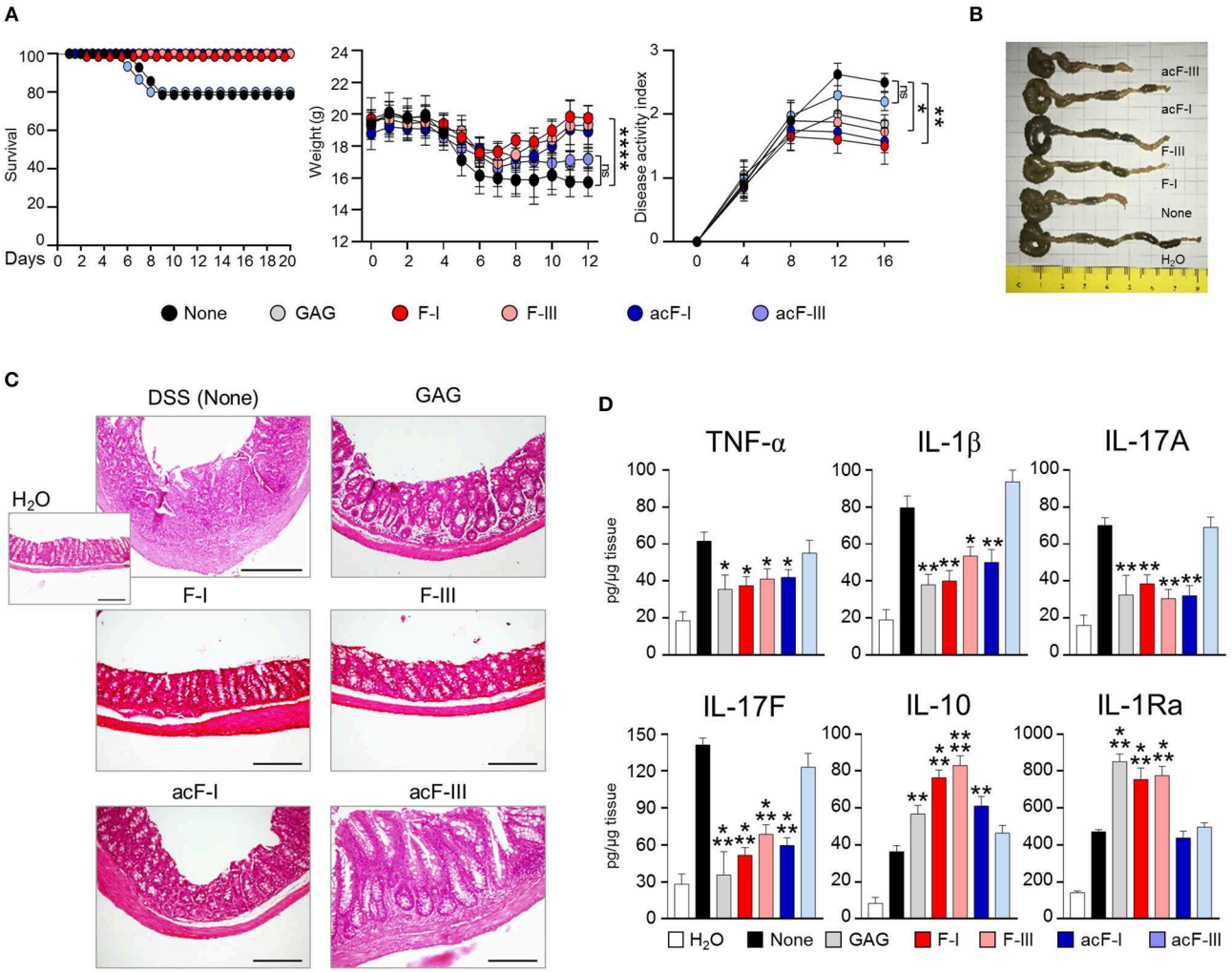

FIGURE 5 | Reduced severity of DSS colitis in C57BL/6 mice treated with modified GAG molecules. DSS or water vehicle was administered *ad libitum* in drinking water for 7 days. Native GAG polymer and GAG oligomers at the dose of 1 mg/kg were given intraperitoneally for 7 consecutive days after DSS treatment. **(A)** Survival, weight (grams) and clinical disease activity index. **(B)** Macroscopic image of colons. **(C)** Histological assessment of colitis severity (20X magnification, bar = 200 µm). **(D)** Levels of colonic cytokines. Data are expressed as mean ± SD. $^{*}P < 0.05$, $^{**}P < 0.01$, $^{***}P < 0.001$, $^{****}p < 0.0001$ GAGs-treated vs. untreated (None) C57BL/6 mice ($n = 10$ mice/group from one experiment). ns, not significant.

species. Moreover, β-glucans isolated from yeast or the hyphal form of *Candida albicans* did not induce similar effects (Smeekens et al., 2015) suggesting that small changes in the chemical composition of the polysaccharides can modify the immune response. Pure chitin isolated from *A. fumigatus* cell wall induces IL-1Ra (Becker et al., 2016). Chitin is composed of *N*-acetylglucosamine residues. However, in contrast to GAG, it is the *N*-acetylated form of glucosamine residues that is required for the IL-1Ra induction (Becker et al., 2016 and data not shown). The seemingly contradictory literature on the immunostimulatory properties of chitin are likely due to many factors including differences in sources of material, purity, readouts for inflammatory responses and the size of particles. Large chitin particles strongly induce pro-inflammatory response whereas small ones are not immunogenic (Alvarez, 2014). The degree of acetylation of cationic polysaccharides such as chitosan is critical for the pro-inflammatory response, showing that the de-*N*-acetylation of osamines not only alter their physicochemical properties but also their immunological activities (Bueter et al., 2011). The respective anti-inflammatory and pro-inflammatory properties of N-acetylated F-III and de-N-acetylated F-III are also an illustration (**Figure 5**). Chitin plays a dual immune response depending of the purity: (1) pure chitin induces an anti-inflammatory response in presence of serum and (2) in presence of other PAMPs (LPS, muramyl dipeptide, but not β-glucans), chitin has a synergistic effect on the induction of pro-inflammatory cytokines in an independent pathway (Becker et al., 2016), showing that the purity and homogeneity of PAMP sample are extremely important to investigate immune response.

β-Glucans induces both inflammatory and anti-inflammatory response that are triggered through independent pathways. Two

main PPRs, the C-type lectin Dectin-1 and the complement receptor CR3 are known to recognize β-glucans (Brown and Gordon, 2001; van Bruggen et al., 2009). In *A.fumigatus* the pathway linking GAG to IL-1Ra production is unknown. IL-1Ra induction by *C. albicans* β-glucans is dependent on a Akt-PI3K dependent PRR (Smeekens et al., 2015). Our data showed that insoluble and soluble GAG oligomers shared an anti-inflammatory response with two independent pathways. Insoluble oligomers may restore a protective effect *in vivo* on colitis through an IL-1Ra independent pathway. In contrast, soluble oligomers induce a specific induction of IL-1Ra where the presence of de-*N*-acetylated galactosamine residues is critical. Although the signaling pathway remains unknown, it is independent on particle size or insolubility of polymer as described for chitin and β-glucans. Our study showed that soluble oligomers composed of an average of 16 α-1,4-linked GalN residues display a specific IL-1Ra induction, suggesting a specific immune pathway. Interestingly, pectin macromolecules have gained significant attention partly because of their immunosuppressive properties (Popov and Ovodov, 2013). Pectin induced *in vitro* a dose-dependent inhibition of IL-1β secretion correlated to an increase secretion of anti-inflammatory cytokines IL-10 and IL-1Ra by human PBMCs (Salman et al., 2008). The anti-inflammatory properties are dependent on a high content of α-1,4-linked galacturonic acid in the main polysaccharidic chain (Popov and Ovodov, 2013). The structural comparison with GAG from *A. fumigatus* suggests a structure-function relationship where linear α-1,4-linked galactose derived monosaccharides may be important for the anti-inflammatory properties of the polymer. However, our data showed that GAG oligomers induce IL-1Ra in PBMCs to a 20–100 fold extend *in vivo* and *in vitro* as compared to pectin (Salman et al., 2008). α-1,4-GalN oligomers are highly water-soluble alternatives to ease medically dose-response-adjustments and to overcome application issues frequently observed for insoluble chitin/chitosan polymers (Vo and Kim, 2014). Finally, our data suggest that the chemical synthesis of α-1,4-GalN oligomers depict new tools to investigate the specific immune pathway of GAG and provide a novel source of anti-inflammatory glycodrugs for treatment of IL-1-driven diseases.

DATA AVAILABILITY STATEMENT

All datasets generated for this study are included in the article/**Supplementary Material**.

ETHICS STATEMENT

The animal study was reviewed and approved by the Italian Animal Welfare Authorization 360/2015-PR and Legislative degree 26/2014.

AUTHOR CONTRIBUTIONS

MG, CH, RS, LR, J-PL, and TF conceived and designed the experiments. MG, CH, IN'G, GR, VO, SM, BC, JG, and TF performed the experiments. MG, CH, BC, RS, LR, JP-L, and TF analyzed the data. MG, CH, GR, VO, SM, BC, JG, RS, LR, J-PL, and TF contributed reagents, materials and analysis tools. MG, TF, and J-PL wrote the paper.

FUNDING

This research was funded by the Aviesan project Aspergillus, the French Government's Investissement d'Avenir program, Laboratoire d'Excellence Integrative Biology of Emerging Infectious Diseases (Grant No ANR-10-LABX-62-IBEID), la Fondation pour la Recherche Médicale (DEQ20150331722 LATGE Equipe FRM 2015). RS thanks Fundação para a Ciência e Tecnologia (FCT) contract IF/00021/2014.

ACKNOWLEDGMENTS

We thank Pauline Robinet, Giorgio Camilli and Jessica Quintin (Institut Pasteur, Paris) for assistance with isolation of PBMC's.

SUPPLEMENTARY MATERIAL

The Supplementary Material for this article can be found online at: https://www.frontiersin.org/articles/10.3389/fcimb.2019.00365/full#supplementary-material

REFERENCES

Alvarez, F. J. (2014). The effect of chitin size, shape, source and purification method on immune recognition. *Molecules* 19, 4433–4451. doi: 10.3390/molecules19044433

Beaussart, A., El-Kirat-Chatel, S., Fontaine, T., Latgé, J.-P., and Dufrêne, Y. F. (2015). Nanoscale biophysical properties of the cell surface galactosaminogalactan from the fungal pathogen *Aspergillus fumigatus*. *Nanoscale* 7, 14996–15004. doi: 10.1039/C5NR04399A

Becker, K. L., Aimanianda, V., Wang, X., Gresnigt, M. S., Ammerdorffer, A., Jacobs, C. W., et al. (2016). Aspergillus cell wall chitin induces anti- and proinflammatory cytokines in human PBMCs via the Fc-γ receptor/Syk/PI3K pathway. *mBio* 7, e01823–e01815. doi: 10.1128/mBio.01823-15

Brown, G. D., and Gordon, S. (2001). A new receptor for β-glucans. *Nature* 413, 36–37. doi: 10.1038/35092620

Bueter, C. L., Lee, C. K., Rathinam, V. A. K., Healy, G. J., Taron, C. H., Specht, C. A., et al. (2011). Chitosan but not chitin activates the inflammasome by a mechanism dependent upon phagocytosis. *J. Biol. Chem.* 286, 35447–35455. doi: 10.1074/jbc.M111.274936

Cavalli, G., and Dinarello, C. A. (2018). Anakinra therapy for non-cancer inflammatory diseases. *Front. Pharmacol.* 9:1157. doi: 10.3389/fphar.2018.01157

Dinarello, C. A., Simon, A., and van der Meer, J. W. M. (2012). Treating inflammation by blocking interleukin-1 in a broad spectrum of diseases. *Nat. Rev. Drug Discov.* 11, 633–652. doi: 10.1038/nrd3800

Finckh, A., and Gabay, C. (2008). At the horizon of innovative therapy in rheumatology: new biologic agents. *Curr. Opin. Rheumatol.* 20, 269–275. doi: 10.1097/BOR.0b013e3282fa13b4

Fontaine, T., Delangle, A., Simenel, C., Coddeville, B., van Vliet, S. J., van Kooyk, Y., et al. (2011). Galactosaminogalactan,

a new immunosuppressive polysaccharide of *Aspergillus fumigatus*. *PLoS Pathog.* 7:e1002372. doi: 10.1371/journal.ppat.1002372

Gabay, C., Lamacchia, C., and Palmer, G. (2010). IL-1 pathways in inflammation and human diseases. *Nat. Rev. Rheumatol.* 6, 232–241. doi: 10.1038/nrrheum.2010.4

Gravelat, F. N., Beauvais, A., Liu, H., Lee, M. J., Snarr, B. D., Chen, D., et al. (2013). Aspergillus galactosaminogalactan mediates adherence to host constituents and conceals hyphal β-glucan from the immune system. *PLoS Pathog.* 9:e1003575. doi: 10.1371/journal.ppat.1003575

Gresnigt, M. S., Bozza, S., Becker, K. L., Joosten, L. A. B., Abdollahi-Roodsaz, S., van der Berg, W. B., et al. (2014). A polysaccharide virulence factor from *Aspergillus fumigatus* elicits anti-inflammatory effects through induction of interleukin-1 receptor antagonist. *PLoS Pathog.* 10:e1003936. doi: 10.1371/journal.ppat.1003936

Hamer, S. N., Cord-Landwehr, S., Biarnés, X., Planas, A., Waegeman, H., Moerschbacher, B. M., et al. (2015). Enzymatic production of defined chitosan oligomers with a specific pattern of acetylation using a combination of chitin oligosaccharide deacetylases. *Sci. Rep.* 5:8716. doi: 10.1038/srep08716

Lavertu, M., Darras, V., and Buschmann, M. D. (2012). Kinetics and efficiency of chitosan reacetylation. *Carbohydr. Polym.* 87, 1192–1198. doi: 10.1016/j.carbpol.2011.08.096

Lee, M. J., Geller, A. M., Bamford, N. C., Liu, H., Gravelat, F. N., Snarr, B. D., et al. (2016). Deacetylation of fungal exopolysaccharide mediates adhesion and biofilm formation. *mBio* 7, e00252–e00216. doi: 10.1128/mBio.00252-16

Lee, M. J., Liu, H., Barker, B. M., Snarr, B. D., Gravelat, F. N., Al Abdallah, Q., et al. (2015). The fungal exopolysaccharide galactosaminogalactan mediates virulence by enhancing resistance to neutrophil extracellular traps. *PLoS Pathog.* 11:e1005187. doi: 10.1371/journal.ppat.1005187

Lever, M. (1972). A new reaction for colorimetric determination of carbohydrates. *Anal. Biochem.* 47, 273–279. doi: 10.1016/0003-2697(72)90301-6

Marx, A., Backes, C., Meese, E., Lenhof, H.-P., and Keller, A. (2016). EDISON-WMW: exact dynamic programing solution of the Wilcoxon-Mann-Whitney test. *Genom. Proteomics Bioinform.* 14, 55–61. doi: 10.1016/j.gpb.2015.11.004

McNamee, E. N., Masterson, J. C., Jedlicka, P., McManus, M., Grenz, A., Collins, C. B., et al. (2011). Interleukin 37 expression protects mice from colitis. *Proc. Natl. Acad. Sci. U.S.A.* 108, 16711–16716. doi: 10.1073/pnas.1111982108

No, H. K., and Meyers, S. P. (1989). Crawfish chitosan as a coagulant in recovery of organic compounds from seafood processing streams. *J. Agric. Food Chem.* 37, 580–583. doi: 10.1021/jf00087a002

Plassard, C., Moussain, D., and Salsac, L. (1982). Plassard, C., D. Mousain, and L. Salsac. Estimation of mycelial growth of basidiomycetes by means of chitin determination. *Phytochemistry* 21, 345–348. doi: 10.1016/S0031-9422(00)95263-4

Popov, S. V., and Ovodov, Y. S. (2013). Polypotency of the immunomodulatory effect of pectins. *Biochem. Mosc.* 78, 823–835. doi: 10.1134/S0006297913070134

Poutsiaka, D. D., Mengozzi, M., Vannier, E., Sinha, B., and Dinarello, C. A. (1993). Cross-linking of the beta-glucan receptor on human monocytes results in interleukin-1 receptor antagonist but not interleukin-1 production. *Blood* 82, 3695–3700.

Robinet, P., Baychelier, F., Fontaine, T., Picard, C., Debr,é, P., Vieillard, V., et al. (2014). A polysaccharide virulence factor of a human fungal pathogen induces neutrophil apoptosis via NK cells. *J. Immunol.* 192, 5332–5342. doi: 10.4049/jimmunol.1303180

Salman, H., Bergman, M., Djaldetti, M., Orlin, J., and Bessler, H. (2008). Citrus pectin affects cytokine production by human peripheral blood mononuclear cells. *Biomed. Pharmacother.* 62, 579–582. doi: 10.1016/j.biopha.2008.07.058

Smeekens, S. P., Gresnigt, M. S., Becker, K. L., Cheng, S.-C., Netea, S. A., Jacobs, L., et al. (2015). An anti-inflammatory property of Candida albicans β-glucan: induction of high levels of interleukin-1 receptor antagonist via a Dectin-1/CR3 independent mechanism. *Cytokine* 71, 215–222. doi: 10.1016/j.cyto.2014.10.013

Tamura, J., Abe, T., Hasegawa, K., and Kadowaki, K. (1992). The mode of action of endo α-1, 4 polygalactosaminidase from *Pseudomonas* sp. 881 on galactosaminooligosaccharides. *Biosci. Biotechnol. Biochem.* 56, 380–383. doi: 10.1271/bbb.56.380

Tamura, J., Takagi, H., and Kadowaki, K. (1988). Purification and some properties of the endo α-1,4 polygalactosaminidase from *Pseudomonas* sp. *Agricult. Biol. Chem.* 52, 2475–2484. doi: 10.1271/bbb1961.52.2475

van Bruggen, R., Drewniak, A., Jansen, M., van Houdt, M., Roos, D., Chapel, H., et al. (2009). Complement receptor 3, not Dectin-1, is the major receptor on human neutrophils for β-glucan-bearing particles. *Mol. Immunol.* 47, 575–581. doi: 10.1016/j.molimm.2009.09.018

Vo, T.-S., and Kim, S.-K. (2014). Marine-derived polysaccharides for regulation of allergic responses. *Adv. Food Nutr. Res.* 73, 1–13. doi: 10.1016/B978-0-12-800268-1.00001-9

Wang, H., Dong, J., Shi, P., Liu, J., Zuo, L., Li, Y., et al. (2015). Anti-mouse CD52 monoclonal antibody ameliorates intestinal epithelial barrier function in interleukin-10 knockout mice with spontaneous chronic colitis. *Immunology* 144, 254–262. doi: 10.1111/imm.12366

Conflict of Interest: The authors declare that the research was conducted in the absence of any commercial or financial relationships that could be construed as a potential conflict of interest.

frontiers in Cellular and Infection Microbiology

ORIGINAL RESEARCH
published: 08 November 2019
doi: 10.3389/fcimb.2019.00378

Importance of *Candida* Antigenic Factors: Structure-Driven Immunomodulation Properties of Synthetically Prepared Mannooligosaccharides in RAW264.7 Macrophages

Ema Paulovičová[1], Lucia Paulovičová[1], Pavol Farkaš[1], Alexander A. Karelin[2], Yury E. Tsvetkov[2], Vadim B. Krylov[2] and Nikolay E. Nifantiev[2]**

[1] Cell Culture & Immunology Laboratory, Department of Immunochemistry of Glycoconjugates, Center for Glycomics, Institute of Chemistry, Slovak Academy of Sciences, Bratislava, Slovakia, [2] Laboratory of Glycoconjugate Chemistry, N.D. Zelinsky Institute of Organic Chemistry, Russian Academy of Sciences, Moscow, Russia

The incidence and prevalence of serious fungal infections is rising, especially in immunosuppressed individuals. Moreover, co-administration of antibiotics and immunosuppressants has driven the emergence of new multidrug-resistant pathogens. The significant increase of multidrug-resistant pathogens, together with their ability to form biofilms, is associated with morbidity and mortality. Research on novel synthetically prepared immunomodulators as potential antifungal immunotherapeutics is of serious interest. Our study demonstrated the immunobiological activity of synthetically prepared biotinylated mannooligosaccharides mimicking *Candida* antigenic factors using RAW264.7 macrophages. Macrophage exposure to the set of eight structurally different mannooligosaccharides induced a release of Th1, Th2, Th17, and Treg cytokine signature patterns. The observed immune responses were tightly associated with structure, dose, exposure time, and selected signature cytokines. The viability/cytotoxicity of the mannooligosaccharide formulas was assessed based on cell proliferation. The structure-based immunomodulatory activity of the formulas was evaluated with respect to the length, branching and conformation of the various formulas. Glycoconjugate formulas with terminal β-mannosyl-units tended to be more potent in terms of *Candida* relevant cytokines IL-12 p70, IL-17, GM-CSF, IL-6, and TNFα induction and cell proliferation, and this tendency was associated with structural differences between the studied glycoconjugate formulas. The eight tested mannooligosaccharide conjugates can be considered potential *in vitro* immunomodulative agents suitable for *in vitro Candida* diagnostics or prospectively for subcellular anti-*Candida* vaccine design.

Keywords: *Candida*, oligomannosides, RAW 264.7, cytokines, proliferation

OPEN ACCESS

Edited by:
Laura Alcazar-Fuoli, Carlos III Health Institute, Spain

Reviewed by:
Jill R. Blankenship, University of Nebraska Omaha, United States
Ian A. Cleary, Grand Valley State University, United States

****Correspondence:***
Ema Paulovičová
ema.paulovicova@savba.sk
Nikolay E. Nifantiev
nen@ioc.ac.ru

Specialty section:
This article was submitted to Fungal Pathogenesis, a section of the journal Frontiers in Cellular and Infection Microbiology

Received: *04 July 2019*
Accepted: *21 October 2019*
Published: *08 November 2019*

Citation:
Paulovičová E, Paulovičová L, Farkaš P, Karelin AA, Tsvetkov YE, Krylov VB and Nifantiev NE (2019) Importance of Candida Antigenic Factors: Structure-Driven Immunomodulation Properties of Synthetically Prepared Mannooligosaccharides in RAW264.7 Macrophages. Front. Cell. Infect. Microbiol. 9:378. doi: 10.3389/fcimb.2019.00378

INTRODUCTION

Most *Candida* species, including the facultative pathogenic strains, belong to the normal commensal mycobiota of immunocompetent individuals. The factors affecting the candidosis are diverse, including the prolonged antifungal treatment in long-term care, immunosuppression associated with anticancer therapy and transplantation of solid organ or bone marrow, immunosuppressive states as diabetes mellitus and HIV, use of vascular devices and hospitalization at intensive care units (Richter et al., 2005; Angiolella et al., 2008; Adiguzel et al., 2010; Cortés and Corrales, 2018). Next, immunocompromised persons with genetic immune system defects are at high risk for mucocutaneous and invasive fungal infections (Vinh, 2011; Cunha and Carvalho, 2012; Pichard et al., 2015; Beenhouwer, 2018). Approximately 17 different *Candida* species are known etiological agents of human infections; more than 90% of systemic infections are caused by *Candida albicans (C. albicans)*, *Candida glabrata (C. glabrata), Candida parapsilosis (C. parapsilosis), Candida tropicalis (C. tropicalis)*, and *Candida krusei (C. krusei)* (Pfaller et al., 2002). The new multidrug-resistant species *Candida auris (C. auris)* was recently isolated (Sears and Schwartz, 2017; Forsberg et al., 2019). $CD4^+$-derived T-cell subpopulations Th1, Th2, and Th17 contribute to anti-*Candida* cellular immune protection. The protective anticandidal Th1 response requires the activity of various cytokines, such as interferon gamma (IFN-γ), transforming growth factor beta (TGF-β), interleukin 6 (IL-6), tumor necrosis factor alpha (TNFα), and IL-12. The induction of the protective antifungal Th1 immune response is inhibited by Th2 cytokines, such as IL-4 and IL-10 (Ito, 2011; Netea et al., 2015; Richardson and Moyes, 2015; Gow et al., 2017). In early infection, neutralization of Th1 cytokines, mainly IFN-γ and IL-12, leads predominately to the onset of Th2 rather than Th1 responses. Th2-type responses are frequently associated with susceptibility to recurrent or persistent infection and fungal allergy. TNFα, IL-1β, IL-6, IL-8, and colony-stimulating factors (CSFs) are among the major proinflammatory cytokines associated with the interaction of immune-competent cells with *Candida* cells. TNFα is thought to be essential in the primary control of disseminated infection caused by *C. albicans.* Although IL-1 shares common properties with TNFα, both IL-1β and IL-6, acting mainly through recruitment of polymorphonuclear neutrophils (PMNs), presumably are not as essential as TNFα in the innate antifungal response. IL-12 is recognized as essential to induce the protective Th1 response to the fungus, simultaneously blocking the Th2 response. The crucial role of the Th17 subset has been associated with anti-*Candida* effectiveness, especially the mucosal immune response (Romani, 2003; Rizzetto et al., 2010; van de Veerdonk and Netea, 2010). Proinflammatory cytokines, such as IL-12, IL-15, and TNFα, have been studied as candidate adjuvants in preclinical trials based on their ability to upregulate the antifungal Th1 response (Ashman and Papadimitriou, 1995; Romani, 2011; Pikman and Ben-Ami, 2012; Naglik, 2014).

Fungal cell wall antigenically active polysaccharides, such as N-linked and O-linked α- and β-mannans, chitin, α- and β-glucans, galactomannan, galactosaminogalactan, glucuronoxylomannan, and some others, are essential immunogens that play crucial roles during host-fungus interactive communication. Cell-wall components act as pathogen-associated molecular patterns (PAMPs), recognized by the immune system through pattern recognition receptors (PRRs) such as TLR2, TLR4, dectin-2, dectin-1, Mincle, DC-SIGN, or galectin-3, on the surfaces of epithelia and myeloid cells (Netea et al., 2006, 2008, 2015; Moyes and Naglik, 2011; Perez-Garcia et al., 2011; Romani, 2011; Cunha and Carvalho, 2012; Salek-Ardakani et al., 2012; Hall and Gow, 2013; Moyes et al., 2015; Zheng et al., 2015; Gow et al., 2017; Snarr et al., 2017).

Generally, specific PAMP–PRR interactions activate the inflammatory response by triggering interleukins and growth factors cell release and phagocytosis. *O*-linked mannans are recognized via TL4 receptor (Netea et al., 2006), α- linked *N*-mannans are sensed through mannose receptor, dectin-2, Mincle, and DC-SIGN (Harris et al., 2009; McKenzie et al., 2010), and the specific receptor for β-mannan is galectin-3 (Jouault et al., 2006; Linden et al., 2013). Chitin cooperates with the mannose receptor and induces TLR9 and NOD-2dependentIL-10 release (Wagener et al., 2014; Erwig and Gow, 2016). Recently, it has been demonstrated that chitin particles of small size stimulated IL-17, IL-12, IL-23, IL-10, and TNF-α in macrophages via a MyD88- and TLR2-dependent pathway (Da Silva et al., 2008, 2009). Additionally, Dectin-1 receptor on macrophages and TLR-2 recognizes β-1,3-glucan (Brown and Gordon, 2001; Brown et al., 2002, 2003; Brown, 2006). Dectin-1 uses Syk kinase and the CARD9 to stimulate IL-10, TLR2 via the MyD88 is required for the production of IL-12p40 (Dennehy et al., 2008; Netea et al., 2008), and both pathways collaborate in TNF- stimulation. Moreover, dectin-1 and galectin-3 interact synergistically to improve the outcome of host immune response to *C. albicans* (Gantner et al., 2003; Taylor et al., 2007; Esteban et al., 2011).

The antigenic factors of mannan from medically relevant *Candida* species have been characterized and their chemical structures determined in several studies (Nishikawa et al., 1982; Suzuki and Fukazawa, 1982; Shibata et al., 1995; Fukazawa et al., 1997; Suzuki, 1997). The antigenic determinants of cell wall polysaccharides and oligosaccharides from medically important yeasts have been studied for their serological specificity and biological activity (Fukazawa et al., 1997). The investigation of species-specific antigenic factor variations of *Candida* mannan and oligomannosyl structures is essential to evaluate the structure-activity relationship, since mannan structure and epitope availability intensely affect its immunobiological behavior (Trinel et al., 1992; Fukazawa et al., 1997; Suzuki, 1997; Shibata et al., 2007). The particular structure of mannan, comprising an α-1,6-mannoside backbone and side chains with α/β-1,2-mannoside or α/β-1,3-mannoside moieties of variable lengths, varies for different *Candida* species and is dependent on the expression of a complex network of mannan biosynthesis, trafficking, and cell wall remodeling genes (Shibata et al., 2012). Different growth conditions are likely to modulate the activation of cell wall signaling cascades, expression of cell wall biosynthesis genes, and alterations in mannan composition (Ernst and Pla, 2011; Lowman et al., 2011). The role of

mannosylation in fungal biology and virulence has been studied using *C. albicans* mutants; the suitability of these mutants for exploring the significance of specific mannan epitopes on cell function, pathogenesis and immune recognition has been proposed (Hall and Gow, 2013; Hall et al., 2013; West et al., 2013). Several studies have attempted to design and develop an anti-*Candida* vaccine based on cell wall-derived structures (Ito, 2011; Richardson and Moyes, 2015; Tso et al., 2018; Piccione et al., 2019). The immunogenic polysaccharide cell wall structures applied in experimental vaccine models include 65 kDa mannoproteins (Sandini et al., 2007), β-1,3-glucan (Torosantucci et al., 2005), and β-1,2- mannosides (Han et al., 1999; Cutler, 2005). These model structures were effective in humoral antibody-mediated antifungal protection. Several monoclonal antibodies were protective in preclinical studies: anti- β-1,3-glucan mAb2G8 (Torosantucci et al., 2005), anti-mannoprotein mAb C7 (Moragues et al., 2003), anti-idiotypic antibodies (Magliani et al., 2004), anti-mannan mAb (Han et al., 1999; Cutler, 2005), and anti-glycosyl mAb (Kavishwar and Shukla, 2006). These antibodies efficiently appeared as candidacidal (Moragues et al., 2003; Magliani et al., 2004; Kavishwar and Shukla, 2006), growth inhibitory, or they neutralized heat shock protein 90 (Hsp90) (Torosantucci et al., 2005). Moreover, mannan conjugated in certain vaccine formulas has already been included in clinical trials (Apostolopoulos et al., 2006; Pashov et al., 2011).

Mannan has also been studied as a promising bioactive material for drug nanocarrier systems and vaccine adjuvant formulations (Tang et al., 2009). Moreover, nanoliposomes with orthogonally bound mannan represent a platform for the development of targeted drug delivery systems and self-adjuvanted carriers for construction of recombinant vaccines (Bartheldyova et al., 2019). Concerning the design of anti-fungal vaccination therapy, apart from *Candida* cell wall moieties, potential new anti-*Candida* drugs have targeted the growth and virulence factors of *C. albicans*, including core signaling components of the high-osmolarity glycerol (HOG) and target of rapamycin (TOR) signaling pathways (Li et al., 2015), as well as various immunomodulators, e.g., colony-stimulating factors and proinflammatory cytokines (Pikman and Ben-Ami, 2012).

Natural *Candida* mannan is a complex polysaccharide structure containing linear and branched fragments composed of α- and β-mannose units, as seen in **Figure 1** (Klis et al., 2001), with the carbohydrate sequences represented according to symbol carbohydrate nomenclature (Varki et al., 1999). Thus, the use of such a heterogenic structure is problematic for the assessment of the biological role of its distinct fragments. However, the application of synthetic mannooligosaccharide derivatives, related to the structures of selected antigenic factors of *Candida* mannan, creates the opportunity to assess the biological roles of each antigenic factor.

Our work investigated the immunomodulation properties of antigenically active distinct parts of *C. albicans* mannan by using a series of structurally related synthetic mannooligosaccharides.

MATERIALS AND METHODS

Synthesis of Biotinylated Oligomannosides 1–8

Mannooligosaccharide conjugate formulas **1** (Krylov et al., 2018a), **2** (Krylov et al., 2018a,b), **3** (Karelin et al., 2007),

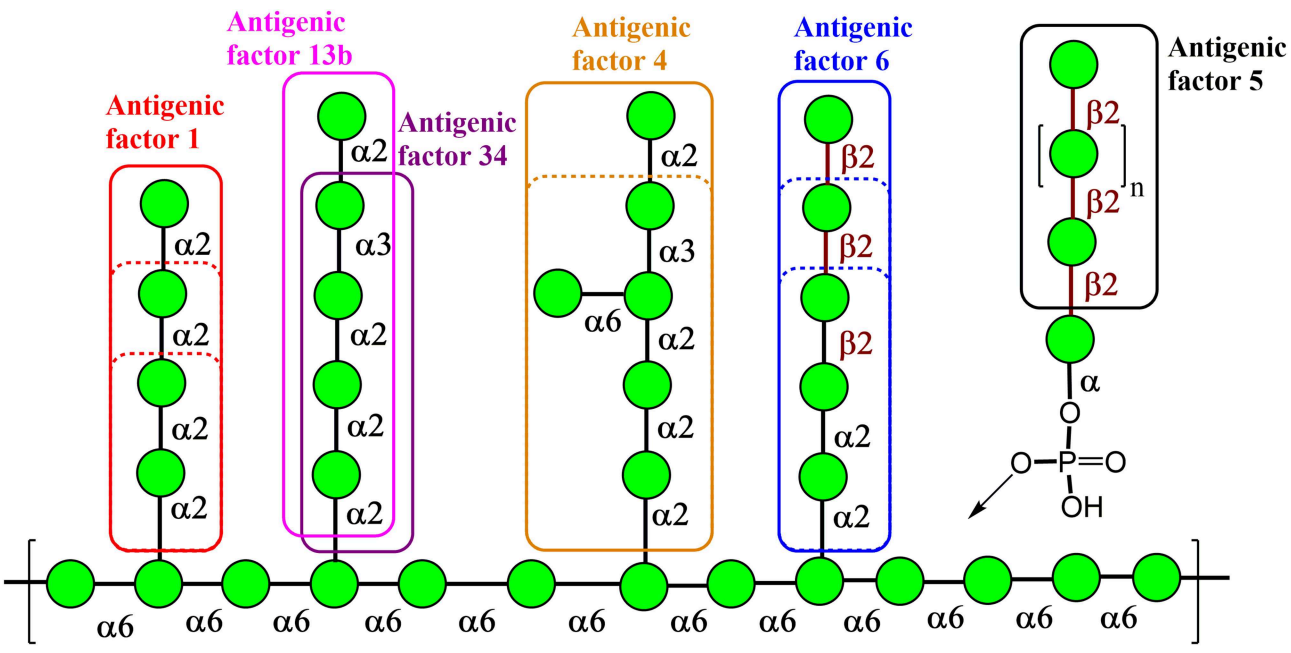

FIGURE 1 | Key structural elements of the cell wall mannan from the fungus *Candida albicans* representing its antigenic factors. The carbohydrate sequences are represented according to symbol carbohydrate nomenclature (Varki et al., 1999).

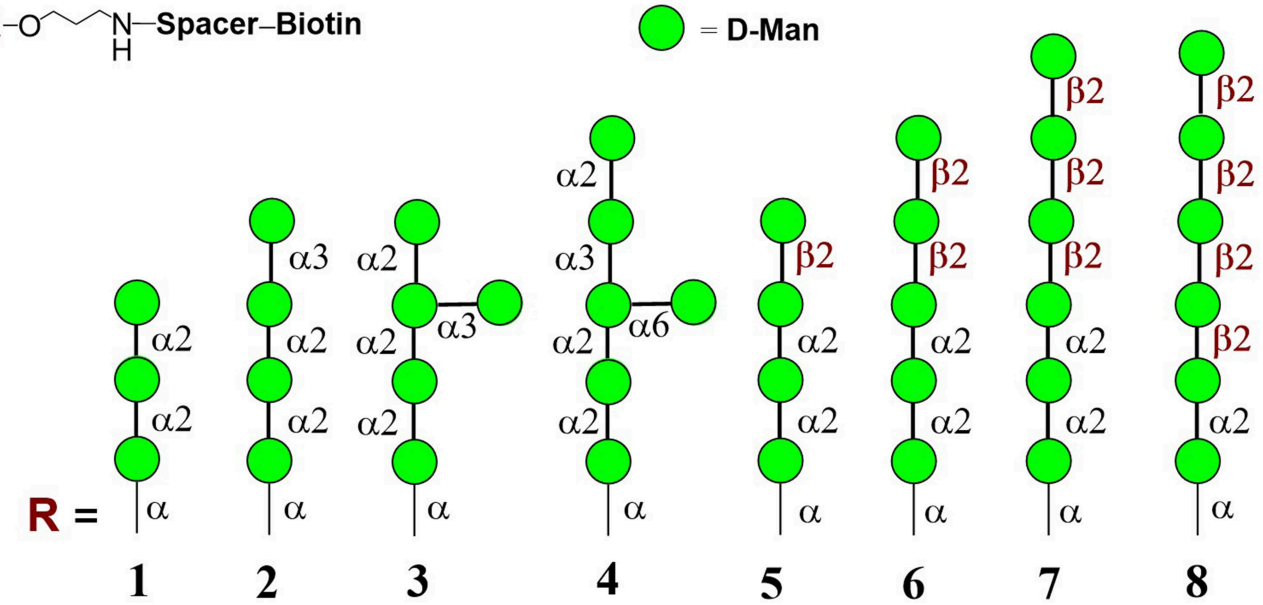

FIGURE 2 | Structures of studied biotinylated mannooligosaccharides **1**–**8** (Argunov et al., 2019).

4 (Karelin et al., 2010), and **5**–**8** (Karelin et al., 2016) were prepared by the biotinylation of parent ligands according to previously described biotinylation protocols (**Figure 2**) (Tsvetkov et al., 2012).

Isolation of Natural Cellular Mannan and Preparation of FITC-Labeled Mannan

The yeast strain *Candida albicans* CCY 29-3-100 (serotype A) (CCY Culture Collection of Yeasts, Institute of Chemistry, Center for Glycomics, Slovak Academy of Sciences, Bratislava, Slovakia) was used to isolate and purify cellular mannan from fresh biomass. Mannan was extracted by autoclaving in 0.2 mol/l NaCl (120°C, 700 kPa) for 10 min and purified using precipitation with Fehling reagent according to a previously described method (Peat et al., 1961).

For the preparation of FITC-labeled mannan, *C. albicans* CCY 29-3-100 mannan (54 mg) was suspended in 1.00 mL of dimethyl sulfoxide and 2.0 μL of pyridine was added. The suspension was heated in a thermoblock at 95°C until the mannan dissolved (3 h). Then, 20 mg of isothiocyanatofluorescein (FITC) was added and heated for another 2 h at 95°C. The reaction was quenched by addition of 10 mL of water, and the result was dialyzed using cellulose membrane tube (cut-off = 14,000, Sigma) against 0.05 % NaHCO3 (1 × 0.9 L, 4 h stirred) and deionized water [8 × 0.9 L, 4 h on stirrer or 12 h in the refrigerator (5°C)] and then lyophilized (FreeZone 18 Liter Console Freeze Dry System, Labconco Corporation, Kansas City, USA).

Preparation of Stock Solutions of Natural Cellular Mannan and Synthetically Prepared Mannooligosaccharides

Stock solutions and different dilutions of natural cellular mannan and glycoconjugate formulas **1**–**8** were prepared aseptically using pre-sterilized disposable plastic wares and sterile, apyrogenic aqua pro injectione (Fresenius Kabi Italia S.r.l., Verona, Italy). All solutions were prepared in a laminar flow hood and sterilized using a 0.2-μm filter (Q-Max® Syringe filter, Frisenette ApS, Knebel, Denmark) before exposure. The laminar flow cabinet was sterilized with 70% ethanol p.a. and UV for 30 min prior to each experiment. The stock solutions were assayed with EndoLISA® ELISA-based Endotoxin Detection Assay (Hyglos, Bernried am Starnberger See, Germany) and evaluated using the Cytation 5 Imager Multi-Mode Reader (BioTek, Winooski, USA) to ascertain endotoxin-free exposure conditions.

Cell Maintenance and Culture, Cell Exposure

The murine macrophage-like RAW 264.7 cell line was selected in the present study because this cell model has been frequently used in *in vitro* studies on phagocytosis, cytokine production, and to evaluate potential bioactive substances to predict their effect *in vivo*.

RAW 264.7 (ATCC® TIB-71™, ATCC, Manassas, USA) cells were cultured in complete Dulbecco's Modified Eagle Medium for 24 h and 48 h, at 37°C under 5% CO_2 atmosphere and 90–100% relative humidity until ∼80% confluence. Viability of cells was determined by Trypan Blue dye exclusion method using a TC20™ automated cell counter (Bio-Rad Laboratories, Inc., Hercules, USA). The starting inoculum of 1×10^5 cells/mL/well (98.3% of viable cells) was seeded in a 24-well cell culture plate (Sigma-Aldrich, St. Louis USA) and exposed to 10 and 100 μg per well of glycoconjugates for 24 and 48 h. Cell mitogens Concanavalin A (Con A; 10 μg/mL, Sigma-Aldrich), phytohemagglutinin (PHA; 10 μg/mL, Sigma-Aldrich), pokeweed mitogen (PWM, 1 μg/mL, Sigma-Aldrich), and lipopolysaccharide (LPS; 1 μg/mL, Sigma-Aldrich) were used

as positive controls. The cell culture media were separated and stored at −20°C until further use. Cell morphology and viability were assayed before ELISA and evaluation of cytotoxicity. The interaction of FITC-labeled *Candida* mannan (100 μg/mL) and RAW 264.7 macrophage cells (1×10^5 cells/mL) was evaluated using either light and fluorescence microscopy (AxioVision Imager A.1, magnification 630x; Zeiss, Wetzlar, Germany) or confocal imaging (Axio Observer LSM 880 employing an Airyscan Plan-Apochromat 63x/1.4 oil DIC M27 optical lens and Zen 2 software) with application of 3D Z-stack imaging (Zeiss).

Cell Proliferation and Cytotoxicity

The influence of glycoconjugates on RAW 264.7 cell proliferation and cytotoxicity was evaluated using the cell proliferation assay ViaLight™ plus kit (Lonza, Rockland, ME, USA) according to the manufacturer's recommendations. Cellular ATP was determined with luciferase-based luminescence quantification. The intensity of emitted light was measured using the Cytation 5 Cell Imaging Multi-Mode Reader (BioTek Instruments, Inc.). Light emission was recorded continuously for 1 s and peak values were evaluated and expressed as relative light units (RLU). The values of unexposed cells were considered the baseline. The proliferation index was calculated as the ratio between the stimulated cells (glycoconjugate formula-treated cells) and the baseline proliferation of unexposed cells. Thus, the proliferation index of the negative control, i.e., unexposed cells, was equal to one.

Determination of Interleukins and Growth Factors

The levels of interleukins and growth factors in cell culture supernates induced by exposure with glycoconjugate formulas **1**–**8** were assayed according to the manufacturer's instructions with Platinum ELISAs® (eBioscience, Thermo Fisher Scientific, Waltham, USA): Mouse IL-12 p70 (MDD 4 pg/mL), Mouse granulocyte-macrophage colony-stimulating factor (GM-CSF;MDD 2 pg/mL), Mouse IL-17 (MDD 1.6 pg/mL), and Mouse IL-6 (MDD 6.5 pg/mL), and Instant ELISAs® (eBioscience): Mouse tumor necrosis factor (TNF)-α (MDD 4 pg/mL), and Mouse IL-10 (MDD 5.28 pg/mL).

To compare the effect of different glycoconjugates on RAW 264.7 macrophage interleukins and growth factors, analyses were performed on raw cytokine concentration data and cytokine concentration data normalized to viable cell counts of untreated control RAW 264.7 cells. The raw concentrations of cytokines determined by ELISA were divided by the RLU [ATP detection systems to quantify viable cells, ViaLightTM plus kit (Lonza, USA)] of living cells in a corresponding sample and multiplied by the RLU of untreated control RAW 264.7 cells.

Statistical Analysis

The experimental results were expressed as mean values ± SD. Normality of data distribution was established according to the Shapiro–Wilk test at the 0.05 level of significance. Statistical comparisons were performed by one-way ANOVA and *post-hoc* Bonferroni tests. Pearson's correlation coefficient was used to compare the strength of the relationship between immunobiological variables. Results were significant when the differences equaled or exceeded the 95% confidence level ($P < 0.05$). Statistics were performed using ORIGIN 7.5 PRO software (OriginLab Corporation, Northampton, USA).

RESULTS

Modern chemical methods enable regio- and stereoselective assembling of linear and branched structures similar to *C. albicans* mannan (Collot et al., 2009; Karelin et al., 2017; Krylov et al., 2017). Here we report the results of our investigation into the structure-driven immunomodulating properties of synthetically prepared mannooligosaccharides in RAW264.7 macrophages using a synthetically prepared panel of biotinylated mannooligosaccharides, formulas **1**–**8** (**Figure 2**). These oligomannosides represented antigenic factor 1 (formula **1**), factor 34 (formula **2**), factor 4 (formula **4**), and factor 6 (formulas **5**–**8**) of *C. albicans* mannan. Side chains related to formula **3** were also found in *C. albicans* mannan (Kogan et al., 1988), but their antigenic specificity is not yet clear.

As natural *Candida* mannan (section Isolation of natural cellular mannan and preparation of FITC-labeled mannan) was utilized in all experiments as a comparative substance, evaluation of its interaction with RAW 264.7 cells was essential. Fluorescently labeled natural mannan was used to visualize the cell interaction and endocytotosis of *Candida* mannan by the murine macrophage RAW 264.7 cells. Evaluation of the interaction was performed with light and fluorescence microscopy (**Figure 3A**) and 3D Z-stack imaging (**Figure 3B**). The patterns documented the ingestion of mannan and its inclusion into subcellular compartments.

Interactions of Natural Mannan and Glycoconjugate Formulas 1–8 With Murine Macrophage Cell Line RAW 264.7, and Influence on Cell Proliferation

The effect of glycoconjugate formulas **1**–**8** on macrophage cell line RAW 264.7 proliferation was monitored by adenosine triphosphate (ATP) bioluminescence as a marker of cell viability (**Figure 4**). The lower concentration of glycoconjugate formulas **1**–**4** (10 μg/mL, **Figure 4A**) slightly decreased the proliferation of RAW 264.7 macrophages. Improved proliferation was observed for formula **1**, which is comprised of three α-1,2-Man units (24 h treatment). The higher concentration of formulas **1**–**4** (100 μg/mL, **Figure 4A**), which are comprised exclusively of α-linkages between Man residues, significantly decreased the proliferation of RAW 264.7 macrophages (between 94 and 98% reduction). As opposed to the α-mannooligosaccharides, treatment of RAW 264.7 macrophages with formulas **5**–**8**, which also contain β-1,2-linked Man units, slightly increased proliferation after 24 h, and the increase was more significant after 48 h stimulation (**Figure 4B**). The highest proliferations were observed for the 10 μg/mL concentration of tetramer formula **5**, which contains one terminal β-1,2-linked Man unit (2.1 times higher than control), and hexamer formula **8**, which contains a tetrameric block of β-1,2-linked Man units (2.2

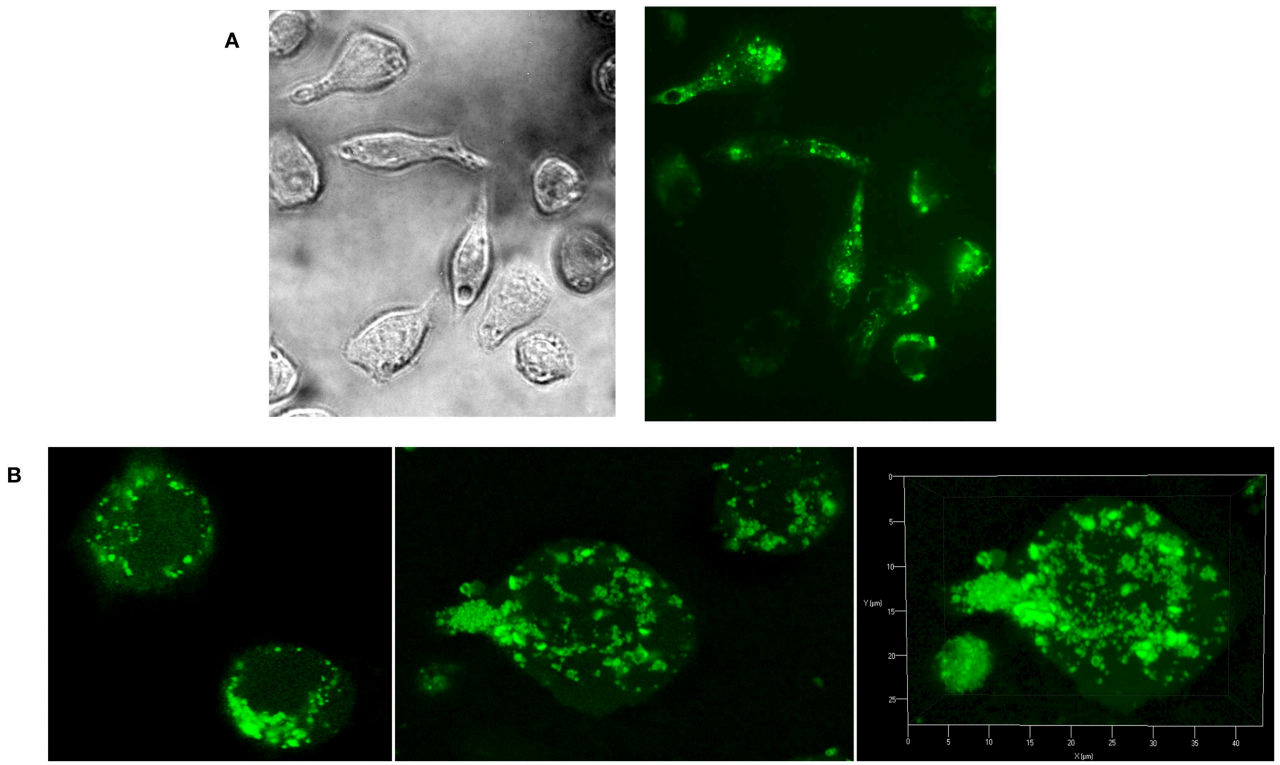

FIGURE 3 | Evaluation of Raw 264.7 cellular interactions with *C. albicans* mannan- FITC conjugated complex. **(A)** light and fluorescence microscopy (magnification 630x); **(B)** confocal microscopy.

times higher than control). The proliferation of RAW 264.7 macrophages treated by glycoconjugates for 48 h was significantly lower (formulas **1**–**4**: $p < 0.01$, formulas **5**–**8**: $p < 0.01$) compared with natural *C. albicans* mannan (M, **Figure 4C**).

Cytokine Responses of RAW 264.7 Macrophages *in vitro* to Glycoconjugate Formulas 1–8

The *in vitro* stimulatory effect of glycoconjugate formulas **1**–**8** on RAW 264.7 macrophage cytokine production was determined by the levels of pro-inflammatory cytokines TNFα, IL-6, IL-17, IL-12, anti-inflammatory cytokine IL-10, and haemopoietic growth factor GM-CSF in supernatants obtained from cultures of RAW264.7 macrophages after 24 or 48 h treatments [not normalized raw cytokine concentrations (**Supplementary Figures 1**, **2**) and cytokine concentrations normalized to viable cell counts of untreated control RAW 264.7 cells (**Figures 5**, **6**)].

Non-normalized raw cytokine concentrations data showed that stimulation of RAW 264.7 cells with the lower concentration of glycoconjugate formulas **1**–**4** (10 μg/mL), which contain linked Man residues, resulted in a slight increase of TNFα production; maximal effect was observed for formula **1** (24 h treatment: 1.37-fold increase and 48 h treatment: 1.48-fold increase, **Supplementary Figure 1**). The stimulation of RAW 264.7 macrophages with the higher concentration of glycoconjugate formulas (100 μg/mL) significantly decreased TNFα production (more than 70% decrease compared to the control). However, IL-6 and GM-CSF production showed different concentration dependencies. The higher concentration of glycoconjugate formulas **1**–**4** (100 μg/mL) induced comparable or higher IL-6 and GM-CSF secretion than the lower concentration (10 μg/mL) (**Supplementary Figure 1**). The highest IL-6 and GM-CSF release was observed for glycoconjugate formula **3** (IL-6: 3.2-fold increase, GM-CSF: 1.9-fold increase).

Glycoconjugate formulas **1**–**4** induced increased IL-17 production (**Supplementary Figure 1**). The higher concentration of glycoconjugate formulas **1**–**4** (100 μg/mL) induced higher IL-17 secretion, except for glycoconjugate formula **3**, for which IL-17 production declined with increasing glycoconjugate concentration (**Supplementary Figure 1**). Production of IL-12 showed a structure related dependency (**Supplementary Figure 1**). The most effective IL-12 inducer was glycoconjugate formula **1**, and induction efficacy declined slightly with increasing number of mannose units in glycoconjugate formulas **1**–**4** (**Supplementary Figure 1**). Glycoconjugate formulas **1**–**4** did not significantly influence IL-10 production (non-normalized data, **Supplementary Figure 1**). The results indicated a higher proinflammatory response associated with glycoconjugate formulas **1**–**4,** containing linked Man residues, with significant reduction of RAW 264.7 macrophage proliferation.

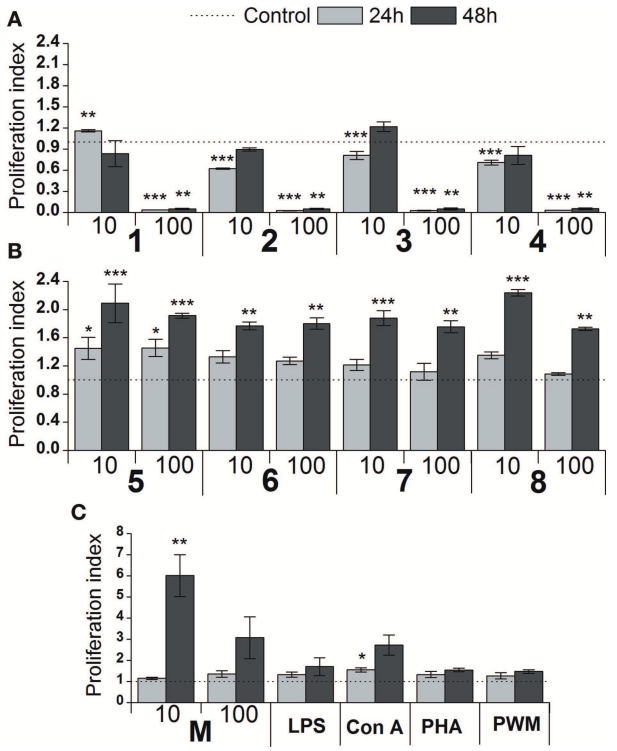

FIGURE 4 | Effect of glycoconjugate formulas **1–8** on proliferation of RAW264.7 macrophages. **(A)**: glycoconjugate formulas **1**, **2**, **3**, and **4**; **(B)**: glycoconjugate formulas **5**, **6**, **7**, and **8**; 10 and 100 μg/mL); **(C)**: *C. albicans* mannan (M, 10 and 100 μg/mL), lipopolysaccharide (LPS, 1 μg/mL), Concanavalin A (Con A, 10 μg/mL), phytohemagglutinin (PHA, 10 μg/mL) and pokeweed mitogen (PWM, 1 μg/mL) for 24 and 48 h. Each value represents the mean ± SD of the proliferation index. The statistical significance of differences between stimulated cells and untreated cells are expressed: *$0.01 < P < 0.05$, **$0.001 < P < 0.01$, ***$P < 0.001$.

The stimulation of RAW 264.7 macrophages with glycoconjugate formulas **5–8** showed a different impact on TNFα production compared to glycoconjugate formulas **1–4** (**Supplementary Figure 2**). Higher TNFα production was observed during the shorter exposure period (24 h). The higher tested concentration (100 μg/mL) significantly increased TNFα production, with maximal efficacy for glycoconjugate formula **6** (24 h: 29.4-fold increase, 48 h: 13.4-fold increase compared to the control). Production of IL-6, GM-CSF, IL-17, and IL-12 also showed a concentration dependency, with higher efficacy for the higher concentrations of glycoconjugate formulas **5–8** (100 μg/mL). The highest IL-6 secretion was induced by glycoconjugate formula **6** (**Supplementary Figure 2**, 24 h: 48.8-fold increase, 48 h: 40.0-fold increase, compared to the control). Additionally, glycoconjugate formula **6** induced a strong increase in IL-17, IL-12, and IL-10 production (**Supplementary Figure 2**). Stimulation with β-mannooligosaccharides **6** and **8** for 24 h markedly increased the production of TNFα (100 μg/mL, $p < 0.001$), IL-6 (100 μg/mL, $p < 0.001$), IL-12 (100 μg/mL, $p < 0.001$), and IL10 (100 μg/mL, $p < 0.001$) compared with natural *C. albicans* mannan.

Due to the tested glycoconjugates having a significant effect on RAW 264.7 macrophage proliferation, especially for glycoconjugate formulas **1–4** that contain α-linked Man residues, the raw data of cytokine concentrations in the culture supernatants were normalized to the viable cell counts of untreated control RAW 264.7 cells for each experiment. We observed that the normalization of cytokine concentration data showed no significant trend change for stimulation of RAW 264.7 macrophages with the β-mannooligosaccharide glycoconjugates (formulas **5–8**) (**Figure 6**). Out of all tested β-mannooligosaccharide glycoconjugates, the most effective cytokine inducers were glycoconjugate formulas **6** and **8**. The highest TNFα (24 h: 23.2-fold increase), IL-6 (24 h, 38.5-fold increase), IL-12 (24 h: 15.6-fold increase), and IL-10 (24 h: 15.3-fold increase) secretion was induced by glycoconjugate formula **6**. The GM-CSF (24 h: 14.5-fold increase) and IL-17 (24 h: 3.1-fold increase) was most effectively induced by β-mannooligosaccharide glycoconjugate formula **8**. Normalization of the cytokine concentration data after stimulation with α-mannooligosaccharide glycoconjugates (formulas **1–4**) (**Figure 5**) accentuated the release of cytokines induced by the higher concentration of glycoconjugates (100 μg/mL). We observed significant capability to induce TNFα, IL-6, GM-CSF, IL-17, and IL-12 production accompanied by an increase of IL-10 after stimulation with all α-mannooligosaccharide glycoconjugates, induced especially with higher 100 μg/mL concentration, that strongly reduced the proliferation of RAW 264.7 cells. The highest production of TNFα, IL-6, GM-CSF, and IL-10 was observed after the shorter exposure time (24 h) with glycoconjugate formula **3**.

The influence of glycoconjugate formulas **1–8** on Th1 and Th2 polarization was revealed based on the TNFα (Th1) to IL-10 (Th2) and IL-6 (Th2) to IL-10 (Th2) ratios (**Figure 7**). Th1 dominance was represented by a higher ratio, while a lower ratio expressed a Th2 dominated environment. Concerning the ratios following 24 and 48 h exposures with 100 and 10 μg/mL of glycoconjugate formulas **1–4**, Th1 dominance based on the TNFα/IL-10 ratio was revealed for conjugate formulas **1** and **4**, while conjugate formulas **2** and **3** exerted Th1 dominance with higher TNFα/IL-10 ratios over IL-6/IL-10 ratios only at the lower concentration (10 μg/mL) after 48 h exposure. For conjugate formulas **5–8**, the values of the TNFα/IL-10 ratios overcame the values of the IL-6/IL-10 ratios following 24 and 48 h exposures with both concentrations for all conjugates, reflecting Th1 dominance.

The resulting *in vitro* proinflammatory effect of glycoconjugate formulas **5-8**, containing terminal β-mannosyls, overcame that of the α-mannooligosaccharides. This was supported by statistically insignificant correlations between the release of proinflammatory cytokines following 24 and 48 h exposures with α-mannooligosaccharides. Significant overall correlations were determined between the release of proinflammatory cytokines induced by individual β-mannooligosaccharides glycoconjugate formulas following 24 h exposure: TNFα and IL-6 ($R = 0.994$ $p = 5.38 \times 10^{-7}$), TNFα and IL-12 ($R = 0.969$ $p = 6.71 \times 10^{-5}$), and IL-12 and IL-6 (R

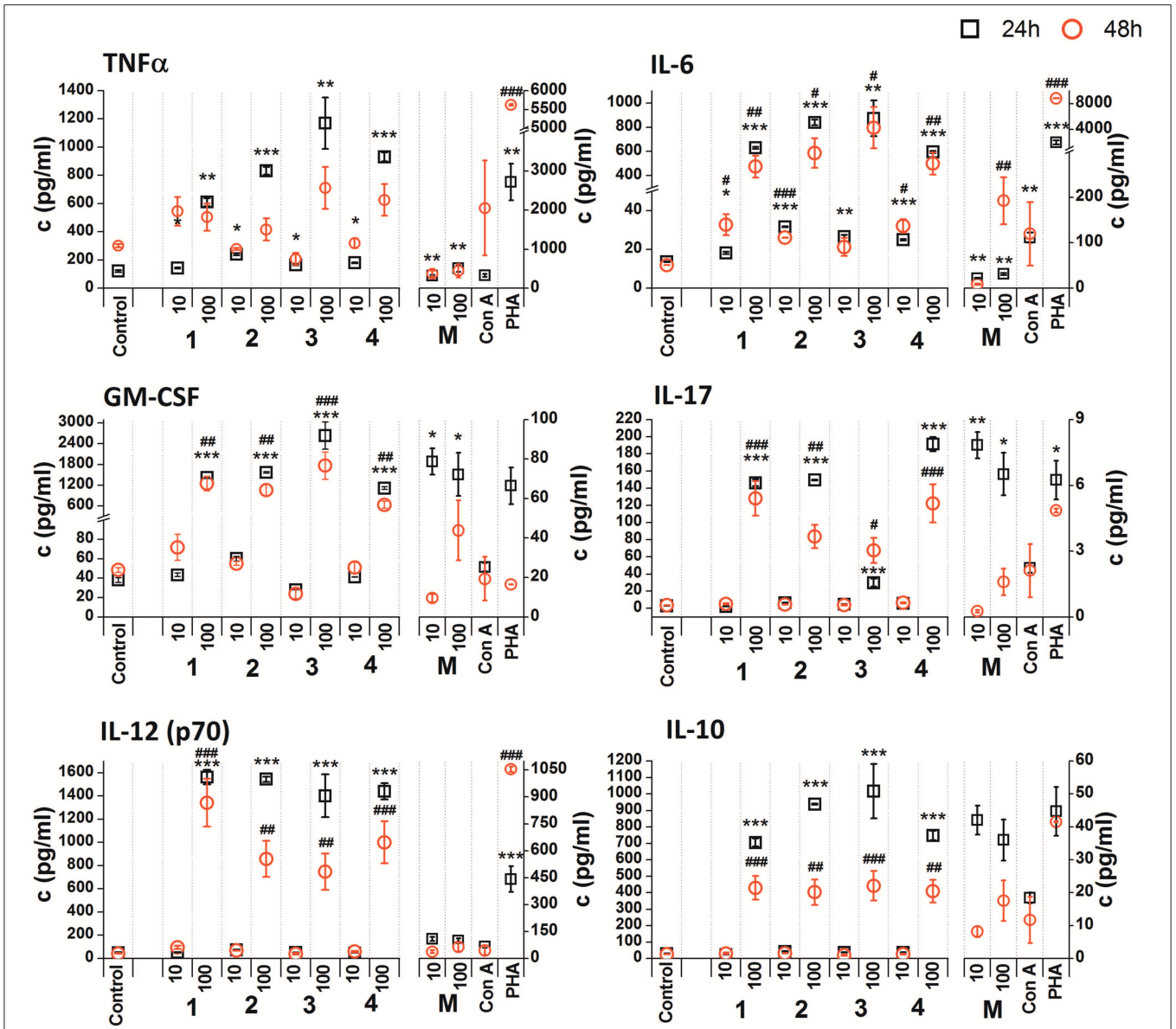

FIGURE 5 | Effect of glycoconjugate formulas **1**–**4** on RAW 264.7 macrophage cytokine production. Negative control represents untreated cells (Control); positive controls: *C. albicans* mannan (M, 10 or 100 μg/mL), Concanavaline A (Con A, 10 μg/mL) and phytohemagglutinin (PHA, 10 μg/mL). All data were normalized to the viable cells' count of untreated control cells of each experiment and are presented as Mean ± SD. Tests were carried out in triplicate. The statistical significance of differences between untreated cells and stimulated cells are expressed: 24 h treatment: $^{***}P < 0.001$, $^{**}0.001 < P < 0.01$, $^{*}0.01 < P < 0.05$; 48 h treatment: $^{\#\#\#}P < 0.001$, $^{\#\#}0.001 < P < 0.01$, $^{\#}0.01 < P < 0.05$.

$= 0.989$ $p = 2.61 \times 10^{-6}$). After 48 h, a significant correlation was also revealed between IL-17 and IL-12 ($R = 0.877$ $p = 0.0042$).

DISCUSSION

Several attempts have been made to synthesize relevant mannan epitopes with immunobiological effectiveness. Synthetically prepared mannooligosaccharides mimicking *Candida* antigenic factors (Karelin et al., 2010, 2015, 2016, 2017) represent promising study models to establish the immunomodulating activity of such formulas on humoral and cellular immunity for subcellular anti-*Candida* vaccine construction (Paulovicova et al., 2010, 2012, 2014; Paulovicova L. et al., 2013).

The immunobiological importance and vaccination potency of synthetically prepared β-1,2-mannopyranosyl trisaccharide mimicking the structure of the *C. albicans* cell surface epitope has previously been studied (Xin et al., 2008, 2012; Costello and Bundle, 2012; Cartmell et al., 2015; Bundle et al.,

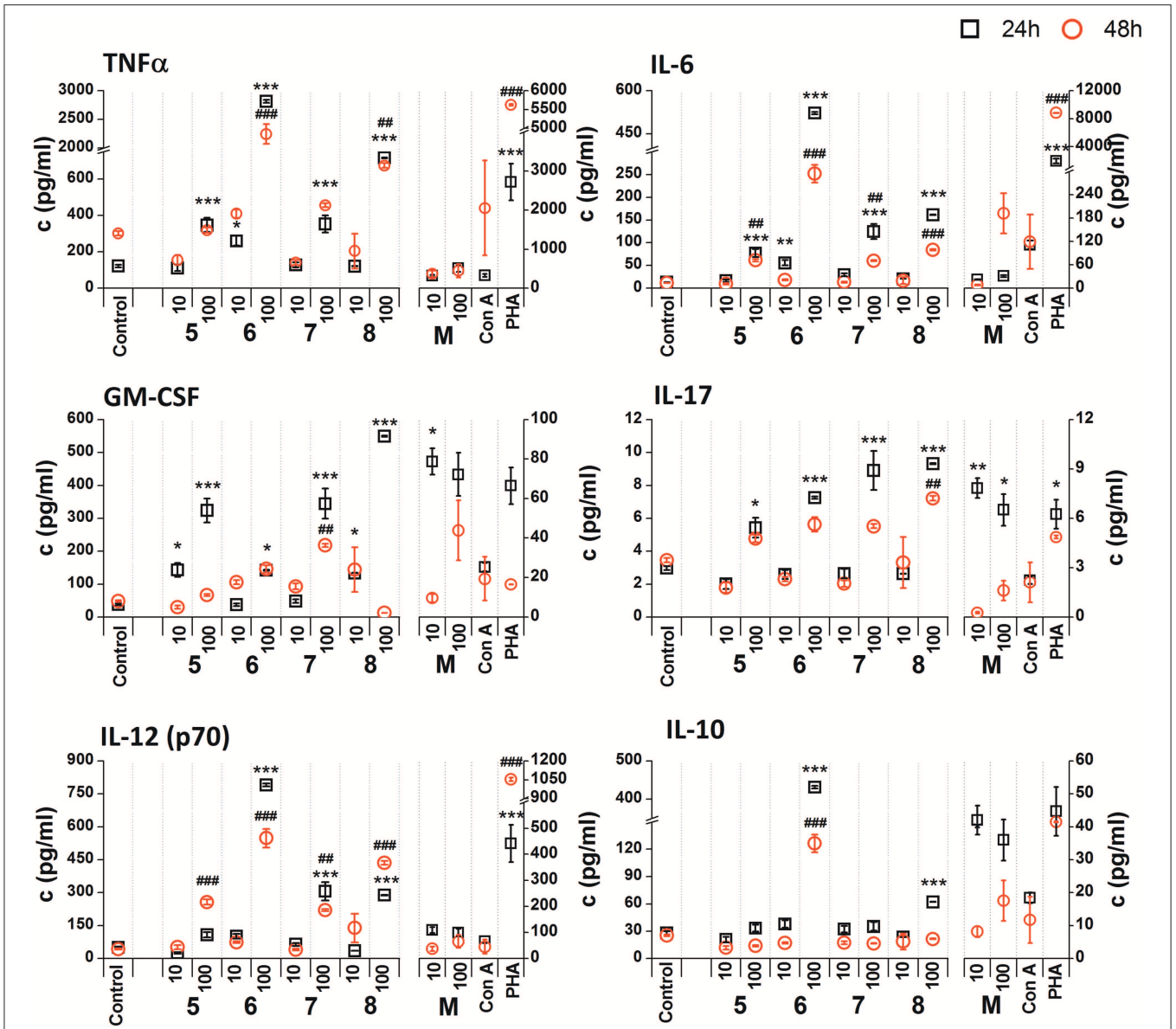

FIGURE 6 | Effect of glycoconjugate formulas **5**–**8** on RAW 264.7 macrophage cytokine production. Negative control represents untreated cells (Control); positive controls: *C. albicans* mannan (M, or 100 μg/mL), Concanavaline A (Con A, 10 μg/mL) and phytohemagglutinin (PHA, 10 μg/mL). All data were normalized to the viable cells' count of untreated control cells of each experiment and are presented as mean ± SD. Tests were carried out in triplicate. The statistical significance of differences between untreated cells and stimulated cells are expressed as follows: 24 h treatment: $^{***}P < 0.001$, $^{**}0.001 < P < 0.01$, $^{*}0.01 < P < 0.05$; 48 h treatment: $^{\#\#\#}P < 0.001$, $^{\#\#}0.001 < P < 0.01$, $^{\#}0.01 < P < 0.05$.

2018). Next, a novel tetrasaccharide construct consisting of β-1,2-mannopyranosyl trisaccharide and α-mannopyranoside was designed and suggested as a model of the *C. albicans* phosphodiester epitope (Dang et al., 2012). Glycoarrays formed by biotinylated oligosaccharides loaded on streptavidin-coated surfaces were previously shown to be indispensable instruments for the investigation of carbohydrate antigen recognition by immune cells (Komarova et al., 2015, 2018; Akhmatova et al., 2016; Paulovicova et al., 2016, 2017; Kurbatova et al., 2017; Argunov et al., 2019; Schubert et al., 2019).

Moreover, the sera reactivity and determination of antigen-specific isotypic antibodies against synthetically prepared mannooligosaccharides were evaluated in a cohort of patients with vulvovaginal candidosis (Karelin et al., 2016; Paulovicova et al., 2016, 2017). Postvaccination antisynthetic heptamannoside polyclonal sera inhibited growth of the azole-resistant clinical strain *C. albicans* CCY 29-3-164 and reduced the number of colony-forming units throughout an experimental mucosal infection (Paulovicova E. et al., 2013). Next, sera cytokine patterns of Th1/Th2/Th17 polarization of immune responses

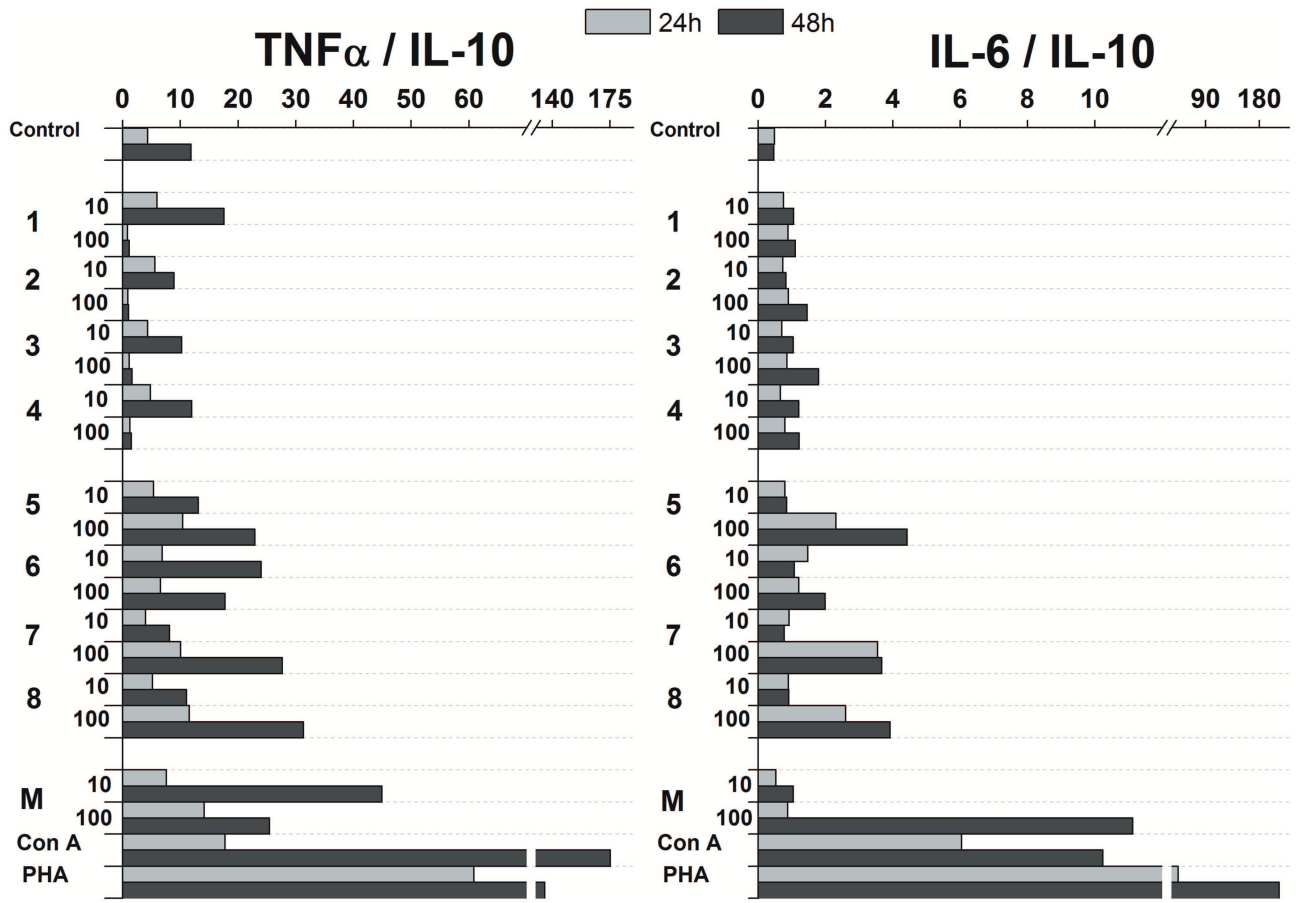

FIGURE 7 | Influence of glycoconjugate formulas **1–8** on Th1 and Th2 polarization based on TNFα to IL-10 and IL-6 to IL-10 ratios.

by synthetic oligosaccharide–BSA conjugates revealed a tight structure-activity relationship (Paulovicova E. et al., 2013; Paulovicova et al., 2017).

Here, the proliferating and cytokine-inducing activities of a series of synthetically prepared nanopolymers mimicking native *C. albicans* cell wall immunogenic moieties were studied using RAW264.7 cell exposure (**Figure 4**). The cell proliferation results revealed almost immunoinhibitory activity of α- mannoside formulas **1–4** (trisaccharide through hexasaccharide), with more pronounced activity with increasing concentration ($p < 0.001$), in contrast with native *C. albicans* cell wall mannan (**Figure 4**). These findings concur with previously published studies (Podzorski et al., 1989, 1990) that reported the immunoinhibitory influence of members of a family of mannose oligosaccharides (disaccharide through hexasaccharide) derived from cetyltrimethylammonium bromide (CTAB) mannan (native *C. albicans* mannan prepared by complexation with CTAB). CTAB mannan was a potent stimulator of lymphoproliferative when added to human peripheral blood mononuclear cells (PMBCs) from donors responsive to *Candida*; it had no inhibitory influence on lymphoproliferation induced by *Candida* or other antigens. Two major oligomannosyl components, mannobiose and mannotriose, of CTAB mannan with an inhibitory effect on cell proliferation were demonstrated to be bound mainly through α(1,2) linkages (Hayette et al., 1992). In contrast, synthetically prepared mannooligosaccharide formulas **5–8** with terminal β-mannosyl units (**Figure 3**) exerted a stimulatory effect on RAW264.7 cell proliferation ($p < 0.001$). Thus, the immunobiological properties of the studied mannooligosaccharides are dose- and structure-dependent. Cell release of interleukins and growth factors associated with inflammation and proliferation was induced by mannooligomers to different extents depending on the oligomer structures (normalized data: **Figures 5**, **6**, not normalized data: **Supplementary Figures 1**, **2**).

Upregulation of cytokines such as TNFα, IL-6, IL-12, GM-CSF was more evident with mannooligosaccharides with terminal β-mannosyl units. Acceleration of secretion of anti-inflammatory cytokine IL-10 with Th1-inhibiting properties was also revealed with β-mannooligosaccharides (**Supplementary Figure 2**). Association between pro- and anti-inflammatory cytokines, in addition to Th1, Th2 and Th17 polarization, is an important prerequisite for the assessment of immunogenic substance behavior. The influence of glycoconjugate formulas **1–8** on

Th1 and Th2 polarization, based on TNFα to IL-10 and IL-6 to IL-10 ratios (**Figure 7**), resulted in a predominant Th1 immune response. Th1 dominance, represented by higher TNFα/IL-10 and IL-6/IL-10 ratios with higher dose and following prolonged treatment, was revealed with tested **1**–**8** formulas, and was more evident for formulas **5**–**8** with β-terminal mannosyls; the Th2 dominated environment was not determined. The observed immune response was tightly associated with dose, exposure time, and selected signature cytokines. The TNFα/IL-10 ratio was more descriptive than the IL-6/IL-10 ratio, presumably due to dual IL-6 roles, i.e., anti-inflammatory activities of IL-6 are mediated by classic signaling, whereas proinflammatory responses of IL-6 are mediated by trans-signaling (Scheller et al., 2011). Saijo et al. reported induced release of cytokines, such as IL-12p40, IL-6, TNFα, and IL-10, from wild-type bone marrow-derived dendritic cells (BMDCs) by treatment with *C. albicans* water soluble fraction (CAWs) and *C. albicans* mannans (Saijo et al., 2010). Moreover, they also observed the secretion of yeast- and hyphae-specific cytokines following cell exposure with both *C. albicans* morphoforms. *C. albicans* mannan, glucomannoprotein and phospholipomannan, containing β-1,2 oligomannosides, induced TNFα in association with degree of polymerization (DP). Jouault et al. noted that TNFα-release occurred most in the presence of relatively long chains of β-oligomannosides (i.e., an oligomannoside comprised of eight mannose units was superior to shorter chains, and oligomannosides of less than four mannose units were not active) (Jouault et al., 1995). Evidently a minimal DP of 4 was necessary to induce production of cytokine (Poulain et al., 1997). With synthetically prepared α- and β- oligomannosides, effective TNFα release was triggered by trimannosides. The ability of β-oligomannosides to induce release of TNFα was also demonstrated by Cutler (2001).

Additionally, cell exposure to conjugate formula **6**, which comprises 2 β and 3α mannosyls, exerted the highest media release of IL-12p70, IL-6, TNFα, and IL-10 (**Figure 6**). Interestingly, conjugate formula **8**, with 4β and 2α-linked mannosyls, induced higher IL-17 and regulatory GM-CSF cell release than the other β-oligomannosides (**Figure 6**).

CONCLUSIONS

Our data suggest an immunobiological role for synthesized mannooligosaccharides that closely resemble *Candida* cell wall mannooligomers. The observed Th1/Th2/Th17 immune responses were tightly associated with structure, dose, exposure time, and selected signature cytokines. Glycoconjugate formulas **5**–**8**, with terminal β-mannosyl-units, tended to be more potent than glycoconjugate formulas **1**–**4** in terms of *Candida* relevant cytokines IL-12 p70, IL-17, GM-CSF, IL-6, and TNFα induction and cell proliferation, and this tendency was associated with structural differences between the studied glycoconjugate formulas. Obtained results warrant further systematic investigation of the immunological properties of carbohydrate antigens of the *Candida* cell wall toward the selection of efficient structures suitable for application as immunomodulative agents either for *in vitro Candida* diagnostics or prospectively for subcellular anti-*Candida* vaccine design.

DATA AVAILABILITY STATEMENT

All datasets generated for this study are included in the article/**Supplementary Material**.

AUTHOR CONTRIBUTIONS

EP, LP, and NN contributed to the conception and design of the study, performed the immunobiological research and analyzed data, acquired funding, and prepared the original draft. PF performed the modification and characterization of mannan. AK, YT, and VK performed the chemical syntheses and analyzed data. All authors contributed to manuscript revision, read, and approved the submitted version.

FUNDING

The synthetic part of this work was supported by the Russian Science Foundation (grant 19-73-30017), while the immunological part of the work was supported by the Scientific Grant Agency of the Slovak Republic VEGA (project 2/0098/17) and the Slovak Research and Development Agency (contract N° APVV-15-0161).

SUPPLEMENTARY MATERIAL

The Supplementary Material for this article can be found online at: https://www.frontiersin.org/articles/10.3389/fcimb.2019.00378/full#supplementary-material

REFERENCES

Adiguzel, N., Karakurt, Z., Gungor, G., Yazicioglu Mocin, O., Acarturk, E., Sogukpinar, O., et al. (2010). Mortality rates and risk factors associated with nosocomial Candida infection in a respiratory intensive care unit. *Tuberkuloz ve toraks* 58, 35–43.

Akhmatova, N. K., Kurbatova, E. A., Akhmatov, E. A., Egorova, N. B., Logunov, D. Y., Gening, M. L., et al. (2016). The effect of a BSA conjugate of a synthetic hexasaccharide related to the fragment of capsular polysaccharide of *Streptococcus pneumoniae* type 14 on the activation of innate and adaptive immune responses. *Front. Immunol.* 7:248. doi: 10.3389/fimmu.2016.00248

Angiolella, L., Stringaro, A. R., De Bernardis, F., Posteraro, B., Bonito, M., Toccacieli, L., et al. (2008). Increase of virulence and its phenotypic traits in drug-resistant strains of *Candida albicans*. *Antimicrob. Agents Chemother.* 52, 927–936. doi: 10.1128/AAC.01223-07

Apostolopoulos, V., Pietersz, G. A., Tsibanis, A., Tsikkinis, A., Drakaki, H., Loveland, B. E., et al. (2006). Pilot phase III immunotherapy study in early-stage breast cancer patients using oxidized mannan-MUC1 [ISRCTN71711835]. *Breast Cancer Res.* 8:R27. doi: 10.1186/bcr1505

Argunov, D. A., Trostianetskaia, A. S., Krylov, V. B., Kurbatova, E. A., and Nifantiev, N. E. (2019). Convergent synthesis of oligosaccharides structurally related to galactan I and galactan II of *Klebsiella pneumoniae* and their use

in screening of antibody specificity. *Eur. J. Org. Chem.* 2019, 4226–4232 doi: 10.1002/ejoc.201900389

Ashman, R. B., and Papadimitriou, J. M. (1995). Production and function of cytokines in natural and acquired immunity to *Candida albicans* infection. *Microbiol. Rev.* 59, 646–672.

Bartheldyova, E., Turanek Knotigova, P., Zachova, K., Masek, J., Kulich, P., Effenberg, R., et al. (2019). N-Oxy lipid-based click chemistry for orthogonal coupling of mannan onto nanoliposomes prepared by microfluidic mixing: synthesis of lipids, characterisation of mannan-coated nanoliposomes and in vitro stimulation of dendritic cells. *Carbohydr. Polym.* 207, 521–532. doi: 10.1016/j.carbpol.2018.10.121

Beenhouwer, D. O. (2018). "Chapter 17 - Molecular basis of diseases of immunity," in *Molecular Pathology, 2nd Edn.* eds W. B. Coleman and G. J. Tsongalis (London: Academic Press), 329–345. doi: 10.1016/B978-0-12-802761-5.00017-1

Brown, G. D. (2006). Dectin-1: a signalling non-TLR pattern-recognition receptor. *Nat. Rev. Immunol.* 6, 33–43. doi: 10.1038/nri1745

Brown, G. D., and Gordon, S. (2001). Immune recognition. A new receptor for beta-glucans. *Nature* 413, 36–37. doi: 10.1038/35092620

Brown, G. D., Herre, J., Williams, D. L., Willment, J. A., Marshall, A. S., and Gordon, S. (2003). Dectin-1 mediates the biological effects of beta-glucans. *J. Exp. Med.* 197, 1119–1124. doi: 10.1084/jem.20021890

Brown, G. D., Taylor, P. R., Reid, D. M., Willment, J. A., Williams, D. L., Martinez-Pomares, L., et al. (2002). Dectin-1 is a major beta-glucan receptor on macrophages. *J. Exp. Med.* 196, 407–412. doi: 10.1084/jem.20020470

Bundle, D. R., Paszkiewicz, E., Elsaidi, H. R. H., Mandal, S. S., and Sarkar, S. (2018). A three component synthetic vaccine containing a beta-Mannan T-cell peptide epitope and a beta-Glucan dendritic cell ligand. *Molecules* 23:E1961. doi: 10.3390/molecules23081961

Cartmell, J., Paszkiewicz, E., Dziadek, S., Tam, P. H., Luu, T., Sarkar, S., et al. (2015). Synthesis of antifungal vaccines by conjugation of beta-1,2 trimannosides with T-cell peptides and covalent anchoring of neoglycopeptide to tetanus toxoid. *Carbohydr. Res.* 403, 123–134. doi: 10.1016/j.carres.2014.06.024

Collot, M., Loukou, C., Mallet, J.-M., and N.E., N. (2009). "Chemical synthesis of the oligosaccharidic fragments of yeast mannans," in *Progress in the Synthesis of Complex Carbohydrate Chains of Plant and Microbial Polysaccharides*, ed N. E. Nifantiev (Trivandrum: Transworld Research Network), 371–398.

Cortés, J. A., and Corrales, F. I. (2018). "Invasive candidiasis: epidemiology and risk factors," in Fungal *Infection*, eds É. S. d. Loreto and J. S. M. Tondolo (London: IntechOpe).

Costello, C., and Bundle, D. R. (2012). Synthesis of three trisaccharide congeners to investigate frame shifting of beta1,2-mannan homo-oligomers in an antibody binding site. *Carbohydr. Res.* 357, 7–15. doi: 10.1016/j.carres.2012.03.019

Cunha, C., and Carvalho, A. (2012). Host genetics and invasive fungal diseases: towards improved diagnosis and therapy? *Expert Rev. Anti Infect. Ther.* 10, 257–259. doi: 10.1586/eri.12.3

Cutler, J. E. (2001). N-glycosylation of yeast, with emphasis on *Candida albicans*. *Med. Mycol.* 39 (Suppl. 1), 75–86. doi: 10.1080/mmy.39.1.75.86

Cutler, J. E. (2005). Defining criteria for anti-mannan antibodies to protect against candidiasis. *Curr. Mol. Med.* 5, 383–392. doi: 10.2174/1566524054022576

Da Silva, C. A., Chalouni, C., Williams, A., Hartl, D., Lee, C. G., and Elias, J. A. (2009). Chitin is a size-dependent regulator of macrophage TNF and IL-10 production. *J. Immunol.* 182, 3573–3582. doi: 10.4049/jimmunol.0802113

Da Silva, C. A., Hartl, D., Liu, W., Lee, C. G., and Elias, J. A. (2008). TLR-2 and IL-17A in chitin-induced macrophage activation and acute inflammation. *J. Immunol.* 181, 4279–4286. doi: 10.4049/jimmunol.181.6.4279

Dang, A. T., Johnson, M. A., and Bundle, D. R. (2012). Synthesis of a *Candida albicans* tetrasaccharide spanning the beta1,2-mannan phosphodiester alpha-mannan junction. *Org. Biomol. Chem.* 10, 8348–8360. doi: 10.1039/c2ob26355f

Dennehy, K. M., Ferwerda, G., Faro-Trindade, I., Pyz, E., Willment, J. A., Taylor, P. R., et al. (2008). Syk kinase is required for collaborative cytokine production induced through Dectin-1 and Toll-like receptors. *Eur. J. Immunol.* 38, 500–506. doi: 10.1002/eji.200737741

Ernst, J. F., and Pla, J. (2011). Signaling the glycoshield: maintenance of the *Candida albicans* cell wall. *Int. J. Med. Microbiol.* 301, 378–383. doi: 10.1016/j.ijmm.2011.04.003

Erwig, L. P., and Gow, N. A. (2016). Interactions of fungal pathogens with phagocytes. *Nat. Rev. Microbiol.* 14, 163–176. doi: 10.1038/nrmicro.2015.21

Esteban, A., Popp, M. W., Vyas, V. K., Strijbis, K., Ploegh, H. L., and Fink, G. R. (2011). Fungal recognition is mediated by the association of dectin-1 and galectin-3 in macrophages. *Proc. Natl. Acad. Sci. U.S.A.* 108, 14270–14275. doi: 10.1073/pnas.1111415108

Forsberg, K., Woodworth, K., Walters, M., Berkow, E. L., Jackson, B., Chiller, T., et al. (2019). Candida auris: the recent emergence of a multidrug-resistant fungal pathogen. *Med. Mycol.* 57, 1–12. doi: 10.1093/mmy/myy054

Fukazawa, Y., Kagaya, K., Suzuki, M., and Shinoda, T. (1997). "Serological specificity and biological activity of cell wall polysaccharides of medically important yeasts," in *Fungal Cells in Biodefense Mechanism,* eds S. Suzuki and M. Suzuki (Tokyo: Saigon Publishing), 17–24.

Gantner, B. N., Simmons, R. M., Canavera, S. J., Akira, S., and Underhill, D. M. (2003). Collaborative induction of inflammatory responses by dectin-1 and Toll-like receptor 2. *J. Exp. Med.* 197, 1107–1117. doi: 10.1084/jem.20021787

Gow, N. A. R., Latge, J. P., and Munro, C. A. (2017). The fungal cell wall: structure, biosynthesis, and function. *Microbiol. Spectr.* 5, 1–25. doi: 10.1128/microbiolspec.FUNK-0035-2016

Hall, R. A., Bates, S., Lenardon, M. D., Maccallum, D. M., Wagener, J., Lowman, D. W., et al. (2013). The Mnn2 mannosyltransferase family modulates mannoprotein fibril length, immune recognition and virulence of *Candida albicans*. *PLoS Pathog.* 9:e1003276. doi: 10.1371/journal.ppat.1003276

Hall, R. A., and Gow, N. A. (2013). Mannosylation in *Candida albicans*: role in cell wall function and immune recognition. *Mol. Microbiol.* 90, 1147–1161. doi: 10.1111/mmi.12426

Han, Y., Ulrich, M. A., and Cutler, J. E. (1999). *Candida albicans* mannan extract-protein conjugates induce a protective immune response against experimental candidiasis. *J. Infect. Dis.* 179, 1477–1484. doi: 10.1086/314779

Harris, M., Mora-Montes, H. M., Gow, N. A., and Coote, P. J. (2009). Loss of mannosylphosphate from *Candida albicans* cell wall proteins results in enhanced resistance to the inhibitory effect of a cationic antimicrobial peptide via reduced peptide binding to the cell surface. *Microbiology* 155, 1058–1070. doi: 10.1099/mic.0.026120-0

Hayette, M. P., Strecker, G., Faille, C., Dive, D., Camus, D., Mackenzie, D. W., et al. (1992). Presence of human antibodies reacting with *Candida albicans* O-linked oligomannosides revealed by using an enzyme-linked immunosorbent assay and neoglycolipids. *J. Clin. Microbiol.* 30, 411–417.

Ito, J. I. (2011). T cell immunity and vaccines against invasive fungal diseases. *Immunol. Invest.* 40, 825–838. doi: 10.3109/08820139.2011.595472

Jouault, T., El Abed-El Behi, M., Martinez-Esparza, M., Breuilh, L., Trinel, P. A., Chamaillard, M., et al. (2006). Specific recognition of *Candida albicans* by macrophages requires galectin-3 to discriminate *Saccharomyces cerevisiae* and needs association with TLR2 for signaling. *J. Immunol.* 177, 4679–4687. doi: 10.4049/jimmunol.177.7.4679

Jouault, T., Lepage, G., Bernigaud, A., Trinel, P. A., Fradin, C., Wieruszeski, J. M., et al. (1995). Beta-1,2-linked oligomannosides from *Candida albicans* act as signals for tumor necrosis factor alpha production. *Infect. Immun.* 63, 2378–2381.

Karelin, A. A., Tsvetkov, Y. E., Kogan, G., Bystricky, S., and Nifantiev, N. E. (2007). Synthesis of oligosaccharide fragments of mannan from *Candida albicans* cell wall and their BSA conjugates. *Russ. J. Bioorg. Chem.* 33, 110–121. doi: 10.1134/S106816200701013X

Karelin, A. A., Tsvetkov, Y. E., and Nifantiev, N. E. (2017). Synthesis of oligosaccharides related to cell wall polysaccharides of the fungi *Candida* and *Aspergillus*. *Russ. Chem. Rev.* 86, 1073–1126. doi: 10.1070/RCR4750

Karelin, A. A., Tsvetkov, Y. E., Paulovičová, E., Paulovičová, L., and Nifantiev, N. E. (2015). Blockwise synthesis of a pentasaccharide structurally related to the mannan fragment from the *Candida albicans* cell wall corresponding to the antigenic factor 6. *Russ. Chem. Bull.* 64, 2942–2948. doi: 10.1007/s11172-015-1251-5

Karelin, A. A., Tsvetkov, Y. E., Paulovicova, E., Paulovicova, L., and Nifantiev, N. E. (2016). A blockwise approach to the synthesis of (1 -> 2)-linked oligosaccharides corresponding to fragments of the acid-stable beta-mannan from the *Candida albicans* cell wall. *Eur. J. Org. Chem.* 2016, 1173–1181. doi: 10.1002/ejoc.201501464

Karelin, A. A., Tsvetkov, Y. E., Paulovicova, L., Bystricky, S., Paulovicova, E., and Nifantiev, N. E. (2010). Synthesis of 3,6-branched oligomannoside fragments of the mannan from *Candida albicans* cell wall corresponding to the antigenic factor 4. *Carbohydr. Res.* 345, 1283–1290. doi: 10.1016/j.carres.2009.11.012

Kavishwar, A., and Shukla, P. K. (2006). Candidacidal activity of a monoclonal antibody that binds with glycosyl moieties of proteins of *Candida albicans*. *Med. Mycol.* 44, 159–167. doi: 10.1080/13693780500266038

Klis, F. M., de Groot, P., and Hellingwerf, K. (2001). Molecular organization of the cell wall of *Candida albicans*. *Med. Mycol.* 39 (Suppl. 1), 1–8. doi: 10.1080/744118876

Kogan, G., Pavliak, V., and Masler, L. (1988). Structural studies of mannans from the cell-walls of the pathogenic yeasts *Candida albicans* Serotype-A and serotype-B and *Candidia parapsilosis*. *Carbohydr. Res.* 172, 243–253. doi: 10.1016/S0008-6215(00)90858-9

Komarova, B. S., Orekhova, M. V., Tsvetkov, Y. E., Beau, R., Aimanianda, V., Latge, J. P., et al. (2015). Synthesis of a pentasaccharide and neoglycoconjugates related to fungal alpha-(1 -> 3)-glucan and their use in the generation of antibodies to trace *Aspergillus fumigatus* cell wall. *Chem. A Eur. J.* 21, 1029–1035. doi: 10.1002/chem.201404770

Komarova, B. S., Wong, S. S. W., Orekhova, M. V., Tsvetkov, Y. E., Krylov, V. B., Beauvais, A., et al. (2018). Chemical synthesis and application of biotinylated oligo-alpha-(1 –> 3)-d-glucosides to study the antibody and cytokine response against the cell wall alpha-(1 –> 3)-d-glucan of *Aspergillus fumigatus*. *J. Org. Chem.* 83, 12965–12976. doi: 10.1021/acs.joc.8b01142

Krylov, V. B., Paulovicova, L., Paulovicova, E., Tsvetkov, Y. E., and Nifantiev, N. E. (2017). Recent advances in the synthesis of fungal antigenic oligosaccharides. *Pure Appl. Chem.* 89, 885–898. doi: 10.1515/pac-2016-1011

Krylov, V. B., Petruk, M. I., Grigoryev, I. V., Lebedin, Y. S., Glushko, N. I., Khaldeeva, E. V., et al. (2018a). Study of the carbohydrate specificity of antibodies against *Aspergillus fumigatus* using the library of synthetic mycoantigens. *Russ. J. Bioorg. Chem.* 44, 80–89. doi: 10.1134/S1068162017060073

Krylov, V. B., Petruk, M. I., Karelin, A. A., Yashunuskii, D. V., Tsvetkov, Y. E., Glushko, N. I., et al. (2018b). Carbohydrate specificity of antibodies against yeast preparations of *Saccharomyces cerevisiae* and *Candida krusei*. *Appl. Biochem. Microbiol.* 54, 665–669. doi: 10.1134/S0003683818060108

Kurbatova, E. A., Akhmatova, N. K., Akhmatova, E. A., Egorova, N. B., Yastrebova, N. E., Sukhova, E. V., et al. (2017). Neoglycoconjugate of tetrasaccharide representing one repeating unit of the *Streptococcus pneumoniae* type 14 capsular polysaccharide induces the production of opsonizing IgG1 antibodies and possesses the highest protective activity as compared to hexa- and octasaccharide conjugates. *Front. Immunol.* 8:659. doi: 10.3389/fimmu.2017.00659

Li, X., Hou, Y., Yue, L., Liu, S., Du, J., and Sun, S. (2015). Potential targets for antifungal drug discovery based on growth and virulence in *Candida albicans*. *Antimicrob. Agents Chemother.* 59, 5885–5891. doi: 10.1128/AAC.00726-15

Linden, J. R., De Paepe, M. E., Laforce-Nesbitt, S. S., and Bliss, J. M. (2013). Galectin-3 plays an important role in protection against disseminated candidiasis. *Med. Mycol.* 51, 641–651. doi: 10.3109/13693786.2013.770607

Lowman, D. W., Ensley, H. E., Greene, R. R., Knagge, K. J., Williams, D. L., and Kruppa, M. D. (2011). Mannan structural complexity is decreased when *Candida albicans* is cultivated in blood or serum at physiological temperature. *Carbohydr. Res.* 346, 2752–2759. doi: 10.1016/j.carres.2011.09.029

Magliani, W., Conti, S., Salati, A., Vaccari, S., Ravanetti, L., Maffei, D. L., et al. (2004). Therapeutic potential of yeast killer toxin-like antibodies and mimotopes. *FEMS Yeast Res.* 5, 11–18. doi: 10.1016/j.femsyr.2004.06.010

McKenzie, C. G., Koser, U., Lewis, L. E., Bain, J. M., Mora-Montes, H. M., Barker, R. N., et al. (2010). Contribution of *Candida albicans* cell wall components to recognition by and escape from murine macrophages. *Infect. Immun.* 78, 1650–1658. doi: 10.1128/IAI.00001-10

Moragues, M. D., Omaetxebarria, M. J., Elguezabal, N., Sevilla, M. J., Conti, S., Polonelli, L., et al. (2003). A monoclonal antibody directed against a *Candida albicans* cell wall mannoprotein exerts three anti-C. albicans activities. *Infect. Immun.* 71, 5273–5279. doi: 10.1128/IAI.71.9.5273-5279.2003

Moyes, D. L., and Naglik, J. R. (2011). Mucosal immunity and *Candida albicans* infection. *Clin. Dev. Immunol.* 2011:346307. doi: 10.1155/2011/346307

Moyes, D. L., Richardson, J. P., and Naglik, J. R. (2015). *Candida albicans*-epithelial interactions and pathogenicity mechanisms: scratching the surface. *Virulence* 6, 338–346. doi: 10.1080/21505594.2015.1012981

Naglik, J. R. (2014). Candida immunity. *N. J. Sci.* 2014:27. doi: 10.1155/2014/390241

Netea, M. G., Brown, G. D., Kullberg, B. J., and Gow, N. A. (2008). An integrated model of the recognition of *Candida albicans* by the innate immune system. *Nat. Rev. Microbiol.* 6, 67–78. doi: 10.1038/nrmicro1815

Netea, M. G., Gow, N. A., Munro, C. A., Bates, S., Collins, C., Ferwerda, G., et al. (2006). Immune sensing of *Candida albicans* requires cooperative recognition of mannans and glucans by lectin and Toll-like receptors. *J. Clin. Invest.* 116, 1642–1650. doi: 10.1172/JCI27114

Netea, M. G., Joosten, L. A., van der Meer, J. W., Kullberg, B. J., and van de Veerdonk, F. L. (2015). Immune defence against *Candida* fungal infections. *Nat. Rev. Immunol.* 15, 630–642. doi: 10.1038/nri3897

Nishikawa, A., Shinoda, T., and Fukazawa, Y. (1982). Immunochemical determinant and serological specificity of *Candida krusei*. *Mol. Immunol.* 19, 367–373. doi: 10.1016/0161-5890(82)90202-4

Pashov, A., Monzavi-Karbassi, B., and Kieber-Emmons, T. (2011). Glycan mediated immune responses to tumor cells. *Hum. Vaccin.* 7, 156–165. doi: 10.4161/hv.7.0.14578

Paulovicova, E., Paulovicova, L., Hrubisko, M., Krylov, V. B., Argunov, D. A., and Nifantiev, N. E. (2017). Immunobiological activity of synthetically prepared immunodominant galactomannosides structurally mimicking *Aspergillus* galactomannan. *Front. Immunol.* 8:1273. doi: 10.3389/fimmu.2017.01273

Paulovicova, E., Paulovicova, L., Pilisiova, R., Bystricky, S., Yashunsky, D. V., Karelin, A. A., et al. (2013). Synthetically prepared glycooligosaccharides mimicking *Candida albicans* cell wall glycan antigens–novel tools to study host-pathogen interactions. *FEMS Yeast Res.* 13, 659–673. doi: 10.1111/1567-1364.12065

Paulovicova, E., Paulovicova, L., Pilisiova, R., Jancinova, V., Yashunsky, D. V., Karelin, A. A., et al. (2016). The evaluation of beta-(1 –> 3)-nonaglucoside as an anti-*Candida albicans* immune response inducer. *Cell. Microbiol.* 18, 1294–1307. doi: 10.1111/cmi.12631

Paulovicova, L., Bystricky, S., Paulovicova, E., Karelin, A. A., Tsvetkov, Y. E., and Nifantiev, N. E. (2010). Model alpha-mannoside conjugates: immunogenicity and induction of candidacidal activity. *FEMS Immunol. Med. Microbiol.* 58, 307–313. doi: 10.1111/j.1574-695X.2009.00642.x

Paulovicova, L., Paulovicova, E., and Bystricky, S. (2014). Immunological basis of anti-Candida vaccines focused on synthetically prepared cell wall mannan-derived manno-oligomers. *Microbiol. Immunol.* 58, 545–551. doi: 10.1111/1348-0421.12195

Paulovicova, L., Paulovicova, E., Karelin, A. A., Tsvetkov, Y. E., Nifantiev, N. E., and Bystricky, S. (2012). Humoral and cell-mediated immunity following vaccination with synthetic *Candida* cell wall mannan derived heptamannoside-protein conjugate Immunomodulatory properties of heptamannoside-BSA conjugate. *Int. Immunopharmacol.* 14, 179–187. doi: 10.1016/j.intimp.2012.07.004

Paulovicova, L., Paulovicova, E., Karelin, A. A., Tsvetkov, Y. E., Nifantiev, N. E., and Bystricky, S. (2013). Effect of branched -oligomannoside structures on induction of anti-Candida humoral immune response. *Scand. J. Immunol.* 77, 431–441. doi: 10.1111/sji.12044

Peat, S., Whelan, W. J., and Edwards, T. E. (1961). 6. Polysaccharides of baker's yeast. Part IV. Mannan. *J. Chem. Soc.* 29–34. doi: 10.1039/jr9610000029

Perez-Garcia, L. A., Diaz-Jimenez, D. F., Lopez-Esparza, A., and Mora-Montes, H. M. (2011). Role of cell wall polysaccharides during recognition of *Candida albicans* by the innate immune system. *J. Glycobiol.* 1, 1–7. doi: 10.4172/jgb.1000102

Pfaller, M. A., Messer, S. A., Hollis, R. J., and Jones, R. N. (2002). Antifungal activities of posaconazole, ravuconazole, and voriconazole compared to those of itraconazole and amphotericin B against 239 clinical isolates of *Aspergillus* spp. and other filamentous fungi: report from SENTRY Antimicrobial Surveillance Program, 2000. *Antimicrob. Agents Chemother.* 46, 1032–1037. doi: 10.1128/AAC.46.4.1032-1037.2002

Piccione, D., Mirabelli, S., Minto, N., and Bouklas, T. (2019). Difficult but not impossible: in search of an anti-Candida vaccine. *Curr. Trop. Med. Rep.* 6, 42–49. doi: 10.1007/s40475-019-00173-2

Pichard, D. C., Freeman, A. F., and Cowen, E. W. (2015). Primary immunodeficiency update: part II. Syndromes associated with mucocutaneous candidiasis and noninfectious cutaneous manifestations. *J. Am. Acad. Dermatol.* 73, 367–381; quiz 381–362. doi: 10.1016/j.jaad.2015.01.055

Pikman, R., and Ben-Ami, R. (2012). Immune modulators as adjuncts for the prevention and treatment of invasive fungal infections. *Immunotherapy* 4, 1869–1882. doi: 10.2217/imt.12.127

Podzorski, R. P., Gray, G. R., and Nelson, R. D. (1990). Different effects of native *Candida albicans* mannan and mannan-derived oligosaccharides on antigen-stimulated lymphoproliferation in vitro. *J. Immunol.* 144, 707–716.

Podzorski, R. P., Herron, M. J., Fast, D. J., and Nelson, R. D. (1989). Pathogenesis of candidiasis. Immunosuppression by cell wall mannan catabolites. *Arch. Surg.* 124, 1290–1294. doi: 10.1001/archsurg.1989.01410110044009

Poulain, D., Jouault, T., and Trinel, P. A. (1997). "Immunoreactivity of *Candida albicans* β-1,2 linked oligomannosides and phospholipomannan," in *Fungal Cells in Biodefense Mechanism*, eds. S. Suzuki and M. Suzuki (Tokyo: Saigon Publishing), 175–181.

Richardson, J. P., and Moyes, D. L. (2015). Adaptive immune responses to *Candida albicans* infection. *Virulence* 6, 327–337. doi: 10.1080/21505594.2015.1004977

Richter, S. S., Galask, R. P., Messer, S. A., Hollis, R. J., Diekema, D. J., and Pfaller, M. A. (2005). Antifungal susceptibilities of Candida species causing vulvovaginitis and epidemiology of recurrent cases. *J. Clin. Microbiol.* 43, 2155–2162. doi: 10.1128/JCM.43.5.2155-2162.2005

Rizzetto, L., Kuka, M., De Filippo, C., Cambi, A., Netea, M. G., Beltrame, L., et al. (2010). Differential IL-17 production and mannan recognition contribute to fungal pathogenicity and commensalism. *J. Immunol.* 184, 4258–4268. doi: 10.4049/jimmunol.0902972

Romani, L. (2003). "Cytokines of innate and adaptive immunity to *Candida albicans*," in *Cytokines and Chemokines in Infectious Diseases Handbook*, eds. M. Kotb and T. Calandra (Totowa, NJ: Humana Press), 227–241. doi: 10.1385/1-59259-309-7:227

Romani, L. (2011). Immunity to fungal infections. *Nat. Rev. Immunol.* 11, 275–288. doi: 10.1038/nri2939

Saijo, S., Ikeda, S., Yamabe, K., Kakuta, S., Ishigame, H., Akitsu, A., et al. (2010). Dectin-2 recognition of alpha-mannans and induction of Th17 cell differentiation is essential for host defense against *Candida albicans*. *Immunity* 32, 681–691. doi: 10.1016/j.immuni.2010.05.001

Salek-Ardakani, S., Cota, E., and Bignell, E. (2012). Host-fungal interactions: key players of antifungal immunity. *Expert Rev. Anti Infect. Ther.* 10, 149–151. doi: 10.1586/eri.11.169

Sandini, S., La Valle, R., De Bernardis, F., Macrì, C., and Cassone, A. (2007). The 65 kDa mannoprotein gene of *Candida albicans* encodes a putative β-glucanase adhesin required for hyphal morphogenesis and experimental pathogenicity. *Cell. Microbiol.* 9, 1223–1238. doi: 10.1111/j.1462-5822.2006.00862.x

Scheller, J., Chalaris, A., Schmidt-Arras, D., and Rose-John, S. (2011). The pro- and anti-inflammatory properties of the cytokine interleukin-6. *Biochim. Biophys. Acta* 1813, 878–888. doi: 10.1016/j.bbamcr.2011.01.034

Schubert, M., Xue, S., Ebel, F., Vaggelas, A., Krylov, V. B., Nifantiev, N. E., et al. (2019). Monoclonal antibody AP3 binds galactomannan antigens displayed by the pathogens *Aspergillus flavus*, *A. fumigatus*, and A. parasiticus. *Front. Cell. Infect. Microbiol.* 9:234. doi: 10.3389/fcimb.2019.00234

Sears, D., and Schwartz, B. S. (2017). *Candida auris*: an emerging multidrug-resistant pathogen. *Int. J. Infect. Dis.* 63, 95–98. doi: 10.1016/j.ijid.2017.08.017

Shibata, N., Ikuta, K., Imai, T., Satoh, Y., Satoh, R., Suzuki, A., et al. (1995). Existence of branched side chains in the cell wall mannan of pathogenic yeast, *Candida albicans*. Structure-antigenicity relationship between the cell wall mannans of *Candida albicans* and Candida parapsilosis. *J. Biol. Chem.* 270, 1113–1122. doi: 10.1074/jbc.270.3.1113

Shibata, N., Kobayashi, H., and Suzuki, S. (2012). Immunochemistry of pathogenic yeast, Candida species, focusing on mannan. *Proc. Jpn. Acad. Ser. B Phys. Biol. Sci.* 88, 250–265. doi: 10.2183/pjab.88.250

Shibata, N., Suzuki, A., Kobayashi, H., and Okawa, Y. (2007). Chemical structure of the cell-wall mannan of *Candida albicans* serotype A and its difference in yeast and hyphal forms. *Biochem. J.* 404, 365–372. doi: 10.1042/BJ20070081

Snarr, B. D., Qureshi, S. T., and Sheppard, D. C. (2017). Immune recognition of fungal polysaccharides. *J. Fungi* 3:47. doi: 10.3390/jof3030047

Suzuki, M., and Fukazawa, Y. (1982). Immunochemical characterization of *Candida albicans* cell wall antigens: specific determinant of *Candida albicans* serotype A mannan. *Microbiol. Immunol.* 26, 387–402. doi: 10.1111/j.1348-0421.1982.tb00189.x

Suzuki, S. (1997). "Structural investigation of mannans of medicinally relevant Candida species; Determination of chemical structures of antigenic factors, 1, 4, 5, 6, 9 and 13b," in *Fungal Cells in Biodefense Mechanism*, eds S. Suzuki and M. Suzuki (Tokyo: Saigon Publishing), 1–16.

Tang, C. K., Sheng, K. C., Esparon, S. E., Proudfoot, O., Apostolopoulos, V., and Pietersz, G. A. (2009). Molecular basis of improved immunogenicity in DNA vaccination mediated by a mannan based carrier. *Biomaterials* 30, 1389–1400. doi: 10.1016/j.biomaterials.2008.11.010

Taylor, P. R., Tsoni, S. V., Willment, J. A., Dennehy, K. M., Rosas, M., Findon, H., et al. (2007). Dectin-1 is required for beta-glucan recognition and control of fungal infection. *Nat. Immunol.* 8, 31–38. doi: 10.1038/ni1408

Torosantucci, A., Bromuro, C., Chiani, P., De Bernardis, F., Berti, F., Galli, C., et al. (2005). A novel glyco-conjugate vaccine against fungal pathogens. *J. Exp. Med.* 202, 597–606. doi: 10.1084/jem.20050749

Trinel, P. A., Faille, C., Jacquinot, P. M., Cailliez, J. C., and Poulain, D. (1992). Mapping of *Candida albicans* oligomannosidic epitopes by using monoclonal antibodies. *Infect. Immun.* 60, 3845–3851.

Tso, G. H. W., Reales-Calderon, J. A., and Pavelka, N. (2018). The elusive anti-Candida vaccine: lessons from the past and opportunities for the future. *Front. Immunol.* 9:897. doi: 10.3389/fimmu.2018.00897

Tsvetkov, Y. E., Burg-Roderfeld, M., Loers, G., Arda, A., Sukhova, E. V., Khatuntseva, E. A., et al. (2012). Synthesis and molecular recognition studies of the HNK-1 trisaccharide and related oligosaccharides. The specificity of monoclonal anti-HNK-1 antibodies as assessed by surface plasmon resonance and STD NMR. *J. Am. Chem. Soc.* 134, 426–435. doi: 10.1021/ja2083015

van de Veerdonk, F. L., and Netea, M. G. (2010). T-cell subsets and antifungal host defenses. *Curr. Fungal Infect. Rep.* 4, 238–243. doi: 10.1007/s12281-010-0034-6

Varki, A., Cummings, R., Esko, J., Freeze, H., Hart, G., and Marth, J. (1999). *Essentials of Glycobiology*. New York, NY: Cold Spring Harbor.

Vinh, D. C. (2011). Insights into human antifungal immunity from primary immunodeficiencies. *Lancet Infect. Dis.* 11, 780–792. doi: 10.1016/S1473-3099(11)70217-1

Wagener, J., Malireddi, R. K., Lenardon, M. D., Koberle, M., Vautier, S., MacCallum, D. M., et al. (2014). Fungal chitin dampens inflammation through IL-10 induction mediated by NOD2 and TLR9 activation. *PLoS Pathog.* 10:e1004050. doi: 10.1371/journal.ppat.1004050

West, L., Lowman, D. W., Mora-Montes, H. M., Grubb, S., Murdoch, C., Thornhill, M. H., et al. (2013). Differential virulence of *Candida glabrata* glycosylation mutants. *J. Biol. Chem.* 288, 22006–22018. doi: 10.1074/jbc.M113.478743

Xin, H., Cartmell, J., Bailey, J. J., Dziadek, S., Bundle, D. R., and Cutler, J. E. (2012). Self-adjuvanting glycopeptide conjugate vaccine against disseminated candidiasis. *PLoS ONE* 7:e35106. doi: 10.1371/journal.pone.0035106

Xin, H., Dziadek, S., Bundle, D. R., and Cutler, J. E. (2008). Synthetic glycopeptide vaccines combining beta-mannan and peptide epitopes induce protection against candidiasis. *Proc. Natl. Acad. Sci. U.S.A.* 105, 13526–13531. doi: 10.1073/pnas.0803195105

Zheng, N. X., Wang, Y., Hu, D. D., Yan, L., and Jiang, Y. Y. (2015). The role of pattern recognition receptors in the innate recognition of *Candida albicans*. *Virulence* 6, 347–361. doi: 10.1080/21505594.2015.1014270

Conflict of Interest: The authors declare that the research was conducted in the absence of any commercial or financial relationships that could be construed as a potential conflict of interest.

frontiers in Cellular and Infection Microbiology

ORIGINAL RESEARCH
published: 12 November 2019
doi: 10.3389/fcimb.2019.00383

Fungal Chitin Reduces Platelet Activation Mediated via TLR8 Stimulation

Jordan Leroy[1,2,3], *Clovis Bortolus*[1,2], *Karine Lecointe*[1,2], *Melissa Parny*[1,2], *Rogatien Charlet*[1,2], *Boualem Sendid*[1,2,3] *and Samir Jawhara*[1,2*]

[1] INSERM, U995/Team2, Lille, France, [2] Lille Inflammation Research International Centre, University of Lille, U995-LIRIC, Lille, France, [3] Service de Parasitologie Mycologie, Pôle de Biologie Pathologie Génétique, CHU Lille, Lille, France

Platelets play an important role in the innate immune response. During candidaemia, circulating fungal polysaccharides, including chitin, are released into the bloodstream and can interact with platelets and induce modulation of platelet activities. However, the role of circulating chitin in platelet modulation has not been investigated. The aims of the present study were to assess the effect of fungal chitin on activation, adhesion, aggregation and receptor expression of platelets and their impact on the host defense against *Candida albicans*. Platelets pre-treated with different concentrations of chitin (10–400 μg/mL) extracted from *C. albicans* were analyzed in terms of activation, Toll-like receptor (TLR) expression, aggregation and adhesion to *C. albicans*. Chitin treatment reduced platelet adhesion to *C. albicans* and neutrophils. P-selectin expression was significantly decreased in platelets challenged with chitin. Aggregation and intracellular Ca^{2+} influx were also decreased in platelets. TLR8 mRNA and proteins were expressed in platelets pre-treated with chitin when compared to untreated platelets. Overall, chitin purified from *C. albicans* reduced the adhesion, activation and aggregation of platelets mediated via TLR8 stimulation by decreasing intracellular Ca^{2+} influx and P-selectin expression.

Keywords: *Candida albicans*, chitin, platelets, neutrophils, Toll-like receptor, P-selectin, thrombin, aggregation

OPEN ACCESS

Edited by:
Laura Alcazar-Fuoli,
Carlos III Health Institute, Spain

Reviewed by:
Slavena Vylkova,
Friedrich Schiller University Jena, Germany
Erika Shor,
Center for Discovery and Innovation, Hackensack Meridian Health, United States

***Correspondence:**
Samir Jawhara
samir.jawhara@univ-lille.fr

Specialty section:
This article was submitted to Fungal Pathogenesis, a section of the journal Frontiers in Cellular and Infection Microbiology

Received: *26 August 2019*
Accepted: *25 October 2019*
Published: *12 November 2019*

Citation:
Leroy J, Bortolus C, Lecointe K, Parny M, Charlet R, Sendid B and Jawhara S (2019) Fungal Chitin Reduces Platelet Activation Mediated via TLR8 Stimulation. Front. Cell. Infect. Microbiol. 9:383. doi: 10.3389/fcimb.2019.00383

INTRODUCTION

Platelets play a crucial role in haemostasis and wound healing (Livio et al., 1988). They are activated by multiple extracellular signals. On an injured endothelial surface, platelets adhere to the exposed subendothelial matrix through a large repertoire of adhesion receptors that lead to platelet activation, resulting in conformational changes to integrin $\alpha_{IIb}\beta_3$ that mediate platelet aggregation by binding to soluble fibrinogen. During this process, platelets start to change their shape by the formation of pseudopods when intracellular Ca^{2+} concentration exceeds a specific threshold and release the contents of their granules including P-selectin (Livio et al., 1988; Guidetti et al., 2019).

Platelets also participate in different immunological processes, including intervention against microbial threat. Platelets interact with various pathogenic fungi including *Candida* species. It has been reported that intravenous (IV) injection of different *Candida* species in mice resulted in the rapid adhesion of platelets to *Candida* and the generation of *C. albicans* pseudohyphal forms (Robert et al., 2000).

In the rabbit model, IV injection of *Candida* results in the formation of massive vegetations and promotes the adhesion of *C. albicans* to fibrin-platelet-erythrocyte deposits (Calderone et al., 1978).

C. albicans is a human commensal yeast and a natural saprophyte of the digestive and vaginal microbiota. Excessive colonization of the digestive mucosa by *C. albicans* is associated with multiple risk factors including immunosuppression and alteration of the mucosal barrier promoting translocation of the yeast through the digestive tract into the blood leading to severe invasive fungal infections. Interaction between the fungus and platelets involves the cell wall, which consists predominantly of polysaccharides associated with proteins and lipids (Gow et al., 2012). Its innermost layers are formed from a dense network of polysaccharides consisting of chitin and β-glucans, which are responsible for the resistance of the cell wall to chemical agents and mechanical action (Gow et al., 2012).

During infection, fungal cell wall components are released into the bloodstream and can be detected up to 10 days before the onset of clinical signs of invasive candidiasis (Sendid et al., 2008, 2013). The fungal cell wall is a dynamic structure and is in perpetual change (Poulain et al., 2009). During hyphal formation, *C. albicans* contains 3–4 times more chitin than in its yeast phase.

Chitin is the second most abundant natural biopolymer of β-1,4-N-acetylglucosamine (GlcNAc) in the world (Park and Kim, 2010). This polysaccharide is an essential component of the exoskeleton of arthropods and crustaceans and the fungal cell wall including that of *C. albicans*, contributing to its rigidity and viability (Mora-Montes et al., 2011). Oligomers of chitin or chito-oligosaccharides exert antimicrobial, anti-tumor and immunomodulatory properties (Park and Kim, 2010). Activation of dectin-1 and Toll-like receptor 2 (TLR2) in macrophages by *C. albicans* results in the activation of a signaling cascade that leads to chitotriosidase secretion that degrades chitin into small fragments. These chitins are recognized by NOD-2 and TLR9 receptors leading to the production of the anti-inflammatory cytokine interleukin (IL)-10 (Wagener et al., 2014). TLRs play a fundamental role in recognizing fungal cell wall components. TLR1, -2, and -4 have been widely described to recognize *C. albicans* (Netea et al., 2004; Choteau et al., 2017). Vancraeyneste et al. showed that soluble short fractions of β-glucans derived from *C. albicans* inhibit platelet activation mediated by TLR4 (Vancraeyneste et al., 2016). Clinically, chitins are released into the blood during fungal infection. Anti-chitin antibodies have also been detected in the serum of patients with candidaemia (Sendid et al., 2008; Poulain, 2015), but the role of chitin in platelet modulation has not yet been investigated (Sendid et al., 2008, 2013). In the current study, we investigated the effects of *C. albicans* chitin on platelet modulation in terms of adhesion, aggregation, activation and receptor expression.

MATERIALS AND METHODS

Ethics Statement

Healthy donors were informed and gave their written consent to participate in the present study. The study protocol was reviewed and approved by the Ethics Committee of Lille University Hospital. The study was conducted according to the principles expressed in the Declaration of Helsinki.

Preparation of Washed Platelets

Whole blood was collected from healthy donors. Platelets were isolated by differential centrifugation and then washed in modified Tyrode's buffer (2.7 mM KCl, 3.3 mM Na_2HPO_4, 137 mM NaCl, 1.2 mM $NaHCO_3$, 1 mg/ml bovine serum albumin, 3.8 mM HEPES, 5 mM glucose) (Byzova and Plow, 1997).

C. albicans Strain and Culture Conditions

C. albicans strain SC5314 was used in this study and maintained at 4°C in yeast peptone dextrose broth (YPD; 1% yeast extract, 2% peptone, 2% dextrose). To prepare the yeast suspension, *C. albicans* cells were cultured in Sabouraud dextrose broth (Sigma-Aldrich, St. Quentin Fallavier, France) for 24 h at 37°C in a rotary shaker. *C. albicans* cells were harvested by centrifugation. After washing several times with phosphate-buffered saline (PBS), *C. albicans* cells were resuspended in PBS.

Preparation of Chitin From *C. albicans*

C. albicans cell pellets were washed twice in PBS. Chitin was extracted from *C. albicans* yeast cells as described previously (Charlet et al., 2018b). Briefly, 20 mL of 10% KOH was added to the *C. albicans* cell pellet. This procedure was repeated twice and the pellet was autoclaved at 120°C for 2 h. After washing with distilled water, the supernatant was removed and 50% acetic acid and 50% hydrogen peroxide were added to the pellet, which was then autoclaved at 120°C for 2 h. After washing with distilled water, the pellet was centrifuged and the chitin fraction was lyophilized. Nuclear magnetic resonance (NMR) analysis was performed to confirm the nature of the chitin. Intact chitin purified from *C. albicans* was added to deuterated hexafluoroisopropanol (Euriso-Top) at 70°C until dissolved. All experiments were performed using a Bruker Avance 600 MHz (13.1 T) spectrometer with Bruker standard pulse programs. MALDI-TOF mass spectra were acquired on a Voyager Elite DE-STR mass spectrometer (Perspective Biosystems, Framingham, MA). A mixture of matrix (1 μL containing 10 mg/mL DHB and 5% acetonitrile) and 1 μL of sample was deposited on a MALDI plate. Small and large soluble chitin fragments were detected by MALDI-TOF mass spectrometry. A BiCinchoninic acid assay was employed to determine the chitin concentration extracted from *C. albicans* (Le Devedec et al., 2008). The standard range for the N-acetyl-glucosamine (GlcNAc) control was 0.1–5 mg/mL.

Platelet Adhesion to Neutrophils or *C. albicans*

Neutrophils were prepared from the peripheral blood of healthy donors by gradient centrifugation, according to the protocol of Pluskota et al. (2003). Fresh platelet poor plasma (200 μL) was added to each well of a 96-well plate and incubated for 2 h at 37°C (Clark et al., 2007). After several washes, a suspension of 10^6 neutrophils in 200 μL of RPMI medium containing 1 mM Mg^{2+}/Ca^{2+} was added to each well of a 96-well plate coated with

Abbreviations: *C. albicans*, *Candida albicans*; CTL, control; DNA, deoxyribonucleic acid; mAb, monoclonal antibody; PAMPs, pathogen associated molecular patterns; PBS, phosphate-buffered saline; RNA, ribonucleic acid; TLR, Toll-like receptor.

platelets. Non-adherent cells were removed and the wells were washed with Hank's balanced salt solution (HBSS) (Bouaouina et al., 2004). To assess platelet adhesion to *C. albicans*, 200 µL of RPMI medium containing 10^5 *C. albicans* cells was added to each well of a 96-well plate. This plate was then incubated at 37°C to allow *C. albicans* to adhere to the bottom of the plate. Thrombin-stimulated platelets (10^6 cells/mL) were labeled with calcein and then pre-treated for 30 min with chitin (20–200 µmol/L) incubated at 37°C for 20 min (Clark et al., 2007). After several washes, the percentage platelet adhesion to *C. albicans* or neutrophils was examined using a fluorometer (FLUOstar® Omega; BMG Labtech, Champigny sur Marne, France). To examine platelet adhesion to *C. albicans* by confocal microscopy, washed human platelets were stained with calcein and *C. albicans* cells were labeled with 5B2 monoclonal antibody (1:2,000 dilution) (Vancraeyneste et al., 2016). Slides were examined by confocal microscopy (Zeiss LSM710). For THP-1 cell culture, THP-1 cells were incubated in RPMI 1640 medium (Gibco by Life Technologies™, France) supplemented with 10% fetal bovine serum, 50 IU/mL penicillin and 50 IU/mL streptomycin. THP-1 cells were differentiated into macrophages in the presence of phorbol-12-myristate 13-acetate (100 nM; Sigma-Aldrich, St. Quentin Fallavier, France) at 37°C and 5% CO_2.

Platelet Aggregation Assay

Washed human platelets (10^8 cells/mL) were pre-treated with chitin (20 µmol/L) for 30 min in HBSS and then treated with thrombin (0.2 U/mL; Sigma-Aldrich, St. Quentin Fallavier, France) to promote platelet aggregation (Cambi et al., 2008). Platelet aggregation was assessed continuously after thrombin addition for 5–10 min using an aggregometer (Labor Biomedical Technologies Gmbh, LABITEC APACT 4004).

Intracellular Ca^{2+} Measurements

Ca^{2+} measurements were performed as described previously (Hussain and Mahaut-Smith, 1999). Briefly, 5 µM fura-2 acetoxymethyl ester (Invitrogen, France) and 0.2 µg/mL Pluronic F-127 were added to washed platelets pre-treated with different concentrations of chitin (20, 50, 100, or 200 µg/mL) in HBSS without Ca^{2+} at 37°C for 30 min. Platelets were then washed once and resuspended in HBSS. After platelet activation with thrombin (0.05 U/mL), the Ca^{2+} response was measured using a fluorometer (FLUOstar® Omega; BMG Labtech, Champigny sur Marne, France). The ratio of absorbance at 340/380 nm was converted into Ca^{2+} concentration (Ca^{2+}).

Analysis of the Expression/Activation of Platelet Receptors and Cell Wall Surface Glycan Expression of *C. albicans*

This was performed in RPMI medium (300 µL) containing 5 × 10^5 platelets/mL; RPMI medium does not induce platelet activation (Speth et al., 2013). Platelets were pre-treated with chitin at different concentrations (20–200 µmol/L) for 2 min and then activated with thrombin (0.05 U/mL). The activation or expression of platelet receptors was assessed using specific or isotype antibodies linked to fluorochromes (anti-human/mouse CD62P P-selectin, anti-human PAC-1, anti-mouse PE IgG1k, Brilliant Violet 421 anti-human CD41; Ozyme, France). After incubation for 30 min in the dark, platelets were washed twice with 300 µl PBS. The platelets were resuspended in 300 µL PBS. Specific isotype controls (mouse IgG1, κ Isotype Control Biolegend®, and mouse IgG1, κ Isotype Control BD Parmagen™) were used in each flow cytometry experiment. The expression/activation of platelet receptors was determined by flow cytometry (BD LSRFortesa® X20). Unstimulated or stimulated platelets with thrombin (0.05 U/mL) were used as controls for each experiment. The data obtained were analyzed using Kaluza software®. To examine the expression of platelet receptors by confocal microscopy, washed human platelets were labeled with TLR monoclonal antibodies (Vancraeyneste et al., 2016). Specific slides (wells 6.7 mm; Thermo Scientific, France) were used in this experiment and the coverslips were examined by confocal microscopy (Zeiss LSM710, Zeiss Airyscan SR mode x6311.4).

Real-Time PCR and Western Blot

A Nucleospin RNA/Protein kit (Macherey-Nagel, France) was used to isolate total RNA and proteins from platelets. Quantification of RNA in each sample was performed by spectrophotometry (Nanodrop; Nyxor Biotech, France). Reverse transcription of mRNA was performed in a final volume of 20 µL containing 1 µg total RNA (high capacity cDNA RT kit; Applied Biosystems). cDNA synthesis was performed according to the High Capacity DNA Reverse Transcription (RT) protocol, using Master Mix (Applied Biosystems). SYBR green dye intensity was determined using one-step software (Jawhara et al., 2008). All results were normalized to the reference gene, *GAPDH*. For Western blot analysis, proteins were recovered in lysis buffer (Tris/HCl 50 mM; Triton-X100, 1%; SDS 0.1%; EDTA 5 mM; NaCl 150 mM). The protein content of each sample was estimated using a BiCinchoninic acid protein assay (Pierce) and adjusted to the same protein concentration prior to analysis by SDS-PAGE on a 10% acrylamide gel [18]. Proteins are transfered onto a nitrocellulose membrane (iBlot 2; Thermofisher Scientific). Membranes were blocked with TBS-BSA 3% for 1 h and then incubated overnight with monoclonal anti-TLR (dilution 1:250) (TLR4 Biotechne®; TLR8 GeneTex®). Horseradish peroxidase-labeled secondary antibody (1:5,000 dilution) (Southern Biotech) were used to detect monoclonal antibodies.

Statistical Analysis

Statistical analysis was performed using XLSTAT and Prism 4.0 (GraphPad). Data were analyzed using the Mann-Whitney *U* test to compare pairs of groups. The results are expressed as the mean ± SD of individual experimental groups. Differences were considered significant when the *P*-value was <0.05.

RESULTS

Effect of Fungal Chitin on Platelet-*C. albicans* or Platelet-Neutrophil Interactions

Platelets can bind directly to different pathogens through different surface glycoproteins. In order to evaluate the effect

of chitin on the *C. albicans*-platelet adhesion process, we used an increasing concentration of fungal chitin ranging from 10 to 200 μg/mL.

These different chitin concentrations were used in the present study as there as there is no routine clinical test to measure the concentration of circulating chitin in the blood of patients with candidaemia.

Increasing concentrations of fungal chitin were associated with a decrease in percentage platelet adhesion to *C. albicans* (**Figure 1**). This decrease was significant for chitin concentrations ≥20 μg/mL. Activated platelets are crucial for the activation of neutrophils and in neutrophil-mediated inflammatory responses. The impact of chitin on platelet-neutrophil interactions was assessed. Platelets pre-treated with chitin (50, 100, or 200 μg/mL) showed a significant decrease in adhesion to neutrophils (**Figure 1**).

Effect of Chitin on Platelet Aggregation

In order to determine the effect of chitin on platelet aggregation involving $\alpha_{IIb}\beta_3$ integrin, platelets were pre-exposed to different chitin concentrations (50, 100, or 200 μg/mL) for 30 min and then stimulated with 0.2 U/mL thrombin (**Figure 2A**). A decrease in the percentage of platelet aggregation was observed in the presence of fungal chitin with a dose-dependent effect. There was a significant decrease in aggregation in the presence of chitin at a concentration of 100 or 200 μg/mL (**Figure 2B**).

Effect of Chitin on Platelet Activation and Receptor Expression

The effect of chitin on platelet activation was determined using fura-2, which exhibits an increase in fluorescence intensity on binding to intracellular Ca^{2+}. The concentration of intracellular calcium in platelets stimulated with thrombin (0.05 U/mL) was higher than that in unstimulated platelets (**Figure 2C**). Pre-treatment of platelets with chitin decreased the concentration of intracellular Ca^{2+} (**Figure 2C**). P-selectin expression, which is a crucial marker of platelet activation, was also investigated. Platelets were labeled with a specific CD41 marker by targeting the 2b chain of the alpha integrin of the GPIIb-IIIa complex. In the presence of thrombin, the majority of the $CD41^+$ platelet population expressed P-selectin while platelets pre-treated with chitin showed a significant decrease in platelet activation proportional to the fungal chitin concentration, with a greater effect of chitin at a concentration of 200 μg/mL suggesting that chitin has a dose-dependent effect (**Figure 3**). In parallel, the activation of integrin $\alpha_{IIb}\beta_3$ was assessed in thrombin-stimulated platelets pretreated with chitin at a concentration of 20 μg/mL (**Supplementary Data**). A significant decrease in integrin $\alpha_{IIb}\beta_3$ activation was observed in thrombin-stimulated platelets when

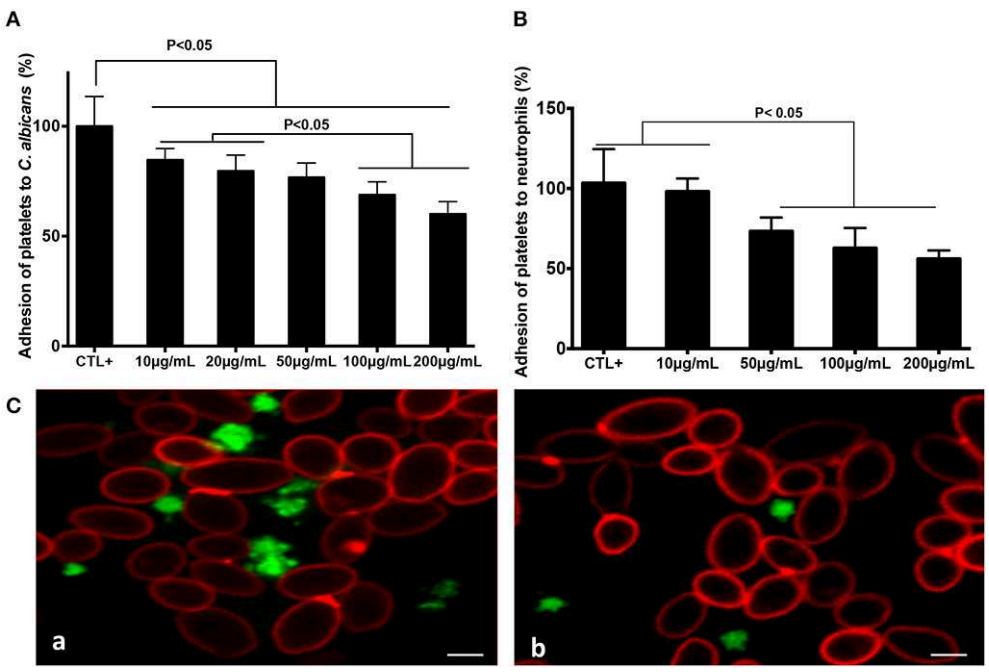

FIGURE 1 | Chitin reduced platelet adhesion to *C. albicans* and neutrophils. Platelet adhesion to *C. albicans* **(A)** or to neutrophils **(B)**. Calcein-labeled washed platelets (10^6 cells/mL) stimulated with thrombin (0.05 U/mL), and untreated as the control (CTL+) or pre-treated with chitin at different concentrations (10, 20, 50, 100, or 200 μg/mL), were incubated with either *C. albicans* or neutrophils. The data obtained from the adhesion of thrombin-activated platelets (CTL+) to *C. albicans* or to neutrophils were assigned a value of 100%. Data are the mean ± SD of five independent experiments (n = 3–4 per group). **(C)** Representative images of platelet adhesion to *C. albicans*. Calcein-labeled washed platelets (green) were untreated with chitin, but received only HBSS (a), or were pre-treated with chitin (b) and then incubated with *C. albicans*. *C. albicans* was stained with anti-phycoerythrin *C. albicans* antibody (5B2). Scale bar = 5 μm.

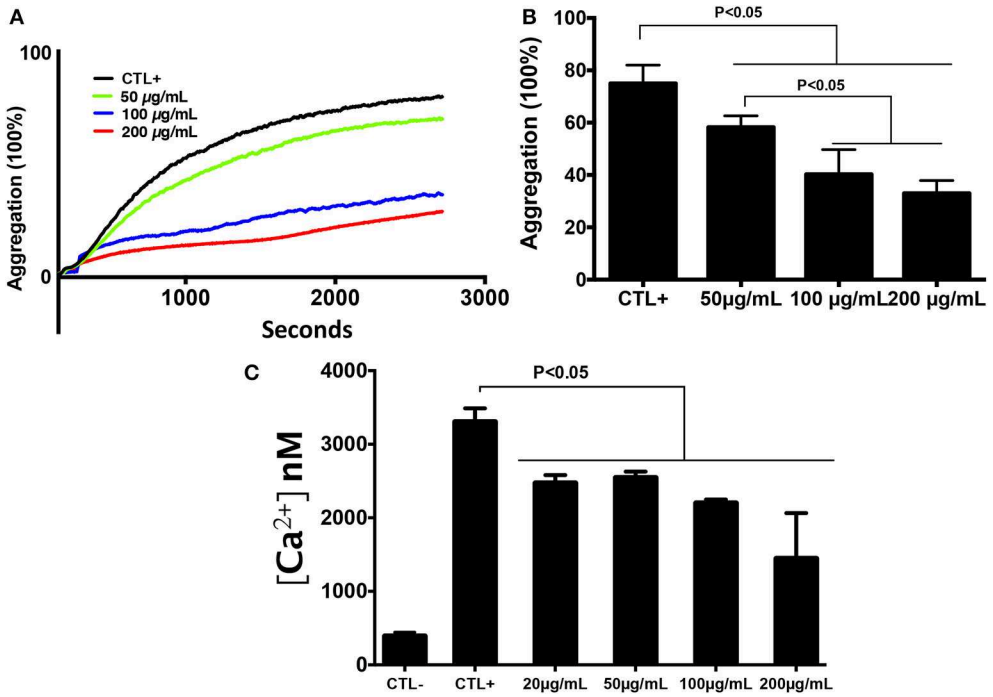

FIGURE 2 | Chitin reduced platelet aggregation and intracellular calcium concentration. **(A)** Representative aggregation curve. Untreated platelets or platelets pre-treated with chitin at different concentrations (50, 100, or 200 µg/mL) were activated with 0.2 U/mL thrombin. **(B)** Percent maximal aggregation in the presence of thrombin. Data are the mean ± SD of three independent experiments (n = 3–4 per group). **(C)** Fura-2 fluorescence reflecting cytosolic Ca^{2+} concentration [Ca^{2+}] of platelets pre-treated with chitin and stimulated with thrombin.

compared to those untreated with chitin. These data corroborate the aggregation assay showing that chitin pre-treatment reduces platelet aggregation.

Using PCR, we also investigated the expression of different TLRs that are known to sense many PAMP molecules, including chitin, promoting the host defense against pathogens (**Figure 4**). Western blot was then performed to confirm the expression of these receptors. A histone marker was used to exclude the presence of leukocytes in the platelet isolate. The human macrophage-differentiated THP-1 cell line was employed as a control. Platelet isolation was histone-free, indicating that the platelet preparation was not contaminated with leukocytes. In terms of mRNA expression levels for TLR2, TLR4, and TLR9, no significant difference was observed between platelets pre-treated with chitin (50 µg/mL) and untreated platelets (**Figure 4**). In contrast, TLR8 mRNA was highly expressed in thrombin-activated platelets pre-treated with chitin compared to that in untreated platelets, and this expression was concentration-dependent, indicating that chitin and thrombin stimulation modulate TLR8 mRNA expression.

The mRNA data correlated with those of Western blot analysis showing that TLR4 expression is independent of chitin exposure while high expression levels of TLR8 were detected in thrombin-activated platelets pre-treated with increasing concentrations of chitin (**Figure 5**). We performed quantification of Western Blot band intensity corresponding to platelets alone (CTL–), platelets in the presence of thrombin (CTL+) and thrombin-stimulated platelets pre-treated with chitin at different concentrations, using ImageJ bundled with 64-bit Java 1.8.0-112. The intensity of each band was normalized to that of beta-actin. We observed an increase in TLR8 band intensity with an increase in chitin concentration (**Supplementary Data**). In parallel, we examined the expression of TLR8 and TLR9 platelet receptors by confocal microscopy. In contrast to TLR9, TLR8 expression was only detected in thrombin-activated platelets pre-treated with chitin (**Figure 5B**).

DISCUSSION

Circulating fungal polysaccharides are in contact with immune cells, including platelets, and these polysaccharides play an important role in modulation of the host response (Poulain et al., 2009; Poulain, 2015). Different studies show that β-glucans derived from *C. albicans* play a crucial role in modulation of the host response, including platelets, but little is known about the effect of fungal chitin on platelet modulation (Jawhara et al., 2012; Vancraeyneste et al., 2016; Charlet et al., 2018a). In the present study, we assessed the effect of chitin purified from the cell wall of *C. albicans* on platelet modulation. During infection, platelets interact directly with leukocytes or pathogens. Pre-treatment of platelets with fungal chitin decreased platelet adhesion to *C. albicans* but also to neutrophils, suggesting that chitin promotes the escape of *C. albicans* from immune cells. We also showed that after platelet activation by thrombin, intracellular Ca^{2+} influx

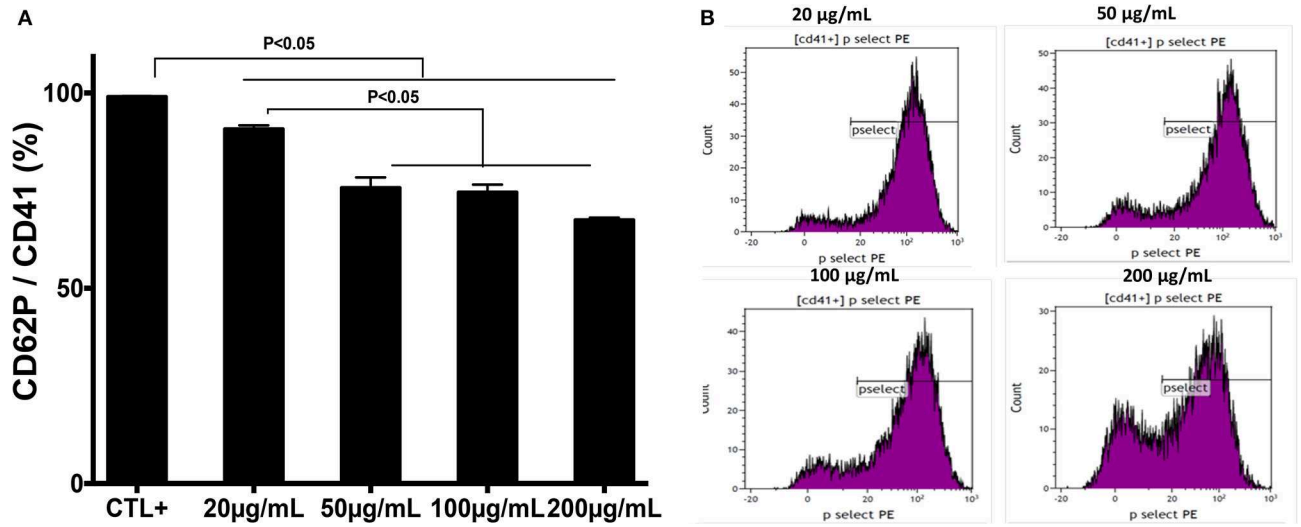

FIGURE 3 | Pre-treatment of platelets with chitin decreases P-selectin expression. **(A)** Platelets (5×10^5 cells/mL) were activated with thrombin (0.05 U/mL) and pre-treated with chitin at a concentration of 20, 50, 100, or 200 µg/mL. CTL+ corresponds to thrombin-activated platelets without chitin treatment. **(B)** The red curve shows the thrombin-activated platelet population treated with chitin at 20, 50, 100, or 200 µg/mL and detected with anti-P-selectin antibodies. Curves are representative of three separate experiments.

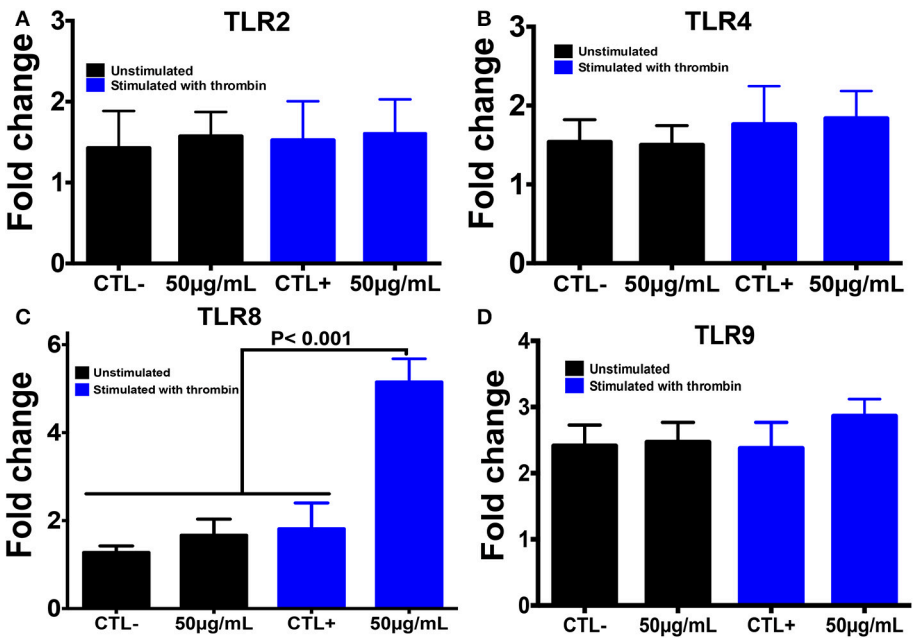

FIGURE 4 | Chitin increases TLR8 expression in thrombin-stimulated platelets. **(A–D)** Relative expression levels of TLR2, TLR4, TLR8, and TLR9 mRNA, respectively, in platelets by real-time PCR. CTL– (control) corresponds to unstimulated platelets, CTL+ (control) represents platelets stimulated with thrombin (0.05 U/mL). 50 µg/mL corresponds to chitin concentration. Data are the mean ± SD of three independent experiments.

increased in platelets. This influx led to platelet aggregation while pre-treatment of platelets with chitin reduced intracellular Ca^{2+} and platelet aggregation. Different studies show that platelet aggregation and enclosure of microorganisms in platelet-fibrin matrices offer protection to microorganisms from antibiotics or clearance by leukocytes (Clawson and White, 1971; Maisch and Calderone, 1981). Maish et al. showed that mannan derived from the *C. albicans* cell wall is involved in the adherence of *C. albicans* to fibrin-platelet matrices, which form *in vivo* on the endocardium of heart valves (Maisch and Calderone, 1981). It has been reported that β-1,3 glucans purified from *C. albicans* reduced platelet aggregation and platelet-*C. albicans*

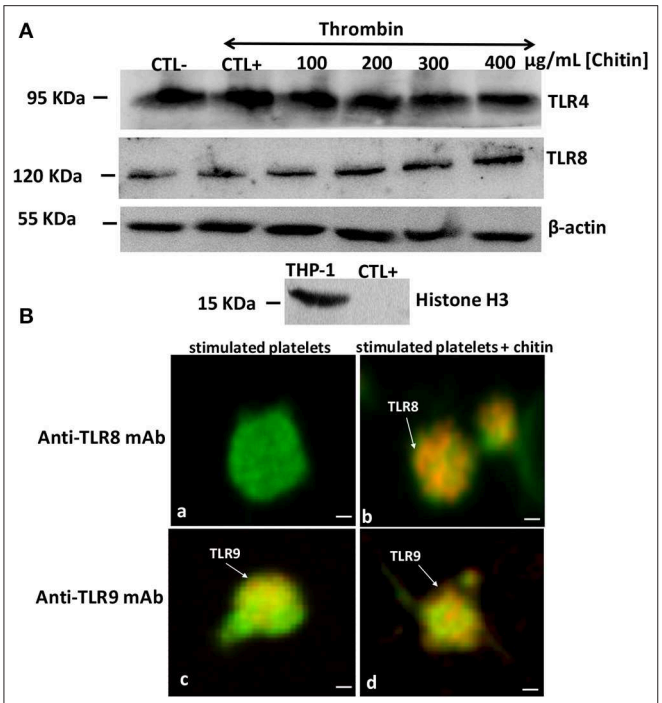

FIGURE 5 | Detection of TLR4 and TLR8 proteins in platelets by Western blot. **(A)** Platelets (10^6 cells/mL) without chitin treatment or thrombin stimulation (CTL–), platelets activated with thrombin at a concentration of 0.05 U/mL (CTL+), platelets activated with thrombin and pre-treated with chitin at different concentrations (100, 200, 300, or 400 µg/mL). Human macrophage-differentiated THP-1 cells used as a control and platelets were labeled with histone marker to exclude the presence of leukocytes in the platelet isolate. Western blots are representative of three independent experiments. **(B)** Representative images of TLR8 detection in platelets. (a,c) Calcein-labeled thrombin-stimulated platelets (green), untreated with chitin and labeled with either anti-TLR8 or anti-TLR9 antibody (red). (b,d) Calcein-labeled thrombin-stimulated platelets (green), pre-treated with chitin and labeled with either anti-TLR8 or anti-TLR9 antibody (red). Scale bar = 1 µm.

and platelet-neutrophil interactions, which protected *C. albicans* from leukocyte activation (Vancraeyneste et al., 2016).

P-selectin expression promotes the adhesion of platelets to leukocytes (Duerschmied et al., 2013; Kral et al., 2016). This platelet-leukocyte interaction induces the recruitment of neutrophils in infected tissues and increases the microbicidal activity of neutrophils (Kral et al., 2016). In this study, a decrease in P-selectin expression was observed in platelets pre-treated with chitin. These data corroborate those for aggregation and platelet adhesion to neutrophils, indicating the involvement of chitin in inhibiting platelet activation.

It is known that fungal polysaccharides can modulate the inflammatory response through their interactions with TLRs, but it remains unclear how fungal chitin modulates TLR expression in platelets (Choteau et al., 2017; Fuchs et al., 2018). TLRs play an important role in the recognition of PAMPs, including fungal chitin, promoting platelets to recognize pathogens in addition to their role in haemostasis (Ward et al., 2005; Schattner, 2019). Activation of platelets with thrombin induces an important modulation of TLR1, TLR6, and TLR9 during vascular lesions potentially mediated by bacterial infection (Shiraki et al., 2004). It has been shown that chitin induces TLR4 expression on keratinocytes at the mRNA and protein level (Koller et al., 2011). Wagener et al. demonstrated that chitin derived from *C. albicans* has the potential to attenuate the inflammatory response via TLR-9 and NOD-2 signaling in macrophages (Wagener et al., 2014). Additionally, Mora-Montes et al. showed that PBMC-treated fungal chitin blocked normal recognition of *C. albicans* cells (Mora-Montes et al., 2011). In a dextran sulfate sodium-induced colitis model, oral administration of fungal chitin reduced the inflammatory parameters and leukocyte infiltration into the gut mucosa and increased IL-10 production via stimulation of NOD-2 and TLR8 (Vancraeyneste et al., 2016). In the present study, a large panel of TLRs receptors were analyzed in platelets by RT-q-PCR (**Supplementary Data**). In contrast to macrophages differentiated from Thp1 cells pre-treated with chitin, which showed high mRNA transcript and protein expression of TLR2 (data not shown), we did not observe any increase in TLR2 mRNA transcripts or protein expression in thrombin-activated platelets pre-treated with chitin. TLR4 was expressed independently of chitin treatment. Of note, treatment of inactivated platelets with chitin did not show any significant increase in TLR8 mRNA levels, while TLR8 transcript levels were significantly increased in thrombin-activated platelets pre-treated with chitin. Additionally, TLR8 mRNA transcript levels in activated platelets were correlated with protein expression levels of TLR8 in a chitin concentration-dependent manner. These data suggest that fungal chitin promotes an increase in TLR8 in thrombin-activated platelets.

In conclusion, chitin purified from *C. albicans* reduces the adhesion, activation and aggregation of activated platelets mediated via TLR8 stimulation by decreasing intracellular Ca^{2+} influx and P-selectin expression. Overall, this study offers a new insight into the role of chitin in modulating platelet activities and platelet-neutrophil interactions, promoting the escape of *C. albicans* from the host defense.

DATA AVAILABILITY STATEMENT

All datasets generated for this study are included in the article/**Supplementary Material**.

ETHICS STATEMENT

The studies involving human participants were reviewed and approved by the Ethics Committee of Lille University Hospital. The patients/participants provided their written informed consent to participate in this study.

AUTHOR CONTRIBUTIONS

JL, CB, KL, MP, RC, and SJ performed the experiments. JL, CB, KL, MP, RC, BS, and SJ

analyzed the data and interpreted the results of the experiments. SJ designed the experiments and drafted the manuscript.

FUNDING

This work was partially funded by the Agence Nationale de la Recherche (ANR) in the setting the project InnateFun, promotional reference ANR-16-IFEC-0003-05, in the Infect-ERA program.

ACKNOWLEDGMENTS

The authors thank Ms. Nadine François, Ms. Nathalie Jouy, and Mr. Antonino Bongiovanni for their excellent technical assistance.

SUPPLEMENTARY MATERIAL

The Supplementary Material for this article can be found online at: https://www.frontiersin.org/articles/10.3389/fcimb.2019.00383/full#supplementary-material

REFERENCES

Bouaouina, M., Blouin, E., Halbwachs-Mecarelli, L., Lesavre, P., and Rieu, P. (2004). TNF-induced beta2 integrin activation involves Src kinases and a redox-regulated activation of p38 MAPK. *J. Immunol.* 173, 1313–1320. doi: 10.4049/jimmunol.173.2.1313

Byzova, T. V., and Plow, E. F. (1997). Networking in the hemostatic system. Integrin alphaiibbeta3 binds prothrombin and influences its activation. *J. Biol. Chem.* 272, 27183–27188. doi: 10.1074/jbc.272.43.27183

Calderone, R. A., Rotondo, M. F., and Sande, M. A. (1978). *Candida albicans* endocarditis: ultrastructural studies of vegetation formation. *Infect. Immun.* 20, 279–289.

Cambi, A., Netea, M. G., Mora-Montes, H. M., Gow, N. A., Hato, S. V., Lowman, D. W., et al. (2008). Dendritic cell interaction with *Candida albicans* critically depends on N-linked mannan. *J. Biol. Chem.* 283, 20590–20599. doi: 10.1074/jbc.M709334200

Charlet, R., Bortolus, C., Barbet, M., Sendid, B., and Jawhara, S. (2018a). A decrease in anaerobic bacteria promotes *Candida glabrata* overgrowth while beta-glucan treatment restores the gut microbiota and attenuates colitis. *Gut. Pathog.* 10:50. doi: 10.1186/s13099-018-0277-2

Charlet, R., Pruvost, Y., Tumba, G., Istel, F., Poulain, D., Kuchler, K., et al. (2018b). Remodeling of the *Candida glabrata* cell wall in the gastrointestinal tract affects the gut microbiota and the immune response. *Sci. Rep.* 8:3316. doi: 10.1038/s41598-018-21422-w

Choteau, L., Vancraeyneste, H., Le Roy, D., Dubuquoy, L., Romani, L., Jouault, T., et al. (2017). Role of TLR1, TLR2 and TLR6 in the modulation of intestinal inflammation and *Candida albicans* elimination. *Gut. Pathog.* 9:9. doi: 10.1186/s13099-017-0158-0

Clark, S. R., Ma, A. C., Tavener, S. A., Mcdonald, B., Goodarzi, Z., Kelly, M. M., et al. (2007). Platelet TLR4 activates neutrophil extracellular traps to ensnare bacteria in septic blood. *Nat. Med.* 13, 463–469. doi: 10.1038/nm1565

Clawson, C. C., and White, J. G. (1971). Platelet interaction with bacteria. II. Fate of the bacteria. *Am. J. Pathol.* 65, 381–397.

Duerschmied, D., Suidan, G. L., Demers, M., Herr, N., Carbo, C., Brill, A., et al. (2013). Platelet serotonin promotes the recruitment of neutrophils to sites of acute inflammation in mice. *Blood* 121, 1008–1015. doi: 10.1182/blood-2012-06-437392

Fuchs, K., Cardona Gloria, Y., Wolz, O. O., Herster, F., Sharma, L., Dillen, C. A., et al. (2018). The fungal ligand chitin directly binds TLR2 and triggers inflammation dependent on oligomer size. *EMBO. Rep.* 19:201846065. doi: 10.15252/embr.201846065

Gow, N. A., Van De Veerdonk, F. L., Brown, A. J., and Netea, M. G. (2012). *Candida albicans* morphogenesis and host defence: discriminating invasion from colonization. *Nat. Rev. Microbiol.* 10, 112–122. doi: 10.1038/nrmicro2711

Guidetti, G. F., Torti, M., and Canobbio, I. (2019). Focal adhesion kinases in platelet function and thrombosis. *Arterioscler. Thromb. Vasc. Biol.* 39, 857–868. doi: 10.1161/ATVBAHA.118.311787

Hussain, J. F., and Mahaut-Smith, M. P. (1999). Reversible and irreversible intracellular Ca^{2+} spiking in single isolated human platelets. *J. Physiol.* 514, 713–718. doi: 10.1111/j.1469-7793.1999.713ad.x

Jawhara, S., Habib, K., Maggiotto, F., Pignede, G., Vandekerckove, P., Maes, E., et al. (2012). Modulation of intestinal inflammation by yeasts and cell wall extracts: strain dependence and unexpected anti-inflammatory role of glucan fractions. *PLoS ONE* 7:e40648. doi: 10.1371/journal.pone.0040648

Jawhara, S., Thuru, X., Standaert-Vitse, A., Jouault, T., Mordon, S., Sendid, B., et al. (2008). Colonization of mice by *Candida* albicans is promoted by chemically induced colitis and augments inflammatory responses through galectin-3. *J. Infect. Dis.* 197, 972–980. doi: 10.1086/528990

Koller, B., Muller-Wiefel, A. S., Rupec, R., Korting, H. C., and Ruzicka, T. (2011). Chitin modulates innate immune responses of keratinocytes. *PLoS ONE* 6:e16594. doi: 10.1371/journal.pone.0016594

Kral, J. B., Schrottmaier, W. C., Salzmann, M., and Assinger, A. (2016). Platelet interaction with innate immune cells. *Transfus. Med. Hemother.* 43, 78–88. doi: 10.1159/000444807

Le Devedec, F., Bazinet, L., Furtos, A., Venne, K., Brunet, S., and Mateescu, M. A. (2008). Separation of chitosan oligomers by immobilized metal affinity chromatography. *J. Chromatogr. A* 1194, 165–171. doi: 10.1016/j.chroma.2008.03.094

Livio, M., Vigano, G., Morigi, M., Ubiali, A., Galbusera, M., and Remuzzi, G. (1988). Role of platelet-activating factor in primary hemostasis. *Am. J. Physiol.* 254, H1218–H1223. doi: 10.1152/ajpheart.1988.254.6.H1218

Maisch, P. A., and Calderone, R. A. (1981). Role of surface mannan in the adherence of *Candida albicans* to fibrin-platelet clots formed *in vitro*. *Infect. Immun.* 32, 92–97.

Mora-Montes, H. M., Netea, M. G., Ferwerda, G., Lenardon, M. D., Brown, G. D., Mistry, A. R., et al. (2011). Recognition and blocking of innate immunity cells by *Candida albicans* chitin. *Infect. Immun.* 79, 1961–1970. doi: 10.1128/IAI.01282-10

Netea, M. G., Sutmuller, R., Hermann, C., Van Der Graaf, C. A., Van Der Meer, J. W., Van Krieken, J. H., et al. (2004). Toll-like receptor 2 suppresses immunity against *Candida albicans* through induction of IL-10 and regulatory T cells. *J. Immunol.* 172, 3712–3718. doi: 10.4049/jimmunol.172.6.3712

Park, B. K., and Kim, M. M. (2010). Applications of chitin and its derivatives in biological medicine. *Int. J. Mol. Sci.* 11, 5152–5164. doi: 10.3390/ijms11125152

Pluskota, E., Soloviev, D. A., and Plow, E. F. (2003). Convergence of the adhesive and fibrinolytic systems: recognition of urokinase by integrin alpha Mbeta 2 as well as by the urokinase receptor regulates cell adhesion and migration. *Blood* 101, 1582–1590. doi: 10.1182/blood-2002-06-1842

Poulain, D. (2015). *Candida albicans*, plasticity and pathogenesis. *Crit. Rev. Microbiol.* 41, 208–217. doi: 10.3109/1040841X.2013.813904

Poulain, D., Sendid, B., Standaert-Vitse, A., Fradin, C., Jouault, T., Jawhara, S., et al. (2009). Yeasts: neglected pathogens. *Dig. Dis.* 27, 104–110. doi: 10.1159/000268129

Robert, R., Nail, S., Marot-Leblond, A., Cottin, J., Miegeville, M., Quenouillere, S., et al. (2000). Adherence of platelets to *Candida* species *in vivo*. *Infect. Immun.* 68, 570–576. doi: 10.1128/IAI.68.2.570-576.2000

Schattner, M. (2019). Platelet TLR4 at the crossroads of thrombosis and the innate immune response. *J. Leukoc. Biol.* 105, 873–880. doi: 10.1002/JLB.MR0618-213R

Sendid, B., Dotan, N., Nseir, S., Savaux, C., Vandewalle, P., Standaert, A., et al. (2008). Antibodies against glucan, chitin, and Saccharomyces cerevisiae mannan as new biomarkers of *Candida albicans* infection that complement tests based on *C. albicans* mannan. *Clin Vaccine Immunol.* 15, 1868–1877. doi: 10.1128/CVI.00200-08

Sendid, B., Francois, N., Decool, V., Poissy, J., and Poulain, D. (2013). Strategy for overcoming serum interferences in detection of serum (1,3)-beta-D-glucans. *J. Clin. Microbiol.* 51, 375–376. doi: 10.1128/JCM.02356-12

Shiraki, R., Inoue, N., Kawasaki, S., Takei, A., Kadotani, M., Ohnishi, Y., et al. (2004). Expression of Toll-like receptors on human platelets. *Thromb. Res.* 113, 379–385. doi: 10.1016/j.thromres.2004.03.023

Speth, C., Hagleitner, M., Ott, H. W., Wurzner, R., Lass-Florl, C., and Rambach, G. (2013). *Aspergillus fumigatus* activates thrombocytes by secretion of soluble compounds. *J. Infect. Dis.* 207, 823–833. doi: 10.1093/infdis/jis743

Vancraeyneste, H., Charlet, R., Guerardel, Y., Choteau, L., Bauters, A., Tardivel, M., et al. (2016). Short fungal fractions of beta-1,3 glucans affect platelet activation. *Am. J. Physiol. Heart Circ. Physiol.* 311, H725–H734. doi: 10.1152/ajpheart.00907.2015

Wagener, J., Malireddi, R. K., Lenardon, M. D., Koberle, M., Vautier, S., Maccallum, D. M., et al. (2014). Fungal chitin dampens inflammation through IL-10 induction mediated by NOD2 and TLR9 activation. *PLoS Pathog.* 10:e1004050. doi: 10.1371/journal.ppat.1004050

Ward, J. R., Bingle, L., Judge, H. M., Brown, S. B., Storey, R. F., Whyte, M. K., et al. (2005). Agonists of toll-like receptor (TLR)2 and TLR4 are unable to modulate platelet activation by adenosine diphosphate and platelet activating factor. *Thromb. Haemost.* 94, 831–838. doi: 10.1160/TH05-01-0009

Conflict of Interest: The authors declare that the research was conducted in the absence of any commercial or financial relationships that could be construed as a potential conflict of interest.

frontiers in Cellular and Infection Microbiology

BRIEF RESEARCH REPORT
published: 22 November 2019
doi: 10.3389/fcimb.2019.00400

The Glucan-Remodeling Enzyme Phr1p and the Chitin Synthase Chs1p Cooperate to Maintain Proper Nuclear Segregation and Cell Integrity in *Candida albicans*

*Genny Degani and Laura Popolo**

Department of Biosciences, University of Milan, Milan, Italy

GH72 family of β-(1,3)-glucanosyltransferases is unique to fungi and is required for cell wall biogenesis, morphogenesis, virulence, and in some species is essential for life. *Candida albicans PHR1* and *PHR2* are pH-regulated genes that encode GH72 enzymes highly similar to Gas1p of *Saccharomyces cerevisiae. PHR1* is expressed at pH $\geq$ 5.5 while *PHR2* is transcribed at pH $\leq$ 5.5. Both are essential for *C. albicans* morphogenesis and virulence. During growth at neutral-alkaline pH, Phr1p-GFP preferentially localizes to sites of active cell wall formation as the incipient bud, the mother-daughter neck, the bud periphery, and concentrates in the septum at cytokinesis. We further investigated this latter localization. In *chs3*Δ cells, lacking the chitin of the chitin ring and lateral cell wall, Phr1p-GFP still concentrated along the thin line of the primary septum formed by chitin deposited by chitin synthase I (whose catalytic subunit is Chs1p) suggesting that it plays a role during formation of the secondary septa. RO-09-3143, a highly specific inhibitor of Chs1p activity, inhibits septum formation and blocks cell division. However, alternative septa are produced and are crucial for cell survival. Phr1p-GFP is excluded from such aberrant septa. Finally, we determined the effects of RO-09-3143 in cells lacking Phr1p. *PHR1* null mutant was more susceptible to the drug than the wild type. The *phr1*Δ cells were larger, devoid of septa, and underwent endomitosis and cell death. Phr1p and Chs1p cooperate in maintaining cell integrity and in coupling morphogenesis with nuclear division in *C. albicans*.

Keywords: cell wall assembly, β-(1,3)-glucanosyltransferases, septum, nuclear segregation, cell integrity, morphogenesis

OPEN ACCESS

Edited by:
Vishukumar Aimanianda, Institut Pasteur, France

Reviewed by:
Carol Munro, University of Aberdeen, United Kingdom
Rebecca Shapiro, University of Guelph, Canada

****Correspondence:***
Laura Popolo
laura.popolo@unimi.it

Specialty section:
This article was submitted to Fungal Pathogenesis, a section of the journal Frontiers in Cellular and Infection Microbiology

Received: *01 August 2019*
Accepted: *07 November 2019*
Published: *22 November 2019*

Citation:
Degani G and Popolo L (2019) The Glucan-Remodeling Enzyme Phr1p and the Chitin Synthase Chs1p Cooperate to Maintain Proper Nuclear Segregation and Cell Integrity in Candida albicans. Front. Cell. Infect. Microbiol. 9:400. doi: 10.3389/fcimb.2019.00400

INTRODUCTION

Candida albicans, a major human fungal pathogen, is a polymorphic fungus endowed of extraordinary morphological plasticity and adaptive capacity. The fight against fungal invasive infections still relies on a small repertoire of drugs, among which the inhibitors of the synthesis of β-(1,3)-glucan (echinocandins) target the fungal cell wall. It is urgent to develop new drugs, or combination of drugs, to counteract the rise of drug resistance and the limited efficacy echinocandins have toward some fungal species such as *Aspergillus fumigatus*.

The fungal cell wall is formed by β-(1,3) and β-(1,6)-glucans, mannoproteins and a tiny amount of chitin, and has the mechanical strength necessary to withstand the high turgor pressure of yeast cells. At the neck most of the bound chitin is cross-linked to β-(1,3)-glucan, the most abundant polysaccharide, whereas in lateral cell walls the attachment of chitin to β-(1,6)-glucan predominates and chitin of the primary septum is free (Cabib and Arroyo, 2013).

The enzymes of the GH72 family are responsible for β-(1,3)-glucan elongation and branching, crucial for the formation of the core of the cell wall and of the high molecular weight glucan-chitin polymer present at the bud neck region in yeast cells (Cabib et al., 2012; Aimanianda et al., 2017). Among the five GH72 encoding genes present in *C. albicans (PHR1, PHR2, PHR3, PGA4,* and *PGA5)* only two, *PHR1* and *PHR2*, appear to encode active enzymes that are anchored to the plasma membrane through a glycosyl-phosphatidylinositol and, in minor amount, are also cross-linked to the cell wall. *PGA4* encodes an inactive enzyme, *PHR3* and *PGA5* transcript level is very low or undetectable and Pga5p has anomalous sequence features (reviewed in Popolo et al., 2017). *PHR1* expression is triggered at external pH values ≥5.5 whereas *PHR2* is expressed at pH ≤5.5. Phr1p and Phr2p act on cell wall remodeling in the growing areas and in the septum both in yeast and hyphal form and, as expected, these enzymes have different pH optimum that mirrors the pH-dependent transcription pattern. Remarkably, β-(1,3)-glucan is shielded by an outer layer of mannoproteins that facilitate the escape of the pathogen from the immune cells (Hopke et al., 2016).

In unicellular yeasts, cell wall biogenesis requires a unique set of enzymes that are strictly regulated to maintain a tight coordination between growth and the discontinuous events of the cell cycle: bud emergence, DNA synthesis, mitosis and cell division. The end of the cell cycle is marked by cytokinesis and division of the septum wall, an essential process. Septation has been extensively studied in budding yeast (Cabib, 2004; Roncero and Sanchez, 2010) and the key enzyme in this process is the plasma membrane chitin synthase II (the catalytic subunit of which is *Sc*Chs2p). This enzyme is synthesized at early mitosis and reaches a maximum at the end of the M phase. It is targeted to the neck during mitosis exit. After execution of its function, *Sc*Chs2p is removed by endocytosis and degraded (Oh et al., 2012; Chin et al., 2016). The chitin disk synthesized by *Sc*Chs2p, named primary septum (PS), defines the plane along which septum abscission will occur and is covered on both sides by the secondary septa, presumably composed of the same material of lateral cell walls. Cell separation requires the help of the chitinases and endo-glucanases *Sc*Cts1p and *Sc*Eng1p, both localized to the daughter side of the septum (Baladron et al., 2002; Cabib, 2004). At cell separation, the secondary septa, the chitin ring and the PS remains on the mother cell forming the bud scar.

In *C. albicans,* septum formation is similar to *S. cerevisiae* and initiates with the synthesis of the chitin ring by recruitment of Chs3p at the site of bud emergence and is completed in G2 by Chs1p, the catalytic subunit of chitin synthase I and the equivalent of *Sc*Chs2p. Chs1p deposits chitin in the invagination that is created between the cell wall and the plasma membrane in concomitance with the closure of the plasma membrane by the cortical actomyosin contractile ring (Bulawa et al., 1995; Mio et al., 1996). As chitin is deposited centripetally, the PS is covered on both sides by cell wall material forming the secondary septa (Roncero and Sanchez, 2010). Cell separation is promoted by Cht3p and Eng1p, the equivalent of *Sc*Cts1p and *Sc*Eng1p, respectively (Dunkler et al., 2005; Esteban et al., 2005). Interestingly in *C. albicans*, the bud scar has a portion of exposed β-(1,3)-glucan (not covered by mannoproteins) that is recognized by Dectin-1 (Gantner et al., 2005). Since cleavage of septa is inhibited in hyphae, β-(1,3)-glucan remains hidden and this promotes the escape from the immune system.

C. albicans Chs1p is an essential enzyme required for PS formation but also for cell integrity (Munro et al., 2001). Other non-essential chitin synthases are Chs3p, Chs2p and Chs8p (Lenardon et al., 2010). Chs3p contributes to the majority of cell wall chitin which is deposited at the chitin ring and lateral walls, in response to a weakening of the cell wall and in the remedial septum. Chs2p and Chs8p are responsible for chitin in the septum and in the remedial septum (Walker et al., 2013; Preechasuth et al., 2015). In response to a pre-treatment with Calcofluor White/calcium chloride that stimulates chitin synthesis, the arrest of PS formation by use of a potent and highly specific inhibitor of Chs1p activity (RO-09-3143), activates the synthesis of remedial septa that are produced by the other active chitin synthases, i.e., Chs3p, Chs2p, and Chs8p, or in *chs3*Δ cells by Chs2p and Chs8p (Walker et al., 2013) and in some conditions restore cell division. This indicates that *C. albicans* possesses redundant salvage pathways to overcome the effects of the inhibition of primary septum formation.

Little is known about the role of β-(1,3)-glucan remodeling enzymes of GH72 family at the septum region. In this work, we deepened the study on the localization of Phr1p in the septum and investigated the impact of glucan remodeling on septum formation. By a chemo-synthetic approach we prove that Phr1p and Chs1p cooperate to maintain cell integrity and proper nuclear segregation.

METHODS

Strains and Growth Conditions

The *Candida albicans* strains used in this work were CAF3-1 (*ura3*Δ::*imm*434/*ura3*Δ::*imm434*) and CAS8 (*ura3*Δ::*imm*434/*ura3*Δ::*imm434 phr1*Δ::*his*G/*phr1*Δ), kindly provided by Prof. W.A. Fonzi (Saporito-Irwin et al., 1995). The two strains expressing Phr1p-GFP, JC94-2 (Hopke et al., 2016) and *chs3*Δ-Phr1p-GFP (this work) harbor one allele of *PHR1* and two copies of *PHR1-GFP* the second of which is on the CIp20 plasmid (*PHR1/PHR1-GFP* CIp20-*PHR1-GFP*). An homozygous *chs3*Δ/*chs3*Δ strain derived from the Ura$^-$ CAI4 strain was kindly provided by Dr. Mio (Mio et al., 1996) (*chs3*Δ::*hisG*/*chs3*Δ::*hisG*). The first copy of *PHR1-GFP* was obtained by a C-terminal internal tagging of GFP in the *PHR1* cds. The nucleotide sequence encoding GFP was inserted between the amino acids G489 and G490 of Phr1p by using a PCR-based strategy (Ragni et al., 2011). The second copy of *PHR1-GFP* was obtained by integration of the *StuI*-linearized

CIp20-*PHR1-GFP* at the *RP10* locus (*PHR1/PHR1-GFP* CIp*20-PHR1-GFP*; Hopke et al., 2016). *C. albicans* cells were routinely grown at 25 or 30°C in YPD (10 g of yeast extract, 20 g of Bacto-peptone, 20 g of glucose, 25 mg of uridine per liter). The experiments were carried out in YPD-150 mM HEPES [4-(2-Hydroxyethyl) piperazine-1-ethanesulfonic acid sodium salt] buffered at the desired pH before sterilization. Growth was monitored as the increase in optical density at 600 nm (OD_{600}). To induce hyphal development we used a protocol previously described (Degani et al., 2016). Briefly, blastospores were obtained by prolonged growth in YPD buffered at pH 6 and then transferred to M199-150 mM HEPES buffered at pH 7.5 at 37°C.

Broth Microdilution and XTT Assays

Susceptibility of *C. albicans cells* to RO-09-3143 was tested by microdilution assay according to the CLS1 guidelines. Inoculum size was 10^5 cells/ml. Cells exponentially growing at 30°C in YPD-150 mM HEPES, pH 8 were harvested by centrifugation and suspended in fresh medium at 2×10^5 cells/ml. In a 96-well microplate, 100 μl of the cell suspension were added to an equal volume of medium containing different concentrations of RO-09-3143 (kindly donated by Roche) dissolved in DMSO (from 0.012 to 25 μM). All determinations were made in quadruplicate. Control wells contained only DMSO. The plates were incubated at 30°C and inspected at 24 h and 48 h. The effect of the treatment was evaluated by reading the turbidity with a Tecan Infinite F200 PRO microplate reader. For the XTT assay, the plate was centrifuged and wells were washed twice with 200 μl PBS. Then, 100 μl of 1 mg/ml XTT solution in PBS containing 1 μM menadione, dissolved at 1 M in acetone, were added to each well. Cells were suspended and the plate was incubated in the dark at 37°C for 1–2 h before reading the absorbance at 490 nm.

Growth and Viability in Yeast and Hyphal Forms in the Presence of the Chs1p Inhibitor

To test the effect on growth in yeast form, exponentially growing cells in YPD-150 mM HEPES buffered at pH 8 at 30°C with shaking at 200 rpm, were collected by centrifugation and inoculated in pre-warmed fresh medium at a cell density of $\sim 10^6$ cells/ml ($\sim$0.1 A_{600}). After 30 min of equilibration, RO-09-3143 [10 μM, a concentration reported as non-lethal for the wild type (Sudoh et al., 2000)] or an equal volume of DMSO were added and cells were monitored at 2.5, 5, and 24 h.

To test the effect of the drug during induction of hyphal growth, blastospores of CAF3-1 and CAS8 were obtained as described at section Strains and Growth Conditions. Blastospores were suspended in pre-warmed M199-pH 7.5 at 2×10^6 cells/ml and the culture was split in two: one received only DMSO and the other RO-09-3143 at 10 μM. At 0, 1, 3, 5, and 24 h after the shift, the formation of hyphae was monitored.

The effect on viability was assessed by methylene blue staining (Degani et al., 2016).

Microscopy

Cells were routinely observed by phase-contrast microscopy after mild sonication consisting in two cycles of 6 s. To maximize Phr1p-GFP expression, cells were grown in YPD-150 mM HEPES buffered at pH 8. For GFP and Calcofluor white (CF), a specific dye for chitin, conventional and confocal microscopy was performed without fixation (Ragni et al., 2011). For the staining of nuclear DNA, cells were processed as previously described (Ragni et al., 2011). Cells with 1, 2, or more nuclei were counted using double beam (bright field and UV filter) to visualize the hyphal compartments and nuclei at the same time.

RESULTS

Altered Localization of Phr1p-GFP in the Presence of Inhibition of Primary Septum Formation

In a previous work we showed that Phr1p-GFP localizes to the septum in *C. albicans* cells at cytokinesis (Ragni et al., 2011). However, only one allele of *PHR1-GFP* was present in the strain used (strain 9.4). To improve the detection of Phr1p-GFP, we repeated the study using strain JC94-2 that contains two copies of *PHR1-GFP* and a wild type *PHR1* allele and whose construction is described elsewhere (Hopke et al., 2016). As expected, a bright fluorescence was detected at the bud periphery, whereas a very intense and thick fluorescent signal was present at the septum supporting the presence of the protein at the chitin ring and septum (**Figure 1**). The optical sections from a confocal microscope analysis indicated that Phr1p-GFP was distributed along the entire septum thickness (**Supplementary Figure 1**). To avoid the interference of the chitin ring that is deposited at the mother-bud neck by Chs3p, we analyzed the localization of Phr1p-GFP in cells lacking Chs3p. *C. albicans chs3*Δ cells showed a faint CF-staining except at the PS where a thin line at the center of the neck constriction was visible (**Figure 1**). In these cells, Phr1p-GFP signal was intense at both sides of the neck constrictions and along the line of the PS. These results indicate that Phr1p-GFP localizes to, or in position proximal to, the chitin disk, either in the secondary septa or in the plasma membrane sides facing the secondary septa and also at the neck constrictions despite the absence of the chitin ring.

Next, we tested the effect of the inhibition of septum formation on the localization of Phr1p-GFP. Since Chs1p is an essential chitin synthase (Munro et al., 2001), we used RO-09-3143, a highly specific inhibitor of this enzyme (Sudoh et al., 2000). RO-09-3143, dissolved in DMSO, was added at the concentration of 10 μM to *C. albicans* exponentially growing cells (see section Growth and Viability in Yeast and Hyphal Forms in the Presence of the Chs1p Inhibitor). In DMSO-treated cells, Phr1p-GFP was detected at the usual sites (plasma membrane, bud periphery, and septum; Ragni et al., 2011). In cells at cytokinesis Phr1p-GFP co-localized with the septum region (**Figure 2Aa–e** and details in **Figure 2Ba'**). After 5 h of treatment with the drug, chains of 4–6 aligned cells were present and a thick CF-positive line separated the cells

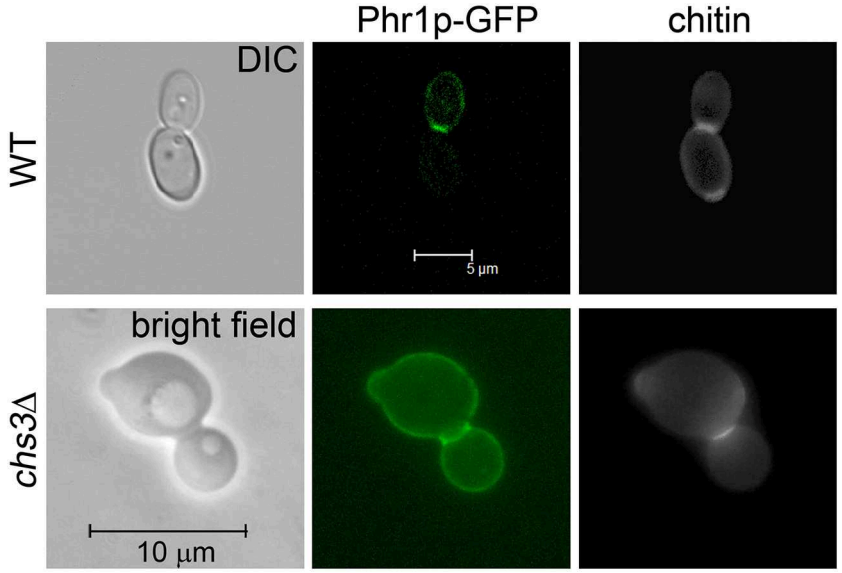

FIGURE 1 | Phr1p-GFP localization at the septum in cells at cytokinesis. Wild type cells (strain JC94-2: *PHR1/PHR1-GFP* RP10::Clp20-*PHR1-GFP*) were grown in YPD-150 mM HEPES pH 8 at 25°C and analyzed by Confocal microscopy. *CHS3* null mutant expressing Phr1p-GFP (*chs3*Δ::*hisG/chs3*Δ::*hisG PHR1/PHR1-GFP* RP10::Clp20-*PHR1-GFP*) was analyzed by conventional fluorescence microscopy.

suggesting that an alternative chitin septum was produced (**Figure 2Af–h**). Interestingly, Phr1p-GFP was present at the cell periphery but did not localized to the new septa as little or no overlap of the green and blue signals was observed and no Phr1p-GFP co-localization with the chitin line was detected in the treated cells (**Figure 2Ai,j** and details in **Figure 2Bb'**). At 24 h of treatment, chains were long and branched and Phr1p-GFP localized to the plasma membrane but was not present in the alternative septa (data not shown). Thus, Phr1p-GFP is excluded from the septa produced in conditions of PS inhibition.

We also analyzed the localization of Phr1p-GFP in a *chs3*Δ mutant treated with DMSO (**Figure 2Ak–o** and detail in **Figure 2Bc'**) or with RO-09-3143 (**Figures 2Ap–t,Bd'**). After 5 h of treatment, the chained cells showed the presence of a chitin-rich septum in which Phr1p-GFP was not detected (details in **Figure 2Bd'**). Thus, Phr1-GFP is excluded from the alternative septum both in the wild type or in the *chs3*Δ mutant (see further Discussion).

Inhibition of Septum Formation Causes Destabilization of the Cell Wall and Defects in Nuclear Segregation in Cells Lacking β-(1,3)-Glucan Remodeling

Effect of RO-09-3143 During Growth in the Yeast Form

The susceptibility of the wild type strain and of a *PHR1* null mutant to RO-09-3143, was tested by broth microdilution assay (see section Broth Microdilution and XTT Assays). Due to the pH-dependent transcriptional pattern of *PHR1*, the phenotype of *phr1*Δ cells is manifested at neutral-alkaline pH values (Saporito-Irwin et al., 1995). Therefore, cells were grown in yeast form in YPD-150 mM HEPES, pH 8. As shown in **Figure 3A,** a *PHR1* null mutant was more sensitive to the drug compared to the wild type (MIC mutant ∼ 6 μM; MIC wild type higher than 25 μM). XTT viability assay showed that the decrease of growth in the wild type was not associated to a decrease in viability suggesting that the drug is cytostatic on the wild type and cytocidal for the mutant (**Figure 3B**).

We analyzed in detail the effects of the inhibitor at a fixed concentration (10 μM) in batch cultures (see section Growth and Viability in Yeast and Hyphal Forms in the Presence of the Chs1p Inhibitor in Methods). Growth, measured as increase of OD_{600}, proceeded in a parallel manner for the two strains and stopped after 8 h of treatment with the drug whereas the control cultures were unaffected for many hours (data not shown). DMSO-treated *phr1*Δ cells were rounder than wild type with wider bud necks and showed a tendency to aggregate (Saporito-Irwin et al., 1995). Cell morphologies and the presence of septa were visible in the CF-stained cells in **Figure 4Aa,b**. After 5 h of treatment with RO-09-3143, wild type cells appeared as linear chains of cells with CF-positive constrictions compared to the DMSO-treated cells between adjacent cells (**Figure 4Ac**) while the majority of *phr1*Δ mutant cells exhibited dramatic morphological changes such as formation of irregular and curved chains of cells, an abnormal enlargement of the bud neck, emergence of buds from random sites and lack of CF-stained alternative septa between the newly formed cells with consequent fusion of cytoplasm (**Figure 4Ad**). At 24 h of treatment, wild type chains of cells were branched with CF-positive constrictions compared to the DMSO-treated cells (**Figure 4Ag**) compared to the normal aspect of DMSO-treated cells (**Figure 4Ae**), whereas the majority of *phr1*Δ cells were 5–6

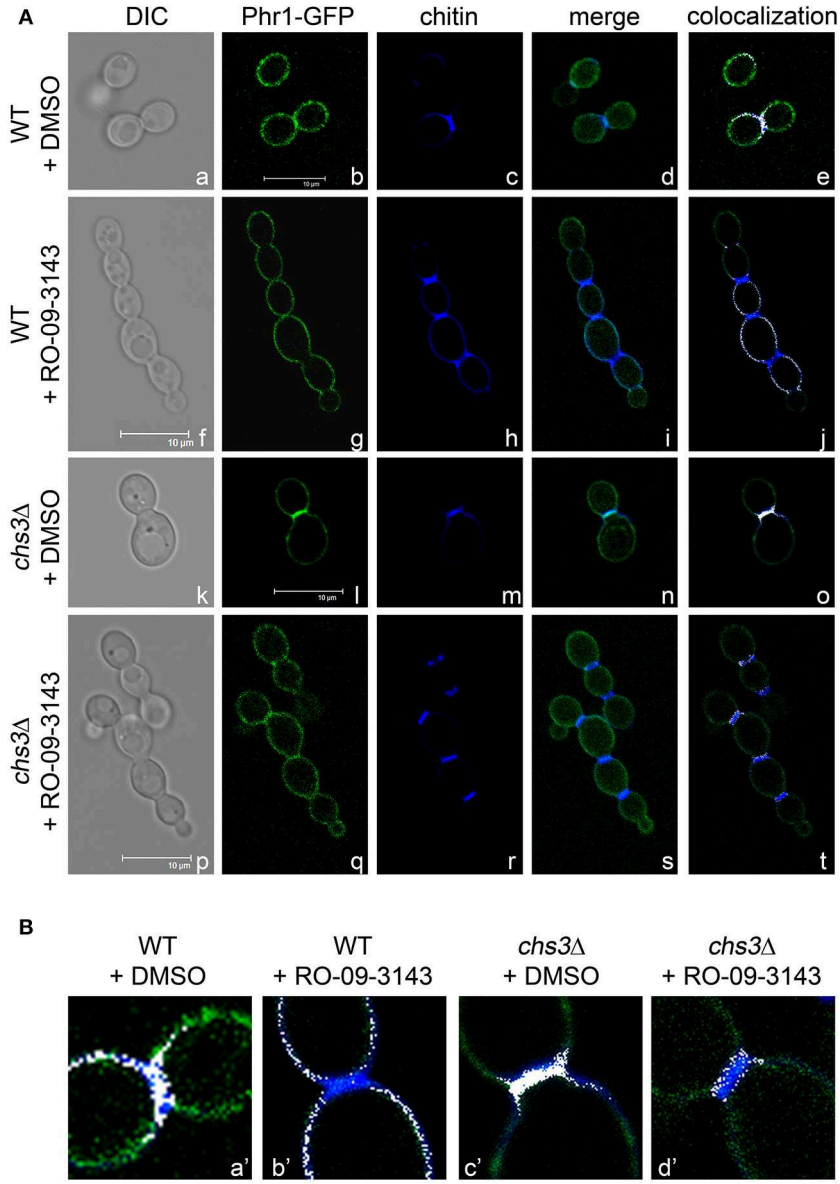

FIGURE 2 | Inhibition of Chs1p alters the localization of Phr1p-GFP in the septum region. **(A)** Formation of alternative septa in wild type and *chs3*Δ cells grown in the presence of Chs1p inhibitor RO-09-3143 (10 μM). Images of Phr1p-fluorescence, CF fluorescence, their merge and the blue and green co-localization depicted in white are shown. **(B)** Magnification of the neck region. The merge of the CF-fluorescence and the green fluorescence (Phr1p-GFP) was artificially colored in white by ImageJ (NIH) and contrast adjusted in Photoshop CS5 (Adobe).

times larger than untreated *phr1*Δ (**Figure 4Af**), had long lines of ruptures with release of cellular material and appearance of cell ghosts, and were full of vacuoles and granules, indicating a total loss of cell integrity and morphology (**Figure 4Ah**).

Next, we analyzed the nuclear content by DAPI staining in DMSO- or RO-09-3143-treated wild type cells (**Figure 4Ba,a',b,b'**) and phr1 mutant cells (**Figure 4Bc,c',d,d'**). At 5 h, *phr1*Δ treated cells contained two or more nuclei, reaching values of 6–7 nuclei in a single cell compartment, and nuclei were abnormally positioned. The increase in nuclei number seems to be a consequence not only of cytoplasm fusion but also of multiple endomitosis (EnM) (**Figure 4Bd,d'**). After 24 h of treatment, most of the treated *phr1*Δ cells were full of amorphous material and DNA, indicating that the majority of the cells lost integrity and died (**Figure 4Bf,f'**) whereas DMSO-treated cells appeared viable and with the expected morphology (**Figure 4Be,e'**). As shown in **Table 1**, the majority of the wild type-treated cells had one nucleus per cell (**Figure 4Bb,b'**). On opposite, almost the totality of *phr1*Δ treated cells contained more than one nucleus in the same cell compartment and the class of cells devoid of a nucleus increased compared to the untreated culture indicating a failure to correctly segregate nuclei to the daughter cells (**Table 1**). Thus, upon inhibition of Chs1p activity, *phr1*Δ cells lose integrity especially at the

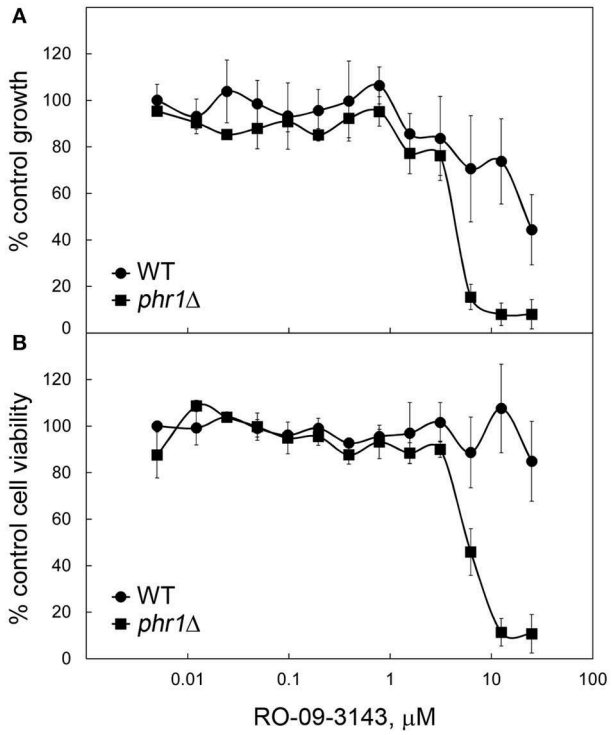

FIGURE 3 | Higher susceptibility to RO-09-3143 of cells lacking β-(1,3)-glucan remodeling. **(A)** Susceptibility of a wild type (CAF3-1) and a *PHR1* null mutant (CAS8) to RO-09-3143 tested in YPD-pH 8 at 30°C in quadruplicates by broth microdilution assay at an inoculum size of 10^5 cells/ml. Absorbance values are relative to the untreated wild type which was set to 100% (untreated wild type: mean $A_{595} = 0.8498 \pm 0.0585$ SD; untreated *phr1*Δ $= 0.8104 \pm 0.0061$ SD). **(B)** After reading the absorbance the plate was used to test cell viability by the XTT method. Data are relative to the absorbance value of the untreated wild type that was set to 100% (wild type $A_{490} = 1.3655 \pm 0.0281$ SD; mutant: $A_{490} = 1.1959 \pm 0.1347$ SD).

neck region, undergo size increase, multiple EnM and aberrant nuclear segregation. To determine cell viability we performed a methylene blue (MB) permeability assay. MB-positive cells, or clusters with at least one blue cell/compartment, were counted as dead/lysed. After 5 h of treatment with RO-09-3143, 3% of wild type cells/chain and 6.8% of the mutant treated cells were MB-positive, respectively, compared to 2.3 or 5% of DMSO-treated wild type and mutant cells. At 24 h, the percentage of viable cells did not change in the wild type (9.4% for treated wild type cells and 1% for DMSO-treated cells) whereas dramatically increased in the mutant (83.5% for treated mutant cells compared to 3.9% for DMSO-treated cells). In conclusion, β-(1,3)-glucan branching/remodeling and Chs1p activity protect cells from abnormal enlargement, EnM and cell lysis.

Effect of RO-09-3143 During Hyphal Development

After 5 h from induction of hyphal growth, wild type germ tubes developed into hyphae whereas *phr1*Δ germ tubes remained short and enlarged with wider septa and swollen aspect (**Supplementary Figures 2a,b**) as expected (Degani et al., 2016). In the presence of RO-09-3143, wild type hyphae were wider than untreated ones with enlarged hyphae apexes and constrictions (**Supplementary Figure 2c**). About 48% of the hyphal compartment had a single nucleus, 57% had more than one nucleus, and 5% had no nucleus, whereas in the DMSO-treated cells all the compartments contained one nucleus and compartments without nuclei were not detected. These data are consistent with those published on the effect of *CHS1* deletion (Munro et al., 2001). In the presence of RO-09-3143, *phr1*Δ mutant cells showed a worsening of the phenotype. Cells formed enlarged and branched short chains with constrictions and abnormal or poorly visible septa and two or more nuclei were detected in the same compartment (**Supplementary Figure 2d**). About 45% of the compartments had more than one nucleus and 19% had no nucleus, whereas in the untreated culture only about 1% underwent EnM (with no more than two nuclei in the same compartment) and no cell was without a nucleus. Similar results were obtained in two independent experiments.

In conclusion, RO-09-3143 induced mis-segregation of nuclei both in wild type and in *phr1*Δ null mutant but in the latter the percentage of compartments with no nuclei increased at the expenses of the category of compartments with more than 1 nucleus, indicating a worsening of the nuclear segregation defect.

At 24 h of treatment, DAPI entered in dead compartments only of the treated mutant and therefore a reliable count of nuclei was not possible (**Supplementary Figures 2e–h**).

DISCUSSION

Phr1p is required for cell wall biogenesis during the entire cell cycle and has a dynamic localization toward the sites of active cell wall growth. Moreover, Phr1p is likely required for the formation of high molecular weight glucan that confers mechanical strength to the bud neck as observed for *Sc*Gas1p (Cabib et al., 2012). In yeast cells, Fks1p concentrates at the division septum with a pattern equivalent to that shown for Gas1p and Phr1p (Utsugi et al., 2002). Phr1p is a new cytokinesis enzyme since the assembly of β-(1,3)-glucan synthesized by Fks1p, during/after invagination of the plasma membrane, and formation of the glucan-rich secondary septa on both sides of the of the chitinous disk (primary septum) requires the elongation and branching of this polysaccharide catalyzed by GH72 family of enzymes (Aimanianda et al., 2017).

In this work, we demonstrated that Phr1p localization at the septum is altered in conditions of primary septum inhibition and leads to the formation of alternative chitin-rich septa. Aberrant septa were previously identified in *S. cerevisiae chs2*Δ mutants that fail to form normal septa and divide, and produce thickened septa synthesized by *Sc*Chs3p (Schmidt et al., 2002; Cabib, 2004). While the normal septa have a typical tri-laminar structure, detectable also in *gas1*Δ mutant cells (Popolo et al., 1993), the aberrant septa are uni-laminar and chitin is deposited in a longitudinal instead of centripetal orientation with respect to the division plate line (Cabib, 2004). Aberrant septa were identified also in *C. albicans* (Walker et al., 2013). Previous studies have shown that chitin of the septum in cells treated with RO-09-3143 is deposited by the other chitin synthases (Chs3p,

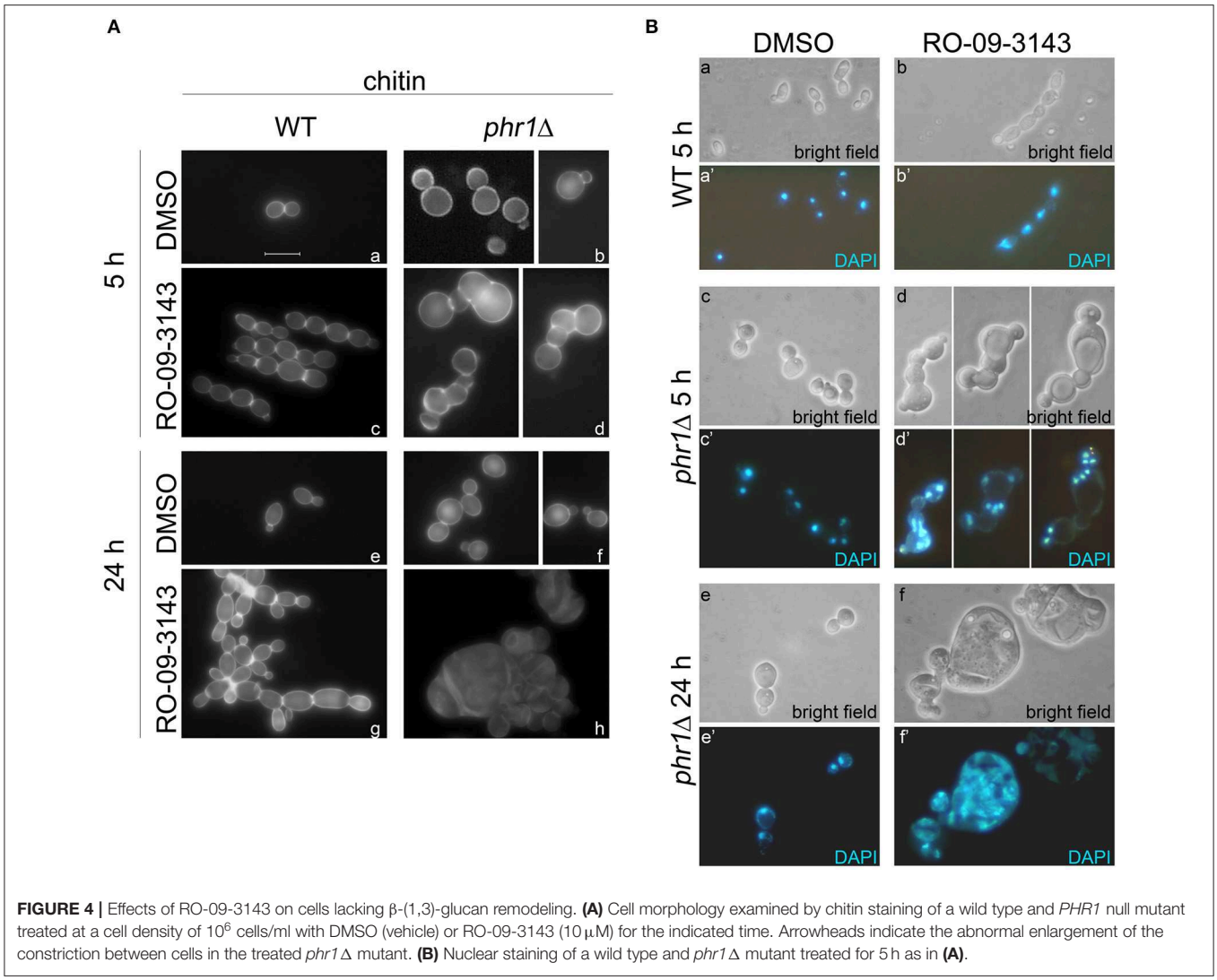

FIGURE 4 | Effects of RO-09-3143 on cells lacking β-(1,3)-glucan remodeling. **(A)** Cell morphology examined by chitin staining of a wild type and *PHR1* null mutant treated at a cell density of 10^6 cells/ml with DMSO (vehicle) or RO-09-3143 (10 μM) for the indicated time. Arrowheads indicate the abnormal enlargement of the constriction between cells in the treated *phr1*Δ mutant. **(B)** Nuclear staining of a wild type and *phr1*Δ mutant treated for 5 h as in **(A)**.

Chs2p or Chs8p). In *chs3*Δ cells treated with the inhibitor, Chs2p and Chs8p are the residual active chitin synthases, and are responsible for the formation of a type of alternative septa (Walker et al., 2013). The absence of β-(1,3)-glucan in these anomalous septa is likely the cause of the exclusion of Phr1p from these structure. These results support the notion that a tight coordination between the synthesis and remodeling of the β-(1,3)-glucan and PS formation exists.

The cell wall of *phr1*Δ cells is weakened but chitin increase operated by Chs3p compensates the defects and prevents cell lysis, as demonstrated by the severe swelling and lysis phenotype of a *phr1*Δ *chs3*Δ double mutant in vegetative growth at pH 8 (data not shown). The percentage of multinucleate cells in the double mutant was unaffected compared to the single mutants and cell lysis was the only predominant phenotypic trait (data not shown).

The inhibition of septum formation exhibited a different but strong phenotype in combination with *PHR1* deletion leading to abnormal enlargement of the neck constriction, and dramatic mis-segregation of the nuclei. These traits prevailed over lysis during the first 5 h of treatment with RO-09-3143. Moreover, the increase of cell mass and loss of cell shape at 24 h, support an additional role of Chs1p in cell integrity in agreement with a previous study (Munro et al., 2001).

TABLE 1 | Distribution of nuclei in cells treated with the inhibitor of primary septum formation[a].

	1 Nucleus (%)	Nuclei ≥ 2 (%)	No nucleus (%)
WT DMSO	97.74 ± 0.49	0.56 ± 0.26	1.69 ± 0.23
WT RO-09-3143	89.76 ± 5.45	3.77 ± 2.33	6.46 ± 3.12
*phr1*Δ DMSO	87.46 ± 2.71	8.06 ± 2.23	4.47 ± 0.49
*phr1*Δ RO-09-3143	4.08 ± 2.32	84.02 ± 0.75	11.90 ± 1.57

[a]*Cells were examined under the microscope with a double beam, bright field, and UV, to simultaneously monitor the cell morphology and the presence of DAPI-stained nucleus/i. The number of nuclei per single cell or per cell in a chain is reported. Cells without a visible nucleus were also counted and were the result of impaired nuclear segregation. A cell with the nucleus in mitosis correctly positioned at the neck between the mother and daughter cell was counted in the class 1 nucleus per cell.*

Schizosaccharomyces pombe has a primary septum constituted of β-(1,3)-glucan. A cell wall β-(1,3)-glucan synthesized by a specific synthase is required to connect the cell wall with the plasma membrane and for contractile ring function at cytokinesis (Munoz et al., 2013; Cortes et al., 2015). We can speculate that Phr1p and Chs1p cooperate to confer rigidity to the cell wall at the membrane invagination site and permit a stable anchorage of AMR to cell wall and plasma membrane. In addition, the cortical region of the bud neck is a crucial site for formation of protein complexes involved in regulatory events leading to proper spindles positioning and cell division (Kusch et al., 2002). Thus, we can envisage that the weakening of the neck cell wall, brought about by the lack of Phr1p and inhibition of Chs1p, causes such severe perturbations that the spindle positioning checkpoint (SPOC) is not operative in arresting mitosis exit and consequently EnM, that are rarely present in normal cells, dramatically increase.

Since *phr1*Δ cells treated with the inhibitor showed lack/reduction of alternative septa, the formation of these septa seems a crucial process to protect cell viability. At this regard, caspofungin is fungistatic in *Aspergillus fumigatus* but becomes fungicidal if treatment is combined with the use of septum inhibitors (Dichtl et al., 2015).

In conclusion, Phr1p and Chs1p of *C. albicans* could be a combination of fungal-specific molecular targets useful for the development of innovative strategies in the fight against invasive fungal infections.

DATA AVAILABILITY STATEMENT

The raw data supporting the conclusions of this manuscript will be made available by the authors, without undue reservation, to any qualified researcher.

AUTHOR CONTRIBUTIONS

LP and GD designed the experiments and analyzed the data. GD performed the experiments and prepared tables and figures. LP wrote the manuscript that was read, discussed, and approved by GD.

FUNDING

This work was partially supported by University of Milan. GD is the recipient of a Post-Doctoral fellowship from the University of Milan (Italy). We do not have a fund number since the work was performed with University of Milan support.

ACKNOWLEDGMENTS

We are grateful to Roche for the kind gift of RO-09-3143. We wish to thank Umberto Fascio and Daniele Cartelli for assistance in confocal microscopy.

SUPPLEMENTARY MATERIAL

The Supplementary Material for this article can be found online at: https://www.frontiersin.org/articles/10.3389/fcimb.2019.00400/full#supplementary-material

Supplementary Figure 1 | Phr1p-GFP concentrates over the entire thickness of the septum. Cell (strain JC94-2) were grown at 25°C in YPD-150 mM HEPES buffered at pH 8. Elaboration by a Leica software provided the integration of image series in cross-sections along the X-Z-axis.

Supplementary Figure 2 | Effects of RO-09-3143 on cells lacking β-(1,3)-glucan remodeling during hyphal development. Analysis of the effects of the inhibition of Chs1p on wild type **(a,c,e,g)** and *phr1*Δ mutant **(b,d,f,h)** during induction of hyphal growth in M199-buffered at pH 7.5 at 37°C. Micrographs of DAPI-stained cells were obtained by dual beam analysis, bright-field and UV light, to show simultaneously cell morphology and nuclei. Bar: 10 μm. Similar results were obtained in two independent experiments.

REFERENCES

Aimanianda, V., Simenel, C., Garnaud, C., Clavaud, C., Tada, R., Barbin, L., et al. (2017). The dual activity responsible for the elongation and branching of beta-(1,3)-glucan in the fungal cell wall. *MBio* 8:e00619-17. doi: 10.1128/mBio.00619-17

Baladron, V., Ufano, S., Duenas, E., Martin-Cuadrado, A. B., del Rey, F., and Vazquez de Aldana, C. R. (2002). Eng1p, an endo-1,3-beta-glucanase localized at the daughter side of the septum, is involved in cell separation in *Saccharomyces cerevisiae*. *Eukaryot. Cell* 1, 774–786. doi: 10.1128/EC.1.5.774-786.2002

Bulawa, C. E., Miller, D. W., Henry, L. K., and Becker, J. M. (1995). Attenuated virulence of chitin-deficient mutants of *Candida albicans*. *Proc. Natl. Acad. Sci. U.S.A.* 92, 10570–10574. doi: 10.1073/pnas.92.23.10570

Cabib, E. (2004). The septation apparatus, a chitin-requiring machine in budding yeast. *Arch. Biochem. Biophys.* 426, 201–207. doi: 10.1016/j.abb.2004.02.030

Cabib, E., and Arroyo, J. (2013). How carbohydrates sculpt cells: chemical control of morphogenesis in the yeast cell wall. *Nat. Rev. Microbiol.* 11, 648–655. doi: 10.1038/nrmicro3090

Cabib, E., Blanco, N., and Arroyo, J. (2012). Presence of a large beta(1-3)glucan linked to chitin at the Saccharomyces cerevisiae mother-bud neck suggests involvement in localized growth control. *Eukaryot. Cell* 11, 388–400. doi: 10.1128/EC.05328-11

Chin, C. F., Tan, K., Onishi, M., Chew, Y., Augustine, B., Lee, W. R., et al. (2016). Timely endocytosis of cytokinetic enzymes prevents premature spindle breakage during mitotic exit. *PLoS Genet.* 12:e1006195. doi: 10.1371/journal.pgen.1006195

Cortes, J. C., Pujol, N., Sato, M., Pinar, M., Ramos, M., Moreno, B., et al. (2015). Cooperation between paxillin-like protein Pxl1 and glucan synthase bgs1 is essential for actomyosin ring stability and septum formation in fission yeast. *PLoS Genet.* 11:e1005358. doi: 10.1371/journal.pgen.1005358

Degani, G., Ragni, E., Botias, P., Ravasio, D., Calderon, J., Pianezzola, E., et al. (2016). Genomic and functional analyses unveil the response to hyphal wall stress in candida albicans cells lacking beta(1,3)-glucan remodeling. *BMC Genomics* 17:482. doi: 10.1186/s12864-016-2853-5

Dichtl, K., Samantaray, S., Aimanianda, V., Zhu, Z., Prevost, M. C., Latge, J. P., et al. (2015). Aspergillus fumigatus devoid of cell wall beta-1,3-glucan is viable, massively sheds galactomannan and is killed by septum formation inhibitors. *Mol. Microbiol.* 95, 458–471. doi: 10.1111/mmi.12877

Dunkler, A., Walther, A., Specht, C. A., and Wendland, J. (2005). *Candida albicans* CHT3 encodes the functional homolog of the Cts1 chitinase of *Saccharomyces cerevisiae*. *Fungal Genet. Biol.* 42, 935–947. doi: 10.1016/j.fgb.2005.08.001

Esteban, P. F., Rios, I., Garcia, R., Duenas, E., Pla, J., Sanchez, M., et al. (2005). Characterization of the CaENG1 gene encoding an endo-1,3-beta-glucanase

involved in cell separation in *Candida albicans*. *Curr. Microbiol.* 51, 385–392. doi: 10.1007/s00284-005-0066-2

Gantner, B. N., Simmons, R. M., and Underhill, D. M. (2005). Dectin-1 mediates macrophage recognition of *Candida albicans* yeast but not filaments. *EMBO J.* 24, 1277–1286. doi: 10.1038/sj.emboj.7600594

Hopke, A., Nicke, N., Hidu, E. E., Degani, G., Popolo, L., and Wheeler, R. T. (2016). Neutrophil attack triggers extracellular trap-dependent candida cell wall remodeling and altered immune recognition. *PLoS Pathog.* 12:e1005644. doi: 10.1371/journal.ppat.1005644

Kusch, J., Meyer, A., Snyder, M. P., and Barral, Y. (2002). Microtubule capture by the cleavage apparatus is required for proper spindle positioning in yeast. *Genes Dev.* 16, 1627–1639. doi: 10.1101/gad.222602

Lenardon, M. D., Munro, C. A., and Gow, N. A. (2010). Chitin synthesis and fungal pathogenesis. *Curr. Opin. Microbiol.* 13, 416–423. doi: 10.1016/j.mib.2010.05.002

Mio, T., Yabe, T., Sudoh, M., Satoh, Y., Nakajima, T., Arisawa, M., et al. (1996). Role of three chitin synthase genes in the growth of *Candida albicans*. *J. Bacteriol.* 178, 2416–2419. doi: 10.1128/jb.178.8.2416-2419.1996

Munoz, J., Cortes, J. C., Sipiczki, M., Ramos, M., Clemente-Ramos, J. A., Moreno, M. B., et al. (2013). Extracellular cell wall beta(1,3)glucan is required to couple septation to actomyosin ring contraction. *J. Cell Biol.* 203, 265–282. doi: 10.1083/jcb.201304132

Munro, C. A., Winter, K., Buchan, A., Henry, K., Becker, J. M., Brown, A. J., et al. (2001). Chs1 of *Candida albicans* is an essential chitin synthase required for synthesis of the septum and for cell integrity. *Mol. Microbiol.* 39, 1414–1426. doi: 10.1046/j.1365-2958.2001.02347.x

Oh, Y., Chang, K. J., Orlean, P., Wloka, C., Deshaies, R., and Bi, E. (2012). Mitotic exit kinase Dbf2 directly phosphorylates chitin synthase Chs2 to regulate cytokinesis in budding yeast. *Mol. Biol. Cell* 23, 2445–2456. doi: 10.1091/mbc.e12-01-0033

Popolo, L., Degani, G., Camilloni, C., and Fonzi, W. A. (2017). The PHR Family: the role of extracellular transglycosylases in shaping *Candida albicans* cells. *J. Fungi.* 3:E59. doi: 10.3390/jof3040059

Popolo, L., Vai, M., Gatti, E., Porello, S., Bonfante, P., Balestrini, R., et al. (1993). Physiological analysis of mutants indicates involvement of the *Saccharomyces cerevisiae* GPI-anchored protein gp115 in morphogenesis and cell separation. *J. Bacteriol.* 175, 1879–1885. doi: 10.1128/jb.175.7.1879-1885.1993

Preechasuth, K., Anderson, J. C., Peck, S. C., Brown, A. J., Gow, N. A., and Lenardon, M. D. (2015). Cell wall protection by the *Candida albicans* class I chitin synthases. *Fungal Genet. Biol.* 82, 264–276. doi: 10.1016/j.fgb.2015.08.001

Ragni, E., Calderon, J., Fascio, U., Sipiczki, M., Fonzi, W. A., and Popolo, L. (2011). Phr1p, a glycosylphosphatidylinsitol-anchored beta(1,3)-glucanosyltransferase critical for hyphal wall formation, localizes to the apical growth sites and septa in *Candida albicans*. *Fungal. Genet. Biol.* 48, 793–805. doi: 10.1016/j.fgb.2011.05.003

Roncero, C., and Sanchez, Y. (2010). Cell separation and the maintenance of cell integrity during cytokinesis in yeast: the assembly of a septum. *Yeast* 27, 521–530. doi: 10.1002/yea.1779

Saporito-Irwin, S. M., Birse, C. E., Sypherd, P. S., and Fonzi, W. A. (1995). PHR1, a pH-regulated gene of *Candida albicans*, is required for morphogenesis. *Mol. Cell Biol.* 15, 601–613. doi: 10.1128/MCB.15.2.601

Schmidt, M., Bowers, B., Varma, A., Roh, D. H., and Cabib, E. (2002). In budding yeast, contraction of the actomyosin ring and formation of the primary septum at cytokinesis depend on each other. *J. Cell Sci.* 115(Pt 2), 293–302.

Sudoh, M., Yamazaki, T., Masubuchi, K., Taniguchi, M., Shimma, N., Arisawa, M., et al. (2000). Identification of a novel inhibitor specific to the fungal chitin synthase. inhibition of chitin synthase 1 arrests the cell growth, but inhibition of chitin synthase 1 and 2 is lethal in the pathogenic fungus *Candida albicans*. *J. Biol. Chem.* 275, 32901–32905. doi: 10.1074/jbc.M003634200

Utsugi, T., Minemura, M., Hirata, A., Abe, M., Watanabe, D., and Ohya, Y. (2002). Movement of yeast 1,3-beta-glucan synthase is essential for uniform cell wall synthesis. *Genes Cells* 7, 1–9. doi: 10.1046/j.1356-9597.2001.00495.x

Walker, L. A., Lenardon, M. D., Preechasuth, K., Munro, C. A., and Gow, N. A. (2013). Cell wall stress induces alternative fungal cytokinesis and septation strategies. *J. Cell Sci.* 126(Pt 12), 2668–2677. doi: 10.1242/jcs.118885

Conflict of Interest: The authors declare that the research was conducted in the absence of any commercial or financial relationships that could be construed as a potential conflict of interest.

frontiers in Cellular and Infection Microbiology

ORIGINAL RESEARCH
published: 06 February 2020
doi: 10.3389/fcimb.2020.00028

What Are the Functions of Chitin Deacetylases in *Aspergillus fumigatus*?

Isabelle Mouyna[1†‡], Sarah Dellière[2‡], Anne Beauvais[1], Fabrice Gravelat[2,3], Brendan Snarr[2,3], Mélanie Lehoux[2], Caitlin Zacharias[2,3], Yan Sun[4], Steven de Jesus Carrion[4], Eric Pearlman[5], Donald C. Sheppard[2,3] and Jean-Paul Latgé[1]*

[1] *Aspergillus Unit, Pasteur Institut, Paris, France,* [2] *Infectious Diseases in Global Health Program, Centre for Translational Biology, McGill University Health Centre, Montréal, QC, Canada,* [3] *Departments of Microbiology and Immunology, Medicine, McGill University, Montréal, QC, Canada,* [4] *Department of Ophthalmology and Visual Sciences, Case Western Reserve University, Cleveland, OH, United States,* [5] *Department of Ophthalmology, University of California, Irvine, Irvine, CA, United States*

OPEN ACCESS

Edited by:
Laura Alcazar-Fuoli, Carlos III Health Institute, Spain

Reviewed by:
Vito Valiante, Leibniz Institute for Natural Product Research and Infection Biology, Germany
Neeraj Chauhan, Rutgers Biomedical and Health Sciences, United States

***Correspondence:**
Jean-Paul Latgé
jplatge@pasteur.fr

†Present address:
Isabelle Mouyna, Neuropathologie Expérimentale, Pasteur Institut, Paris, France

‡*These authors have contributed equally to this work*

Specialty section:
This article was submitted to Fungal Pathogenesis, a section of the journal Frontiers in Cellular and Infection Microbiology

Received: *16 October 2019*
Accepted: *15 January 2020*
Published: *06 February 2020*

Citation:
Mouyna I, Dellière S, Beauvais A, Gravelat F, Snarr B, Lehoux M, Zacharias C, Sun Y, de Jesus Carrion S, Pearlman E, Sheppard DC and Latgé J-P (2020) What Are the Functions of Chitin Deacetylases in Aspergillus fumigatus? Front. Cell. Infect. Microbiol. 10:28. doi: 10.3389/fcimb.2020.00028

Deacetylation of chitin by chitin deacetylases (Cda) results in the formation of chitosan. Chitosan, a polymer of β1,4 linked glucosamine, plays multiple roles in the function of the fungal cell wall, including virulence and evasion of host immune responses. In this study, the roles of chitosan and putative *CDA*s in cell wall structure and virulence of *Aspergillus fumigatus* were investigated. Low levels of chitosan were found in the conidial and cell wall of *A. fumigatus*. Seven putative *CDA* genes were identified, disrupted and the phenotype of the single mutants and the septuple mutants were investigated. No alterations in fungal cell wall chitosan levels, changes in fungal growth or alterations in virulence were detected in the single or septuple Δ*cda1-7* mutant strains. Collectively, these results suggest that chitosan is a minority component of the *A. fumigatus* cell wall, and that the seven candidate Cda proteins do not play major roles in fungal cell wall synthesis or virulence. However, Cda2 is involved in conidiation, suggesting that this enzyme may play a role in N-acetyl-glucosamine metabolism.

Keywords: ***Aspergillus fumigatus*, filamentous fungi, cell wall, chitin deacetylase, chitosan, chitin, conidia**

INTRODUCTION

The fungal cell wall is a complex exoskeleton that protects the cell from osmotic pressure changes and other environmental stresses, yet allows the cell to interact with its environment. Importantly, the fungal cell wall constitutes the first interface between pathogenic fungi and their host. Its components are fungal-specific and are therefore ideal targets for recognition as non-self by immune cells as well as ideal targets for antifungals drugs (Lee and Sheppard, 2016; van de Veerdonk et al., 2017).

Chitin, a homopolymer of N-acetyl-glucosamine (GlcNAc) linked in ß1,4, is produced by many living organisms including crustaceous, insects, and fungi. Chitin can comprise up to 20% of the inner fungal cell wall and can be partially de-N-acetylated to form chitosan, a polymer containing glucosamine (GlcN) as well as GlcNAc. The distinction between these two molecules is not absolute. Polymers with 50% or more acetylation are generally termed chitin, while those with acetylation levels less than this are commonly referred to as chitosan (Kasaai, 2009). Chitin deacetylation is catalyzed by a family of conserved carbohydrate esterase enzymes of type 4 (CE-4 family) known as

chitin-deacetylases (E.C. 3.5.1.41) (Pochanavanich and Suntornsuk, 2002). Deacetylation alters the physical properties of the polymer to enhance solubility, flexibility, and confers a positive charge at neutral pH (Wang et al., 2016). A dynamic equilibrium between the quantity of chitin and chitosan exist in the cell wall but the environmental factors and regulatory elements governing this equilibrium are largely unknown.

The role of chitin deacetylation was first described in non-pathogenic yeast. In *Saccharomyces cerevisiae* (Christodoulidou et al., 1996) two functionally redundant *CDAs* were found to deacetylate chitin specifically in the ascospore cell wall, as the double Δ*cda1cda2* mutant exhibited a complete loss of chitosan from the ascospore. In *Schizosaccharomyces pombe*, a single chitin deacetylase, Cda1, is required for proper spore formation (Matsuo et al., 2005).

The role of chitosan in pathogenicity has been best studied in the fungal plant pathogens *Puccinia graminis*, *Colletotrichum graminicola* (El Gueddari et al., 2002), and more recently in *Magnaporte oryzae* (Geoghegan and Gurr, 2016, 2017; Kuroki et al., 2017). During infection with these organisms, chitin is deacetylated to chitosan within the appressorium, a flattened thickened hyphal tip by which these fungi attach to, and penetrate their host (El Gueddari et al., 2002). Conversion of chitin into chitosan is hypothesized to protect the appressoria from hydrolytic attack by chitinases present in the plant tissue. This approach also serves to prevent the detection of chitin from plant pattern recognition receptors such as CEBiP (Chitin Elicitor Binding Protein) to evade plant immunity (Geoghegan and Gurr, 2016). *M. oryzae* mutants lacking *CDAs* are unable to produce appressorium *in vitro*. However, appressorium development was restored in the mutant during infection of rice leaves and the mutant retained the ability to cause infection, suggesting other polymers may play a compensatory role *in planta* (Geoghegan and Gurr, 2016). Six *CDAs* were found in the genome of *A. nidulans* (Liu et al., 2017). However, in the absence of mutants, the role of *A. nidulans CDAs* could not be determined.

The role of chitosan in human pathogenic fungi has been well-studied in the yeast *Cryptococcus neoformans* which causes meningoencephalitis in immunocompromised patients. Chitosan is an important component of the *C. neoformans* vegetative cell wall (Baker et al., 2007). Three genes, *CDA1*, *CDA2,* and *CDA3*, were identified as coding for putative secreted Cdap in this yeast. Mutants lacking these genes were devoid of cell wall chitosan and exhibited increased susceptibility to cell wall stressors suggesting a role for chitosan in fungal cell wall integrity (Baker et al., 2007). Additionally, the triple Δ*cda* mutant (Δ*cda123*) exhibited attenuated virulence in a mice model of infection (Baker et al., 2011). It has been also reported recently that *CDA1* was required for fungal virulence (Upadhya et al., 2018). Accordingly, Upadhya et al. (2016) showed that protective immunity was induced in mice vaccinated with heat-killed Δ*cda123* cells and was effective in multiple mouse strains. The role of chitosan in other human fungal pathogens such as *A. fumigatus* has not been studied, although two putative chitin deacetylase genes have been annotated within the fungal genome, Afu4g09940 (*CDA5*) and Afu6g10430 (*CDA6*) (Gastebois et al., 2009).

Based on early studies in filamentous phytopathogenic ascomycetes, we hypothesized that chitosan might play a role in cell wall morphogenesis and in host-pathogen interactions in *A. fumigatus*. We explored this hypothesis with the following three specific questions: (i) is chitosan present in the mycelial or conidial cell wall of *A. fumigatus*? (ii) how many *CDAs* genes are present in *A. fumigatus* genome and (iii) what is the role of these *CDA*s in *A. fumigatus*? To answer these questions, we characterized the percentage of deacetylation of the chitosan in the mycelium and conidia. We constructed mutants deficient in *CDA*s and studied the effects of these gene deletions on mycelial and conidial cell wall integrity, morphogenesis, adherence, biofilm formation, and virulence.

MATERIALS AND METHODS

Fungal Strains and Growth Media

The fungal parental strains used in this study was akuBKu80 pyrG+ (KU80) deficient for non-homologous end joining recombination (da Silva Ferreira et al., 2006) that was derived from the *A. fumigatus* strain CEA10 and retained the same virulence potential. Transformations were performed on minimal medium (Glc-MM) (10 g/L glucose (Glc), 0.92 g/L ammonium tartrate, 0.52 g/L KCl, 0.52 g/L $MgSO4{\cdot}7H_2O$, 1.52 g/L KH_2PO_4, 1 mL/L trace element solution (Cove, 1966), pH adjusted to 7.0). Hygromycin B (hph) (Sigma®, St Louis, MO, USA Sigma, Kawasaki, Japan) was added to transformation plates in an overlay after one night of incubation at room temperature, resulting in a final concentration of 150 μg/mL. For DNA extraction, cultures were grown in Sabouraud liquid medium (2% glucose + 1% mycopeptone) and DNA was isolated from *A. fumigatus* as previously described (Girardin et al., 1993). Strains constructed for this work are listed in the **Table 1**. Fungal strains were grown on different culture media: 2% malt-agar, Yeast Potato Dextrose (YPD) (1% yeast extract, 2% peptone, 2% dextrose), Glc-MM, GlcNAc-MM (MM in which Glc was replaced by GlcNAc), Brian (Brian et al., 1961), RPMI (Invitrogen) buffered with 34.53 g/L of MOPS or Dulbecco's Modified Eagle Medium (DMEM) (Invitrogen). Solid media was obtained by supplementation with 1.5–2% agar. Conidia were collected from agar slants/plates after 7 days of growth at room temperature using 0.05% Tween 20 solution.

Chitin Deacetylation Analysis

Two methods were used to quantify the degree of chitin deacetylation in *A. fumigatus* mycelium and conidia. First, the level of deacetylated chitin was measured in mycelial and conidial alkali-insoluble-(AI) and soluble-(AS) cell wall fractions by gas chromatography. Briefly, conidia were recovered with 0.05% tween 20 from 3 weeks old malt tubes at room temperature, and filtered using BD Falcon filters (BD Biosciences) to remove mycelium. Mycelium was obtained after growing conidia for 6 h at 37°C in Sabouraud medium to obtain germ tubes, which were inoculated in shaken flasks in RPMI-MOPS medium for 16 h at 37°C. Mycelium and conidia were disrupted with 1 and 0.17 mm diameter glass beads, respectively, for 2 min in Fast-prep cell breaker (MP Biomedical) at 4°C. The cell wall was

TABLE 1 | Fungal strains used and constructed in the present study.

Strains	Genotypes	Source
Parental strain KU80	CEA17Δ*akuB*^{KU80}	da Silva Ferreira et al., 2006
Δ*cda1*	CEA17_Δ*akuB*^{KU80}Δ*cda1::six-β-rec-hygroR-six*	This study
Δ*cda2*	CEA17_Δ*akuB*^{KU80}Δ*cda2::six-β-rec-hygroR-six*	This study
Δ*cda3*	CEA17_ΔakuB ^{KU80}Δcda3::six-β-rec-hygroR-six	This study
Δ*cda4*	CEA17_Δ*akuB*^{KU80}Δ*cda4::six-β-rec-hygroR-six*	This study
Δ*cda5*	CEA17_Δ*akuB*^{KU80}Δ*cda5::six-β-rec-hygroR-six*	This study
Δ*cda6*	CEA17_Δ*akuB*^{KU80}Δ*cda6::six-β-rec-hygroR-six*	This study
Δ*cda7*	CEA17_Δ*akuB*^{KU80}Δ*cda7::six-β-rec-hygroR-six*	This study
Δ*cda4/5*	CEA17_Δ*akuB*^{KU80} Δ*cda4::six/*Δ*cda5::six-β-rec-hygroR-six*	This study
Δ*cda4/5/6*	CEA17_Δ*akuB*^{KU80} Δ*cda4::six/*Δ*cda5::six/*Δ*cda6::six-β-rec-hygroR-six*	This study
Δ*cda4/5/6/3*	CEA17_Δ*akuB*^{KU80}Δ*cda4::six/*Δ*cda5::six/*Δ*cda6::six/*Δ*cda3::six-β-rec-hygroR-six*	This study
Δ*cda4/5/6/3/2*	CEA17_Δ*akuB*^{KU80}Δ*cda4::six/*Δ*cda5::six/*Δ*cda6::six/*Δ*cda3::six/*Δ*cda2::six-β-rec-hygroR-six*	This study
Δ*cda4/5/6/3/2/1*	CEA17_Δ*akuB*^{KU80}Δ*cda4::six/*Δ*cda5::six/*Δ*cda6::six/*Δ*cda3::six/*Δ*cda2::six*Δ*cda1::six-β-rec-hygroR-six*	This study
Δ*cda4/5/6/3/2/1/7* (Δ*cda1-7*)	CEA17_Δ*akuB*^{KU80}Δ*cda4::six/*Δ*cda5::six/*Δ*cda6::six/*Δ*cda3::six/*Δ*cda2::six*Δ*cda1::six*Δ*cda7::six-β-rec-hygroR-six*	This study

recovered by centrifugation, washed three times in distilled water and lyophilized. Freeze-dried cell walls were boiled 10 min, twice in 50 mM Tris-HCl pH 7.4 containing 50 mM EDTA, 2% SDS and 40 mM β-mercaptoethanol, and extensively washed with water. The AS and AI fractions were extracted as described previously (Beauvais et al., 2005). For chitin deacetylation measurement, 5 mg AS and AI were incubated in 1 mL 2 M $NaNO_2$ and 0.33 mL 2 N HCl for 6 h at room temperature. After evaporation of HNO_2 under nitrogen for 30 min and centrifugation, the supernatant was loaded on 50 × 8 (H^+) and 1 × 8 resin (acetate-O^-), separated by a GF/C whatman filter. The water-eluted fraction was recovered and lyophilized. Half of the eluted fraction was reduced and peracetylated prior anhydromannitol quantification (representing the deacetylated chitin fraction degraded by HNO_2) by gas chromatography (GC) (Sawardeker and Sloneker, 1965). The remaining half of the eluted fraction was hydrolyzed by 8 N HCl for 4 h at 100°C, reduced and peractylated prior determination of the total GlcN (by gas chromatography with meso-inositol as internal standard (Mouyna et al., 2010). The results were expressed in μg of deacetylated chitin in AI and AS fractions.

The degree of chitin deacetylation was also quantified using a colorimetric approach based on the specific absorbance of the free amine groups present on GalN sugars (Dubois, 1956). Briefly, 200 μL (10 mg/mL) cell wall were incubated in 200 μL 5% $KHSO_4$ + 200 μL 5% $NaNO_2$ for 1 h at 50°C. As a control, the cell wall was incubated in 5% NaCl instead of 5% $NaNO_2$. After evaporation of HNO_2 using 200 μL 12.5% ammonium sulfamate for 5 min, 200 μL 0.5% 3-methyl-2-benzothiazolinone hydrazine hydrochloride hydrate was added to the mixture. After incubation 30 min at 37°C, 200 μL 0.5% $FeCl_3$ was added and the incubation was continued for 5 min. The OD of the extract was measured at 650 nm (800 nm as reference), using GlcN for the calibration curve. In parallel, 200 μL (10 mg/mL) conidial cell wall were hydrolyzed by 8 N HCl as above. The extract was then dried, solubilized in 200 μL of water and the amount of GlcN was quantified by HPLC with a CarboPAC PA-1 column (Dionex) and a pulsed electrochemical detector as previously described (Hartland et al., 1996).

Construction of the Δ*cda* Deletion Strains

The single and multiple *CDA* deletion mutants were constructed in KU80 background (da Silva Ferreira et al., 2006) using the β-rec/six site-specific recombination system (Hartmann et al., 2010). The self-excising β-rec/six blaster cassette containing the hph resistance marker was released from the plasmid pSK529 via *Fsp*I restriction enzyme. Using the GeneArt® Seamless Cloning and Assembly (Life technologies, Carlsbad, CA 92008 USA) the *CDA* replacement cassette containing the marker module flanked by 5′ and 3′ homologous regions of the target gene generated by PCR (**Table S1**), was cloned into the pUC19 vector. The corresponding replacement cassettes were released from the resulting vector via *Sma*I or *Fsp*I. The KU80 parental strain was transformed with the *CDA* replacement cassette by electroporation as described by Sanchez and Aguirre to generate the single deletion mutants (Sánchez and Aguirre, 1996). For the construction of multiple deletion strains, single deletion strain was cultivated in presence of 2% xylose-containing MM (instead of glucose) that allows the excision of the selection marker by recombination of the six recognition regions. All gene deletions were confirmed by Southern blotting (**Figure S1**).

Growth, Sporulation, Germination, and Morphology of the Δ*cda* Mutant Strains

Fungal growth was measured at 37or 50°C in agar based media: malt, Sabouraud, RPMI, Glc-MM, and GlcNAc-MM. Plates were spotted at the center with 10^5 conidia suspended in 5 μL of 0.01% Tween 20 and the diameter of the colony was measured daily. Growth of the parental and mutant strains were also monitored at 37°C in 50 mL (3% glucose + 1% yeast extract) liquid medium shaken at 150 rpm and the dry weight determined.

Conidiation rates were quantified by inoculating 10^5 conidia in tubes containing 2% Malt-agar medium. After 1 week of growth at RT, conidia were recovered with 5 mL of an aqueous 0.05% Tween 20 solution and the absorbance was measured at 600 nm (OD_{600} nm = 0.620 ≈ 2 × 10^7 conidia/mL). Conidial germination was followed microscopically every 30 min after 4 h of growth at 37°C (inoculation of 5 μL of conidia at 10^6 cell/mL on a glass slide with 2% Malt-agar medium). For the viability assays, conidia on agar slants were stored at 37°C for 2 months, conidial suspensions were then recovered in 0.05% Tween 20 water, and the viability of conidia was evaluated by quantitative culture on 2% malt medium.

Susceptibility to Antifungal Drugs

The susceptibility of mutant strains to antifungal cell wall drugs was determined by spotting 3 μL of a suspension of conidia at 5 × 10^6 cell/mL on plates supplemented with each drug. The sensitivity to Congo Red® (CR) and CFW was estimated on Glc-MM-agar containing 0–300 μg/mL CR or 0–200 μg/mL CFW. Plates were incubated for 48 h at 37°C and growth was measured. Resistance to caspofungin (0.07–38 μg/ml) was assessed in liquid RPMI-MOPS medium by the resazurin method (Clavaud et al., 2012).

Biofilm Quantification

Biofilm cultures were grown statically for 20 h in tissue culture-treated 96 wells-plates (Falcon) in Brian media at 10^5 conidia/mL as described previously (Snarr et al., 2017). Following incubation, non-adherent cells were removed by washing the wells twice with distilled water. The wells were stained with 0.1% (w/v) crystal violet for 10 min at room temperature and then rinsed twice with water. The remaining dye was extracted by addition of 70% (v/v) ethanol and left for 10 min, after which the absorbance was measured at 600 nm using Infinite M200 Pro spectrophotometer (Tecan).

RNA Isolation and Gene Expression Level by Quantitative RT-PCR

The expression level of the sporulation involved-genes *BRLA*, *ABAA*, *WETA* was performed by reverse-transcriptase real-time PCR using primers designed using the Beacon Designer 4.0 software (**Table S1**). One hundred conidia were spotted on Glc-MM and GlcNAc-MM and let them grow 7 days at 37°C. Conidia from sporulating colonies were recovered in 500 μL phenol, disrupted with 0.5 mm diameter glass beads and RNA was isolated by using the phenol-chloroform method. Reverse transcription and real-time PCR were performed as described previously (Mouyna et al., 2010). The expression ratios were normalized to *TEF1* expression and calculated according to the ΔΔCt method (Livak and Schmittgen, 2001). Three independent biological replicates were performed.

Virulence Studies

Murine Model of Invasive Pulmonary Aspergillosis

The virulence of the parental KU80 strain and the Δ*cda1-7* mutant was tested in a murine model of invasive pulmonary aspergillosis. Mice were immunosuppressed with cortisone acetate, 250 mg/kg subcutaneously on days−2 and +3, and cyclophosphamide (Western Medical Supply), 250 mg/kg intraperitonealy on day−2 and 200 mg/kg on day +3 (Sheppard et al., 2004, 2006). For each fungal strain tested, groups of 16 mice were infected using an aerosol chamber as previously described (Sheppard et al., 2004). An additional 8 mice were immunosuppressed but not infected. To prevent bacterial infections, enrofloxacin was added to the drinking water while the mice were immunosuppressed. Mice were monitored for signs of illness and moribund animals were euthanized. All procedures involving mice were approved by the Animal Care Committees of the McGill University Health Center and followed the National Institutes of Health guidelines for animal housing and care. For fungal burden determination, 8 mice out of 16 were sacrificed 4 days after infection. The lungs were immediately homogenized in ice cold PBS containing 10 mL of protease inhibitor mix/mL (Sigma Aldrich), and then aliquoted and stored at −80°C until use. Pulmonary galactomannan (GM) content of lung homogenates was used as a surrogate measure of fungal burden using the Platelia Aspergillus EIA kit (Bio-Rad) as described previously (Gravelat et al., 2013). Lung homogenates were clarified by centrifugation, diluted 1:20 and assayed as per manufacturer's recommendations. Samples were compared to a standard curve composed of serial dilutions of lung homogenate from a mouse heavily infected.

Murine Model of *A. fumigatus* Keratitis

C57BL/6 mice were purchased from The Jackson Laboratory (Bar Harbor, ME) and AMCase$^{-/-}$ mice were obtained from Dr. Lori Fitz through a material transfer agreement between UC Irvine and Pfizer. Mice were bred under specific pathogen-free conditions and maintained according to institutional guidelines. All animals were treated in accordance with the guidelines provided in the Association for Research in Vision and Ophthalmology (ARVO) statement for the Use of Animals in Ophthalmic and Vision Research, and were approved by Case Western Reserve University and UC Irvine IACUC committees.

Mice were infected as previously described (de Jesus Carrion et al., 2013; Leal et al., 2013). *A. fumigatus* strains were cultured in VMM agar in 25 cm^2 tissue culture flasks. Dormant conidia were recovered with a bacterial L-loop and harvested in 5 ml PBS. Pure conidial suspensions were obtained by passing the culture suspension through PBS-soaked sterile gauges placed at the tip of a 10 ml syringe. Conidia were quantified and a stock was made at a final concentration of 2.5 × 10^4 conidia/μl in PBS. Mice were anesthetized and the corneal epithelium was abraded with a 30 gauge needle to allow insertion of a 33-gauge Hamilton needle through which 2 μl PBS containing 4 × 10^4 conidia were injected into the corneal stroma as described by (de Jesus Carrion et al., 2019). For assessment of fungal viability, whole eyes were homogenized under sterile conditions in 1 ml PBS, using the Mixer Mill MM300 (Retsch, Qiagen, Valencia, CA) at 33 Hz for 4 min. Subsequently, serial log dilutions were performed and plated onto Sabouraud dextrose agar plates (Becton Dickenson). Following incubation for 24 h at 37°C, the number of CFUs was determined by direct counting.

Statistical Analyses and Graphs

All analyses were performed with GraphPad Prism software v6.0 (GraphPad Software). *P*-values were determined by student's *t*-test. A *P*-value of <0.05 (two-tailed) is considered statistically significant.

RESULTS

Quantification of Chitosan in the Cell Wall of *A. fumigatus*

Gas chromatography analysis of cell wall fractions from *A. fumigatus* revealed a total concentration of 1.1 μg/mg of free GlcN group in the mycelial cell wall, and 2.6 μg/mg in the the conidial cell wall (**Figure 1A**). These data indicate a chitin deacetylation fraction of 1.5% in the mycelium (AI fraction) and 7.8% in conidia (**Figure 1B**). Free amine quantification confirmed that 8.5% of conidial chitin is deacetylated (**Figure 2**). Unfortunately, due to the insufficient sensitivity of the method used to quantify free amine and to the low amount of deacetylated chitin in the mycelium, it was impossible to obtain reliable quantification of free amine on hyphal samples. Interestingly, glucosamine polymer was found in the AI and AS fractions of the conidial cell wall whereas it was only found in the AI fraction of the mycelial cell wall. Collectively these data suggest that chitosan is only a significant component of the conidial cell wall.

Characterization of the *CDA* Gene Family in *A. fumigatus*

To identify putative *CDA*-encoding genes in *A. fumigatus*, the sequence of the well-characterized fungal chitin deacetylase from *Colletotrichum lindemuthianum* (AY633657) (Blair et al., 2006), was used to perform a BLAST search of the *A. fumigatus* genome (https://blast.ncbi.nlm.nih.gov/Blast.cgi). Seven putative *A. fumigatus* open reading frames predicted to encode a polysaccharide/chitin de-N-acetylase domain (Pfam 01522) were identified (http://pfam.xfam.org/) belonging to CE-4 family of the CaZy database (http://www.cazy.org:) *CDA1*, AFUA_1G15280; *CDA2*, AFUA_6G05030; *CDA3*, AFUA_3G07210; *CDA4*, AFUA_5G11410; *CDA5*, AFUA_4G09940, *CDA6*, AFUA_6G10430, and *CDA7*, AFUA_5G09130. The characteristics of these putative chitin deacetylases are given in **Table S2**. Conserved domains, including transmembrane domains and peptide signals, were characterized with SMART for each putative protein (http://smart.embl-heidelberg.de/). Cda3, Cda4, and Cda6 have a predicted N-terminal peptide signal, suggesting that these proteins are secreted while Cda1, Cda2, and Cda7 are predicted to be intracellular proteins. Cda6 contains a Carbohydrate Binding Domain (CBM18) and is likely GPI anchored (mendel.imp.ac.at/gpi/fungi). There was 4–20% of identity between all the putative Cda proteins except Cda2 and Cda7 which are very closely related (almost 80% of identity; **Table S3**). Amino acid conserved between all the Cdap are presented in **Figure 3**. A phylogenic tree containing all known and putative Cdas was created including the putative Cdap of *S. cerevisiae*, *S. pombe*, *C. neoformans*, and *M. oryzae* (**Figure S2**). Three distinct

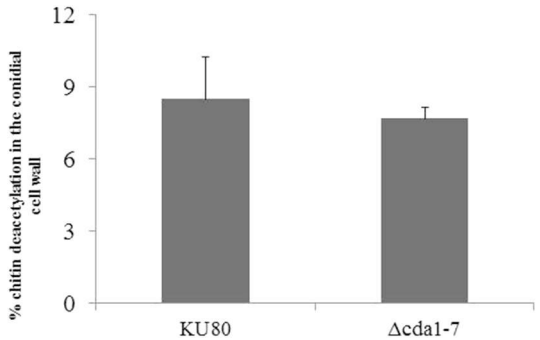

FIGURE 2 | Percentage of chitin deacetylation in KU80 and Δ*cda1-7* conidial cell wall by the method of Dubois (1956).

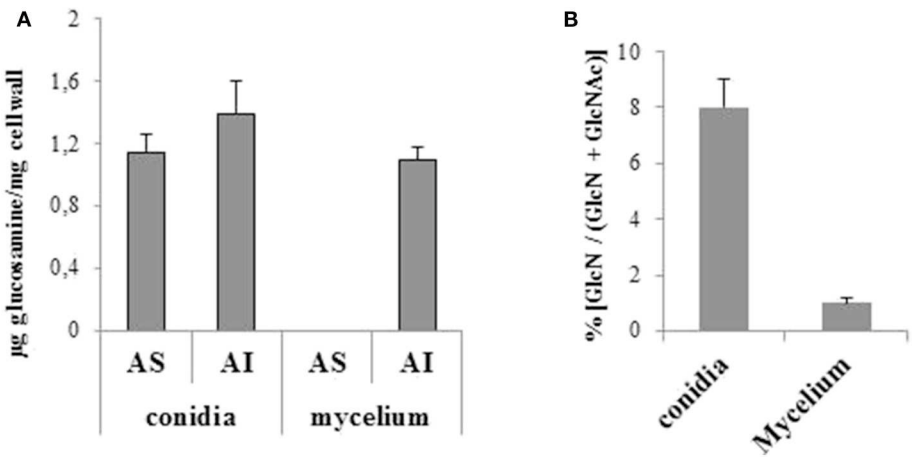

FIGURE 1 | Quantification of glucosamine and N-acetyl glucosamine in the alkali-soluble and -insoluble fractions of mycelial and conidial cell wall. **(A)** Total amount of glucosamine determined by anhydromannitol quantification after HNO_2 deamination followed by GC. **(B)** Percentage of deacetylation of chitin in the cell wall.

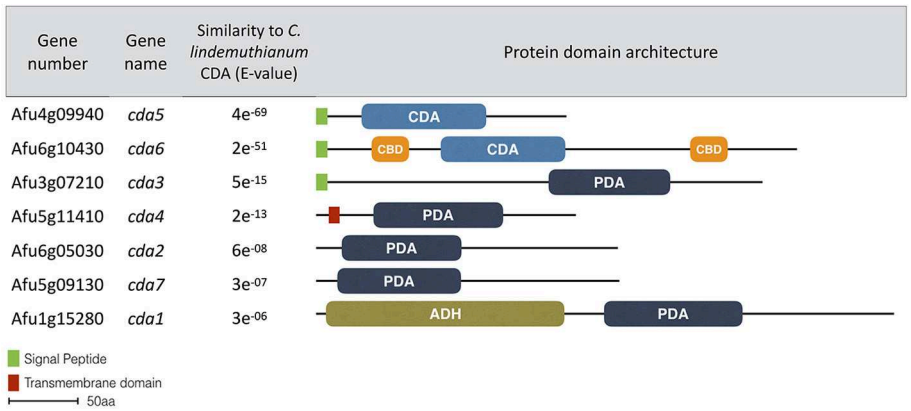

FIGURE 3 | Bioinformatic analysis of *CDA* genes in fungi. Conserved domains and architecture of seven putative chitin de-N-acetylase in *A. fumigatus*. CDA, chitin deacetylase domain; PDA, polysaccharide deacetylase domain; CBD, chitin binding domain; ADH, deshydrogenase domain (Pfam 00106).

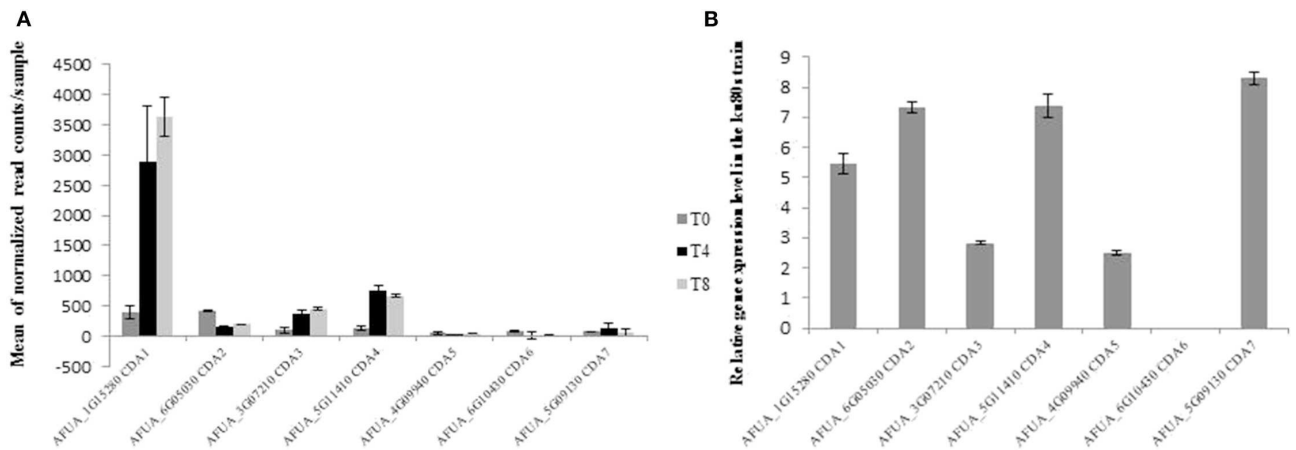

FIGURE 4 | *CDA* gene expression level in *A. fumigatus* **(A)** Gene expression profile of the KU80 *CDA* family genes in dormant (T 0 h), swollen (T 4 h), and germinated conidia (T 8 h) in Glucose 3%/YE 1% medium. The data are extracted from RNAseq analysis data (Mouyna et al., 2016). The errors bars represent standard deviation from the mean values of three different experiments. The data have been normalized/size of the gene **(B)** Relative Gene expression level of the *CDA* genes in the mycelium during conidiation of the parental strain (WT). The expression ratios were relative to *TEF1* gene. Values are taken from the RNA-seq data analysis of Valsecchi et al. (2017). For this RNA-sequencing experiment, the fungus was grown for seven days on malt agar at 37°C at room temperature. The errors bars represent standard deviation from the mean values of three different experiments.

groups are observed: the first group including *A. fumigatus* Cda1, Cda2, and Cda7 with *S. pombe* Cda1p and *M. oryzae* Cbl5p, the second one including *A. fumigatus* Cda4, Cda5, and Cda6 related to all the putative Cdap of the yeast *S. cerevisiae*, *C. neoformans* and the other homologs of *M. oryzae*, and finally a third group including only *A. fumigatus* Cda3.

Gene Level Expression of the CDA Family During Growth

We used the expression data from a RNA sequencing analysis performed to quantify the expression of glycosyl-hydrolases in dormant, swollen, and germinated conidia (Mouyna et al., 2016; **Figure 4A**). In addition, since the level of glucosamine was the highest in the conidia, we undertook a specific analysis of the expression of the CDAs during the conidiation (**Figure 4B**). The gene *CDA1* was highly expressed especially in swollen and germinated conidia. Genes *CDA2, CDA3,* and *CDA4* were expressed in both stages, while *CDA7*, *CDA5,* and *CDA6* were only weakly expressed (**Figure 4A**). Genes *CDA1*, *CDA2*, *CDA7,* and *CDA4* were strongly expressed during conidiation (**Figure 4B**). The combined transcriptional profiling data suggested that *CDA1* may be involved in chitin deacetylation during germination and vegetative development and *CDA1*, *CDA2*, *CDA7,* and *CDA4* during conidiogenesis.

Phenotypic Analysis of Δ*cda* Mutants

To determine the role of candidate *CDA* genes in chitosan synthesis, single deletion mutants for each *CDA* gene, and a septuple mutant lacking all seven *CDA* genes (Δ*cda1-7*) were constructed. Quantification of chitosan by free amine

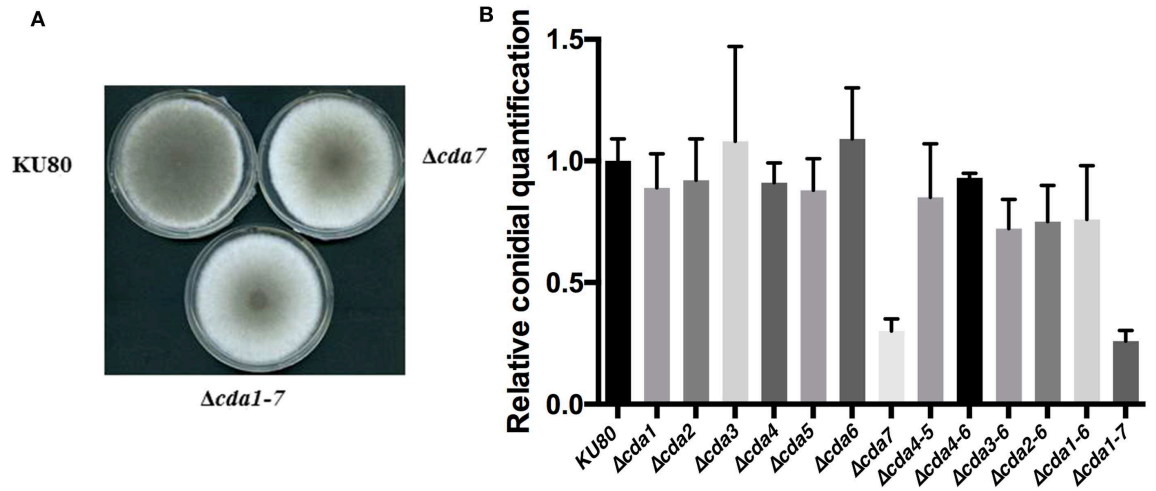

FIGURE 5 | Vegetative growth of *A. fumigatus* wild-type strain and Δ*cda* mutants on GlcNAc as sole carbon source. **(A)** Colonies of the KU80, Δ*cda*7, and Δ*cda1-7* on GlcNAc-MM; **(B)** Conidia quantification on GlcNAc-MM. Data are normalized to parental strain KU80.

determination revealed no differences in the percentage of chitin deacetylation in the conidia of the Δ*cda1-7* mutant strain and the parental strain, suggesting that these seven candidate *CDA* genes do not play a role in the deacetylation of chitin in *A. fumigatus* conidia (**Figure 2**).

The effects of the deletion of putative *CDA* genes on *A. fumigatus* germination, growth and resistance to cell wall stress were evaluated. No differences in germination, growth in liquid or solid medium or biofilm growth were observed between wild-type *A. fumigatus* and the septuple Δ*cda1-7* mutant (**Figure S3**; data not shown). No difference in susceptibility to the ß1,3 glucan synthase inhibitor caspofungin was observed, with both strains exhibiting an MIC of 0.3 μg/mL. Similarly, agar dilution assays demonstrated that both strains displayed similar growth on media containing CR or CFW (data not shown). Moreover, no microscopic differences in hyphal morphology or branching pattern were observed between these strains in presence of any of these cell wall stressors (data not shown). These results confirmed that the chitosan does not play a role in the morphogenesis of the mycelial cell wall.

The effect of *CDA* deletions on conidiation was tested by examining the ability of the parental and Δ*cda1-7* mutant strains to conidiate on different solid media. No difference in conidiation of KU80 and Δ*cda1-7* was observed on regular glucose media (data not shown). However, when grown on GlcNAc as the sole carbon source (GlcNAc-MM), the Δ*cda1-7* mutant exhibited reduced conidiation, with 74 (±4.3)% fewer conidia produced as compared with the wild-type KU80 strain ($p < 0.001$) (**Figures 5A,B**). However, in presence of glucosamine conidiation was similar to the parental and other mutant strains (**Figure S4**). The conidiation defect of the Δ*cda1-7* mutant was uniquely dependent on the deletion of *CDA7,* since the single Δ*cda7* mutant exhibited a similar reduction in conidiation (70 ± 5.0%) as was observed in the septuple mutant (**Figure 5B**). In accordance with the observed conidiation defect of the Δ*cda7* and Δ*cda1-7* mutants, expression of *BrlA, WetA, and AbaA* were significantly down regulated in these strains (**Figure S5**). These results suggest that Cda7 may not function as a chitin deacetylase, but rather plays a role in GlcNAc-metabolism and/or sensing.

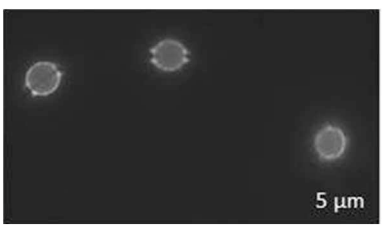

FIGURE 6 | Ascospores of *A. fumigatus* labeled by Eosin Y.

Since studies in plant pathogens suggest that the importance of the *CDAs* may be different *in vivo* and *in vitro*, we evaluated the role of putative *CDAs* in the pathogenesis of *Aspergillus* infection in a neutropenic mouse model of pulmonary invasive aspergillosis and in an *Aspergillus* corneal infection model in immunocompetent mice. No difference in the survival rate (**Figure S6A**) or pulmonary fungal burden of immunosuppressed mice infected by wild-type strain or the Δ*cda1-7* mutant strain were observed (**Figure S6B**). Similarly, there was no difference in fungal burden between these strains in infected corneas (**Figure S7**). Collectively these data showed that these candidate *CDA* genes are dispensable for the virulence of *A. fumigatus*.

DISCUSSION

In the plant pathogenic fungi *M. oryzae, P. graminis,* and *C. graminicola*, chitosan was located in the cell wall of the invasive and adhesive germ tube (El Gueddari et al., 2002;

Geoghegan and Gurr, 2016). This observation initially suggested the possibility that chitosan in conidia and appressorium plays a role in host-adherence. In contrast, in *A. fumigatus* the amount of deacetylated chitin is minimal in the hyphal cell wall. This finding is in agreement with the lack of any role of the putative Cda proteins in vegetative growth or infection. These findings suggest that other positively charged-osamine polymers such as the ones present in GAG, mediate adhesion of *A. fumigatus* mycelium to host tissues (Lee et al., 2016).

In the conidia of *A. fumigatus*, we found that deacetylation of cell wall chitin was not due to the activity of the Cdas. Deacetylation of chitin in *A. fumigatus* conidial cell wall could be mediated by other *A. fumigatus* CE-4 family deacetylases such as Agd3, already known to deacetylate GalNac residues within GAG (Lee et al., 2016). CE-4 family included many other deacetylases with low specificity, which are active toward a variety of substrates. *A. nidulans* chitin deacetylase has been produced as a recombinant protein. It was able to fully deacetylate a partially acetylated chitosan and active only on chitin which is not-crystallized. As with other Cda, this protein exhibited poor substrate specificity as it was able to act on acetylated- xylan and glucuroxylan (Liu et al., 2017). The bacterial deacetylases, PelA in *Pseudomonas aeruginosa*, IcaB in *Staphylococcus epidermidis,* PgaB in *Escherichia coli* and PssB in *Listeria monocytogenes*, all homologous to the *A. fumigatus* Agd3, are also poorly specific since they are able to deacetylate different polymers of GlcNAC or N-acetylmannosamine residues (Lee et al., 2016; Ostapska et al., 2018).

Is deacetylated chitin necessary during the vegetative life of *A. fumigatus*? Probably not, since the deletion of *CDAs* did not alter the growth, germination, resistance to antifungal cell wall compounds, nor pathogenicity of *A. fumigatus*. However, the mutant deficient for *CDA7* showed impaired conidiation on MM containing GlcNAc as sole carbon source, which was confirmed in the septuple mutant. Cda7 is not a functional deacetylase since the same amount of deacetylated chitin was found in the sextuple mutant Δ*cda1*-7 but this esterase could be involved in GlcNAc catabolism necessary to produce primary carbon source for the fungal cell allowing normal conidial development. The function of AfCda7 is different from *A. nidulans's* Cda which deacetylated *in vitro* a minimum of two GlcNAc monomers (Liu et al., 2017). Another hypothesis is that Cda7 could be involved in glucosamine sensing. GlcNAc has been shown to activate intracellular signalization pathways through different mechanisms in microbial pathogens regulating different functions including virulence function in some species (Naseem and Konopka, 2015). For instance, it promotes hyphal growth in *Candida albicans*. GlcNAc catabolism increases medium pH by releasing ammonia, while glucose catabolism decreases the pH. A synergy between basic extracellular medium and GlcNAc recognition by GlcNAc sensors promotes hyphae formation in the yeast independently from hyphal-specific genes (Naseem and Konopka, 2015). *C. albicans* Gig1, another member of the CE-4 family is specifically induced by GlcNAc and not by other sugars (Gunasekera et al., 2010). Gig1 is not essential for GlcNAc metabolism or induction of hyphae but the Δ*gig1* mutant displayed increased resistance to nikkomycin Y, which inhibits chitin synthase from converting UDP-GlcNAc into cell wall chitin. Two orthologs with 20–26% of homology have been identified in the *A. fumigatus* genome. Yet, no protein homology was observed between Cda7 and the GlcNAc sensors such as Ngs1, the GlcNAc deacetylase Nag2 which is part of the NAG regulon governing the GlcNAc signalization pathway in *C. albicans*, nor Gig1 (Su et al., 2016; Naseem et al., 2017). The production of recombinant Cda proteins of *A. fumigatus,* as well as the analysis of the expression of the different *CDA*'s in presence of GlcNAc or GlcN will be required to elucidate the role of *CDAs* in *A. fumigatus*.

CDA's could also play a role in the formation of ascospores in *A. fumigatus*. Ascospores are the fungal structures with the highest proportion of chitosan (Zhang et al., 2017). In *S. cerevisiae*, *CDA*'s are specifically expressed during ascospore formation and chitosan appears to have a structural role (Pammer et al., 1992; Christodoulidou et al., 1996). The sexual form of *A. fumigatus* was recently discovered (O'Gorman et al., 2009). *A. fumigatus* ascospores have not been described in nature and require very specific conditions to be produced *in vitro* as they have been obtained only in oatmeal agar medium incubated in the dark at 30°C for several months before sexual reproduction was completed. *A. fumigatus* ascospores were eosin Y positive, showing that they contained substantial amount of chitosan (**Figure 6**). *CDA*'s could be responsible for the deacetylation of chitin in *A. fumigatus* ascospores and defect in chitosan may inhibit ascospore formation like in *S. cerevisiae* (Pammer et al., 1992).

In conclusion, despite the fact that chitin deacetylases are present throughout the Fungi kingdom and exhibit similar catalytic sites in their protein sequences, they appeared to mediate very different biological processes depending on the organism. In *A. fumigatus*, our study suggests that chitin in conidia was not deacetylated by Cda proteins. The enzyme responsible for deacetylation of chitin within the conidial cell wall is still unknown but could be due to other CE4 deacetylases. In *A. fumigatus* the deletion of *CDA* genes did not play any role in morphogenesis, cell wall integrity, adherence and virulence. While *A. fumigatus* is able to produce ascospores with a chitosan-rich cell wall, the involvement of *CDA*s for the formation of chitosan in these structures remains to be demonstrated.

DATA AVAILABILITY STATEMENT

The raw data supporting the conclusions of this article will be made available by the authors, without undue reservation, to any qualified researcher.

ETHICS STATEMENT

All procedures involving mice were approved by the Animal Care Committees of the McGill University Health Center and followed the National Institutes of Health guidelines for animal housing and care.

AUTHOR CONTRIBUTIONS

IM, SD, AB, EP, DS, and J-PL conceived and designed the experiments, analyzed the data, and wrote the paper. IM, SD, AB, FG, BS, ML, CZ, YS, and SJ performed the experiments.

FUNDING

This research was funded by AVIESAN grant (to complete), la Fondation pour la Recherche Médicale for the grant Espoirs de la recherche to fulfill SD's MSc project. This research was also supported by NIH grant RO1 EY18612 (EP).

ACKNOWLEDGMENTS

We would like to thank Prof. Holger Deising for kindly providing anti-chitosan antibodies. We also thank Prof. Françoise Botterel for sharing her human resources.

SUPPLEMENTARY MATERIAL

The Supplementary Material for this article can be found online at: https://www.frontiersin.org/articles/10.3389/fcimb.2020.00028/full#supplementary-material

Figure S1 | Targeted replacement strategies used for *A. fumigatus CDA* genes.

Figure S2 | Phylogeny of the proteins of Af, *A. fumigatus*; Mo, *M. oryzae*; Sc, *S. cerevisiae*; Cn, *C. neoformans*; Sp, *S. pombe* and *Mucor* rouxii. Sequence alignment and phylogenetic reconstructions have been done using clustalW (https://www.genome.jp/tools-bin/clustalw) The tree was constructed using FastTree v2.1.8 with default parameters (Price et al., 2009).

Figure S3 | Growth on agar Malt medium of the parental strain KU80, the single deletion Δ*cda* mutants as well as the Δ*cda1-7* deletion mutant.

Figure S4 | Growth on agar glucosamine-MM medium of the parental strain KU80, the single deletion Δ*cda7* mutants as well as the Δ*cda1-7* deletion mutant.

Figure S5 | Transcription factor gene expression level by QPCR on GlcNAc-MM medium. Gene expression data expressed as $2^{-\Delta\Delta Ct}$ are the mean of at least three replicates ± standard error and were calculated as the ratio of the target gene compared with the Elongation factor 1 (EF1α) gene used as a reference.

Figure S6 | Virulence of Δ*cda* deficient strain in a mice model of invasive aspergillosis. A total of 16 animals were infected by each strain. **(A)** Survival of immunosuppressed mice infected intranasally with *A. fumigatus* parental strain KU80 and Δ*cda1-7* mutant and of uninfected strain **(B)** Quantification of fungal burden in lung homogenates of mice after 4 days of infection using pulmonary galactomannan content as a surrogate measure. Error bars indicate standard errors.

Figure S7 | Role of the Cdas in *A. fumigatus* survival in corneal infection. CFU of infected corneas for the parental strain KU80 and the Δ*cda 1-7* mutant. Each data point represents a single infected cornea. Significance was determined by student's *T*-test to compare two groups. *P*-values: * < 0.05, *** < 0.0001. Experiments were repeated three times with similar results.

Table S1 | Primers used in this study.

Table S2 | Characteristics of *A. fumigatus CDA* family.

Table S3 | Percent of identity between the *A. fumigatus CDA* family members, *CDA* from *C. lindemuthianum* (Cl CDA-col) and *CDA1* from *S. cerevisiae* (Sc), *S. pombe* (Sp), *C. neoformans* (Cn), and *M. grisea* (Mg). The% of identities between these proteins have been calculated after sequence alignment using clustalW (https://www.genome.jp/tools-bin/clustalw) and GeneDoc 2.7 software.

REFERENCES

Baker, L. G., Specht, C. A., Donlin, M. J., and Lodge, J. K. (2007). Chitosan, the deacetylated form of chitin, is necessary for cell wall integrity in *Cryptococcus neoformans*. *Eukaryot. Cell* 6, 855–867. doi: 10.1128/EC.00399-06

Baker, L. G., Specht, C. A., and Lodge, J. K. (2011). Cell wall chitosan is necessary for virulence in the opportunistic pathogen *Cryptococcus neoformans*. *Eukaryot. Cell* 10, 1264–1268. doi: 10.1128/EC.05138-11

Beauvais, A., Maubon, D., Park, S., Morelle, W., Tanguy, M., Huerre, M., et al. (2005). Two (1-3) glucan synthases with different functions in *Aspergillus fumigatus*. *Appl. Environ. Microbiol.* 71, 1531–1538. doi: 10.1128/AEM.71.3.1531-1538.2005

Blair, D. E., Hekmat, O., Schüttelkopf, A. W., Shrestha, B., Tokuyasu, K., Withers, S. G., et al. (2006). Structure and mechanism of chitin deacetylase from the fungal pathogen *Colletotrichum lindemuthianum*. *Biochemistry* 45, 9416–9426. doi: 10.1021/bi0606694

Brian, P. W., Dawkins, A. W., and Grove, J. F. (1961). Phytotoxic compounds produced by *Fusarium equiseti*. *J. Exp. Bot.* 12, 1–12. doi: 10.1093/jxb/12.1.1

Christodoulidou, A., Bouriotis, V., and Thireos, G. (1996). Two sporulation-specific chitin deacetylase-encoding genes are required for the ascospore wall rigidity of *Saccharomyces cerevisiae*. *J. Biol. Chem.* 271, 31420–31425. doi: 10.1074/jbc.271.49.31420

Clavaud, C., Beauvais, A., Barbin, L., Munier-Lehmann, H., and Latgé, J. P. (2012). The composition of the culture medium influences the β-1,3-glucan metabolism of *Aspergillus fumigatus* and the antifungal activity of inhibitors of β-1,3-glucan synthesis. *Antimicr. Agents Chemother.* 56, 3428–3431. doi: 10.1128/AAC.05661-11

Cove, D. J. (1966). The induction and repression of nitrate reductase in the fungus *Aspergillus nidulans*. *Biochim. Biophys. Acta* 113, 51–56. doi: 10.1016/S0926-6593(66)80120-0

da Silva Ferreira, M. E., Kress, M. R. V. Z., Savoldi, M., Goldman, M. H. S., Hartl, A., Heinekamp, T., et al. (2006). The akuBKU80 mutant deficient for nonhomologous end joining is a powerful tool for analyzing pathogenicity in *Aspergillus fumigatus*. *Eukaryot. Cell* 5, 207–211. doi: 10.1128/EC.5.1.207-211.2006

de Jesus Carrion, S., Abbondante, S., Clark, H. L., Marshall, M. E., Mouyna, I., Beauvais, A., et al. (2019). *Aspergillus fumigatus* corneal infection is regulated by chitin synthases and by neutrophil-derived acidic mammalian chitinase. *Eur. J. Immunol.* 49, 918–927. doi: 10.1002/eji.201847851

de Jesus Carrion, S., Leal, S. M. Jr., Ghannoum, M. A., Aimanianda, V., Latgé, J. P., Pearlman, E., et al. (2013). The RodA hydrophobin on *Aspergillus fumigatus* spores masks dectin-1– and dectin-2–dependent responses and enhances fungal survival *in vivo*. *J. Immunol.* 191, 2581–2588. doi: 10.4049/jimmunol.1300748

Dubois, M. (1956). Colorimetric method for determination of sugars and related substances. *Anal. Chem.* 28, 350–356. doi: 10.1021/ac60111a017

El Gueddari, N. E., Rauchhaus, U., Moerschbacher, B. M., and Deising, H. B. (2002). Developmentally regulated conversion of surface-exposed chitin to chitosan in cell walls of plant pathogenic fungi. *New Phytol.* 156, 103–112. doi: 10.1046/j.1469-8137.2002.00487.x

Gastebois, A., Clavaud, C., Aimanianda, V., and Latgé, J. P. (2009). *Aspergillus fumigatus*: cell wall polysaccharides, their biosynthesis and organization. *Fut. Microbiol.* 4, 583–595. doi: 10.2217/fmb.09.29

Geoghegan, I. A., and Gurr, S. J. (2016). Chitosan mediates germling adhesion in *Magnaporthe oryzae* and is required for surface sensing and germling morphogenesis. *PLoS Pathog.* 12: e1005703. doi: 10.1371/journal.ppat.1005703

Geoghegan, I. A., and Gurr, S. J. (2017). Investigating chitin deacetylation and chitosan hydrolysis during vegetative growth in *Magnaporthe oryzae*. *Cell. Microbiol.* 19:e12743. doi: 10.1111/cmi.12743

Girardin, H., Latgé, J. P., Srikantha, T., Morrow, B., and Soll, D. R. (1993). Development of DNA probes for fingerprinting *Aspergillus fumigatus*. *J. Clin. Microbiol.* 31, 1547–1554. doi: 10.1128/JCM.31.6.1547-1554.1993

Gravelat, F. N., Beauvais, A., Liu, H., Lee, M. J., Snarr, B. D., Chen, D., et al. (2013). *Aspergillus* galactosaminogalactan mediates adherence to host constituents and

conceals hyphal β-glucan from the immune system. *PLoS Pathog.* 9:e1003575. doi: 10.1371/journal.ppat.1003575

Gunasekera, A., Alvarez, F. J., Douglas, L. M., Wang, H. X., Rosebrock, A. P., and Konopka, J. B. (2010). Identification of GIG1, a GlcNAc-induced gene in *Candida albicans* needed for normal sensitivity to the chitin synthase inhibitor nikkomycin Z. *Eukaryot. Cell* 9, 1476–1483. doi: 10.1128/EC.00178-10

Hartland, R. P., Fontaine, T., Debeaupuis, J. P., Simenel, C., Delepierre, M., and Latgé, J. P. (1996). A novel beta-(1-3)-glucanosyltransferase from the cell wall of *Aspergillus fumigatus*. *J. Biol. Chem.* 271, 26843–26849. doi: 10.1074/jbc.271.43.26843

Hartmann, T., Dümig, M., Jaber, B. M., Szewczyk, E., Olbermann, P., Morschhäuser, J., et al. (2010). Validation of a self-excising marker in the human pathogen *Aspergillus fumigatus* by employing the beta-rec/six site-specific recombination system. *Appl. Environ. Microbiol.* 76, 6313–6317. doi: 10.1128/AEM.00882-10

Kasaai, M. R. (2009). Various methods for determination of the degree of N-acetylation of chitin and chitosan: a review. *J. Agr. Food Chem.* 57, 1667–1676. doi: 10.1021/jf803001m

Kuroki, M., Okauchi, K., Yoshida, S., Ohno, Y., Murata, S., Nakajima, Y., et al. (2017). Chitin-deacetylase activity induces appressorium differentiation in the rice blast fungus *Magnaporthe oryzae*. *Sci. Rep.* 7, 1–8. doi: 10.1038/s41598-017-10322-0

Leal, S. M., Roy, S., Vareechon, C., Carrion, S. D., Clark, H., Lopez-Berges, M. S., et al. (2013). Targeting iron acquisition blocks infection with the fungal pathogens *Aspergillus fumigatus* and *Fusarium oxysporum*. *PLoS Pathog.* 9:e1003436. doi: 10.1371/journal.ppat.1003436

Lee, M. J., Geller, A. M., Bamford, N. C., Liu, H., Gravelat, F. N., Snarr, B. D., et al. (2016). Deacetylation of fungal exopolysaccharide mediates adhesion and biofilm formation. *mBio* 7, e00252–e00216. doi: 10.1128/mBio.00252-16

Lee, M. J., and Sheppard, D. C. (2016). Recent advances in the understanding of the *Aspergillus fumigatus* cell wall. *J. Microbiol.* 54, 232–242. doi: 10.1007/s12275-016-6045-4

Liu, Z., Gay, L. M., Tuveng, T. R., Agger, J. W., Westereng, B., Mathiesen, G., et al. (2017). Structure and function of a broad-specificity chitin deacetylase from *Aspergillus nidulans* FGSC A4. *Sci. Rep.* 7:1746. doi: 10.1038/s41598-017-02043-1

Livak, K. J., and Schmittgen, T. D. (2001). Analysis of relative gene expression data using real-time quantitative PCR and the 2−ΔΔCT method. *Methods* 25, 402–408. doi: 10.1006/meth.2001.1262

Matsuo, Y., Tanaka, K., Matsuda, H., and Kawamukai, M. (2005). cda1+, encoding chitin deacetylase is required for proper spore formation in *Schizosaccharomyces pombe*. *FEBS Lett.* 579, 2737–2743. doi: 10.1016/j.febslet.2005.04.008

Mouyna, I., Aimanianda, V., Hartl, L., Prevost, M.-C., Sismeiro, O., Dillies, M. A., et al. (2016). GH16 and GH81 family β-(1,3)-glucanases in *Aspergillus fumigatus* are essential for conidial cell wall morphogenesis. *Cell. Microbiol.* 18, 1285–1293. doi: 10.1111/cmi.12630

Mouyna, I., Kniemeyer, O., Jank, T., Loussert, C., Mellado, E., Aimanianda, V., et al. (2010). Members of protein O-mannosyltransferase family in *Aspergillus fumigatus* differentially affect growth, morphogenesis and viability. *Mol. Microbiol.* 76, 1205–1221. doi: 10.1111/j.1365-2958.2010.07164.x

Naseem, S., and Konopka, J. B. (2015). N-acetylglucosamine regulates virulence properties in microbial pathogens. *PLoS Pathog.* 11:e1004947. doi: 10.1371/journal.ppat.1004947

Naseem, S., Min, K., Spitzer, D., Gardin, J., and Konopka, J. B. (2017). Regulation of hyphal growth and N-acetylglucosamine catabolism by two transcription factors in *Candida albicans*. *Genetics* 206, 299–314. doi: 10.1534/genetics.117.201491

O'Gorman, C. M., Fuller, H. T., and Dyer, P. S. (2009). Discovery of a sexual cycle in the opportunistic fungal pathogen *Aspergillus fumigatus*. *Nature* 457, 1–5. doi: 10.1038/nature07528

Ostapska, H., Howell, P. L., and Sheppard, D. C. (2018). Deacetylated microbial biofilm exopolysaccharides: it pays to be positive. *PLoS Pathog.* 14:e1007411. doi: 10.1371/journal.ppat.1007411

Pammer, M., Briza, P., Ellinger, A., Schuster, T., Stucka, R., Feldmann, H., et al. (1992). DIT101 (CSD2, CAL1), a cell cycle-regulated yeast gene required for synthesis of chitin in cell walls and chitosan in spore walls. *Yeast* 8, 1089–1099. doi: 10.1002/yea.320081211

Pochanavanich, P., and Suntornsuk, W. (2002). Fungal chitosan production and its characterization. *Lett. Appl. Microbiol.* 35, 17–21. doi: 10.1046/j.1472-765X.2002.01118.x

Price, M. N., Dehal, P. S., and Arkin, A. P., (2009). FastTree: computing large minimum evolution trees with profiles instead of a distance matrix. *Mol. Biol. Evol.* 26, 1641–1650. doi: 10.1093/molbev/msp077

Sánchez, O., and Aguirre, J. (1996). Efficient transformation of *Aspergillus nidulans* by electroporation of germinated conidia. *Fung. Genet. Rep.* 43, 48–51. doi: 10.4148/1941-4765.1317

Sawardeker, J. S., and Sloneker, J. S. (1965). Quantitative determination of monosaccharides by gas liquid chromatography. *Anal. Chem.* 37, 945–947. doi: 10.1021/ac60226a048

Sheppard, D. C., Graybill, J. R., Najvar, L. K., Chiang, L. Y., Doedt, T., Kirkpatrick, W. R., et al. (2006). Standardization of an experimental murine model of invasive pulmonary aspergillosis. *Antimicr. Agents Chemother.* 50, 3501–3503. doi: 10.1128/AAC.00787-06

Sheppard, D. C., Rieg, G., Chiang, L. Y., Filler, S. G., Edwards, J. E., and Ibrahim, A. S. (2004). Novel inhalational murine model of invasive pulmonary aspergillosis. *Antimicr. Agents Chemother.* 48, 1908–1911. doi: 10.1128/AAC.48.5.1908-1911.2004

Snarr, B. D., Baker, P., Bamford, N. C., Sato, Y., Liu, H., Lehoux, M., et al. (2017). Microbial glycoside hydrolases as antibiofilm agents with cross-kingdom activity. *Proc. Natl. Acad. Sci. U.S.A.* 3, 7124–7129. doi: 10.1073/pnas.1702798114

Su, C., Lu, Y., and Liu, H. (2016). N-acetylglucosamine sensing by a GCN5-related N-acetyltransferase induces transcription via chromatin histone acetylation in fungi. *Nat. Commun.* 7, 1–12. doi: 10.1038/ncomms12916

Upadhya, R., Baker, L. G., Lam, W. C., Specht, C. A., Donlin, M. J., and Lodge, J. K. (2018). *Cryptococcus neoformans* Cda1 and its chitin deacetylase activity are required for fungal pathogenesis. *mBio* 9, 873–819. doi: 10.1128/mBio.02087-18

Upadhya, R., Lam, W. C., Maybruck, B., Specht, C. A., Levitz, S. M., and Lodge, J. K. (2016). Induction of protective immunity to cryptococcal infection in mice by a heat-killed, chitosan-deficient strain of *Cryptococcus neoformans*. *mBio* 7, 525–514. doi: 10.1128/mBio.00547-16

Valsecchi, I., Sarikaya-Bayram, Ö., Wong Sak Hoi, J., Muszkieta, L., Gibbons, J., Prevost, MC, et al. (2017). MybA, a transcription factor involved in conidiation and conidial viability of the human pathogen *Aspergillus fumigatus*. *Mol Microbiol.* 105:880–900. doi: 10.1111/mmi.13744

van de Veerdonk, F. L., Gresnigt, M. S., Romani, L., Netea, M. G., and Latgé, J. P. (2017). *Aspergillus fumigatus* morphology and dynamic host interactions. *Nat. Biotechnol.* 15, 1–14. doi: 10.1038/nrmicro.2017.90

Wang, J., Wang, L., Yu, H., Zain-ul-Abdin, Chen, Y., Chen, Q., et al. (2016). Recent progress on synthesis, property and application of modified chitosan: an overview. *Int. J. Biol. Macromol.* 88, 333–344. doi: 10.1016/j.ijbiomac.2016.04.002

Zhang, K., Needleman, L., Zhou, S., and Neiman, A. (2017). A novel assay reveals a maturation process during ascospore wall formation. *J. Fungi* 3, 54–12. doi: 10.3390/jof3040054

Conflict of Interest: The authors declare that the research was conducted in the absence of any commercial or financial relationships that could be construed as a potential conflict of interest.

frontiers in Cellular and Infection Microbiology

ORIGINAL RESEARCH
published: 06 May 2020
doi: 10.3389/fcimb.2020.00205

Local Activation of the Alternative Pathway of Complement System in Mycotic Keratitis Patient Tear

Mohammed Razeeth Shait Mohammed[1], *Sandhya Krishnan*[1], *Rabbind Singh Amrathlal*[2], *Jeya Maheshwari Jayapal*[1], *Venkatesh Prajna Namperumalsamy*[3], *Lalitha Prajna*[4] *and Dharmalingam Kuppamuthu*[1]*

[1] Department of Proteomics, Aravind Medical Research Foundation, Dr. G. Venkataswamy Eye Research Institute, Aravind Eye Care System, Madurai, India, [2] Department of Microbiology, Aravind Medical Research Foundation, Dr. G. Venkataswamy Eye Research Institute, Aravind Eye Care System, Madurai, India, [3] Cornea Clinic, Aravind Eye Hospital, Aravind Eye Care System, Madurai, India, [4] Department of Ocular Microbiology, Aravind Eye Hospital, Aravind Eye Care System, Madurai, India

Aspergillus flavus and Fusarium solani are the predominant causative agents of mycotic keratitis in the tropical part of the world. Tear proteins play a major role in the innate immune response against these fungal infections as has been shown by the presence of complement proteins and neutrophil extracellular trap proteins in keratitis patients tear. In this study, we established the presence of the components of the alternate pathway of complement system and their functional state in the tear film of mycotic keratitis patients. The complement proteins namely, C3 and CFH were found only in the open-eye tear of patients but not in control individuals. *In vitro* analysis showed binding of purified C3b and CFH to fungal spores, which confirmed that the spores can provide a foreign surface for forming the complement complex. Analysis of spore bound tear proteins by mass spectrometry exhibited the presence of known proteins of the alternate pathway complement cascade in keratitis patient tear. Hemolytic assay using rabbit RBC confirmed the presence of a functional alternate pathway of complement cascade in the tear proteome of the patients. The presence of negative regulators, CFH and CFI, in the patient tear indicate that the complement activity is tightly regulated during fungal infection. Mass spectrometry data show vitronectin and clusterin, two known inhibitors of the membrane attack complex only in the patient tear. These data demonstrate the activation of the alternate pathway of complement cascade during the early stages of infection. Interestingly, the production of multiple negative regulators of complement cascade implies the pathogen can effectively evade the host complement system during infection.

Keywords: fungal keratitis, *A. flavus*, complement alternate pathway, C3b, factor H and factor I

OPEN ACCESS

Edited by:
Laura Alcazar-Fuoli,
Carlos III Health Institute, Spain

Reviewed by:
Aylin Döğen,
Mersin University, Turkey
Lukasz Kozubowski,
Clemson University, United States

****Correspondence:***
Dharmalingam Kuppamuthu
dharmalingam.k@gmail.com

Specialty section:
This article was submitted to Fungal Pathogenesis, a section of the journal Frontiers in Cellular and Infection Microbiology

Received: *13 December 2019*
Accepted: *16 April 2020*
Published: *06 May 2020*

Citation:
Shait Mohammed MR, Krishnan S, Amrathlal RS, Jayapal JM, Namperumalsamy VP, Prajna L and Kuppamuthu D (2020) Local Activation of the Alternative Pathway of Complement System in Mycotic Keratitis Patient Tear. Front. Cell. Infect. Microbiol. 10:205. doi: 10.3389/fcimb.2020.00205

INTRODUCTION

Fungal keratitis is one of the sight-threatening corneal infections, which develops in immunocompetent individuals also (Selvam et al., 2015). Mycotic keratitis is more widespread in India and other tropical parts of the world (Erie et al., 1993; Mohammed et al., 2019b). Tear film plays a crucial role in immune defense against the invading microbes and the presence of most of

the proteins involved in the alternate pathway of complement cascade has been demonstrated in patient tear (Ananthi et al., 2013; Kandhavelu et al., 2017). Previous studies showed the presence of several innate immune response associated proteins such as NET proteins, wound healing proteins and complement proteins in patient tear (Kandhavelu et al., 2017). Activation of the alternate pathway requires appropriate foreign surface for binding of the complement proteins and their subsequent activation. The complement system is controlled by negative regulators including factor H-like protein 1 (FHL-1), factor H (CFH), and complement factor I (CFI). CFH is the key regulator of C3b amplification and prevents non-specific damage to host cells (Ram et al., 1998; Zipfel and Skerka, 1999; Behnsen et al., 2008; Schmidt et al., 2016). CFH accelerates irreversible decay of C3bBb by displacing Bb, as well as complement factor I (CFI) mediated cleavage of C3b (Kuhn and Zipfel, 1996, Pangburn et al., 1977; Irmscher et al., 2018), yielding iC3b that cannot bind CFB. Subsequently iC3b cleavage ultimately yields C3d, and these regulatory functions prevent host damage by terminating the complement cascade. Among the fungi studied, *Candida albicans* (Meri et al., 2002) and *A. fumigatus* (Kozel et al., 1989; Johnsson et al., 1998) are shown to bind complement regulators to their surfaces leading to immune evasion due to the down regulation of complement activation. The presence of complement proteins C1q, C3, CFB, C4, C5, and C9 have been shown in closed- eye tears. However, only C3, CFB, and C4 are found in open-eye tears (Willcox et al., 1997). These proteins in the tear are shown to be active functionally. Our previous studies have shown the presence of several complement proteins in the tear proteome of keratitis patients (Kandhavelu et al., 2017). We also showed the presence of negative regulators namely, CFH, vitronectin and clusterin (inhibitors of the membrane attack complex), and lactoferrin (acts on soluble C3) (Kandhavelu et al., 2017). Previous reports clearly showed lactoferrin, an abundant protein found in human tear, inhibit the classical pathway of complement cascade but not the alternative pathway (Kievjts and Kijlstra, 1985).

The aim of the present work was to confirm the presence of alternative pathway of complement proteins and the complement regulatory proteins in the tear film of keratitis patients and to show their functional competence.

MATERIALS AND METHODS

Tear Protein Samples, *A. flavus* Strains and Their Growth Conditions

Aspergillus flavus strain CI1123 used in this study has been described previously (Selvam et al., 2015; Mohammed et al., 2019b). Conidia were harvested using 0.05% (v/v) Tween 20 in PBS (pH 7.2), filtered, counted using a Neubauer counting chamber and the spore suspension was stored in 20% glycerol at −80°C. For liquid culture, 50 ml of Czapek Dox broth (Himedia) was inoculated with conidia and incubated at 30°C for 2 h to obtain swollen spores.

This study was approved by the Institutional Ethical committee of Aravind Eye Hospital Madurai and informed consent was obtained from all study participants. Tear samples were collected from patients and uninfected age-matched controls as described previously (Kandhavelu et al., 2017). The method used for tear collection has been optimized to avoid contamination of cells from corneal epithelial layer. All the samples used in this study were open-tear samples. We did not find any significant variation in the total volume of tear collected from individuals from both groups.

Identification of CFH and C3b in Patient Tear

Tear samples from keratitis patients were pooled and 12 μg of tear proteins were subjected to sodium dodecyl sulfate-polyacrylamide gel electrophoresis (SDS-PAGE). Proteins were transferred onto a nitrocellulose (NC) membrane using a semi dry blotter (Thermo Scientific). The NC membrane was equilibrated with Towbin transfer buffer [39 mM glycine, 48 mM Tris-Cl, pH 7.5, and 20% methanol] and blocked with 5% skimmed milk powder in Tween 20-Tris buffered saline (TBS-T) to prevent non-specific binding. Immuno detection was performed by incubating the membrane overnight with rabbit anti-human Complement factor H antibody (H-300; SC33156, Santa Cruz Biotechnology) diluted 1:5,000 in TBS containing 0.1% skim milk powder to detect CFH and C3b was detected using rabbit monoclonal anti-C3 antibody (EPR2988 [Recombinant rabbit monoclonal antibody raised using synthetic peptide spanning human C3dg region (aa 1,200–1,300) of C3 protein], Abcam). This antibody can detect the breakdown products of C3 alpha chain, namely C3α, C3bα', iC3bα'1, C3dg, and C3d. After three washes with TBS-T and TBS, the membrane was incubated with goat anti-rabbit IgG HRP conjugate (Abcam) diluted 1:5,000 in TBS containing 0.1% skim milk powder at RT for 45 min. After three washes with TBS-T, the membrane was developed using 3, 3′-diaminobenzidine chromogenic substrate. The color development was stopped by rinsing the membrane in Milli-Q water. The membrane was then air-dried and imaged using Gel Doc™ (Bio-Rad Laboratories). In all these experiments, in the absence of a tear protein that is unaltered in level for use as a loading control, extra care was taken to quantify the exact concentration of tear proteins using Bradford assay followed by a check gel confirmation. Rainbow protein marker allowed the confirmation of transfer efficiency in western blot assay.

Binding Assay to Determine CFH and Spore Interaction

Aspergillus flavus swollen spores (2×10^8), were suspended in 150 μl of binding buffer (100 mM NaCl, 50 mM Tris [pH 7.4]) and incubated with 2 μg of CFH (Merck Millipore) at 37°C for 1 h with mixing (4 rpm). At the end of incubation period, the conidia were washed five times with one ml of wash buffer (100 mM NaCl, 50 mM Tris, 0.05% Tween 20 [pH 7.4]) (Behnsen et al., 2008) and, the bound proteins were eluted by boiling spores in 50 μl of 1X Laemmli buffer for 5 min. After removing spores by centrifugation, the proteins in the supernatant were resolved by SDS-PAGE followed by western blot using anti-CFH antibody.

Immunofluorescence Assays

Aspergillus flavus swollen spores (1×10^8) were mixed with 10 μg of factor H pure protein and incubated at 37°C for 1 h. The conidia were washed three times with ice-cold PBS (0.03 M phosphate, 0.15 M NaCl [pH 7.2]), and suspended in 2% BSA in PBS to avoid non-specific binding and incubated for 30 min at 37°C. Factor H bound conidia were incubated with anti-factor H primary antibody for 1 h at 37°C (1:200 dilution), followed by three washes in PBS and then mixed with the goat anti-rabbit IgG-FITC secondary antibody [F9887, Sigma, dilution of 1:400 in 2% (w/v) BSA-PBS] for 1 h. The conidia were washed once with PBS and mixed with 10 μg/ml calcofluor for 30 min at RT. Excess calcofluor was removed by washing and the stained conidia were examined using the Leica Live confocal microscope. The experiment was repeated as above for C3b immunofluorescence detection.

Assay of Binding of Tear Proteins to Spores

Aspergillus flavus swollen spores (2×10^8) were mixed with 100 μg of infected tear proteins in 150 μl of binding buffer and the mixture was incubated for 1 h at 37°C. Unbound proteins were removed by washing the conidia five times with one ml of wash buffer (100 mM NaCl, 50 mM Tris, 0.05% Tween 20 [pH 7.4]). Proteins bound to conidia were eluted by boiling in 50 μl of 1X Laemmli buffer. The supernatant containing eluted proteins were collected by centrifugation and used for SDS-PAGE separation and probed with anti-C3 antibody or anti-CFH antibody in western blots.

Heparin Competition Experiments

Heparin (heparin sodium salt, Himedia, TC138; 5,000 IU/ml) was mixed with 5 μg of CFH and incubated for 30 min at 37°C. The complex was added to swollen conidia (2×10^8) and incubated for 1 h with constant mixing. Washing and elution of the bound CFH was examined as described above.

Assay of Cleavage of C3b by CFI

Swollen conidia (2×10^8) were incubated with 100 μg of *A. flavus* keratitis patient tear for 1 h at 37°C on a shaker with or without the addition of 1.5 μg of CFI (Merck Millipore). At the end of the incubation period, conidia were separated by centrifugation and the supernatant was taken for SDS-PAGE and western blot analysis using anti-C3 antibody.

Spore Surface Bound CFH Accelerates Proteolysis of C3b by CFI

Swollen conidia (2×10^8) were incubated with purified CFH (5 μg) for 1 h at 37°C on a shaker. The mixture was washed five times with washing buffer and resuspended in 150 μl of binding buffer. Three micrograms of C3b (Merck Millipore) and 1.5 μg of CFI were added. The conidia were incubated for 1 h at 37°C, the conidia were removed by centrifugation, and the released cleavage products were separated by SDS-PAGE and analyzed by immunoblotting.

MS Analysis of Spore Bound Tear Proteins

Swollen conidia (2×10^8) were incubated with 100 μg of tear from *A. flavus* keratitis patient (intermediate stage) or healthy person and the bound proteins were eluted by boiling in 50 μl of 1X Laemmli buffer for 5 min as discussed above. Proteins in the supernatant were fractionated on a 12% SDS-PAGE. Electrophoresis was stopped when the tracking dye reached one cm into the separating gel. After staining with coomassie blue, a single band was cut and processed for in-gel tryptic digestion and mass spectrometry as described previously by Kandhavelu et al. (2017) with minor modifications. In brief, gel pieces were destained with repeated washes with 25 mM ammonium bicarbonate in 50% acetonitrile. The gel pieces were dehydrated using 100% acetonitrile followed by reduction of disulfide bridges using 50 μl of 10 mM DTT in 25 mM ammonium bicarbonate for 45 min at 55°C and alkylated with 55 mM IAA in 25 mM ammonium bicarbonate. After reduction and alkylation, gel pieces were washed three times with 100 μl of 100 mM ammonium bicarbonate, and dehydrated using 100% acetonitrile. Dehydrated gel pieces were dried under vacuum and rehydrated for 30 min on ice with 600 ng of trypsin (Invitrogen). Tryptic peptides were purified using C18 tips and analyzed using Thermo Easy nLC 1000 coupled with Orbitrap Velos Pro mass spectrometer (Thermo, USA) and MS parameters are discussed in detail in our previous paper (Mohammed et al., 2019a).

Data Processing

All MS/MS raw data for experimental and biological replicates acquired from Orbitrap Velos Pro Mass Spectrometer were analyzed by Proteome Discoverer v1.4 using Mascot and the inbuilt SequestHT algorithm. Both SequestHT and Mascot was set up to search against human proteome database from UniProt (141,139 entries) with parameters of peptide tolerance of 10 PPM with two missed cleavages. Carbamidomethylation was given as fixed modification and methionine oxidation, N-terminal acetylation and phosphorylation (S, T, Y) as variable modifications (Selvam et al., 2015; Mohammed et al., 2019a).

Functional Assay for Alternative Pathway of Complement System

Functional assay using rabbit blood was done as described previously (Sohn et al., 2000) with minor modification. Five ml of rabbit blood was mixed with an equal volume of Alsever solution and kept on ice for 5–10 min. RBCs were washed twice using DGHB buffer and suspended in fresh DGHB and kept at 4°C. Cells were counted using a Neubauer counting chamber. Hemolytic assay was performed by diluting human serum from a healthy person in DGHB buffer at ratio of 1:4 and 1:6 or with different concentrations (200 μg, 400 μg, 600 μg, 800 μg, 2 mg) of control/keratitis tear. Tear or serum was mixed with 1×10^8 rabbit RBCs and incubated for 60 min at 37°C. Reaction was terminated by adding 1.2 ml of ice-cold 0.15 M NaCl. After centrifugation (1,250 x g) for 10 min at 4°C, the clear supernatant was used for optical density measurement at 412 nm using spectrophotometer (Evolution UV- VIS Thermo Fisher). Optical density of the control experiment, where

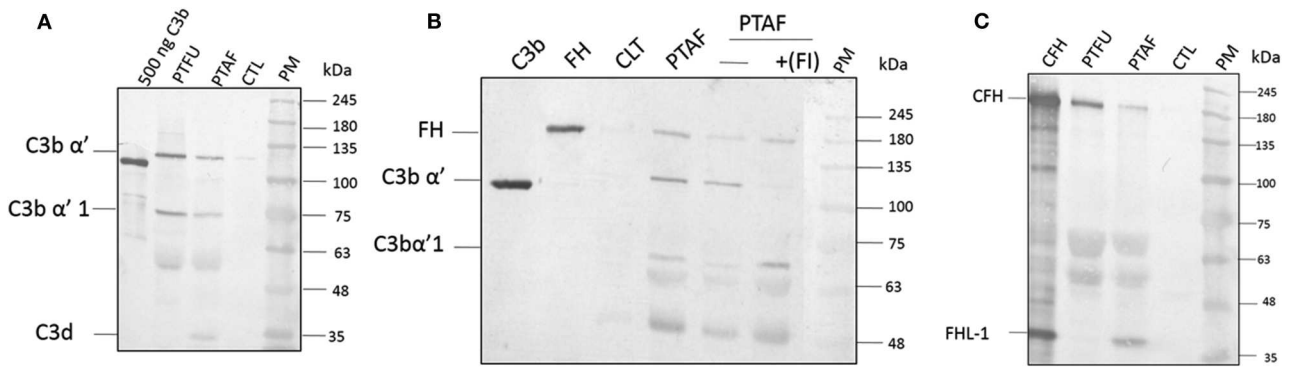

FIGURE 1 | Complement C3, factor H and factor I are present in keratitis patient tear and are functional. **(A)** C3 protein and its cleavage products in keratitis patient tear. Twelve microgram of tear proteins was separated on a 12% SDS-PAGE and probed with anti-C3 antibody as described in materials and methods. The monoclonal antibody used recognized the C3dg portion of the C3 protein. Lanes 1, Purified C3b (500 ng); 2, *Fusarium* keratitis patient tear (PTFU); 3, *A. flavus* keratitis patient tear (PTAF); 4, normal person tear (CTL); 5, protein marker (PM). **(B)** Alpha chain of C3 is cleaved by patient tear and externally added CFI can accelerate this cleavage. *A. flavus* swollen conidia (2×10^8) were incubated with 50 μg of keratitis patient tear in the presence or absence of Factor I (1.5 μg) and the supernatant was separated in a SDS-PAGE and transferred to NC membrane. The membrane was probed with a mix of anti-FH and anti-C3 antibodies. Lanes 1, Purified C3b; 2, Purified CFH; 3, Control tear; 4, *A. flavus* keratitis patient tear (PFTA); 5, *A. flavus* keratitis patient tear without factor I (FI); 6, *A. flavus* keratitis patient tear mixed with FI; 7, protein marker (PM). **(C)** Complement factor H in keratitis patient tear. Twelve microgram of tear protein was separated on a 12% SDS page and probed with anti-CFH antibody in western blots as described in materials and methods. Lanes 1, Purified CFH (500 ng); 2, *Fusarium* keratitis patient tear (PTFU); 3, *A. flavus* keratitis patient tear (PTAF); 4, normal person tear (CTL); 5, protein marker (PM).

water was substituted for proteins, was taken as 100% lysis (Sohn et al., 2000).

RESULTS

C3 Protein and Its Cleavage Products in Keratitis Patient's Tear

Proteins from tear films were fractionated on acrylamide gels and, the presence of C3 and its processed products were examined using a monoclonal antibody that recognizes an epitope in the C3dg portion of C3-alpha chain. This antibody was shown to recognize C3 (α, 120 kDa), C3b (α', 110 kDa), iC3b (α'1,68 kDa), C3dg (41 kDa), and, C3d (31 kDa). Data in **Figure 1A** show the presence of the C3 alpha chain belonging to uncleaved C3, migrating as a 120 kDa band as well as the cleaved forms of C3. The presence of uncleaved form of C3 was previously reported by us (Kandhavelu et al., 2017) and, our current data confirm this finding. In the control sample, only a faint band migrating at the 120 kDa region could be detected compared to the patient's tear, indicating the induction of C3 upon fungal infection. The presence of the alpha fragment of iC3b in both *Fusarium* and *A. flavus* keratitis patient tear implied the activation of complement pathway. Unlike the tear from *A. flavus* keratitis patients, the quantity of C3 and its cleaved products were slightly higher in *Fusarium* keratitis patient tear, even though same amount of total tear proteins were loaded in each track (**Figure 1A**). C3 and its cleavage products were significantly reduced in control tear.

C3 Convertase Is Cleaved in Patient Tear

The presence of CFH well as the formation of iC3b (**Figure 1B**) indicated the cleavage of C3 in patients' tear, presumably mediated by complement factor I (CFI). Data in **Figure 1B** show the presence of CFH and C3 in *A. flavus* keratitis tear. Previous studies using *A. fumigatus* spores showed that the alternative pathway of complement can be assembled on the spore surface (Behnsen et al., 2008). Therefore, we examined the formation of C3 convertase on the surface of *A. flavus* spores. Swollen spores when added to tear proteins led to the reduction in the amount of C3 in the tear samples (compare the 120 kDa C3 protein band in lanes 4 and 5 of **Figure 1B**). Further, the addition of purified CFI led to complete cleavage of C3, which implied the reduced cleavage seen in patient tear is due to the limitation in the amount of CFI. Further experiments are needed to confirm the absence of other inhibitors of C3 cleavage.

Identification of Complement Factor H in Tear Samples

Previous mass spectrometry data (Kandhavelu et al., 2017) show the presence of CFH, the major negative regulatory factor of the alternative complement pathway, in keratitis patient's tear. This data was further confirmed in this study by western blot analysis of CFH in the tear sample from the patients and control (**Figure 1C**). The protein band corresponding to 180 kDa co-migrating with purified CFH showed the presence of CFH in keratitis patients' tear but not in control tear. The anti-CFH antibody recognized an additional protein migrating as a 37 kDa band even in purified CFH sample lane. This protein has been shown to be factor H like (FHL) protein (unpublished results) and has been identified from keratitis patient tear as well (see later). FHL, however, could not be found in *Fusarium* keratitis patient tear. Two other cross-reacting proteins detected have not been identified yet. The presence of CFH implies the negative regulation of the alternative pathway since CFH catalyzes CFI mediated cleavage of C3b, leading to the inhibition of C3 convertase formation.

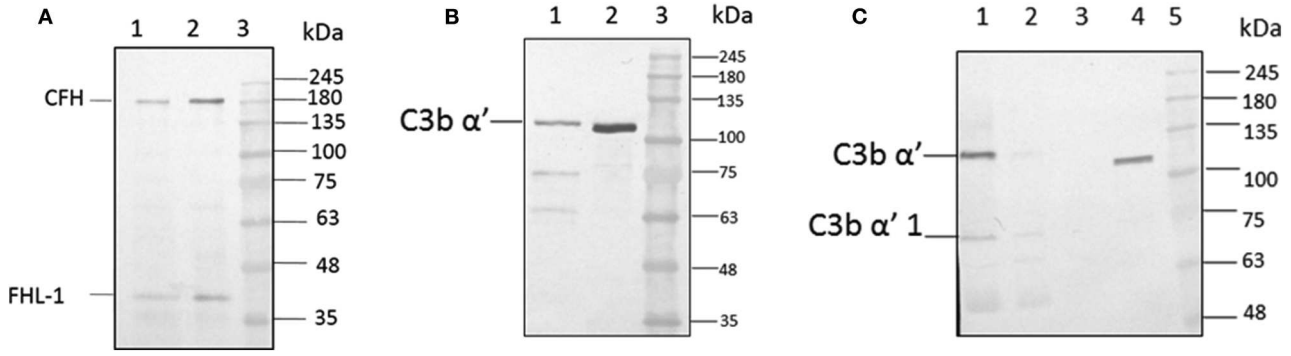

FIGURE 2 | C3b and CFH binds to conidial surface. **(A)** *A. flavus* conidia were incubated with 2.0 μg factor H, washed and eluted the surace bound proteins, which were separated by SDS-PAGE, transferred to a NC membrane and probed with anti-CFH antibody. Lanes 1, Eluate of 2.0 μg of CFH bound to the spore; 2, 200 ng of pure protein CFH; 3, protein marker (PM). **(B)** *A. flavus* conidia (2×10^8) were incubated with purified C3b (5 μg). After extensive washing, bound proteins were eluted with 1X Laemmli buffer. Proteins in eluate were separated in a SDS-PAGE, transferred to a NC membrane and probed with anti-C3b antibody. Lanes 1, Eluate of 5 μg of C3b bound to the spore; 2, 500 ng of pure protein C3b; 3, protein marker (PM). **(C)** Binding of C3b in keratitis patient tear to conidial surface. *A. flavus* conidia were incubated with purified 50 μg of *A. flavus* keratitis patient tear. After extensive washing, bound proteins were eluted with 1X Laemmli buffer. Proteins in the eluate were separated in a SDS-PAGE, transferred to a NC membrane and probed with anti-C3b antibody. Lanes 1, 10 μg of keratitis patient tear; 2, unbound proteins of keratitis patient tear; 3, wash fraction; 4, eluate of patient tear proteins bound to the spore surface; 5, protein marker (PM).

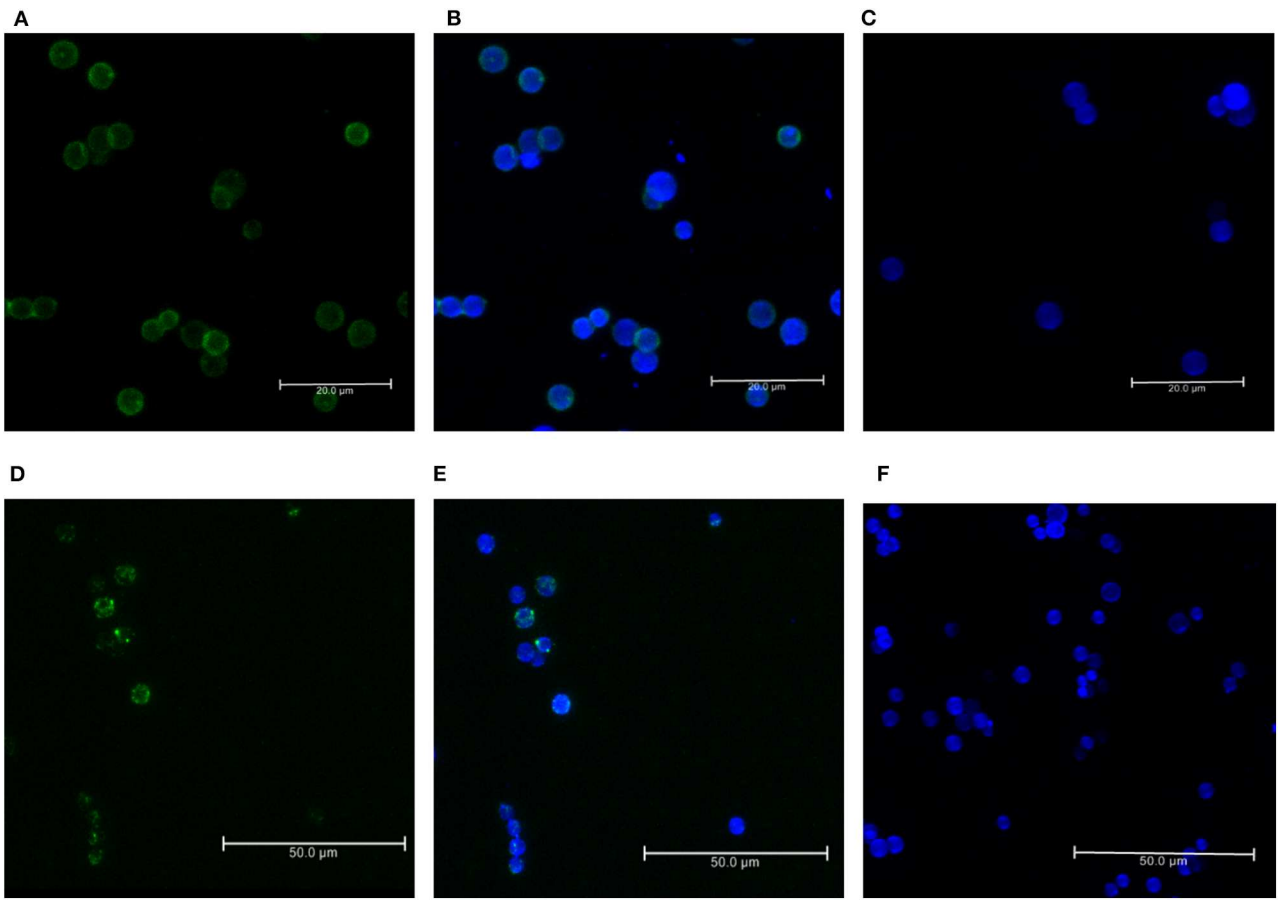

FIGURE 3 | Immunofluorescence of C3b and CFH binds to conidial surface. Binding of factor H and C3b to *A. flavus* conidia. Conidia were incubated with purified factor H and C3b separately and binding was visualized by immunofluorescence with rabbit anti-CFH antibody and an Alexa 488-coupled secondary antibody (green). The cell wall was stained with calcofluor (blue). **(A)** Immunofluorescence of conidia labeled with C3b (FITC-green). **(B)** Merged image of conidia labeled with C3b-FITC and calcofluor. **(C)** Negative control without the C3b. **(D)** Immunofluorescence of conidia labeled with CFH (FITC-green). **(E)** Merged image of conidia labeled with CFH-FITC and calcofluor. **(F)** Negative control without C3b.

C3b and CFH Bind Efficiently to the Conidial Surface

For the formation of functional complement components, C3 and C3b should bind to the surface of spores of *A. flavus* and the cleavage of bound C3b by CFH also depends on the binding of CFH to surface. In order to examine this, conidia were incubated with purified CFH or C3b and at the end of the incubation period, the conidia were washed extensively, and the proteins bound to the spores were eluted and examined. Proteins in the eluted fraction were separated by SDS-PAGE and analyzed by Western blotting using appropriate antibodies. **Figures 2A,B** shows the presence of CFH and C3b, respectively, in the bound fraction. In both cases, the binding is nearly complete since the wash fractions did not have any proteins (data not shown). Binding of CFH and C3b to *A. flavus* was also analyzed by immunofluorescence as described in materials and methods section. **Figure 3** shows the fluorescence of antibody bound to *A. flavus* spores pre-incubated with C3b and CFH but not in untreated spores. These experiments confirm that the *A. flavus* spore surface can act as an activating surface for the assembly of the C3 convertase as well as its inhibitory components (**Figure 2C**).

Inhibition of C3b and CFH Binding to Spore Surface by Heparin

Among the SCR domains of CFH, SCR 7, SCR 9, SCR 13, and SCR 20 are responsible for binding heparin (Behnsen et al., 2008). Since these same sites are also involved in the binding of CFH to the microbial surface, we examined the role of these sites in the binding of *A. flavus* spores. At a concentration of 5,000 IU/ml, heparin completely inhibited the attachment of CFH to conidia, as demonstrated by western blot analysis (**Figure 4A**, compare lane 1 and 2). Binding of CrFH in keratitis patients' tear to the *A. flavus* spore surface was inhibited when the tear was pretreated with heparin. In a similar experiment, C3b was pre-incubated with heparin (5,000 IU/ml) and the binding of C3b to spores was shown to be inhibited (**Figure 4B**). The actual mechanism of C3b binding to spore surface is unknown, however, the above data imply that the heparin-binding sites in C3b are the ones involved in spore binding.

Heparin Accelerated Inhibition of CFH Mediated Cleavage of C3b by CFI

Earlier study show the CFH binding to foreign surface leads to the CFH mediated CFI cleavage of C3b (Behnsen et al., 2008). In order to examine the effect of heparin on CFH mediated cleavage of C3b through CFI, conidia were incubated with CFH prior to the addition of heparin (5,000 IU/ml) and after extensive washing, purified CFI and C3b were added. After incubation, the bound proteins were eluted and separated by SDS-PAGE. The proteolytic cleavage of α'chain of C3b was assayed by western blotting. In the presence of CFI and C3b, CFH-coated conidia accelerated the cleavage of C3b as expected (**Figure 5**, lane 3). However, the addition of heparin inhibits CFH (**Figure 5**, lane 2) mediated cleavage confirming the inhibition of C3b binding to spores.

Assembly of Complement Proteins in Tear on the Spore Surface

Previous studies show the presence of several complement proteins in patient tear but not in control tear. In order to examine the binding of complement proteins to spores, tear proteins were incubated with conidia and the bound proteins were eluted and analyzed using mass spectrometry as described under materials and methods. **Table 1A** shows the list of

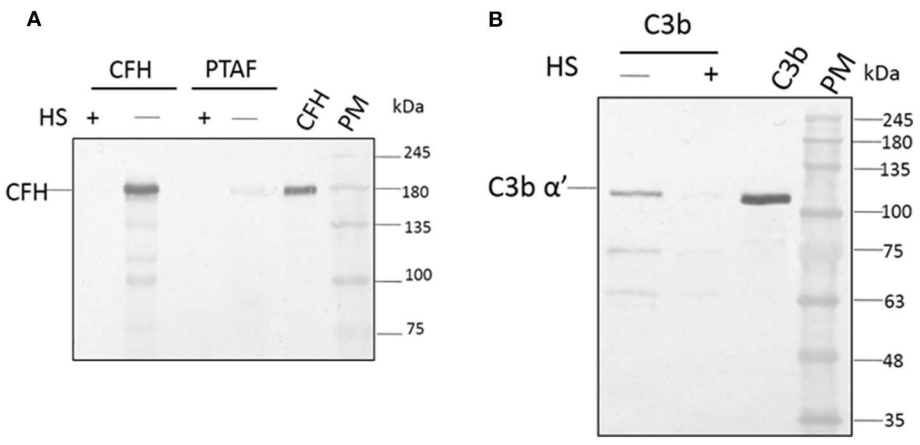

FIGURE 4 | Heparin inhibits the binding of factor H to conidial surfaces. **(A)** *A. flavus* swollen conidia (2×10^8) were incubated with purified factor H (5 μg) in the presence or absence of 5,000 IU of heparin sulfate (HS) or with 100μg of *A. flavus* infected tear in the presence of heparin (5,000 IU). Bound proteins were eluted with a 1X Laemmli buffer, eluate fractions were separated on a SDS-PAGE and western blot analysis performed using anti-CFH antibody. Two hundred nanogram of purified factor H was used as a control. Lanes 1, Eluate of 5,000 IU of HS with 5 μg CFH; 2, eluate of 5 μg CFH bound to spores; 3, eluate of 5,000 IU of HS with 100μg *A. flavus* infected tear; 4, 12 μg of *A. flavus* keratitis patient tear; 5, purified CFH 200 ng; 6, protein marker (PM). **(B)** *A. flavus* swollen conidia (2×10^8) were incubated with purified C3b (5 μg) in the presence and absence of 5,000 IU of heparin sulfate (HS). After extensive washing, bound proteins were eluted with 1X Laemmli buffer. Proteins in eluate were separated in a SDS-PAGE, transferred to a NC membrane and probed with anti-C3b antibody. Lanes 1, eluate of 5 μg of C3 bound to spores; 2, eluate of 5,000 IU of HS with 5 μg C3b; 3, purified C3b; 4, protein marker (PM).

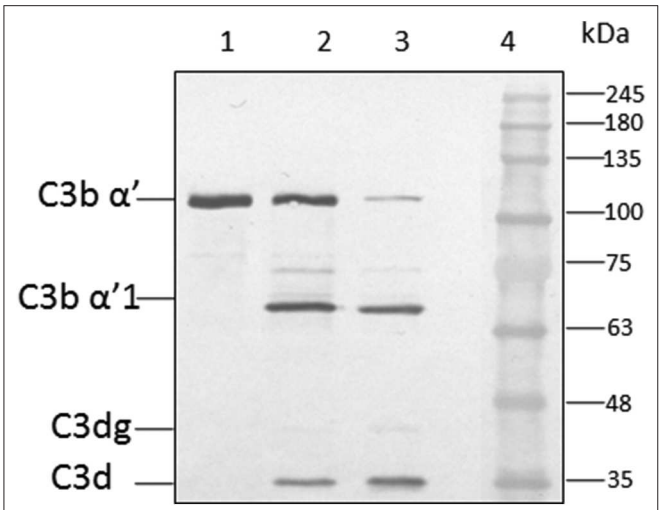

FIGURE 5 | Co-factor assay. Conidia of *A. flavus* were incubated with purified factor H in the presence or absence of 5,000 IU of heparin sulfate (HS). After extensive washing, both factor I and C3b were added. After incubation for 1 h, the supernatant was separated and proteins resolved by SDS-PAGE, transferred to a NC membrane and probed with anti-C3 antibody. The positions of the C3bα' and it's cleaved forms are indicated. Lanes 1, purified C3b control (500 ng); 2, supernatant of C3b and FI after incubation with 5,000 UI of Heparin sulfate and 5 μg CFH; 3, supernatant of C3b and FI after incubation with 5 μg CFH on conidia; 4, protein marker (PM).

complement proteins in keratitis patients' tear bound to *A. flavus* spores. In addition to the complement proteins, vitronectin, and clusterin that are inhibitors of MAC complex formation, were also found in patient tear (**Table 1B**). We also found proteins involved in neutrophil extracellular trap formation along with lactoferrin, a protein that regulates complement activity in the spore bound protein fraction.

Demonstration of Functional Competence of the Alternate Pathway in the Keratitis Patient Tear

Rabbit erythrocytes are not protected from CFH mediated inhibition of hemolysis when mixed with human serum (Herbert et al., 2015). This assay is useful to demonstrate the presence of all the complement components and the formation of the final membrane attack complex that lyses intact cells. Data in **Figure 6** show 55% hemolysis of rabbit RBCs in six-fold diluted serum. RBC hemolysis could be demonstrated with tear proteins from keratitis patients only at higher concentrations. The presence of lower amount of complement components as well as inhibitors of the complement cascade could be the reason for the decreased hemolysis in tear film compared to serum. Unlike the patient tear, tear from controls did not show any hemolytic activity even at a high concentration of 2 mg.

DISCUSSION

The significant findings of the current work are, one, fungal infection induces all components of the alternative pathway of

TABLE 1 | Hundred microgram of *A. flavus* keratitis patient tear was incubated with *A. flavus* conidia for 60 min at 37°C.

(A) IDENTIFICATION OF KERATITIS PATIENT TEAR PROTEINS BOUND TO *A. flavus* CONIDIAL SURFACE

Uniprot ID.	Protein description	Number of unique peptides	PSMs
P01024	Complement C3	12	42
A8K5T0	cDNA FLJ75416, highly similar to CFH	9	28
F5GXS0	Complement C4-B	3	10
P02747	Complement C1q subunit C	3	12
D6RA08	Complement C1 subunit B	2	4
F8WCZ6	Complement C1s	2	4
B0UXW4	Complement factor B	3	10
B4E1B0	cDNA FLJ54318, highly similar to Complement C1r	2	3
B1AKG0	Complement factor H-related protein 1	1	2
P01625	Ig kappa chain V-IV region Len	2	8
B7Z553	cDNA FLJ51266, Vitronectin OS	1	14
P10909-4	Isoform 4 of Clusterin	6	24
P80188	Neutrophil gelatinase-associated lipocalin	2	6
B0QY04	Neutrophil cytosol factor 4	1	4
P59665	Neutrophil defensin 1	1	1
B1ALB7	Neutrophil cytosol factor 2	1	1
B3VMW0	Lactoferrin	31	717
B2MV14	Truncated lactoferrin	22	609
B3KSL2	cDNA FLJ36533, highly similar to lactotransferrin	31	769
P08311	Cathepsin G	3	9
P05164-2	Isoform H14 of Myeloperoxidase	4	18
B4DNT5	Proteinase 3	1	2
P61626	Lysozyme C	11	764

(B) COMPARISON OF THE SPORE BOUND PROTEINS OF CONTROL AND PATIENT TEAR FILM

Uniprot ID	Protein description	Control tear (PSMs)	Patient tear (PSMs)
E7ER44	Kaliocin-1	1,676	–
B3VMWO	Lactoferrin	1,663	674
B3KSL2	cDNA FLJ36533 highly similar to lactotransferrin	–	642
Q5EK51	Lactoferrin	1,652	–
Q2TUW9	Lactoferrin	1,610	–
P02787	Sero transferrin	–	136
B2MV14	Truncated Lactoferrin	1,410	475
H6VRF8	Keratin 1	267	307
Q6MZV7	Uncharacterized protein DKFZp686C11235	–	165
P13645	Keratin, type I cytoskeletal 10	178	222
P02647	Apolipoprotein A-I	–	83
P35908	Keratin, type II cytoskeletal 2 epidermal	99	168
P35527	Keratin, type I cytoskeletal 9	105	126
F6KPG5	Albumin	77	1,220

(Continued)

TABLE 1 | Continued

(B) COMPARISON OF THE SPORE BOUND PROTEINS OF CONTROL AND PATIENT TEAR FILM			
Uniprot ID	**Protein description**	**Control tear (PSMs)**	**Patient tear (PSMs)**
P61626	Lysozyme C	652	488
P12273	Prolactin-inducible protein	–	49
A8K008	cDNA FLJ78387	–	156
P05109	Protein S100-A8	–	55
Q6GMX6	IGH protein	–	155
B4E335	cDNA FLJ52842, highly similar to Actin, cytoplasmic 1	–	–
Q6MZQ6	Uncharacterized protein DKFZp686G11190	–	144
Q6N096	Uncharacterized protein DKFZp686I15196	–	146
P01859	Ig gamma-2 chain c region	–	114
P01860	Ig gamma-3 chain c region	–	98
Q6MZU6	Putative uncharacterized protein DKFZp686C15213	–	111
B4DW52	cDNA FLJ55253, highly similar to Actin, cytoplasmic 1	–	99
Q0KKI6	Immunoglobulin light chain (fragment)	–	98
P31025	Lipocalin-1	93	197
P25311	Zinc-alpha-2-glycoprotein	33	18

*After extensive washing, bound proteins were eluted by using sample buffer. Eluate fraction was processed for shot-gun MS sample preparation. Raw files were analyzed in Proteome Discoverer. Comparison of complement protein bound to conidia present in infection tear is given in **(A,B)** shows comparison of bound proteins using control and infected tear in the spore binding assay.*

the complement cascade, and two, these complement proteins can form a functional membrane attack complex.

This study confirms the previous mass spectrometry study (Kandhavelu et al., 2017), in which all the proteins of the alternative pathway of complement have been identified in keratitis patient's tear. It has been reported previously that in the case of control open eye-tear and closed-eye tear, some proteins of the complement pathway are present but at a very low level (Willcox et al., 1997). Our data showing the presence of a low level of some of the complement proteins in control reflex tear supports this finding. Among the proteins found in control reflex tear, complement factor C4, C3, CFB, vitronectin, and lactoferrin have also been demonstrated in normal person open-eye tear and closed-eye tear in a previous study (Willcox et al., 1997). However, in keratitis patient tear, these and other alternative complement pathway proteins were upregulated considerably resulting in the representation of the entire alternative pathway of the complement system.

Complement pathways contribute significantly to the innate immune defense against fungal infections by activating host inflammatory response leading to the fungal clearing (Sturtevant and Latgé, 1992b; Morgan and Gasque, 1997; Herbert et al., 2015; Lubbers et al., 2017). Even though the membrane attack complex-mediated lysis of fungal pathogens was not demonstrated, data presented in this study show that an active membrane attack complex in keratitis tear. Ghosh et al. (2015) showed that the low-density membrane attack complexes are involved in signaling. The tear film has a lower level of complement proteins compared to blood. The tear film also has negative regulators such as CFH, clusterin, vitronectin and lactoferrin and these may be reducing the complement activity.

C3 convertase, the alternate pathway convertase, is central to the elaboration of complement function, including formation of C5 convertase. Among the two C3 convertases, the classical pathway C3 convertase, C4b2b is inhibited by lactoferrin (Kievjts and Kijlstra, 1985). Previous reports show the presence of C4 even in control tear, and lactoferrin in tear film can inhibit the classical pathways of complement function (Kandhavelu et al., 2017). There is no change in the amount of lactoferrin in a patient tear compared to the control tear and hence, the role of classical pathway convertases in innate defense in antifungal immunity is minimal or none. Western blot analysis showed increased amount of C3 in a patient tear compared to the control, which has negligible amount of C3 confirming the previous report (Kandhavelu et al., 2017). Under reducing conditions of electrophoresis, alpha chain of purified C3b protein appeared as a 110 kDa band indicating the cleavage of C3a from native C3 alpha chain, which is 120 kDa in molecular weight. Under similar reducing electrophoresis conditions, C3 alpha chain of C3 protein in tear appeared as a 120 kDa protein indicating the absence of cleavage of C3 in a patient tear. Even in blood, very low amount of fluid phase C3b has been demonstrated and hence, it is likely that C3b is not formed in tear film in fluid phase. Examination of the mass spectrometry data from our previous report show the identification of the four peptides (Kandhavelu et al., 2017) belonging to the region covering C3a from patient tear confirming the presence of unprocessed C3 in patient tear.

Spore surface bound forms of C3 and C3 (H_2O) can in turn bind CFB, which leads to the formation of alternative pathway C3 convertase (Sturtevant and Latgé, 1992a). The presence of factor D and properdin in keratitis patient tear imply that C3bBb convertase could be formed and stabilized on fungal surface. The identification of C3α'1 and C3d in the patient tear shows cleavage of C3b alpha chain presumably by CFH and CFI present in the patient tear film. These results imply the formation of functional MAC complexes, but, their half-life is short due to the cleavage of C3b by CFI. Cleavage of native C3 and C3 (H_2O) is less effective in the fluid phase, which could be the reason for the presence of uncleaved C3 alpha in patient tear.

In our experiments, pre-incubation of spores with heparin prevents binding of purified C3b and tear C3 to spores. When thiol ester bond is cleaved, any surface with hydroxyl group can bind C3, and hence, it is likely that heparin masks all these sites leading to the inhibition of C3 binding. The actual mechanism of C3b binding to the spore surface is unknown. However, it is interesting to identify ligands that could inhibit C3 binding to spores and such ligands

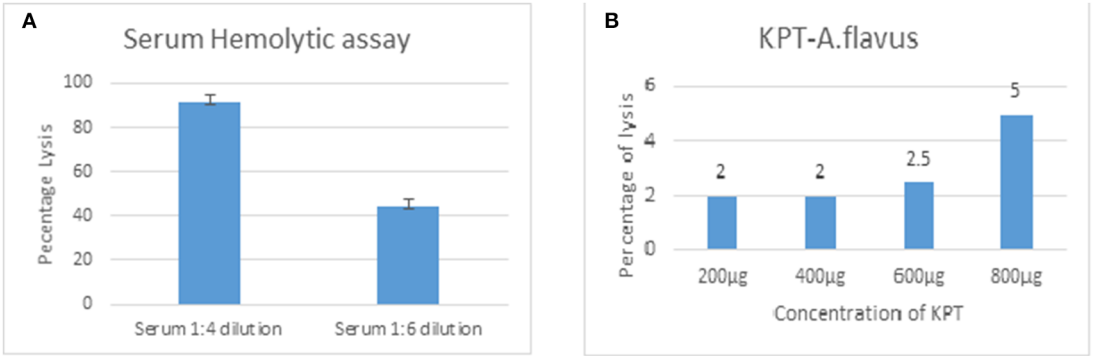

FIGURE 6 | Functional assay of complement proteins. Different concentrations of human serum **(A)** or *A. flavus* keratitis patient tear **(B)** was added to 1 × 10^8 to rabbit RBCs and incubated in DGHB buffer for 60 min at 37°C. After centrifugation, the supernatant was collected and the absorbance measured at 412 nm.

could be used as inhibitors of complement activation and excessive inflammation.

In order to demonstrate the binding of complement proteins of the alternative pathway of complement cascade as well as other proteins that interact with fungal spores, we examined the spectrum of proteins from keratitis tear and healthy person tear films that were bound tightly when incubated with fungal spores. Apart from complement cascade proteins, neutrophil extracellular trap proteins, and inhibitors of MAC were found interacting with fungal spores.

Overall, to the best of our knowledge, this is the first report showing the induction of an active alternative pathway of the complement cascade in keratitis patient's tear. Further, there are other proteins which interact with the fungal spores and these proteins have a significant role to play in the modulation of complement-mediated anti-fungal defense. Induction of the negative regulators implies that the outcome of *A. flavus* infection depends on the host and fungal pathogen interaction in each individual, even though the formation of an active alternative pathway of the complement system is found in all keratitis patients. The identification of swollen conidial surface proteins and their interacting partners in the keratitis patient tear will help in the identification of new virulence mechanisms as well as their role in host immune modulation.

DATA AVAILABILITY STATEMENT

The raw data supporting the conclusions of this article will be made available by the authors, without undue reservation, to any qualified researcher.

ETHICS STATEMENT

This study was ethically approved from Aravind Eye Hospital Madurai and we have got written informed consent form from all participants in this study.

AUTHOR CONTRIBUTIONS

MS performed the experiment and wrote the first draft of manuscript. SK performed hemolysis experiment. RA and JJ guidance and proofreading of manuscript. VN and LP provided tear samples, supervised and reviewed manuscript. DK proposed, designed and supervised the entire study and also, wrote and proofread the manuscript.

FUNDING

This study was supported by the grant from the Department of Biotechnology BT/01/CEIB/11/VI/09 (Programme Support for Research on Human Mycotic Keratitis). The funders had no role in study design, data collection, and analysis, decision to publish, or preparation of the manuscript.

ACKNOWLEDGMENTS

The authors thank Dr. C. Gowri Priya Chidambaranathan, Scientist, Department of Immunology, Aravind Medical Research Foundation, for help in confocal imaging, M. Sujitha, M. P. Kalaiselvi for their help in mass spectrometry and T. Parameswari, G. Rekha for tear sample collection.

REFERENCES

Ananthi, S., Prajna, N. V., Lalitha, P., Valarnila, M., and Dharmalingam, K. (2013). Pathogen induced changes in the protein profile of human tears from *Fusarium* keratitis patients. *PLoS ONE* 8:E53018. doi: 10.1371/journal.pone.0053018

Behnsen, J., Hartmann, A., Schmaler, J., Gehrke, A., Brakhage, A. A., and Zipfel, P. F. (2008). The opportunistic human pathogenic fungus *Aspergillus fumigatus* evades the host complement system. *Infect. Immun.* 76, 820–827. doi: 10.1128/IAI.01037-07

Erie, J. C., Nevitt, M. P., Hodge, D. O., and Ballard, D. J. (1993). Incidence of ulcerative keratitis in a defined population from 1950 through 1988. *Arch. Ophthalmol.* 111, 1665–1671. doi: 10.1001/archopht.1993.01090120087027

Ghosh, P., Sahoo, R., Vaidya, A., Chore, M., and Halperin, J. A. (2015). Role of complement and complement regulatory proteins in the complications of diabetes. *Endocr. Rev.* 36, 272–288. doi: 10.1210/er.2014-1099

Herbert, A. P., Makou, E., Chen, Z. A., Kerr, H., Richards, A., Rappsilber, J., et al. (2015). Complement evasion mediated by enhancement of captured factor h: implications for protection of self-surfaces from complement. *J. Immunol.* 195, 4986–4998. doi: 10.4049/jimmunol.1501388

Irmscher, S., Döring, N., Halder, L.D., Kopka, I., Dunker, C., Jacobsen, I.D., et al. (2018). Kallikrein cleaves C3 and activates complement. *J. Innate Immun.* 10, 94–105. doi: 10.1159/000484257

Johnsson, E., Berggård, K., Kotarsky, H., Hellwage, J., Sjöbring, U., and Lindah, L. G. (1998). Role of the hypervariable region in streptococcal m proteins: binding of a human complement inhibitor. *J. Immunol.* 161, 4894–4901.

Kandhavelu, J., Demonte, N. L., Namperumalsamy, V. P., Prajna, L., Thangavel, C., Jayapal, J. M., et al. (2017). *Aspergillus flavus* induced alterations in tear protein profile reveal pathogen-induced host response to fungal infection. *J. Proteomics* 152, 13–21. doi: 10.1016/j.jprot.2016.10.009

Kievjts, F., and Kijlstra, A. N. (1985). Inhibition of C3 deposition on solid phase bound immune complexes by lactoferrin. *Immunology* 54, 449–456.

Kozel, T. R., Wilson, M., Farrell, T., and Levitz, S. (1989). Activation of C3 and binding to *Aspergillus fumigatus* conidia and hyphae. *Infect. Immun.* 57, 3412–3417. doi: 10.1128/IAI.57.11.3412-3417.1989

Kuhn, S., and Zipfel, P. F. (1996). Mapping of the domains required for decay acceleration activity of the human factor H-like protein 1 and factor H. *Eur. J. Immunol.* 26, 2383–2387. doi: 10.1002/eji.18302 61017

Lubbers, R., Van Essen, M. F., Van Kooten, C., and Trouw, L. A. (2017). Production of complement components by cells of the immune system. *Clin. Exp. Immunol.* 188, 183–194. doi: 10.1111/cei.12952

Meri, T., Hartmann, A., Lenk, D., Eck, R., Würzner, R., and Hellwage, J. (2002). The yeast candida albicans binds complement regulators factor H and Fhl-1. *Infect. Immun.* 70, 5185–5192. doi: 10.1128/IAI.70.9.5185-519 2.2002

Mohammed, M. R. S., Balamurgan, M. K., Amrathlal, R. S., Kannan, P., Jayapal, J. M., Namperumalsamy, V. P. et al. (2019a). Dataset for the spore surface proteome and hydrophobin A/roda proteoforms of *A. flavus*. *Data Brief* 23:103817. doi: 10.1016/j.dib.2019.103817

Mohammed, M. R. S., Balamurugan, M., Amrathlal, R. S., Kannan, P., Jayapal, J. M., Namperumalsamy, V. P., et al. (2019b). Identification of the proteoforms of surface localized rod a of *Aspergillus flavus* and determination of the mechanism of proteoform generation. *J. Proteomics* 193, 62–70. doi: 10.1016/j.jprot.2018.12.016

Morgan, B. P., and Gasque, P. (1997). Extrahepatic complement biosynthesis: where, when and why? *Clin. Exp. Immunol.* 107, 1–7. doi: 10.1046/j.1365-2249.1997.d01-890.x

Pangburn, M. K., Schreiber, R. D., and Müller-Eberhard, H. J. (1977). Human complement C3b inactivator: isolation, characterization, and demonstration of an absolute requirement for the serum protein beta1h for cleavage of C3b and C4b in solution. *J. Exp. Med.* 146, 257–270. doi: 10.1084/jem.146.1.257

Ram, S., Mcquillen, D. P., Gulati, S., Elkins, C., Pangburn, M. K., and Rice, P. A. (1998). Binding of complement factor H to loop 5 of porin protein 1a: a molecular mechanism of serum resistance of *Nonsialylated neisseria* gonorrhoeae. *J. Exp. Med.* 188, 671–680. doi: 10.1084/jem.188.4.671

Schmidt, C. Q., Lambris, J. D., and Ricklin, D. (2016). Protection of host cells by complement regulators. *Immunol. Rev.* 274, 152–171. doi: 10.1111/imr.12475

Selvam, R. M., Nithya, R., Devi, P. N., Shree, R. B., Nila, M. V., Demonte, N. L., et al. (2015). Exoproteome of *Aspergillus flavus* corneal isolates and saprophytes: identification of proteoforms of an oversecreted alkaline protease. *J. Proteomics* 115, 23–35. doi: 10.1016/j.jprot.2014.11.017

Sohn, J.-H., Kaplan, H. J., Suk, H.-J., Bora, P. S., and Bora, N. S. (2000). Complement regulatory activity of normal human intraocular fluid is mediated by Mcp, Daf, and Cd59. *Invest. Ophthalmol. Vis. Sci.* 41, 4195–4202.

Sturtevant, J., and Latgé, J. P. (1992a). Interactions between conidia of *Aspergillus fumigatus* and human complement component C3. *Infect. Immun.* 60, 1913–1918. doi: 10.1128/IAI.60.5.1913-1918.1992

Sturtevant, J., and Latgé, J. P. (1992b). Participation of complement in the phagocytosis of the conidia of *Aspergillus fumigatus* by human polymorphonuclear cells. *J. Infect. Dis.* 166, 580–586. doi: 10.1093/infdis/166.3.580

Willcox, M., Morris, C., Thakur, A., Sack, R., Wickson, J., and Boey, W. (1997). Complement and complement regulatory proteins in human tears. *Invest. Ophthalmol. Vis. Sci.* 38, 1–8.

Zipfel, P. F., and Skerka, C. (1999). Fhl-1/reconectin: a human complement and immune regulator with cell-adhesive function. *Immunol. Today* 20, 135–140. doi: 10.1016/S0167-5699(98)01432-7

Conflict of Interest: The authors declare that the research was conducted in the absence of any commercial or financial relationships that could be construed as a potential conflict of interest.

frontiers in Cellular and Infection Microbiology

ORIGINAL RESEARCH
published: 12 May 2020
doi: 10.3389/fcimb.2020.00164

Caspofungin Induced Cell Wall Changes of *Candida* Species Influences Macrophage Interactions

Louise A. Walker and Carol A. Munro*

School of Medicine, Medical Sciences and Nutrition, Institute of Medical Sciences, University of Aberdeen, Aberdeen, United Kingdom

Candida species are known to differ in their ability to cause infection and have been shown to display varied susceptibilities to antifungal drugs. Treatment with the echinocandin, caspofungin, leads to compensatory alterations in the fungal cell wall. This study was performed to compare the structure and composition of the cell walls of different *Candida* species alone and in response to caspofungin treatment, and to evaluate how changes at the fungal cell surface affects interactions with macrophages. We demonstrated that the length of the outer fibrillar layer varied between *Candida* species and that, in most cases, reduced fibril length correlated with increased exposure of β-1,3-glucan on the cell surface. *Candida glabrata* and *Candida guilliermondii*, which had naturally more β-1,3-glucan exposed on the cell surface, were phagocytosed significantly more efficiently by J774 macrophages. Treatment with caspofungin resulted in increased exposure of chitin and β-1,3-glucan on the surface of the majority of *Candida* species isolates that were tested, with the exception of *C. glabrata* and *Candida parapsilosis* isolates. This increase in exposure of the inner cell wall polysaccharides, in most cases, correlated with reduced uptake by macrophages and in turn, a decrease in production of TNFα. Here we show that differences in the exposure of cell wall carbohydrates and variations in the repertoire of covalently attached surface proteins of different *Candida* species contributes to their recognition by immune cells.

Keywords: chitin, β-1,3-glucan, GPI-anchored proteins, fungal cell wall, echinocandin, macrophages, immune response

OPEN ACCESS

Edited by:
James Bernard Konopka, Stony Brook University, United States

Reviewed by:
Jeniel E. Nett, University of Wisconsin-Madison, United States
Robert T. Wheeler, University of Maine, United States

****Correspondence:***
Louise A. Walker
louise.walker@abdn.ac.uk

Specialty section:
This article was submitted to Fungal Pathogenesis, a section of the journal Frontiers in Cellular and Infection Microbiology

Received: *19 December 2019*
Accepted: *27 March 2020*
Published: *12 May 2020*

Citation:
Walker LA and Munro CA (2020) Caspofungin Induced Cell Wall Changes of Candida Species Influences Macrophage Interactions. Front. Cell. Infect. Microbiol. 10:164. doi: 10.3389/fcimb.2020.00164

INTRODUCTION

Candida species differ in their ability to cause infection. *Candida albicans* is the most common cause of *Candida* bloodstream infections (40%), followed by *Candida glabrata* (29%), *Candida parapsilosis* (11%), *Candida tropicalis* (4%), *Candida dubliniensis* (2%), and *Candida lusitaniae* (<1%) (Data captured from England; Health Protection Report, 2018). *Candida* species also have varied susceptibilities to antifungal drugs. The echinocandins act by specifically inhibiting the synthesis of β-1,3-glucan in the fungal cell wall. The inhibition of β-1,3-glucan synthesis occurs predominantly through inhibition of the catalytic Fks glucan synthase subunits (Kurtz and Douglas, 1997). Caspofungin is one of the most widely used of the echinocandins in the clinic and has fungicidal activity against the majority of *Candida* species. *C. lusitaniae*, *C. parapsilosis*, and *Candida guilliermondii* are known to have relatively reduced susceptibility compared to *C. albicans* and in recent years the incidence of clinical isolates of *C. glabrata*, which have acquired resistance

to the echinocandins has increased (Garcia-Effron et al., 2010; Pfaller et al., 2013). Alarmingly echinocandin-resistant *C. glabrata* isolates (up to 38%) were also cross-resistant to fluconazole (Pfaller et al., 2012, 2013). Acquired resistance is predominantly mediated by point mutations within hotspot regions in the *FKS* genes (Park et al., 2005; Balashov et al., 2006; Garcia-Effron et al., 2010; Alexander et al., 2013; Pham et al., 2014; Marti-Carrizosa et al., 2015).

The fungal cell wall determines cell shape, maintains cell wall integrity and is recognized by the innate immune system. The cell walls of *Candida* spp. in general are composed of an inner core of chitin and β-1,3-glucan, which is covered by an outer layer of cell wall proteins, the majority of which are covalently linked to β-1,6-glucan by modified glycosylphosphatidylinositol (GPI) anchors (Gow et al., 2017). The cell wall is a dynamic structure which alters its composition in response to cell wall stress by upregulating genes involved in cell wall synthesis, in an attempt to restore the robustness of the cell wall (Walker et al., 2008). Treatment of *C. albicans* with caspofungin has been shown to lead to a compensatory increase in chitin content, *in vitro* and *in vivo* (Walker et al., 2008; Lee et al., 2012). This compensatory increase in chitin is not specific to *C. albicans* as *C. tropicalis*, *C. parapsilosis*, *C. guilliermondii,* and isolates of *C. krusei* also demonstrated an elevation in chitin content in response to caspofungin treatment (Walker et al., 2013). In addition, isolates of *C. albicans*, *C. krusei*, *C. parapsilosis,* and *C. guilliermondii,* which have increased chitin content are less susceptible to caspofungin (Walker et al., 2008, 2013). *C. albicans* cells with elevated chitin contents have also been shown to be less susceptible to caspofungin in a murine model of systemic infection (Lee et al., 2012).

Putative GPI-modified cell wall proteins have been implicated in susceptibility to caspofungin as deletion of specific proteins leads to alterations in cell wall composition and subsequently to differences in susceptibility to caspofungin (Plaine et al., 2008). As a result of the cell wall remodeling that occurs in response to caspofungin treatment, chitin and β-1,3-glucan also become more exposed on the cell surface (Wheeler and Fink, 2006; Wheeler et al., 2008; Mora-Montes et al., 2011).

The fungal cell wall plays an important role in immune recognition as it is the first point of contact between the host and pathogen. The main innate immune cells that are involved in the recognition of invading pathogens are neutrophils, monocytes and macrophages (Netea et al., 2008). Components of the cell wall act as pathogen associated molecular patterns (PAMPs), which are recognized by pattern recognition receptors (PRRs) on host cells (Brown and Gordon, 2001; Porcaro et al., 2003; Kohatsu et al., 2006; McGreal et al., 2006; Netea et al., 2006, 2008). The two main classes of PRRs are the Toll-like receptors (TLRs) and the C-type lectin receptors (CLRs). The TLRs recognize phospholipomannan and *O*-linked mannan, whereas the C-type lectin receptors recognize β-1,3-glucan and mannan (Stahl et al., 1978; Wileman et al., 1986; Jouault et al., 2003; McGreal et al., 2006; Netea et al., 2006, 2008; Sato et al., 2006; Gow et al., 2007; Taylor et al., 2007). The increased exposure of chitin and β-1,3-glucan on the cell surface of *C. albicans*, in response to caspofungin treatment, results in altered cytokine production by immune cells, indicating that remodeling of the cell wall influences interactions with host cells (Wheeler and Fink, 2006; Wheeler et al., 2008; Mora-Montes et al., 2011; Baltch et al., 2012a,b; Fidan et al., 2014). Caspofungin treatment of *C. albicans* cells, followed by UV inactivation led to increased recognition of fungal cells by the C-type lectin, Dectin-1, which in turn increased cytokine production (Wheeler and Fink, 2006; Wheeler et al., 2008). In contrast, increased exposure of chitin on the surface of *C. albicans* has been shown to result in reduced cytokine production (Mora-Montes et al., 2011). Naturally occurring variations in the cell walls of different *C. albicans* isolates influences the dependency on dectin-1 for recognition and clearance of fungal cells (Marakalala et al., 2013). In addition the role of dectin-1 in recognition of four different *Candida* species, with differences in their cell wall carbohydrate composition, also varies (Thompson et al., 2019).

Because different *Candida* species vary in their ability to cause infection and vary in their cell wall composition, we aimed to perform a detailed comparison of the cell wall architectures of seven most prevalent *Candida* spp. and examine how their surface carbohydrates and proteomes change in response to caspofungin (CSF) treatment. In addition, the effect of caspofungin-induced cell wall changes of the different *Candida* species on the response of host immune cells was investigated.

MATERIALS AND METHODS

Strains, Media, and Growth Conditions

The strains of each *Candida* species that were used in this study had been typed and their genomes sequenced, these strains are listed in **Table 1**. Strains were maintained on solid YPD medium [1% (w/v) yeast extract, 2% (w/v) mycological peptone, 2% (w/v) glucose, 2% (w/v) agar]. RPMI-1640 medium (Gibco, Paisley, UK) was used for drug susceptibility testing and for growing cultures for HPLC and proteomic analysis.

TABLE 1 | Caspofungin susceptibilities of sequenced strains of different *Candida* species[a].

Species	Strain name	Caspofungin IC_{50} (μg/ml)	References
Candida albicans	SC5314	0.032	(Gillum et al., 1984)
Candida dubliniensis	CD36	0.064	(Sullivan et al., 1995)
Candida glabrata	ATCC2001	0.064	American Type Culture Collection
Candida tropicalis	MYA-3404	0.125	American Type Culture Collection
Candida lusitaniae	ATCC42720	0.5	American Type Culture Collection
Candida parapsilosis	ATCC22019	1	American Type Culture Collection
Candida guilliermondii	ATCC6260	8	American Type Culture Collection

[a] *As determined by broth microdilution testing. The IC_{50} was defined as the concentration of caspofungin that inhibited 50% growth of each Candida species when cultured in RPMI-1640 for 24 h at 37°C.*

Preparation of FITC-Stained *Candida* spp

Staining of *Candida* spp. yeast cells with fluorescein isothiocyanate (FITC) was performed as previously described (Graham et al., 2006). Briefly, *Candida* spp. were grown in YPD in the presence or absence of an IC_{50} concentration of caspofungin (Walker et al., 2013) in YPD at 30°C for 6 h. *Candida* spp. cells were washed twice with PBS and stained for 10 min at room temperature in the dark with 1 mg/ml fluorescein isothiocyanate (FITC) (Sigma, Dorset, United Kingdom) in 0.05 M carbonate-bicarbonate buffer (pH 9.6) (BDH Chemicals, VWR International, Leicestershire, United Kingdom). Cells were then washed three times in 1x PBS to remove residual FITC and were resuspended in 1x PBS. FITC-stained $6x10^5$ *Candida* spp. cells that had been pre-grown with or without IC_{50} caspofungin were then added to the macrophages at a multiplicity of infection (MOI) of 3 *Candida* spp. cells per macrophage, and incubated at 37°C for 4 h before visualization.

Phagocytosis and Cytokine Assays

Macrophage Cell Culture

J774.1 murine macrophages (European Collection of Cell Culture) were cultured in Dulbecco's modified Eagle's medium (DMEM; Lonza Group, Ltd., Braine-l'Alleud, Belgium), supplemented with 10% (vol/vol) fetal calf serum, 2% (wt/vol) penicillin and streptomycin antibiotics (Invitrogen, Ltd., Paisley, United Kingdom) in tissue culture flasks (Nalge Nunc, International, Hereford, United Kingdom) at 37°C and 5% (vol/vol) CO_2. For phagocytosis assays, 2×10^5 J774.1 macrophages in 2 ml supplemented DMEM medium were seeded onto glass-based imaging dishes [Imaging dish CG 1.0; MACS Miltenyi Biotec (130-098-282), Surrey, UK] and incubated at 37°C with 5% CO_2 for at least 2 h to allow for macrophage adherence to the dish. Immediately prior to experiments, DMEM medium was replaced with 2 ml pre-warmed supplemented CO_2-independent medium (Gibco, Invitrogen, Paisley, UK) and cultures used immediately for phagocytosis assays.

After 4 h of co-incubation 50 μl of supernatant was removed from phagocytosis assays to allow determination of TNFα production from J774 macrophages as a result of incubation with each *Candida* species. TNFα concentrations were determined using enzyme-linked immunosorbent assays (R&D Systems) according to the manufacturer's instructions.

Cell Wall Staining of Exposed Chitin and Glucan

Candida spp. yeast cells were grown in YPD in the presence or absence of an IC_{50} concentration of caspofungin in YPD at 30°C for 6 h. Cells were stained with 5 μg/ml Fc:Dectin1 protein to visualize exposed β-1,3-glucan, as previously described (52). Briefly, 1×10^6 cells/sample were blocked with FACS block (0.5% BSA, 5% HI-rabbit serum, 5 mM ETDA, 2 mM NaAzide in PBS) for 30 min. Cell pellets were harvested and washed 3 × with 1 ml FACS wash (0.5% BSA, 5 mM EDTA, 2 mM NaAzide in PBS) at 4°C. After washing, the cell pellet was resuspended in 100 μl of 5 μg/ml Fc:Dectin1 protein (diluted from stock in FACS block) and incubated for 1 h on ice. Cells were then washed 3 times with 1 ml FACS wash and resuspended in 200 μl FACS block plus 1/200 anti-human Fc+Alexa-488 and incubated for 45 min on ice. After incubation cells were washed three times with 1 ml FACS wash and fixed with 200 μl 1% formaldehyde. After fixing cells were also stained with 25 μg/ml Wheat Germ Agglutinin conjugated to Texas Red (WGA-TR). All samples were examined by DIC and fluorescence microscopy using a Zeiss Axioplan 2 microscope. Images were recorded digitally using the Openlab system (Openlab v 4.04, Improvision, Coventry, UK) and a Hamamatsu C4742- 95 digital camera (Hamamatsu Photonics, Hamamatsu, Hertfordshire, UK). In all experiments the exposure time for a series of fluorescence images was fixed so the intensity of fluorescence relative to a control was used as standard. Chitin and β-1,3-glucan exposure were measured by quantifying WGA-TR and Fc:Dectin1-488 fluorescence, respectively, of individual yeast cells (Walker et al., 2008). Mean fluorescence intensities were calculated for 50 individual cells of each *Candida* species, for each condition.

High-Pressure Freezing (HPF)-Transmission Electron Microscopy (TEM)

Candida spp. yeast cells were grown in YPD at 30°C for 6 h and HPF was carried out as described previously (Walker et al., 2010) with the following modifications. Briefly, samples were prepared by high-pressure freezing with an EMPACT2 high-pressure freezer and rapid transport system (Leica Microsystems Ltd., Milton Keynes, United Kingdom). After freezing, cells were freeze-substituted in substitution reagent (1% [wt/vol] OsO_4 in acetone) with a Leica EMAFS2. Samples were then embedded in Epoxy resin and additional infiltration was provided under a vacuum at 60°C before embedding in Leica FSP specimen containers and polymerizing at 60°C for 48 h. Semithin survey sections, 0.5 μm thick, were stained with 1% toluidine blue to identify areas containing cells. Ultrathin sections (60 nm) were prepared with a Diatome diamond knife on a Leica UC6 ultramicrotome and stained with uranyl acetate and lead citrate for examination with a Philips CM10 transmission microscope (FEI UK Ltd., Cambridge, United Kingdom) and imaging with a Gatan Bioscan 792 (Gatan United Kingdom, Abingdon, United Kingdom). Image J was used to measure the thickness of the inner (chitin and glucan) and outer cell wall by averaging measurements for 30 cells, for each condition.

Antifungal Susceptibility Testing

CSF (Merck Research Laboratories, New Jersey, USA) minimum inhibitory concentrations were determined by broth micro-dilution testing using the CLSI guidelines M27-A3. Drug concentrations ranged from 0.016 to 16 μg/ml CSF. Exponentially grown cultures were diluted to 2×10^6 cells/ml in 2x RPMI-1640 and 100 μl of culture was added to each well. Plates were incubated for 24 h at 37°C. After incubation, optical densities were read in a VERSAmax tunable microplate reader (Molecular Devices, California, USA) at 405 nm.

HPLC Analysis of Cell Wall Composition

Cell walls were extracted as described previously (Mora-Montes et al., 2011). Briefly, each *Candida* species was grown in

RPMI-1640 for 3 h at 37°C with shaking at 200 rpm. Each *Candida* species was then subsequently treated with a sub-MIC concentration of CSF (as determined from **Table 1**) for an additional 2 h, or grown without addition of drug for a further 2 h, as an untreated control. Cells were collected by centrifugation at 4,000 g for 5 min, washed once with chilled deionized water, resuspended in deionized water, and physically fractured with glass beads in a FastPrep machine (Qbiogene). The lysed cells were collected by centrifugation at 4,000 g for 5 min. The pellet containing the cell debris and walls was washed five times with 1 M NaCl, resuspended in extraction buffer (500 mM Tris-HCl buffer, pH 7.5, 2% [wt/vol] SDS, 0.3 M β-mercaptoethanol, and 1 mM EDTA), boiled at 100°C for 10 min, and freeze-dried. To quantify glucan, mannan, and chitin the cell walls were acid hydrolyzed as previously described (Lee et al., 2012). The hydrolyzed samples were analyzed by high-performance anion exchange chromatography with pulsed amperometric detection (HPAEC-PAD) in a carbohydrate analyzer system from Dionex (Surrey, United Kingdom) as described previously (Plaine et al., 2008). The total concentration of each cell wall component was expressed as μg per mg of dried cell wall which was determined by calibration from the standard curves of glucosamine, glucose, and mannose monomers, and converted to a percentage of the total cell wall.

Proteomic Analysis

Analysis of cell wall proteins was as described previously (Dutton et al., 2014). *Candida* species were grown with or without CSF as described for the HPLC analysis above. Briefly, 2 mg of freeze dried cell wall was mixed with 0.5 M ammonium bicarbonate in water containing 3 mM dithiothreitol and heated at 60°C for 20 min. Iodoacetamide (30 μl of 55 mM stock solution) was then added, and the suspension was incubated in the dark, at 25°C for 10 min. Following addition of 30 μl of 20 mg/ml trypsin, the suspension was incubated at 37°C for 14 h and centrifuged at 14,000 × g for 10 min. The supernatant was freeze-dried and extracted with 10% formic acid, and peptides were purified using ZipTip mC18 pipette tips (Millipore) and dissolved in 0.1% formic acid.

Samples (3 μl) were injected into an LC-MS system which comprised an UltiMate 3000 LC instrument (Dionex Ltd., United Kingdom) fitted with a PepSwift monolithic poly(styrene-codivinylbenzene) (PS-DVB) column (200 μm inside diameter [i.d.] by 5 cm; Dionex) coupled to an HCTultra ion trap mass spectrometer (Bruker Daltonik GmbH, Bremen, Germany) fitted with a low-flow nebulizer in the electrospray ionization (ESI) source and controlled by HyStar software (version 4.0; Bruker Daltonik). Peptides were separated at a flow rate of 2 μl/min using a linear gradient of 0–40% acetonitrile-water-formic acid (80:20:0.04) (solvent B) in water-acetonitrile-formic acid (97:3:0.05) (solvent A) over 40 min, followed by a 1 min column wash in 90% solvent B and a 12-min equilibration step in solvent A. MS/MS data (scan range, m/z 100–2,200; averages 2) were acquired in positive data-dependent AutoMS(n) mode using the esquireControl software program (version 6.2; Bruker Daltonik). Up to three precursor ions were selected from the MS scan (range, m/z 300–1,500; averages 3) in each AutoMS(n) cycle. Precursors were actively excluded after being selected twice within a 1-min window, and singly charged ions were also excluded. Peptide peaks were detected (maximum of 9,999 compounds above an intensity threshold of 50,000) and deconvoluted automatically using Data Analysis software (version 3.4; Bruker Daltonik). Mass lists in the form of Mascot Generic Format (*. mgf) files were created automatically and used as inputs to Mascot MS/MS ion searches via a local Mascot server (version 2.2; Matrix Science, London, United Kingdom) with a database built from sequence files available from Candida Genome Database (32). The Search parameters used were the following: enzyme = trypsin; fixed modifications = carbamidomethyl (C); variable modifications = oxidation (M); mass values = monoisotopic; peptide mass tolerance = 1.5 Da; fragment mass tolerance = 0.5 Da; max missed cleavages = 1; instrument type = ESI-TRAP. Search results were displayed by Mascot after selection of the following parameters: standard scoring; require bold red; ion score or expect cutoff = 0.05.

Statistical Analyses

Results from independent replicate experiments are expressed as means ± SD. One-way ANOVA with a Dunnett's *post-hoc* test was used for statistical analysis. Significance was determined as $p < 0.05$.

RESULTS

IC_{50} of *Candida* spp to Caspofungin

The susceptibility of each of the sequenced *Candida* spp. strains, used in this study, to CSF was determined following the CLSI-M27-A3 guidelines. *C. albicans*, *C. dublinensis*, *C. glabrata,* and *C. tropicalis* were the most susceptible to CSF (**Table 1**). The IC_{50} range for these susceptible species was between 0.032 and 0.064 μg/ml CSF (**Table 1**). *C. lusitaniae* and *C. parapsilosis* had CSF IC_{50} measurements of 0.5 and 1 μg/ml, respectively, which was classified as intermediate susceptibility and *C. guilliermondii* was resistant to CSF (**Table 1**). Therefore, the order of susceptibility to CSF from most susceptible to most resistant of the isolates of the *Candida* spp. tested here was: *C. albicans* > *C. dubliniensis* > *C. glabrata* > *C. tropicalis* > *C. lusitaniae* > *C. parapsilosis* > *C. guilliermondii*.

Candida Species Have Differences in the Ultrastructure of Their Cell Wall

Ultrastructural differences in the cell wall of each *Candida* species were investigated using high pressure freezing transmission electron microscopy (TEM) which conserves the fungal cell wall architecture. TEM analysis revealed that the inner core of the cell wall of *C. glabrata* (**Figure 1A**, v) and *C. tropicalis* (**Figure 1A,** ii) isolates was significantly thicker than the inner core of *C. albicans* isolate (**Figure 1A**, i; **Figure 1B**). In contrast to this the inner core of the *C. guilliermondii* cell wall (**Figure 1A**, vii) was significantly thinner, in comparison to *C. albicans* (**Figure 1A**, i; **Figure 1B**). Overall, the largest difference in the cell wall between the *Candida* species was in the outer fibrillar layer (**Figure 1B**). The variations

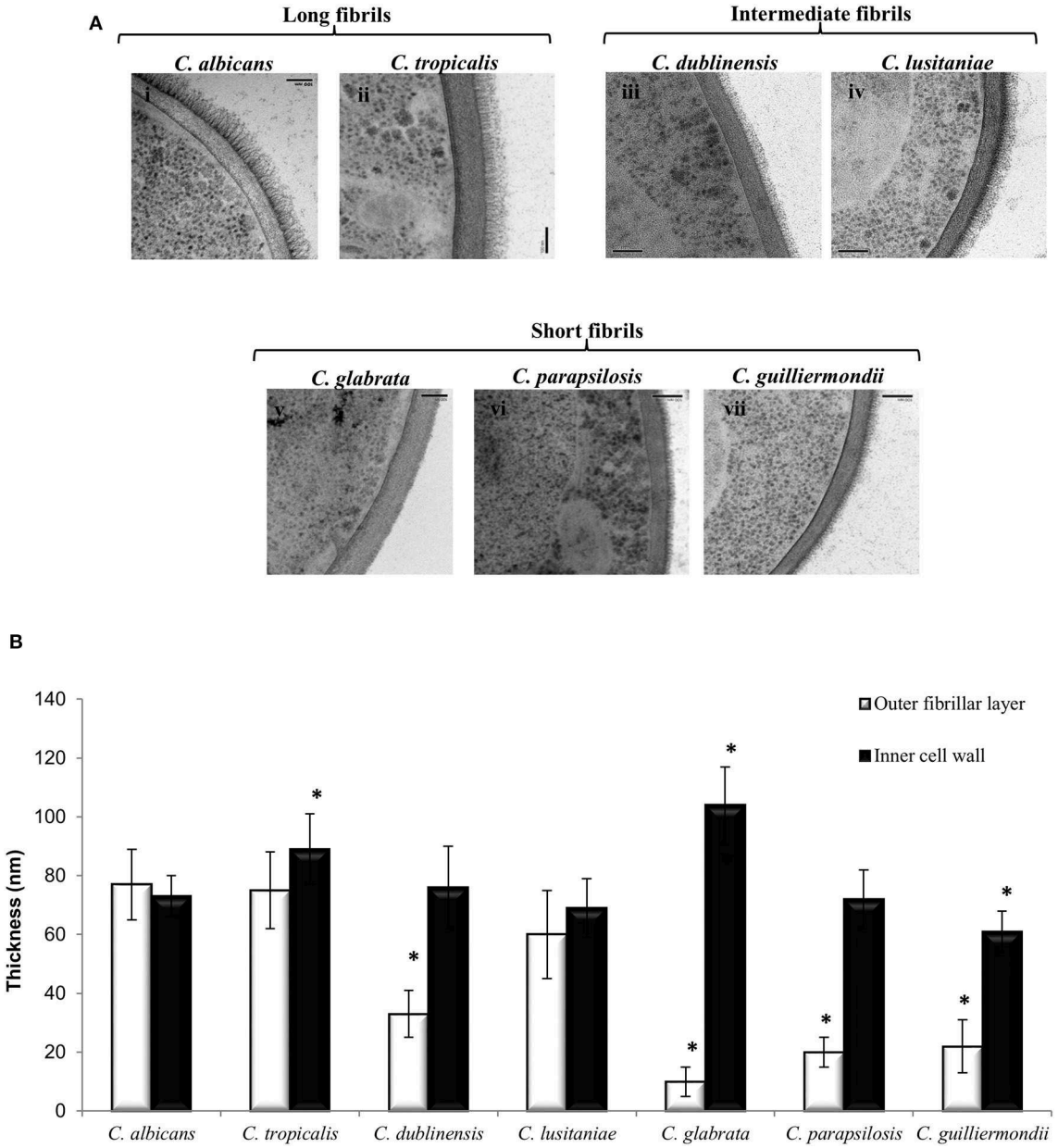

FIGURE 1 | The ultrastructure of the cell wall varies between *Candida* species. **(A)** TEMs of the cell wall of different *Candida* species: *C. albicans* (i), *C. tropicalis* (ii), *C. dublinensis* (iii), *C. lusitaniae* (iv), *C. glabrata* (v), *C. parapsilosis* (vi) and *C. guilliermondii* (vii). Scale bars are 100 nm. **(B)** The thickness of the inner cell wall (glucan and chitin) and outer fibrillar layer was determined from TEM pictures. Measurements from 30 cells that were sectioned so that cell wall thickness was even all around the cell periphery. Significant differences (*$p < 0.05$) compared to *C. albicans*. Error bars are SD ($n = 30$).

in length of the outer fibrillar layer were classified as either long (>65 nm), intermediate (30–65 nm), or short (<30 nm) (**Figure 1B**). *C. albicans* and *C. tropicalis* had the longest outer fibrillar layers, followed by *C. dubliniensis* and *C. lusitaniae* which were classified as having intermediate fibril length (**Figure 1B**). *C. glabrata*, *C. parapsilosis,* and *C. guilliermondii* isolates had short outer fibrils on the cell surface, in comparison to the *C. albicans* isolate (**Figure 1B**).

Candida Species Have Species Specific GPI-Anchored Proteins Present on Their Cell Surface

To determine the differences in the cell wall proteome between the different *Candida* species, LC-MS/MS was used to identify which covalently attached, predicted GPI-modified proteins were present on the surface of each *Candida* species when they were cultured in RPMI-1640 medium (**Table 2**). Here we

TABLE 2 | *Candida* species-specific detection of cell wall GPI-anchored proteins by LC/MS/MS proteomics.

Species specific detection of putative GPI-anchored proteins[a,b,c]						
C. albicans	***C. dubliniensis***	***C. lusitaniae***	***C. parapsilosis***	***C. tropicalis***	***C. glabrata***	***C. guilliermondii***
Hyr1 (C1_13450W_A)	Als4 (CD36_64610)	Pga31 (CLUG_00164)	Pga24/Ywp1 (CPAR2_806670)	Pga24/Ywp1 (CTRG_01856)	Epa6 (CAGL0C00110g)	Pga24/Ywp1 (DEHA2A14366g)
	Als2 (CD36_64800)	Rbt1 (CLUG_03306)	Pga30 (CPAR2_402000)		Epa3 (CAGL0E06688g)	
	Sap9 (CD36_83850)				Awp4 (CAGL0J12001g)	

[a] *Proteins assigned common names according to their C. albicans orthologs (Butler et al., 2009). Unique protein IDs in brackets.*
[b] *Detected in at least one of three biological replicate samples.*
[c] *In addition the following proteins were detected in all samples: Ssr1 (C7_00860W_A), Pga4 (C5_05390C_A), Crh11 (C4_02900C_A).*

TABLE 3 | Caspofungin treatment specific proteins in different *Candida* species in RPMI-1640 medium.

Species	Cell wall proteins specific to CSF-treated cells[a,b,c]				
C. albicans	Utr2 (C3_01730C_A)	Pga31 (C4_04080C_A)	Ecm33 (C1_03190C_A)	Rbt1 (C4_03520C_A)	Pga29 (C4_04050C_A)
C. dubliniensis	Utr2 (CD36_81610)	Pga31 (CD36_43780)	Phr2 (CD36_00220)		
C. lusitaniae	Utr2 (CLUG_02005)	Pga62 (CLUG_00242)	Als1	Phr1 (CLUG_01043)	Pga24 (CLUG_00242)
C. parapsilosis	Utr2 (CPAR2_503190)		Als1		
C. tropicalis	Utr2 (CTRG_02140)	Pga31 (CTRG_00350)	Ecm33 (CTRG_00105)		
C. glabrata	Pir3 (CAGL0M08492g)	Crh1 (CAGL0G09449g)			
C. guilliermondii	Utr2 (PGUG_00573)	Pga30 (PGUG_01942)	Plb5 (PGUG_01288)		

[a] *Proteins assigned common names according to their C. albicans orthologs (Butler et al., 2009). Unique protein IDs in brackets.*
[b] *Detected in at least one of three biological replicate samples.*
[c] *These proteins were not detected in the cell walls of untreated cultures.*

have annotated the proteins according to their *C. albicans* orthologs based on sequence similarity according to Candida Genome Database (Skrzypek et al., 2016). A core set of predicted cell wall proteins were identified in all species (**Table 2**). The hyphal specific protein, Hyr1, was uniquely detected in the cell wall of *C. albicans*, commensurate with it being a *C. albicans*-specific hyphal-associated protein and *C. albicans* will undergo filamentation in RPMI-1640 medium. GPI-anchored proteins that were identified specifically in the cell wall of *C. dubliniensis* included two Als proteins involved in adhesion and the secreted aspartyl protease, Sap9 (**Table 2**). A fungal-specific phospholipase and Pga59 orthologs were detected only on the cell surface of *C. lusitaniae* (**Table 2**). The cell wall of *C. parapsilosis* was found to contain orthologs of the yeast wall protein, Ywp1/Pga24, and Pga30, a protein of unknown function (**Table 2**).

Caspofungin treatment has been previously shown to alter cell wall architecture and increases chitin production in *C. albicans*, *C. tropicalis*, *C. krusei*, *C. parapsilosis,* and *C. guilliermondii* (9). The effect of CSF treatment on the cell wall proteome of each *Candida* species was also investigated by treating each *Candida* spp. with their IC_{50} concentration of caspofungin (**Table 3**). Certain proteins were detected only at the cell surface in response to CSF treatment in addition to the proteins listed that are found on the surface of untreated cells. The proteins expressed in response to caspofungin varied between the different *Candida* spp. Orthologs of the transglycosidase, Utr2, were detected on the cell surface of the majority of *Candida* species in response to CSF treatment with the exception of *C. glabrata* (**Table 3**). Orthologs of Pga31, a GPI-anchored protein of unknown function was detected on the surface of the species that were most sensitive to CSF, such as *C. albicans, C. dublinensis,* and *C. tropicalis* in response to CSF treatment (**Table 3**). A protein related to Pga30, a member of the same family as Pga31 was detected in the cell wall of *C. guilliermondii* treated with CSF. *C. lusitaniae* and *C. parapsilosis*, which have intermediate susceptibility to CSF, were found to have Als-like proteins on their cell surface in response to CSF treatment (**Table 3**).

Cell Wall Composition of Different *Candida* Species in the Presence or Absence of CSF

The carbohydrate composition of the cell walls of the different *Candida* spp., in the presence or absence of an IC_{50} concentration of caspofungin, was determined by acid hydrolysis of isolated cell walls and analysis by high-performance liquid chromatography. *C. tropicalis* had substantially higher chitin content than *C. albicans*, whereas *C. glabrata* and *C. guilliermondii* had significantly less chitin compared to *C. albicans* (**Table 4**). The majority of *Candida* spp. had comparable levels of glucan in the cell wall, with the exception of *C. tropicalis,* which had significantly reduced glucan compared to *C. albicans* and *C. glabrata*, which had a higher glucan content (**Table 4**). The quantity of mannan in the cell wall was significantly reduced in *C. glabrata*, *C. parapsilosis,* and *C. guilliermondii* compared

TABLE 4 | Quantification of the components of the cell wall of *Candida* species, with and without caspofungin treatment a,b,c*#.

Candida spp.	% Dried cell wall		
	Chitin	**Glucan**	**Mannan**
C. albicans	4 ± 0.2 (100%)	66 ± 3 (100%)	30 ± 2 (100%)
C. albicans + CSF[c]	8 ± 1[#] (200%)	43 ± 5[#] (65%)	49 ± 3[#] (163%)
C. tropicalis	5 ± 0.5* (100%)	54 ± 2* (100%)	41 ± 6 (100%)
C. tropicalis + CSF	12 ± 4 (240%)[#]	40 ± 7 (74%)[#]	49 ± 2 (120%)
C. dubliniensis	5 ± 0.8 (100%)	63 ± 4 (100%)	32 ± 1 (100%)
C. dubliniensis + CSF	13 ± 2[#] (260%)	49 ± 6[#] (78%)	38 ± 3 (119%)
C. lusitaniae	4 ± 0.1 (100%)	70 ± 8 (100%)	26 ± 2 (100%)
C. lusitaniae + CSF	9 ± 3[#] (225%)	53 ± 11[#] (76%)	38 ± 3[#] (146%)
C. glabrata	2 ± 0.1* (100%)	81 ± 5* (100%)	17 ± 4* (100%)
C. glabrata + CSF	1 ± 0.2 (50%)	67 ± 3[#] (83%)	32 ± 2[#] (188%)
C. parapsilosis	7 ± 5 (100%)	75 ± 4 (100%)	18 ± 3* (100%)
C. parapsilosis +CSF	8 ± 3 (114%)	62 ± 2[#] (83%)	30 ± 6[#] (167%)
C. guilliermondii	2 ± 1* (100%)	79 ± 6 (100%)	19 ± 2* (100%)
C. guilliermondii + CSF	6 ± 0.5[#] (300%)	59 ± 8[#] (75%)	36 ± 5[#] (189%)

[a] *Cell walls were acid hydrolyzed and released monosaccharide was detected.*
[b] *Results are expressed as a % of dried cell wall of the untreated data ± SD. n = 3 biological replicates. For + CSF samples % in brackets is relative to untreated samples which were set as 100%.*
[c] *IC_{50} concentration of CSF was used for each species.*
**Significantly different compared to untreated cells of C. albicans (P = 0.05).*
[#] *Significantly different compared to untreated cells of the same species (P = 0.05).*

to *C. albicans* (**Table 4**) in agreement with the TEM analysis which suggested these species have shorter mannan fibrils on their outer surfaces. In most cases treatment with CSF resulted in an increase in chitin content, with the exception of *C. glabrata* and *C. parapsilosis* (**Table 4**). As expected all *Candida* spp. isolates tested had a reduction in β-1,3-glucan in response to CSF treatment. Exposure to an IC_{50} concentration of CSF led to a significant increase in mannan content in all *Candida* spp., with the exception of *C. tropicalis* and *C. dublinensis* isolates (**Table 4**).

Candida Species Have Differences in Surface Exposure of Chitin and Glucan in Response to CSF Treatment

Exposure of chitin and glucan on the cell surface is known to influence the immune recognition of fungal cells (Wheeler and Fink, 2006; Wheeler et al., 2008; Mora-Montes et al., 2011). Fluorescent staining was used to determine whether the differences in outer fibril length between the *Candida* species isolates correlated with variations in exposure of chitin and β-1,3-glucan on the cell surface. The exposure of chitin was determined using 25 μg/ml Wheat Germ Agglutinin-Texas Red (WGA-TR) and exposed β-1,3-glucan was stained with 5 μg/ml Fc:Dectin1- Alexa 488 (**Table 5**, **Supplementary Figure 1**). The exposure of chitin and β-1,3-glucan, after treatment with an IC_{50} concentration of CSF for 6 h, was determined for each *Candida* species isolate. Exposure of β-1,3-glucan was significantly higher on the surface of untreated *C. glabrata* and *C. guilliermondii* compared to *C. albicans* (**Table 5**). Treatment with CSF, at the IC_{50}, resulted in increased exposure of β-1,3-glucan on the surface of *C. albicans*, *C. tropicalis*, *C. dubliniensis*, *C. lusitaniae,* and *C. guilliermondii* (**Table 5**). However, CSF treatment had no effect on the exposure of β-1,3-glucan of *C. glabrata* and *C. parapsilosis* (**Table 5**). Measurement of exposed chitin on the cell surface determined that the *C. glabrata* isolate had less chitin exposed on the outer surface compared to *C. albicans* isolate (**Table 5**). Treatment of *C. albicans*, *C. tropicalis*, *C. dubliniensis*, *C. lusitaniae,* and *C. guilliermondii* with CSF resulted in increased detection of chitin on the cell surface (**Table 5**). The exception to this was *C. glabrata* and *C. parapsilosis* which had no change in exposure of chitin, in response to CSF treatment (**Table 5**).

Relationship Between Phagocytosis and Exposure of Chitin and Glucan

To determine the effect of exposure of chitin and glucan on phagocytosis, the uptake of isolates of each *Candida* species by J774 macrophages was determined. The yeasts were cultured with and without sub-MIC CSF treatment and phagocytosis correlated to the exposure of chitin and β-1,3-glucan on the cell surface (**Figure 2**, **Supplementary Table 1**). The majority of *Candida* species had low levels of chitin and β-1,3-glucan exposed naturally on the cell surface, under the growth conditions used (**Figure 2A**). The exception was *C. glabrata* and *C. guilliermondii* which had significantly more β-1,3-glucan exposed on the cell surface, compared to *C. albicans*, which correlated with these *Candida* species having the highest phagocytosis by J774 macrophages (**Figure 2A**). To determine the effect of altered exposure of β-1,3-glucan and chitin, the phagocytosis of CSF-treated cells was also measured (**Figure 2B**). In all cases the combined increase in exposure of chitin and β-1,3-glucan, in CSF-treated cells, resulted in a significant decrease in phagocytosis by macrophages (**Figure 2B**). Treatment of *C. glabrata* and *C. parapsilosis* with CSF had little effect on the exposure of the outer cell wall components and consequently there was no significant change in their phagocytosis by macrophages (**Figure 2B**). Pearson Correlation analysis demonstrated that there was a positive correlation between glucan exposure and chitin exposure and caspofungin treatment [$r_{(12)} = 0.703$, $p = 0.005$; $r_{(12)} = 0.699$, $p = 0.005$ respectively] but a negative correlation between % phagocytosis and caspofungin treatment [$r_{(12)} = -0.763$, $p = 0.002$].

TABLE 5 | Quantification of the exposure of β-1,3-glucan and chitin of *Candida* species, with and without caspofungin treatment[a].

Candida species	Glucan exposure (mean fluorescence intensity)		Chitin exposure (mean fluorescence intensity)	
	No treatment	Caspofungin treatment	No treatment	Caspofungin treatment
C. albicans	179 ± 20	450 ± 34[#]	167 ± 17	488 ± 51[#]
C. dubliniensis	211 ± 14	374 ± 52[#]	160 ± 26	404 ± 40[#]
C. glabrata	273 ± 21*	257 ± 39	89 ± 18*	79 ± 20
C. tropicalis	185 ± 41	607 ± 66[#]	178 ± 22	516 ± 54[#]
C. lusitaniae	171 ± 29	468 ± 49[#]	159 ± 31	438 ± 35[#]
C. parapsilosis	201 ± 13	189 ± 30	172 ± 28	202 ± 45
C. guilliermondii	263 ± 36*	537 ± 72[#]	160 ± 29	445 ± 49[#]

[a] *The average relative β-1,3-glucan and chitin contents of individual cells from different Candida species were determined by measuring the intensity of Fc:Dectin1–Alexa488 and WGA-Texas Red fluorescence. Measurements were made on untreated control cultures and after growth with caspofungin at the specific IC_{50} for each species (as determined in* ***Table 1****). Statistical differences are shown for comparison to untreated cells of C. albicans (*P = 0.05) or untreated cells of the same species (#P = 0.05), and data are means with standard deviations (n = 50).*

Cytokine Production Varies Between *Candida* Species and Is Reduced in Response to CSF Treatment

Increased exposure of β-1,3-glucan has previously been shown to stimulate cytokine production whereas increased exposure of chitin has been shown to result in a decrease in cytokine production (Wheeler and Fink, 2006; Wheeler et al., 2008; Mora-Montes et al., 2011). To determine the cytokine production stimulated by the different *Candida* species, TNFα production was measured when untreated live cells of each *Candida* species were exposed to J774 macrophages for 4 h (**Figure 3**). Live cells of *C. albicans* and *C. dubliniensis* stimulated the highest levels of TNFα production (**Figure 3**). The other *Candida* species all stimulated very low levels of TNFα (**Figure 3**), which remained unchanged even after 24 h (data not shown). Treatment with an IC_{50} concentration of CSF, specific to each *Candida* species, led to a significant decrease in TNFα production in *C. albicans* and *C. dubliniensis*, compared to untreated cells (**Figure 3**). Treatment with CSF had no effect on TNFα production in the other *Candida* species isolates, with the exception of the *C. tropicalis* isolate which had a significant increase in TNFα production compared to untreated cells (**Figure 3**). *C. tropicalis* also had the highest level of surface-exposed β(1,3)-glucan when treated with CSF.

DISCUSSION

This study aimed to directly compare the structure and composition of the cell walls of different *Candida* species, examine how the cell wall was altered in response to caspofungin treatment and assess how this impacted on fungal: murine macrophage interactions. We demonstrated that the length of the outer fibrillar layer varied between the species isolates tested and that, in most cases, reduced fibril length correlated with increased exposure of β-1,3-glucan on the cell surface. *C. glabrata* and *C. guilliermondii*, which had naturally more β-1,3-glucan exposed on the cell surface, were phagocytosed more efficiently by J774 macrophages. This is in agreement with a previous study that showed that in a mixed population of *C. albicans* and *C. glabrata* cells, *C. glabrata* is preferentially phagocytosed over *C. albicans* (Keppler-Ross et al., 2010). Similar to our observations, Estrada-Mata et al. (2016) also demonstrated that *C. parapsilosis* had less mannan content but more β-1,3-glucan exposed on the surface compared to *C. albicans* which correlated with an increase in cytokine production by human PBMCs (Estrada-Mata et al., 2016). Dectin-1 has been shown to play an important role in recognition of *C. parapsilosis* by human PBMCs (Toth et al., 2013). In our study *C. parapsilosis* induced little cytokine production from J774 macrophages at 4 h, but differences in the source of immune cells and the time that *Candida* cells were exposed to immune cells before performing the ELISAs may account for these differences.

There were also notable differences in the cell wall proteins that reside on the surface of the different *Candida* species, for example, the GPI-anchored proteins, Epa3, Epa6, and Awp4, were identified specifically on the cell wall of *C. glabrata* under the growth conditions tested. These are known to be adhesion proteins in *C. glabrata* which are associated with biofilm formation (de Groot et al., 2008; Kraneveld et al., 2011). The presence of cell wall proteins on the cell surface of *C. glabrata*, *C. parapsilosis,* and *C. tropicalis* has been shown to be dependent on the growth conditions tested (Karkowska-Kuleta et al., 2019).

Treatment with CSF is known to result in a compensatory increase in cell wall chitin levels and result in increased exposure of chitin and β-1,3-glucan on the surface of *C. albicans* cells (Wheeler and Fink, 2006; Walker et al., 2008, 2013; Wheeler et al., 2008; Mora-Montes et al., 2011). All of the *Candida* species isolates tested, with the exception of *C. glabrata* and *C. parapsilosis* isolates, demonstrated a compensatory increase in cell wall chitin content in response to CSF treatment. Likewise, treatment with CSF also resulted in an increase in exposure of chitin and β-1,3-glucan on the cell surface for the majority of species tested. Notable exceptions were *C. glabrata* and *C. parapsilosis* with no changes in glucan exposure in response to caspofungin treatment. This increase in exposure of the inner cell wall polysaccharides, did not increase the number of macrophages that had engulfed the fungal cells in fact caspofungin treatment resulted in a reduction in % phagocytosis.

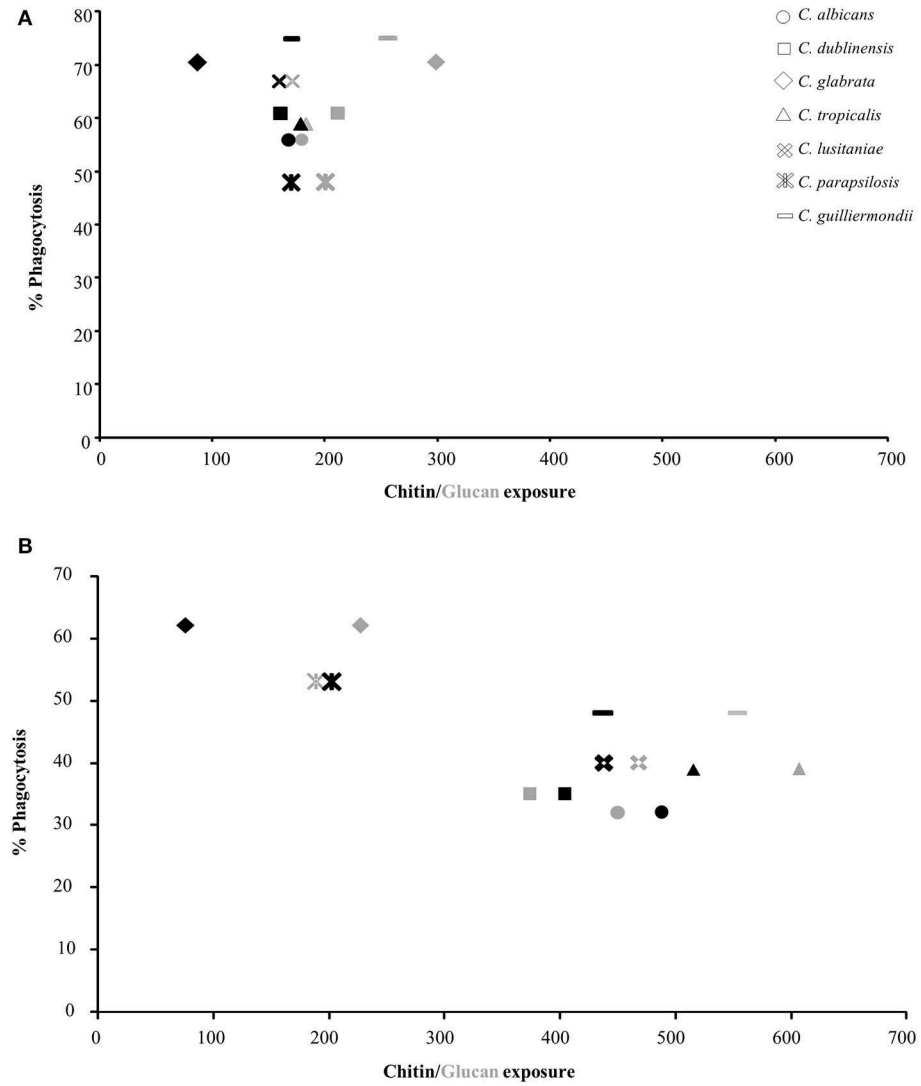

FIGURE 2 | Correlation between exposure of chitin and glucan on the cell surface of *Candida* species and phagocytosis by J774 macrophages. The values for exposure of chitin and β-1,3-glucan were taken from **Table 5**. Phagocytosis of *Candida* spp. by macrophages was determined by fluorescence microscopy. All cells were stained with 10 μg/ml FITC prior to exposure to macrophages. FITC-stained cells were exposed to J774 macrophages for 1 h, after which non-phagocytosed cells were stained with 25 μg/ml CFW. The number of macrophages which had phagocytosed *Candida* cells were then counted ($n = 300$). **(A)** Untreated *Candida* spp. cells. **(B)** CSF treated *Candida* cells. Black shapes = chitin (WGA-TR), gray shapes = glucan (Fc:dectin1-alexa488).

The majority of live *Candida* spp. cells stimulated low levels of TNFα production. In comparison the *C. albicans* and *C. dublinensis* isolates stimulated elevated levels of TNFα but these levels were significantly reduced when macrophages were exposed to the same isolates after caspofungin treatment. A notable exception to this trend was CSF-treated *C. tropicalis* isolate which stimulated significantly elevated TNFα production compared to untreated cells attaining a level comparable to *C. albicans* and *C. dublinensis*. *C. tropicalis* had the highest level of Fc-dectin1-Alex488 staining with and without caspofungin treatment. These findings suggested that the immune stimulatory properties of the different *Candida* species is not solely dependent upon β-1,3-glucan exposure and recognition by Dectin-1 and other factors may come into play (Wagener et al., 2014). Recently, treatment with either fragments of chitin or β-1,3-glucan from *Aspergillus fumigatus* were shown to stimulate production of TNFα. In addition, combined treatment with both chitin and β-1,3-glucan resulted in a synergistic increase in TNFα production (Dubey et al., 2014). This is in contrast with the findings here where other changes at the cell surface including increased chitin exposure appeared to override any stimulation of the immune response elicited by glucan exposure. The differences in stimulation of the immune response may be due to variations in size of the cell wall polysaccharides and the way the polymer is presented to immune cells. Small particles of chitin are known to illicit a greater cytokine response compared to larger

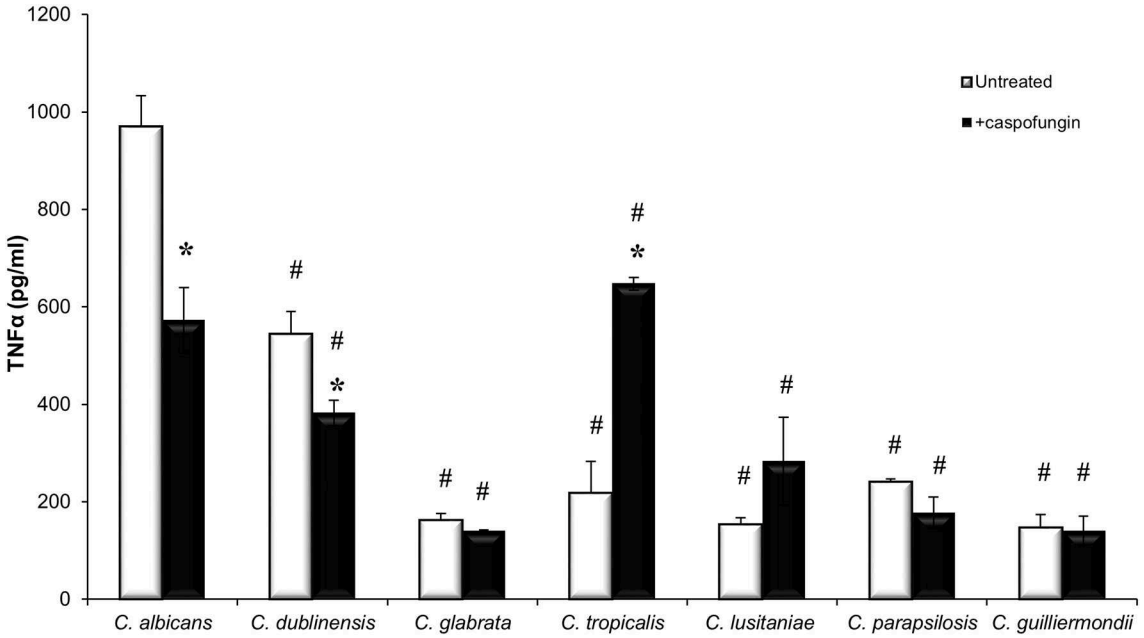

FIGURE 3 | *Candida* species stimulate different immune responses. Live cells of each *Candida* species, which had been grown with or without an IC_{50} concentration of caspofungin for 6 h, were exposed to J774 macrophages for 4 h. After 4 h of co-incubation, supernatants were collected and cytokine production was measured. Significant differences ($^{\#}p < 0.05$) compared to *C. albicans*. Significant differences ($^{*}p < 0.05$) compared to untreated cells of the same species. Error bars are SD ($n = 3$).

chitin fragments (Da Silva et al., 2009). Likewise, differences in polysaccharide structure may influence the immune response. The chitin microfibrils of *A. fumigatus* and *C. albicans* may have a different architecture, which could influence the immune response (Gow and Gooday, 1983; Lenardon et al., 2007). Recently, hyphal β-1,3-glucan of *C. albicans* was found to have a unique cyclical structure that is absent in β-1,3-glucan from the yeast form (Lowman et al., 2014). Compared to β-1,3-glucan from yeast cells, hyphal glucan was shown to induce an immune response in macrophages and human peripheral blood mononuclear cells through a Dectin-1-dependent mechanism. In addition CSF treatment has also been shown to not only effect β-1,3-glucan exposure but also its nano-structure with the density of dectin-1 binding sites increasing leading to increased phagocytosis by dendritic cells (Lin et al., 2016). To dissect further whether glucan and/or chitin plays the main role in caspofungin-mediated dampening of the immune response, it would be interesting to evaluate the effect of blocking receptors of both polysaccharides on interaction with macrophages. Another consideration is that the change in GPI-modified proteins on the cell surface, in response to CSF treatment, may also influence the interaction with immune cells. For example, the transglycosidase, Utr2, was detected on the surface of the majority of *Candida* species in response to CSF treatment. Utr2 is involved in crosslinking chitin and β-1,3-glucan and forms part of a compensatory mechanism activated in response to cell weakening induced by echinocandin treatment (Pardini et al., 2006). A *C. albicans utr2*Δ mutant was found to have the same susceptibility to micafungin as the wild type (Alberti-Segui et al., 2004). Deletion of *UTR2* in *C. albicans* resulted in attenuated virulence in a mouse model of systemic candidiasis. Despite this attenuation in virulence the fungal burdens from the kidneys of mice infected with the *utr2*Δ mutant were comparable to that of mice infected with wild-type *C. albicans*. This suggests that in the absence of *UTR2*, cells do not elicit the same inflammatory response as wild-type cells and enables the *utr2*Δ mutant to be tolerated by the host, leading to survival of the infected mice (Pardini et al., 2006). Therefore, the increased abundance of Utr2 on the cell surface in response to caspofungin treatment may also contribute to altered interactions with host cells.

Candida guilliermondii and *C. parapsilosis* are known to be intrinsically less sensitive to the echinocandins. Both species had thin walls and their cell wall proteomes differed from CSF-susceptible species. Pga24/Ywp1 orthologs were detected on their cell surfaces when grown on RPMI-1640 medium. In *C. albicans* Pga24 is associated with the yeast cell wall (Granger et al., 2005) and here was not detected when *C. albicans* was grown on RPMI-1640 medium. Mutation of *PGA24* did not alter echinocandin susceptibility of *C. albicans* (Plaine et al., 2008). The role of this surface protein in echinocandin susceptibility of *C. guilliermondii* and *C. parapsilosis* remains to be determined.

The ability of live cells of each isolate of the different *Candida* species to stimulate cytokine production varied significantly (**Figure 3**). *C. albicans* and *C. dubliniensis* isolates, tested here, elicited the highest production of TNFα. In contrast to this the other isolates representing the different *Candida* species

stimulated negligible levels of TNFα when exposed to J774 macrophages for 4 h. Previous work has demonstrated that *C. parapsilosis*, *C. tropicalis*, *C. lusitaniae,* and *C. guilliermondii* in addition to *C. albicans* and *C. dubliniensis*, stimulated production of TNFα from murine peritoneal macrophages and human PBMCs after 24 h (Aybay and Imir, 1996; Navarro-Arias et al., 2019). The most likely reason for the difference observed at the 4 h time point is that *C. albicans* and *C. dubliniensis* are the only two species which form true hyphae and were capable of germinating within macrophages, and consequently escaping from macrophages, faster than any of the other *Candida* species. For example, *C. glabrata* yeast cells have been shown to replicate within macrophages for up to 3 days before causing lysis of the macrophage (Seider et al., 2011). Therefore, the low levels of cytokine production that have been observed as a result of exposure of macrophages to live *C. glabrata* is thought to be due to *C. glabrata* evading host defenses by hiding within immune cells (Seider et al., 2011, 2014; Brunke et al., 2014). However, it is possible for *C. glabrata* to filament under certain conditions. Prolonged exposure of *C. glabrata* to macrophages led to filamentous growth which was a result of a point mutation in *CHS2* (Lewis et al., 2013). Treatment of *C. albicans* and *C. dubliniensis* with CSF resulted in a decrease in production of TNFα and reduced phagocytosis by macrophages. Exposure of *C. albicans* to caspofungin has previously been shown to reduce cytokine production in both live and heat killed *C. albicans* cells, as a result of increased exposure of chitin on the cell surface (Mora-Montes et al., 2011).

Here we examined caspofungin induced changes at the cell surface of representative isolates of different *Candida* species. We detected drug-induced changes in the repertoire of covalently attached surface proteins and alterations in the exposure of cell wall carbohydrates of contributing to their recognition by J774 macrophages. The cell surface is highly variable both between and within species and so these investigations should be expanded to a wider range of isolates of the different species to determine the extent of cell surface variability and how it impacts on host interactions and drug susceptibility.

DATA AVAILABILITY STATEMENT

The raw data supporting the conclusions of this article will be made available by the authors, without undue reservation, to any qualified researcher.

AUTHOR CONTRIBUTIONS

LW and CM contributed to acquisition, analysis, and interpretation of data for the work. All authors contributed to the design of the work and approved the submitted and final version.

FUNDING

We acknowledge funding from the British Society for Antimicrobial Chemotherapy, the Medical Research Council (G0400284) and Wellcome Trust Strategic Award for Medical Mycology and Fungal Immunology 097377.

ACKNOWLEDGMENTS

We thank Gillian Milne from the University of Aberdeen Microscopy and Histology facility for help with EM, Dr. David Stead (Aberdeen Proteomics) for proteomics analysis and Prof. Gordon Brown for Fc:Dectin1. We thank Dr. Judith Bain and Prof. Lars Erwig for advice on the macrophage assays.

SUPPLEMENTARY MATERIAL

The Supplementary Material for this article can be found online at: https://www.frontiersin.org/articles/10.3389/fcimb.2020.00164/full#supplementary-material

REFERENCES

Alberti-Segui, C., Morales, A. J., Xing, H., Kessler, M. M., Willins, D. A., Weinstock, K. G., et al. (2004). Identification of potential cell-surface proteins in *Candida albicans* and investigation of the role of a putative cell-surface glycosidase in adhesion and virulence. *Yeast* 21, 285–302. doi: 10.1002/yea.1061

Alexander, B. D., Johnson, M. D., Pfeiffer, C. D., Jimenez-Ortigosa, C., Catania, J., Booker, R., et al. (2013). Increasing echinocandin resistance in *Candida glabrata*: clinical failure correlates with presence of *FKS* mutations and elevated minimum inhibitory concentrations. *Clin. Infect. Dis.* 56, 1724–1732. doi: 10.1093/cid/cit136

Aybay, C., and Imir, T. (1996). Tumor necrosis factor (TNF) induction from monocyte/macrophages by *Candida* species. *Immunobiology* 196, 363–374. doi: 10.1016/S0171-2985(96)80059-3

Balashov, S. V., Park, S., and Perlin, D. S. (2006). Assessing resistance to the echinocandin antifungal drug caspofungin in *Candida albicans* by profiling mutations in *FKS1*. *Antimicrob. Agents Chemother.* 50, 2058–2063. doi: 10.1128/AAC.01653-05

Baltch, A. L., Lawrence, D., Ritz, W. J., Andersen, N., Bopp, L. H., Michelsen, P. B., et al. (2012b). Effects of anidulafungin and voriconazole, singly and in combination, on cytokine/chemokine production by human monocyte-derived macrophages infected with *Candida glabrata* or activated by lipopolysaccharide. *Chemotherapy* 58, 146–151. doi: 10.1159/000337076

Baltch, A. L., Lawrence, D. A., Ritz, W. J., Andersen, N. J., Bopp, L. H., Michelsen, P. B., et al. (2012a). Effects of echinocandins on cytokine/chemokine production by human monocytes activated by infection with *Candida glabrata* or by lipopolysaccharide. *Diagn. Microbiol. Infect. Dis.* 72, 226–233. doi: 10.1016/j.diagmicrobio.2011.11.004

Brown, G. D., and Gordon, S. (2001). Immune recognition. A new receptor for beta-glucans. *Nature* 413, 36–37. doi: 10.1038/35092620

Brunke, S., Seider, K., Fischer, D., Jacobsen, I. D., Kasper, L., Jablonowski, N., et al. (2014). One small step for a yeast–microevolution within macrophages renders *Candida glabrata* hypervirulent due to a single point mutation. *PLoS Pathog.* 10:e1004478. doi: 10.1371/journal.ppat.1004478

Butler, G., Rasmussen, M. D., Lin, M. F., Santos, M. A., Sakthikumar, S., Munro, C. A., et al. (2009). Evolution of pathogenicity and sexual reproduction in eight Candida genomes. *Nature.* 459, 657–662. doi: 10.1038/nature08064

Da Silva, C. A., Chalouni, C., Williams, A., Hartl, D., Lee, C. G., and Elias, J. A. (2009). Chitin is a size-dependent regulator of macrophage TNF and IL-10 production. *J. Immunol.* 182, 3573–3582. doi: 10.4049/jimmunol.0802113

de Groot, P. W., Kraneveld, E. A., Yin, Q. Y., Dekker, H. L., Gross, U., Crielaard, W., et al. (2008). The cell wall of the human pathogen *Candida glabrata*: differential incorporation of novel adhesin-like wall proteins. *Eukaryot. Cell* 7, 1951–1964. doi: 10.1128/EC.00284-08

Dubey, L. K., Moeller, J. B., Schlosser, A., Sorensen, G. L., and Holmskov, U. (2014). Induction of innate immunity by *Aspergillus fumigatus* cell wall polysaccharides is enhanced by the composite presentation of chitin and beta-glucan. *Immunobiology* 219, 179–188. doi: 10.1016/j.imbio.2013.10.003

Dutton, L. C., Nobbs, A. H., Jepson, K., Jepson, M. A., Vickerman, M. M., Aqeel Alawfi, S., et al. (2014). *O*-mannosylation in *Candida albicans* enables development of interkingdom biofilm communities. *MBio* 5:e00911-14. doi: 10.1128/mBio.00911-14

Estrada-Mata, E., Navarro-Arias, M. J., Perez-Garcia, L. A., Mellado-Mojica, E., Lopez, M. G., Csonka, K., et al. (2016). Members of the *Candida parapsilosis* complex and *Candida albicans* are differentially recognized by human peripheral blood mononuclear cells. *Front. Microbiol.* 6:1527. doi: 10.3389/fmicb.2015.01527

Fidan, I., Yesilyurt, E., Kalkanci, A., Aslan, S. O., Sahin, N., Ogan, M. C., et al. (2014). Immunomodulatory effects of voriconazole and caspofungin on human peripheral blood mononuclear cells stimulated by *Candida albicans* and *Candida krusei*. *Am. J. Med. Sci.* 348, 219–223. doi: 10.1097/MAJ.0000000000000236

Garcia-Effron, G., Chua, D. J., Tomada, J. R., DiPersio, J., Perlin, D. S., Ghannoum, M., et al. (2010). Novel *FKS* mutations associated with echinocandin resistance in *Candida* species. *Antimicrob. Agents Chemother.* 54, 2225–2227. doi: 10.1128/AAC.00998-09

Gillum, A. M., Tsay, E. Y., and Kirsch, D. R. (1984). Isolation of the *Candida albicans* gene for orotidine-5'-phosphate decarboxylase by complementation of S. cerevisiae ura3 and *E. coli* pyrF mutations. *Mol. Gen. Genet.* 198, 179–182. doi: 10.1007/bf00328721

Gow, N. A., Netea, M. G., Munro, C. A., Ferwerda, G., Bates, S., Mora-Montes, H. M., et al. (2007). Immune recognition of *Candida albicans* beta-glucan by dectin-1. *J. Infect. Dis.* 196, 1565–1571. doi: 10.1086/523110

Gow, N. A. R., and Gooday, G. W. (1983). Ultrastructure of chitin in hyphae of *Candida albicans* and other dimorphic and mycelial fungi. *Protoplasma* 115, 52–58. doi: 10.1007/BF01293580

Gow, N. A. R., Latge, J.-P., and Munro, C. A. (2017). The fungal cell wall: structure, biosynthesis, and function. *Microbiol. Spectr.* 5, 1–25. doi: 10.1128/microbiolspec.FUNK-0035-2016

Graham, L. M., Tsoni, S. V., Willment, J. A., Williams, D. L., Taylor, P. R., Gordon, S., et al. (2006). Soluble Dectin-1 as a tool to detect beta-glucans. *J. Immunol. Methods* 314, 164–169. doi: 10.1016/j.jim.2006.05.013

Granger, B. L., Flenniken, M. L., Davis, D. A., Mitchell, A. P., and Cutler, J. E. (2005). Yeast wall protein 1 of *Candida albicans*. *Microbiology* 151, 1631–1644. doi: 10.1099/mic.0.27663-0

Jouault, T., Ibata-Ombetta, S., Takeuchi, O., Trinel, P. A., Sacchetti, P., Lefebvre, P., et al. (2003). *Candida albicans* phospholipomannan is sensed through toll-like receptors. *J. Infect. Dis.* 188, 165–172. doi: 10.1086/375784

Karkowska-Kuleta, J., Satala, D., Bochenska, O., Rapala-Kozik, M., and Kozik, A. (2019). Moonlighting proteins are variably exposed at the cell surfaces of *Candida glabrata*, *Candida parapsilosis* and *Candida tropicalis* under certain growth conditions. *BMC Microbiol.* 19, 145–149. doi: 10.1186/s12866-019-1524-5

Keppler-Ross, S., Douglas, L., Konopka, J. B., and Dean, N. (2010). Recognition of yeast by murine macrophages requires mannan but not glucan. *Eukaryot. Cell* 9, 1776–1787. doi: 10.1128/EC.00156-10

Kohatsu, L., Hsu, D. K., Jegalian, A. G., Liu, F. T., and Baum, L. G. (2006). Galectin-3 induces death of *Candida* species expressing specific beta-1,2-linked mannans. *J. Immunol.* 177, 4718–4726. doi: 10.4049/jimmunol.177.7.4718

Kraneveld, E. A., de Soet, J. J., Deng, D. M., Dekker, H. L., de Koster, C. G., Klis, F. M., et al. (2011). Identification and differential gene expression of adhesin-like wall proteins in *Candida glabrata* biofilms. *Mycopathologia* 172, 415–427. doi: 10.1007/s11046-011-9446-2

Kurtz, M. B., and Douglas, C. M. (1997). Lipopeptide inhibitors of fungal glucan synthase. *Med. Mycol.* 35, 79–86. doi: 10.1080/02681219780000961

Lee, K. K., Maccallum, D. M., Jacobsen, M. D., Walker, L. A., Odds, F. C., Gow, N. A., et al. (2012). Elevated cell wall chitin in *Candida albicans* confers echinocandin resistance *in vivo*. *Antimicrob. Agents Chemother.* 56, 208–217. doi: 10.1128/AAC.00683-11

Lenardon, M. D., Whitton, R. K., Munro, C. A., Marshall, D., and Gow, N. A. (2007). Individual chitin synthase enzymes synthesize microfibrils of differing structure at specific locations in the *Candida albicans* cell wall. *Mol. Microbiol.* 66, 1164–1173. doi: 10.1111/j.1365-2958.2007.05990.x

Lewis, L. E., Bain, J. M., Okai, B., Gow, N. A., and Erwig, L. P. (2013). Live-cell video microscopy of fungal pathogen phagocytosis. *J. Vis. Exp.* 2013:50196. doi: 10.3791/50196

Lin, J., Wester, M. J., Graus, M. S., Lidke, K. A., and Neumann, A. K. (2016). Nanoscopic cell-wall architecture of an immunogenic ligand in *Candida albicans* during antifungal drug treatment. *Mol. Biol. Cell* 27, 1002–1014. doi: 10.1091/mbc.E15-06-0355

Lowman, D. W., Greene, R. R., Bearden, D. W., Kruppa, M. D., Pottier, M., Monteiro, M. A., et al. (2014). Novel structural features in *Candida albicans* hyphal glucan provide a basis for differential innate immune recognition of hyphae versus yeast. *J. Biol. Chem.* 289, 3432–3443. doi: 10.1074/jbc.M113.529131

Marakalala, M. J., Vautier, S., Potrykus, J., Walker, L. A., Shepardson, K. M., Hopke, A., et al. (2013). Differential adaptation of *Candida albicans in vivo* modulates immune recognition by dectin-1. *PLoS Pathog.* 9:e1003315. doi: 10.1371/journal.ppat.1003315

Marti-Carrizosa, M., Sanchez-Reus, F., March, F., Canton, E., and Coll, P. (2015). Implication of *Candida parapsilosis FKS1* and *FKS2* mutations in reduced echinocandin susceptibility. *Antimicrob. Agents Chemother.* 59, 3570–3573. doi: 10.1128/AAC.04922-14

McGreal, E. P., Rosas, M., Brown, G. D., Zamze, S., Wong, S. Y., Gordon, S., et al. (2006). The carbohydrate-recognition domain of Dectin-2 is a C-type lectin with specificity for high mannose. *Glycobiology* 16, 422–430. doi: 10.1093/glycob/cwj077

Mora-Montes, H. M., Netea, M. G., Ferwerda, G., Lenardon, M. D., Brown, G. D., Mistry, A. R., et al. (2011). Recognition and blocking of innate immunity cells by *Candida albicans* chitin. *Infect. Immun.* 79, 1961–1970. doi: 10.1128/IAI.01282-10

Navarro-Arias, M. J., Hernandez-Chavez, M. J., Garcia-Carnero, L. C., Amezcua-Hernandez, D. G., Lozoya-Perez, N. E., Estrada-Mata, E., et al. (2019). Differential recognition of *Candida tropicalis*, *Candida guilliermondii*, *Candida krusei*, and *Candida auris* by human innate immune cells. *Infect. Drug Resist.* 12, 783–794. doi: 10.2147/IDR.S197531

Netea, M. G., Brown, G. D., Kullberg, B. J., and Gow, N. A. (2008). An integrated model of the recognition of *Candida albicans* by the innate immune system. *Nat. Rev.* 6, 67–78. doi: 10.1038/nrmicro1815

Netea, M. G., Gow, N. A., Munro, C. A., Bates, S., Collins, C., Ferwerda, G., et al. (2006). Immune sensing of *Candida albicans* requires cooperative recognition of mannans and glucans by lectin and Toll-like receptors. *J. Clin. Invest.* 116, 1642–1650. doi: 10.1172/JCI27114

Pardini, G., De Groot, P. W., Coste, A. T., Karababa, M., Klis, F. M., de Koster, C. G., et al. (2006). The *CRH* family coding for cell wall glycosylphosphatidylinositol proteins with a predicted transglycosidase domain affects cell wall organization and virulence of *Candida albicans*. *J. Biol. Chem.* 281, 40399–40411. doi: 10.1074/jbc.M606361200

Park, S., Kelly, R., Kahn, J. N., Robles, J., Hsu, M. J., Register, E., et al. (2005). Specific substitutions in the echinocandin target Fks1p account for reduced susceptibility of rare laboratory and clinical *Candida* sp. isolates. *Antimicrob. Agents Chemother.* 49, 3264–3273. doi: 10.1128/AAC.49.8.3264-3273.2005

Pfaller, M., Neofytos, D., Diekema, D., Azie, N., Meier-Kriesche, H. U., Quan, S. P., et al. (2012). Epidemiology and outcomes of candidemia in 3648 patients: data from the Prospective Antifungal Therapy [PATH Alliance(R)] registry, 2004-2008. *Diagn. Microbiol. Infect. Dis.* 74, 323–331. doi: 10.1016/j.diagmicrobio.2012.10.003

Pfaller, M. A., Messer, S. A., Woosley, L. N., Jones, R. N., and Castanheira, M. (2013). Echinocandin and triazole antifungal susceptibility profiles for clinical opportunistic yeast and mold isolates collected from 2010 to 2011: application of new CLSI clinical breakpoints and epidemiological cutoff

values for characterization of geographic. *J. Clin. Microbiol.* 51, 2571–2581. doi: 10.1128/JCM.00308-13

Pham, C. D., Iqbal, N., Bolden, C. B., Kuykendall, R. J., Harrison, L. H., Farley, M. M., et al. (2014). Role of *FKS* mutations in *Candida glabrata*: MIC values, echinocandin resistance, and multidrug resistance. *Antimicrob. Agents Chemother.* 58, 4690–4696. doi: 10.1128/AAC.03255-14

Plaine, A., Walker, L., Da Costa, G., Mora-Montes, H. M., McKinnon, A., Gow, N. A., et al. (2008). Functional analysis of *Candida albicans* GPI-anchored proteins: roles in cell wall integrity and caspofungin sensitivity. *Fungal Genet. Biol.* 45, 1404–1414. doi: 10.1016/j.fgb.2008.08.003

Porcaro, I., Vidal, M., Jouvert, S., Stahl, P. D., and Giaimis, J. (2003). Mannose receptor contribution to *Candida albicans* phagocytosis by murine E-clone J774 macrophages. *J. Leukoc. Biol.* 74, 206–215. doi: 10.1189/jlb.1202608

Sato, K., Yang, X. L., Yudate, T., Chung, J. S., Wu, J., Luby-Phelps, K., et al. (2006). Dectin-2 is a pattern recognition receptor for fungi that couples with the Fc receptor gamma chain to induce innate immune responses. *J. Biol. Chem.* 281, 38854–38866. doi: 10.1074/jbc.M606542200

Seider, K., Brunke, S., Schild, L., Jablonowski, N., Wilson, D., Majer, O., et al. (2011). The facultative intracellular pathogen *Candida glabrata* subverts macrophage cytokine production and phagolysosome maturation. *J. Immunol.* 187, 3072–3086. doi: 10.4049/jimmunol.1003730

Seider, K., Gerwien, F., Kasper, L., Allert, S., Brunke, S., Jablonowski, N., et al. (2014). Immune evasion, stress resistance, and efficient nutrient acquisition are crucial for intracellular survival of *Candida glabrata* within macrophages. *Eukaryot. Cell* 13, 170–183. doi: 10.1128/EC.00262-13

Skrzypek, M. S., Binkley, J., Binkley, G., Miyasato, S. R., Simison, M., and Sherlock, G. (2016). The *Candida* Genome Database (CGD): incorporation of Assembly 22, systematic identifiers and visualization of high throughput sequencing data. *Nucleic Acids Res.* 45, D592–D596. doi: 10.1093/nar/gkw924

Stahl, P. D., Rodman, J. S., Miller, M. J., and Schlesinger, P. H. (1978). Evidence for receptor-mediated binding of glycoproteins, glycoconjugates, and lysosomal glycosidases by alveolar macrophages. *Proc. Natl. Acad. Sci. U.S.A.* 75, 1399–1403. doi: 10.1073/pnas.75.3.1399

Sullivan, D. J., Westerneng, T. J., Haynes, K. A., Bennett, D. E., and Coleman, D. C. (1995). *Candida dubliniensis* sp. nov.: phenotypic and molecular characterization of a novel species associated with oral candidosis in HIV-infected individuals. *Microbiology* 141, 1507–1521. doi: 10.1099/13500872-141-7-1507

Taylor, P. R., Tsoni, S. V., Willment, J. A., Dennehy, K. M., Rosas, M., Findon, H., et al. (2007). Dectin-1 is required for beta-glucan recognition and control of fungal infection. *Nat. Immunol.* 8, 31–38. doi: 10.1038/ni1408

Thompson, A., Griffiths, J. S., Walker, L., da Fonseca, D. M., Lee, K. K., Taylor, P. R., et al. (2019). Dependence on Dectin-1 Varies With Multiple *Candida* Species. *Front. Microbiol.* 10:1800. doi: 10.3389/fmicb.2019.01800

Toth, A., Csonka, K., Jacobs, C., Vagvolgyi, C., Nosanchuk, J. D., Netea, M. G., et al. (2013). *Candida albicans* and *Candida parapsilosis* induce different T-cell responses in human peripheral blood mononuclear cells. *J. Infect. Dis.* 208, 690–698. doi: 10.1093/infdis/jit188

Wagener, J., Malireddi, R. K., Lenardon, M. D., Koberle, M., Vautier, S., MacCallum, D. M., et al. (2014). Fungal chitin dampens inflammation through IL-10 induction mediated by *NOD2* and *TLR9* activation. *PLoS Pathog.* 10:e1004050. doi: 10.1371/journal.ppat.1004050

Walker, C. A., Gomez, B. L., Mora-Montes, H. M., Mackenzie, K. S., Munro, C. A., Brown, A. J., et al. (2010). Melanin externalization in *Candida albicans* depends on cell wall chitin structures. *Eukaryot. Cell* 9, 1329–1342. doi: 10.1128/EC.00051-10

Walker, L. A., Gow, N. A., and Munro, C. A. (2013). Elevated chitin content reduces the susceptibility of *Candida* species to caspofungin. *Antimicrob. Agents Chemother.* 57, 146–154. doi: 10.1128/AAC.01486-12

Walker, L. A., Munro, C. A., de Bruijn, I., Lenardon, M. D., McKinnon, A., and Gow, N. A. (2008). Stimulation of chitin synthesis rescues *Candida albicans* from echinocandins. *PLoS Pathog.* 4:e1000040. doi: 10.1371/journal.ppat.1000040

Wheeler, R. T., and Fink, G. R. (2006). A drug-sensitive genetic network masks fungi from the immune system. *PLoS Pathog.* 2:e35. doi: 10.1371/journal.ppat.0020035

Wheeler, R. T., Kombe, D., Agarwala, S. D., and Fink, G. R. (2008). Dynamic, morphotype-specific *Candida albicans* beta-glucan exposure during infection and drug treatment. *PLoS Pathog.* 4:e1000227. doi: 10.1371/journal.ppat.1000227

Wileman, T. E., Lennartz, M. R., and Stahl, P. D. (1986). Identification of the macrophage mannose receptor as a 175-kDa membrane protein. *Proc. Natl. Acad. Sci. U.S.A.* 83, 2501–2505. doi: 10.1073/pnas.83.8.2501

Conflict of Interest: The authors declare that the research was conducted in the absence of any commercial or financial relationships that could be construed as a potential conflict of interest.

frontiers in Cellular and Infection Microbiology

REVIEW
published: 29 May 2020
doi: 10.3389/fcimb.2020.00229

Surfactant Protein D Recognizes Multiple Fungal Ligands: A Key Step to Initiate and Intensify the Anti-fungal Host Defense

Taruna Madan[1]* *and Uday Kishore*[2]

[1] Department of Innate Immunity, ICMR-National Institute for Research in Reproductive Health, Mumbai, India, [2] Biosciences, College of Health and Life Sciences, Brunel University London, Uxbridge, United Kingdom

OPEN ACCESS

Edited by:
Jagadeesh Bayry, Institut National de la Santé et de la Recherche Médicale (INSERM), France

Reviewed by:
Grith Lykke Sorensen, University of Southern Denmark, Denmark
Jiu-Yao Wang, National Cheng Kung University, Taiwan

***Correspondence:**
Taruna Madan
taruna_m@hotmail.com

Specialty section:
This article was submitted to Fungal Pathogenesis, a section of the journal Frontiers in Cellular and Infection Microbiology

Received: 27 January 2020
Accepted: 23 April 2020
Published: 29 May 2020

Citation:
Madan T and Kishore U (2020) Surfactant Protein D Recognizes Multiple Fungal Ligands: A Key Step to Initiate and Intensify the Anti-fungal Host Defense. Front. Cell. Infect. Microbiol. 10:229. doi: 10.3389/fcimb.2020.00229

With limited therapeutic options and associated severe adverse effects, fungal infections are a serious threat to human health. Innate immune response mediated by pattern recognition proteins is integral to host defense against fungi. A soluble pattern recognition protein, Surfactant protein D (SP-D), plays an important role in immune surveillance to detect and eliminate human pathogens. SP-D exerts its immunomodulatory activity via direct interaction with several receptors on the epithelial cells lining the mucosal tracts, as well as on innate and adaptive immune cells. Being a C-type lectin, SP-D shows calcium- and sugar-dependent interactions with several glycosylated ligands present on fungal cell walls. The interactome includes cell wall polysaccharides such as 1,3-β-D-glucan, 1,6-β-D-glucan, Galactosaminogalactan Galactomannan, Glucuronoxylomannan, Mannoprotein 1, and glycosylated proteins such as gp45, gp55, major surface glycoprotein complex (gpA). Recently, binding of a recombinant fragment of human SP-D to melanin on the dormant conidia of *Aspergillus fumigatus* was demonstrated that was not inhibited by sugars, suggesting a likely protein-protein interaction. Interactions of the ligands on the fungal spores with the oligomeric forms of full-length SP-D resulted in formation of spore-aggregates, increased uptake by phagocytes and rapid clearance besides a direct fungicidal effect against *C. albicans*. Exogenous administration of SP-D showed significant therapeutic potential in murine models of allergic and invasive mycoses. Altered susceptibility of SP-D gene-deficient mice to various fungal infections emphasized relevance of SP-D as an important sentinel of anti-fungal immunity. Levels of SP-D in the serum or lung lavage were significantly altered in the murine models and patients of fungal infections and allergies. Here, we review the cell wall ligands of clinically relevant fungal pathogens and allergens that are recognized by SP-D and their impact on the host defense. Elucidation of the molecular interactions between innate immune humoral such as SP-D and fungal pathogens would facilitate the development of novel therapeutic interventions.

Keywords: SP-D, fungi, cell wall, polysaccharides, glycoprotein, mycoses, allergy

INTRODUCTION

Fungal infections range from asymptomatic, mild mucocutaneous infections to potentially life-threatening systemic infections. With more than a billion people with mild infections, several millions mucosal candidiasis cases and 150 million people with serious fungal diseases, fungi have a huge impact on public health (Bongomin et al., 2017). Cells of the innate immune system (e.g., dendritic cells and macrophages) bind components of fungal cell walls using surface or soluble pattern recognition receptors (PRRs). The C-type lectin receptors and the Toll-like receptors are particularly involved in anti-fungal immunity (Salazar and Brown, 2018). Surfactant protein D (SP-D), a soluble C-type lectin, recognizes several fungal ligands and inhibits their interactions with target host cells (Pandit et al., 2012; Carreto-Binaghi et al., 2016). Importantly, SP-D can activate or inhibit the pro-inflammatory signaling in the target cells via a range of activating or inhibitory receptors (Kishore et al., 2006).

Surfactant Protein D, a Soluble Collectin

The human SP-D gene is located proximal to the centromere of chromosome 10 in humans and Chromosome 14 in mouse. The primary structure of the SP-D protein comprises of four distinct regions: an N-terminal non-collagenous domain, a triple-helical collagenous region, an α-helical coiled-coil neck region, and the C-terminal carbohydrate recognition domain (CRD) (Kishore et al., 2005). This primary structural organization exists as a trimeric subunit, which can form further oligomeric units up to dodecamers. It is quite usual to visualize, under electron microscopy, fuzzy balls of SP-D proteins in lung washings.

SP-D is produced by different cell types, including type II pneumocytes, non-ciliated bronchiolar cells, submucosal gland and epithelial cells of trachea in the lung. Other sources include ductal epithelial cells in the lacrimal apparatus, mucosal and glandular/ductal epithelial cells in the gastrointestinal tract, skin, male and female genitourinary tracts (Kishore et al., 2005). Vascular endothelial cells in the heart and brain tissues also synthesize significant levels of SP-D (Sorensen et al., 2006; Schob et al., 2013). SP-D expression is considerably increased in a human corneal cell line challenged with *A. fumigatus* via TLR4 signaling, and corneal tissue of rats challenged with *Fusarium solani* (Che et al., 2012a,b; Wu et al., 2015). Such a widespread existence of SP-D in various tissues and fluids and its increased expression in response to fungal pathogens emphasizes its importance as an innate immune surveillance molecule at the mucosal barriers.

SP-D mediates immune regulation by direct interaction with multiple receptors on immune and epithelial cells, leading to altered cytokine and free radical production (Jakel et al., 2013; Sorensen, 2018) (**Table 1**). SP-D stimulates antigen presentation by dendritic cells but inhibits T cell proliferation. SP-D via its collagen domain, binds calreticulin/CD91 receptor complex and activates macrophages. The globular CRD domain promotes an anti-inflammatory effect through a signal inhibitory regulatory protein α (SIRPα) on macrophages (Gardai et al., 2003). Various immunomodulatory mechanisms mediated by SP-D that strengthen host defense against fungi are summarized in **Figure 1**.

Being a calcium-dependent lectin, SP-D binds maltose, glucose, mannose, fucose, galactose, lactose, glucosamine, and N-acetylglucosamine, and to complex carbohydrates on the surface of fungal pathogens (Pandit et al., 2012). The binding of SP-D to a variety of opportunistic fungi results in the direct inhibition of fungal growth, aggregation and enhanced phagocytosis (Pandit et al., 2012). Importantly, the downstream immune response elicited by SP-D also contributes to the reduction/elimination of fungal infection in mice (Pandit et al., 2012).

Here, we review the cell wall ligands of clinically relevant fungal pathogens and allergens that are recognized by SP-D and their impact on the host defense (**Table 2**). Elucidation of the interactions between SP-D and fungal ligands could lead to the development of novel therapeutic interventions for both allergic and invasive mycoses. We also provide an update on the cellular receptors of SP-D involved in immunomodulation, serum and BAL levels of SP-D, polymorphisms of SP-D, oligomeric forms of SP-D, proteolytic degradation of SP-D and a possible road map to pursue clinical applications of SP-D.

SP-D RECOGNIZES AND STRENGTHENS HOST DEFENSE AGAINST *Aspergillus fumigatus*

Aspergillus fumigatus is a prominent fungal pathogen in immunocompromised individuals, and can cause invasive aspergillosis. In the immunocompetent host, it causes allergic disorders such as allergic rhinitis, allergic sinusitis, hypersensitivity pneumonitis, and allergic bronchopulmonary Aspergillosis (ABPA).

With a series of *in vitro* and *in vivo* studies, we established that SP-D was relevant in host defense against *A. fumigatus* (Madan et al., 2005a). SP-D bound and agglutinated *A. fumigatus* conidia in a calcium-dependent manner, and enhanced uptake of opsonized conidia by the alveolar macrophages and neutrophils (Madan et al., 1997a). Rat SP-D bound the *A. fumigatus* conidia via CRD; EDTA, mannose, glucose, maltose, and inositol inhibited the binding (Allen et al., 2001). Human SP-D binding to conidia was unaffected by hydrophobic surfactant components. However, SP-D did not increase the association of conidia with rat alveolar macrophages. SP-D-enriched rat BAL fluid inhibited spore binding to extracellular matrix (ECM) proteins and epithelial cells (Yang et al., 2000). Pre-incubation of ECM proteins and epithelial cells with SP-D-enriched BAL fluid prevented the enhancement of spore binding induced by *A. fumigatus* spore diffusate. SP-D localized to *A. fumigatus* surface and stayed bound through the different stages of infection of Calu-3 cells (a human airway epithelial cell line) grown on an air-liquid interface (Ordonez et al., 2019). Importantly, fungal adhesion to the epithelium decreased and fungal clearance by neutrophils increased in the presence of SP-D. Human monocyte-derived macrophages phagocytosed SP-D opsonized dormant conidia more efficiently and upregulated the secretion of pro-inflammatory cytokines (Wong et al., 2018). In a

TABLE 1 | Various cellular receptors that interact with SP-D.

Cell type	Cellular receptors	Function	References
Myeloid cells and soluble form in serum	Cluster of differentiation 14 (CD14)	Inhibition of CD14 interaction with LPS	Sano et al., 2000
Alveolar macrophages, monocyte-derived dendritic cells	CD14/TLR	Inhibition of der p (mite allergen)-induced activation	Liu et al., 2010
Alveolar macrophages	Toll-like receptor 4 (TLR4), MD-2, TLR-2	Inhibition of TLR-2, TLR4 and MD-2 interaction with LPS	Ohya et al., 2006; Nie et al., 2008; Yamazoe et al., 2008
Alveolar macrophages, monocyte-derived macrophages	Signal-regulatory protein-α (SIRP-α)/calreticulin/CD91	SIRP-α interaction with CRD prevents nuclear factor-κB activation, and secretion of inflammatory cytokines Collagen domain interaction with calreticulin/CD91 promotes secretion of inflammatory cytokines	Gardai et al., 2003
Neutrophils	Leukocyte-associated immunoglobulin-like receptor 1 (LAIR-1)	Collagen domain interaction leads to reduction of reactive oxygen species signaling	Olde Nordkamp et al., 2014
Alveolar macrophages	Osteoclast-associated receptor (OSCAR)	Collagen domain interaction results in pro-inflammatory response	Barrow et al., 2015
Eosinophils	Fc receptor γII (FcγRII/CD32)	Inhibitory effect on IgG and serum-triggered eosinophilic cationic protein degranulation by eosinophils	von Bredow et al., 2006
NK cells	NKp46	Secretion of IFN-g and lymph node homing of DCs	Ge et al., 2016
Type II pneumocytes	G Protein-coupled receptor 116 (GPR116)	Regulation of lung surfactant levels	Fukuzawa et al., 2013
Bladder epithelial cells	Uroplakin Ia	Inhibits the adherence and cytotoxicity of uropathogenic *E. coli*	Kurimura et al., 2012
Lung adenocarcinoma epithelial cells	Epidermal growth factor receptor (EGFR)	Suppressing EGF signaling and inhibiting the proliferation and migration	Hasegawa et al., 2015
Dendritic cells and soluble DC-SIGN	DC-SIGN	Reduces HIV-1 capture and transfer to CD4+ T cells	Dodagatta-Marri et al., 2017

murine model of immunocompromised pulmonary invasive aspergillosis, intranasal SP-D treatment rescued mice from death, concomitant with enhanced local production of protective Th1 cytokines, TNF-α and IFN-γ, and that of protective C-C chemokine, MIP-1α (Singh et al., 2009). Immunosuppressed SP-D gene-deficient mice showed an early death upon conidial challenge, a higher hyphal density and tissue injury in lungs. Treatment with SP-D, or a recombinant fragment of human SP-D composed of trimeric neck and CRD regions (rfhSP-D), reduced the mortality, concomitant with higher IFN-γ to IL-4 ratios in treated SP-D gene-deficient mice (Madan et al., 2010). SP-D gene-deficient immunocompetent mice displayed significantly reduced pro-inflammatory cytokines in the lung upon intranasal challenge with wild-type conidia or melanin ghosts (i.e., hollow melanin spheres) (Wong et al., 2018).

In mice mimicking human ABPA, intranasal treatment with native SP-D (or rfhSP-D) suppressed *A. fumigatus* allergen-specific IgE levels, eosinophilia, pulmonary cellular infiltration and switched the cytokine profile from a pathogenic Th2 to a protective Th1 (Madan et al., 2001). The exogenous SP-D reduced allergen-induced early airway response, bronchial hyper-responsiveness, blood eosinophilia, and Th2 cytokines in murine models of *A. fumigatus* induced allergic asthma possibly by reducing eotaxin levels in the lung (Erpenbeck et al., 2006). SP-D treatment reduced the allergen-induced histamine release from peripheral blood cells. A 9-fold increase in SP-D protein levels with no concomitant changes in SP-D mRNA was observed in the BALB/c mice sensitized intraperitoneally and challenged intranasally with *A. fumigatus* allergenic extract (Haczku et al., 2001). C57BL/6 mice have attenuated *A. fumigatus*-induced allergic airway hyper-responsiveness (AHR) when compared with Balb/c mice owing to a markedly increased SP-D protein expression (Atochina et al., 2003). SP-D gene-deficient mice exhibited intrinsic hypereosinophilia and several-fold increase in levels of IL-5 and IL-13, and lower of IFN-γ to IL-4 ratio in the lungs, suggesting a Th2 bias of immune response (Madan et al., 2005b). SP-D gene-deficient mice were more susceptible than wild-type mice to pulmonary hypersensitivity induced by *A. fumigatus* allergens. Intranasal treatment with SP-D or rfhSP-D was effective in rescuing the *A. fumigatus*-sensitized SP-D gene-deficient mice (Madan et al., 2005b).

SP-D Interactome on *Aspergillus fumigatus*: Involvement of Both CRD and Collagen Domains

Purified human SP-D bound to the allergens present in the 3-week culture filtrate of *A. fumigatus* as well as purified allergens, gp55 and gp45, in a carbohydrate and calcium-dependent manner but not to the deglycosylated forms of these allergens (Madan et al., 1997b). SP-D inhibited binding of the glycosylated allergens to specific IgE antibodies and induction of histamine release from sensitized basophils. The calcium-activated protein phosphatase, calcineurin, which regulates production of several

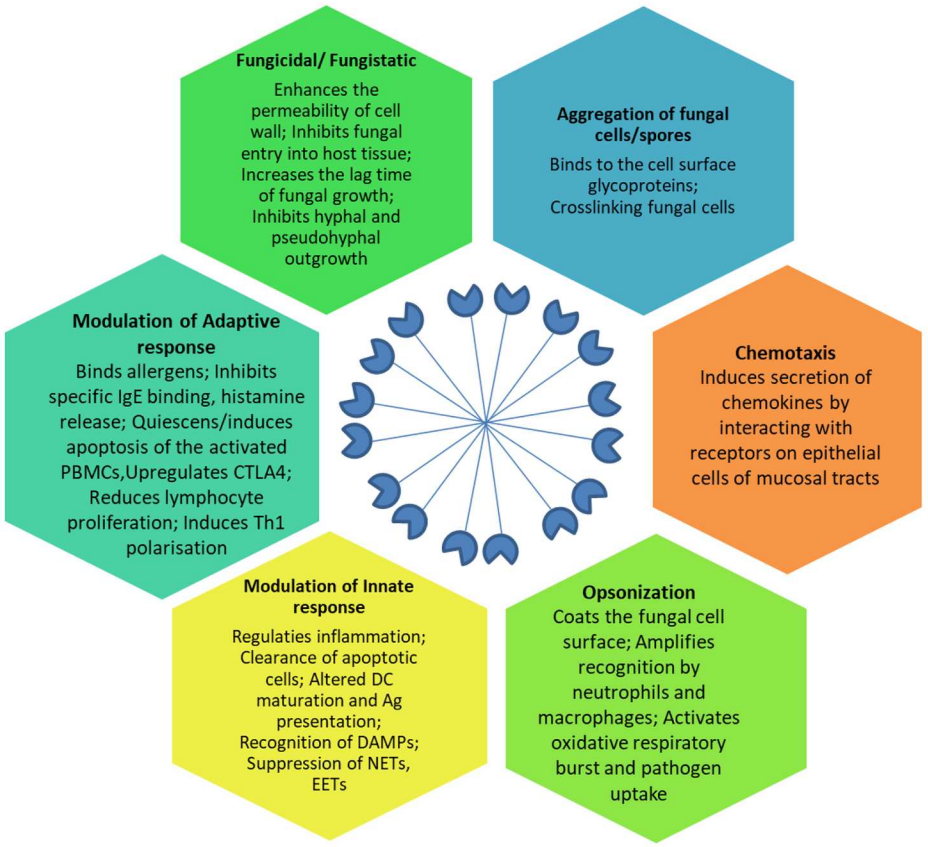

FIGURE 1 | Effector anti-fungal mechanisms mediated by SP-D. The cartoon in the center of the figure depicts the fuzzy ball structure of SP-D formed from several dodecameric structural units. Ag, Antigen; CTLA-4, Cytotoxic T-lymphocyte Associated protein 4; DAMPs, Damage Associated Molecular Patterns; DC, Dendritic cells; EETs, Eosinophil Extracellular Traps; IgE, Immunoglobulin E antibodies; NETs, Neutrophil Extracellular Traps; PBMCs, Peripheral Blood Mononuclear Cells; Th1, T helper 1 lymphocytes.

cell wall molecules, such as 1, 3-β-D-glucan, seems to be a critical factor for SP-D binding to *A. fumigatus* hyphae (Geunes-Boyer et al., 2010). Calcineurin-deficient hyphae [generated via either deletion of the catalytic subunit calcineurin A (Delta cna A) or pharmacologic inhibition by FK506] were not recognized by SP-D. In presence of Caspofungin (which inhibits 1,3-β-D-glucan synthesis) and nikkomycin Z (which inhibits chitin synthesis), SP-D binding to the wild-type strain was enhanced. These observations suggested presence of multiple SP-D ligands, leaving little room for *Aspergillus* to escape immune surveillance mediated by SP-D.

To unravel the SP-D ligands present on dormant conidia, the first pathogen entity that enters the host, various conidial cell wall components were purified and examined for their interaction with SP-D via ELISA (Wong et al., 2018). SP-D significantly bound to melanin pigment (polymer of 1,8-dihydroxynaphthalene), a virulent factor that contributes to immune suppression of the host. Germinating conidia, which lacks in melanin layer, bound to SP-D via two cell-wall polysaccharides, galactomannan (GM) and galactosaminogalactan (GAG). As per the localization of melanin, GM and GAG on the conidial surface, SP-D binding was punctate on the dormant conidia, while it was uniform on germinating conidia. SP-D interacted with melanin via its collagen domain whereas its CRD region was involved in binding to GM and GAG.

SP-D BINDS 1, 3 β-GLUCAN ON *Blastomyces dermatitidis* AND INHIBITS TNF-α PRODUCTION

Inhaled spores of *Blastomyces dermatitidis* may cause flu-like symptoms, leading to blastomycosis, an invasive and often serious fungal infection in immunocompromised patients. Bronchoalveolar lavage fluid (BALF)-treated *B. dermatitidis* showed presence of bound-SP-D that was significantly reduced in the presence of 1,3-β-Glucan, a cell wall component of *B. dermatitidis* spores. BALF as well as purified SP-D-supplemented SP-D$^{-/-}$ BALF reduced the TNF-α level from β-Glucan-stimulated murine alveolar macrophages. BALF, pre-incubated with *B. dermatitidis* or β-Glucan, lost the ability to inhibit TNF-α production (Lekkala et al., 2006).

TABLE 2 | Ligands of Various Fungi that Interact with SP-D.

Fungi	Fungal ligands recognized by SP-D	Source
Aspergillus fumigatus	Glycosylated allergen gp45	3 week culture filtrate
	Glycosylated allergen gp55	3 week culture filtrate
	1,3-β-D-Glucan	Germinating conidia, mycelia
	Melanin (on dormant conidia)	Dormant conidia
	Galactoseaminogalactan (GAG)	Germinating conidia, mycelia
	Galactomannan (GM)	Germinating conidia, mycelia
Blastomyces dermatitidis	1,3-β-D-Glucan	Cell wall component of spores
Cryptococcus neoformans	Glucuronoxylomannan	Capsule
	Mannoprotein 1	Capsule
Pneumocystis carinii	Major surface glycoprotein complex	Cyst and trophozoite
	1,3-β-D-Glucan	Cyst
Coccidiodes posadasii	Culture filtrate antigen	Culture filtrate
Saccharomyces cerevisiae	Mannoprotein	External cell wall
	1,6-β-D-Glucan	Yeast cell wall

SP-D DIRECTLY INHIBITS THE GROWTH OF *Candida albicans* AND ITS ADHERENCE TO THE MUCOSAL EPITHELIAL CELLS

Candida albicans colonizes the mucosal surfaces of humans and is a common member of the human gut and vaginal flora. Immunocompromised individuals develop fatal candidiasis. SP-D bound and agglutinated *C. albicans* (yeast form) in a calcium-dependent manner; this interaction was inhibited by competing sugars such as maltose or mannose. Importantly, incubation with SP-D had a fungicidal effect on *C. albicans*. However, SP-D inhibited phagocytosis of *C. albicans* by alveolar macrophages (van Rozendaal et al., 2000). SP-D strongly bound to *C. albicans* infecting Calu-3 cells grown on an air-liquid interface. Binding with SP-D interfered with adhesion of *Candida* to the epithelium and enhanced neutrophil mediated clearance of opsonized *Candida* (Ordonez et al., 2019). Thus, SP-D seems to facilitate *C. albicans* clearance by making the pathogen readily available for neutrophils away from macrophages and epithelial cells.

SP-D BINDS TO CULTURE FILTRATE ANTIGENS OF *Coccidioides posadasii*

Coccidioidomycosis is a fungal disease caused by highly virulent, soil-fungus *Coccidioides immitis* or *C. posadasiie*. Inhalation of air-borne arthroconidia leads to initiation of the primary infection. Clinical manifestations include a severe fatal mycosis involving extra-pulmonary tissues. SP-D binds to coccidiodal culture filtrate antigens. Lungs of mice infected intranasally with a lethal dose of *C. posadasii* had significantly reduced levels of SP-D (Awasthi et al., 2004).

SP-D RECOGNIZES GLUCURONOXYLOMANNAN AND MANNOPROTEIN 1 OF *Cryptococcus neoformans* CAPSULE

Cryptococcus neoformans causes infection as a primary human pathogen, or may cause invasive cryptococcosis as an opportunistic pathogen invading the immunocompromised hosts including AIDS patients. Inhalation of acapsular, or sparsely encapsulated cells of *C. neoformans* leads to development of infection with capsule as the chief virulence factor.

SP-D bound and agglutinated acapsular *C. neoformans*, but not the encapsulated form, in a calcium- and sugar-dependent manner (Schelenz et al., 1995). Another study reported that SP-D bound acapsular form with a higher affinity than the encapsulated cryptococci leading to their aggregation (van de Wetering et al., 2004). The cryptococcal capsular components, glucuronoxylomannan (GXM) and mannoprotein 1 (MP1), were identified as SP-D ligands; secreted GXM inhibited SP-D-mediated aggregation of acapsular *C. neoformans*.

SP-D binds and protects *C. neoformans* cells against macrophage-mediated defense mechanisms *in vitro* and *in vivo* (Geunes-Boyer et al., 2009). SP-D binding to *C. neoformans* was calcineurin-independent (Geunes-Boyer et al., 2010). SP-D-deficient mice infected with *C. neoformans* showed reduced eosinophil infiltration, IL-5, fungal burden, and increased survival than wild type control animals (Geunes-Boyer et al., 2012; Holmer et al., 2014). The evidence provided by murine models of fungal infections treated with exogenous native or recombinant human SP-D is direct and reliable. SP-D gene-deficient mice develop increased pulmonary inflammation, emphysema, and surfactant phospholipid accumulations (Botas et al., 1998; Korfhagen et al., 1998; Ikegami et al., 2000, 2005; Wert et al., 2000; Fisher et al., 2002). Further, there is a significant increase in activated lymphocytes, apoptotic alveolar macrophages as well as enlarged, lipid-laden, macrophages that release metalloproteinases and reactive oxygen species (Botas et al., 1998; Korfhagen et al., 1998; Ikegami et al., 2000, 2005; Wert et al., 2000; Fisher et al., 2002). Importantly, oxygen radical release and production of the pro-inflammatory mediators, TNF-α, IL-1, and IL-6, were increased in response to either viral or bacterial pathogens (LeVine et al., 2000, 2001, 2004). These coexisting pulmonary abnormalities of SP-D gene deficient mice complicate the interpretation of challenge models. For example, lymphocyte and macrophage activation along with the increased pro-inflammatory mediators might enhance killing and offset

any increase of pathogen survival that results more directly from SP-D deficiency.

SP-D MEDIATED DIRECT KILLING OF *Histoplasma capsulatum*

Histoplasma capsulatum is an intracellular fungal pathogen that causes a self-limiting flu-like illness, and sometimes, a more serious pneumonitis or a chronic cavitary pulmonary infection. In immunosuppressed patients, the fungus can act as an opportunistic pathogen causing a progressive, disseminated disease. Though the ligand on the fungus is not known, exposure to SP-D resulted in increased *H. capsulatum* permeability in a dose-dependent manner, and hence, decrease in viability. However, SP-D did not aggregate *H. capsulatum*, or inhibit the phagocytosis of *H. capsulatum* and growth of macrophage-internalized *H. capsulatum* (McCormack et al., 2003).

SP-D BINDS AND AGGREGATES *Pneumocystis carinii* VIA MAJOR SURFACE GLYCOPROTEIN COMPLEX AND β-GLUCANS

A 3-fold increase in the total alveolar SP-D protein content was observed in the pulmonary fluid samples from *Pneumocystis*-infected humans and rats (Aliouat et al., 1998; Qu et al., 2001). SP-D bound to *P. carinii* via glucose-, mannose-, and N-acetyl-glucosamine-rich major surface glycoprotein complex (gpA), and augmented the adherence of the organisms to alveolar macrophages (O'Riordan et al., 1995). The binding was calcium-dependent and competitively inhibited by maltose > glucose > mannose > N-acetyl-glucosamine, with a higher affinity toward oligomeric forms of SP-D (Vuk-Pavlovic et al., 2001). Maximal SP-D binding was at pH 7.4, with significant inhibition at pH 4. Though SP-D induced aggregation, the phagocytosis of *P. carinii* was not enhanced. SP-D also bound to fungal β-glucans present on Pneumocystis' cystic forms, which are potent stimulators of TNF-α release (Vuk-Pavlovic et al., 1998).

Vuk-Pavlovic et al. generated human SP-D overexpressing transgenic mice that produced approximately 30-50-fold higher level of SP-D and noted that the mice did not had any significant differences in lung morphology and function (Vuk-Pavlovic et al., 2006). These mice were then depleted of $CD4^+$ lymphocytes, before and during the *Pneumocystis murina* challenge. SP-D-overexpressing mice exhibited significantly higher fungal burden, with increased levels of TNF-α and macrophage inflammatory protein-2 as well as increased lymphocyte and eosinophil infiltration in BAL on 10 and 14th week (Allen et al., 2001). Though the study inferred increased levels of SP-D led to formation of higher aggregates of *Pneumocystis*, basal levels of other pattern recognition proteins or immunoregulatory molecules were not examined in the SP-D overexpressing mice.

SP-D BINDS MANNOPROTEIN AND 1,6-β-D-GLUCAN, TWO CELL WALL COMPONENTS OF *Saccharomyces cerevisiae*

S. cerevisiae, an opportunistic pathogen, causes severe infections such as fungemia, endocarditis, pneumonia, peritonitis, urinary tract infections, skin infections, and esophagitis in patients with chronic disease, cancer, and immunosuppression. SP-D bound and aggregated *Saccharomyces cerevisiae* cells and isolated cell walls. Cell wall mannoprotein and 1,6-β-D-glucan of yeast were SP-D ligands but SP-D failed to aggregate chitin. Pustulan [a 1,6-β-linked glucose homopolymer] inhibited SP-D binding to yeast as well as to *A. fumigatus*. $F4/80^+$ cells, isolated from the BAL of SP-D gene-deficient mice, internalized considerably less zymosan particles (a glucan with repeating glucose units connected by β-1,3-glycosidic linkages) than $F4/80^+$ WT cells (Allen et al., 2001).

SP-D REVERSED THE PULMONARY NEUTROPHILIC INFILTRATION AND TNF-α LEVELS INDUCED IN 1,3-β-GLUCAN-MODULATED ALLERGIC INFLAMMATION

As mentioned above, 1,3-β-glucan is an important fungal ligand recognized by SP-D. Sensitization with 1,3-β-Glucan induced pulmonary neutrophilic infiltration and increased TNF-α level in the BAL of SP-D gene-deficient mice (Fakih et al., 2015). This infiltration was significantly reversed by treatment with rfhSP-D. Thus, a high-dose of SP-D could potentially offer protection against mold-induced exacerbations of allergic asthma.

COMPETITIVE INTERACTION OF SP-D WITH OTHER PRRs FOR THE COMMON FUNGAL LIGANDS

Other PRRs such as Dectins, Surfactant Protein-A (SP-A), Mannan-Binding Lectin (MBL), Mannose Receptor (MR), Macrophage inducible calcium dependent lectin receptor (Mincle), Macrophage C-type Lectin (MCL), Complement receptor 3 (CR3), Dendritic Cell-Specific Intercellular adhesion molecule-3-Grabbing Non-integrin (DC-SIGN), Langerin, and melanin-sensing C-type lectin receptor (MelLec) bind to common fungal ligands as SP-D (Goyal et al., 2018). Another complexity in the anti-fungal host defense is brought in by the fact that SP-D binds to other PRRs such as SP-A (Kuroki et al., 1991), TLR-2, TLR-4 (Ohya et al., 2006) and DC-SIGN (Dodagatta-Marri et al., 2017). These complex interactions need further investigation in pre-clinical studies to realize the true translation potential of PRRs.

IMPACT OF SP-D GENETIC POLYMORPHISMS AND PROPORTION OF OLIGOMERIC FORMS

Genetic polymorphisms of SP-D have been shown to be associated with an increased susceptibility to infections. Allelic variations can influence the quantity and multimerisation of SP-D produced in the serum with differential effects on its binding properties. Individuals with the Thr/Thr (Che et al., 2012b)-encoding genotype had significantly lower SP-D serum levels with predominantly the monomeric form of SP-D than individuals with the Met/Met (Che et al., 2012b) genotype with higher oligomeric forms (Leth-Larsen et al., 2005). However, there has been no study correlating SP-D polymorphisms with susceptibility to fungal infections.

SP-D LEVELS IN FUNGAL ALLERGY AND INFECTIONS

Serum levels of SP-D are altered in asthma, lung hypersensitivity and pulmonary infection caused by *P. carinii* during AIDS. Median SP-D in BAL was significantly decreased in the lung bacterial infection (12.17 ng/ml) compared with the control group (641 ng/ml), and was below assay limits for the majority of cystic fibrosis children (Postle et al., 1999). In asthmatics and allergics, SP-D levels increased in BAL and serum that went down following corticosteroid therapy (Cheng et al., 2000; Koopmans et al., 2004).

P. carinii pneumonia is associated with raised levels of alveolar SP-D, probably as a result of increased expression and accumulation. The synthesis and secretion of SP-D increased with acute injury and epithelial activation (Atochina et al., 2001).

SP-D levels have not been determined for other fungal infections. SP-D serum levels may be a useful and non-invasive diagnostic tool for fungal infections. The successive monitoring of serum levels of SP-A and/or SPD may predict disease activity, although it is presently unclear if these alterations are a cause or consequence of the disease.

PREDISPOSITION OF TYPE-2 DIABETES TO FUNGAL INFECTIONS AND SERUM SP-D LEVELS

Patients with type-2 diabetes (T2D) exhibited higher serum SP-D concentrations than control subjects (P = 0.006) (López-Cano et al., 2017). There was an inverse association between forced expiratory volume in 1 s (FEV1) and serum SP-D ($r = -0.265$; $P = 0.029$), as well as a significant positive relationship between SP-D concentration and residual volume ($r = 0.293$; $P = 0.043$). Endurance exercise training with improvement in aerobic fitness induced a significant reduction in serum SP-D levels in obese women with T2D (Rezaei et al., 2017). Significantly increased leukocyte SFTPD mRNA levels were observed in hyperglycemic gestational diabetes mellitus (GDM) patients ($P < 0.05$) with a significant positive association with C-reactive protein (Wojcik et al., 2016). Additionally, transcript level of SFTPD also correlated positively with fasting glycemia and insulin resistance. These reports suggest that serum levels of SP-D are increased in T2D patients in response to the increased systemic inflammation and get reduced by endurance exercise. However, none of the studies have evaluated the proportion of various oligomeric forms and functional competence of the serum SP-D for host defense in T2D patients. Importantly, T2D obese patients having respiratory tract infections had lower serum SP-D levels than those who did not have infections ($p = 0.01$) (Jawed et al., 2015). It is likely that in the presence of a respiratory infection, SP-D from the serum moved to the lungs to fight off the pathogen. There are no reports on the association of SP-D levels with respiratory or non-respiratory fungal infections in T2D patients.

PROTEOLYTIC DEGRADATION OF SP-D

SP-D levels and proportion of oligomeric forms could be significantly altered by proteolytic degradation. Mildly acidic pH, as might be found in endocytic compartments, may disrupt the lectin-dependent activities of SP-D (Persson et al., 1990). Importantly, SP-D was highly resistant to degradation by a wide variety of neutral proteases *in vitro*, and degradation products have not yet been shown to accumulate under pathological conditions *in vivo* (Brown-Augsburger et al., 1996). Dodecamers of recombinant rat SP-D were not degraded by human leukocyte elastase (HLE) (1 μM) or a variety of secreted mammalian neutral proteases at 37°C in the presence of physiologic calcium concentrations (Crouch, 2000). In the absence of calcium, multimeric SP-D was partially digested by 1,000-fold higher molar concentrations of HLE (50 μM) in a dose- and time-dependent manner with complete digestion happening in 24 h (Griese et al., 2003). Functional studies showed that digested SP-D had lost its calcium-dependent lectin properties, i.e., it neither bound to mannose nor agglutinated bacteria. These studies demonstrate that elastase results in the limited proteolysis of SP-D with loss of its CRD-dependent activities. HLE is present up to 19 U/ml in BAL in patients with cystic fibrosis. Results in patients with CF and high elastase activity in the BAL fluid indicated decreased SP-D in some, but not in all subjects (Griese et al., 2003). In contrast, lung diseases without significant neutrophilic inflammation in BAL fluid are not expected to exhibit degraded SP-D. This observed resistance of native SP-D to proteolytic damage might lead to enhancement of host defense functions on exogenous intranasal administration as validated by the murine model studies (Madan et al., 2001, 2005b, 2010; Singh et al., 2009). Incubation of cell-free BAL fluid with protease IV of *P. aeruginosa* resulted in degradation of SP-D in a time- and dose-dependent fashion; this degradation was inhibited by the trypsin-like serine protease inhibitor N-α-p-tosyl-L-lysine-chloromethyl ketone (TLCK) (Malloy et al., 2005). Degradation by protease IV led to inhibition of SP-D-mediated bacterial aggregation and uptake by macrophages.

PERSPECTIVES

Interaction of SP-D with several fungal pathogens has been established beyond doubt. SP-D binds multiple ligands of several fungi and modulates the immune response of the host geared mostly toward elimination of the pathogen, and alleviation of fungal allergies. Although the studies are limited mostly to respiratory fungal pathogens, with the presence of SP-D in digestive tract mucosa, reproductive tract mucosa, and most importantly skin, it is quite likely that SP-D may impact other fungal infections too.

Functionally competent purified recombinant forms of full length and truncated human SP-D have been evaluated extensively using *in vitro*, *in vivo,* and *ex vivo* systems, and are available in adequate amounts for therapeutic intervention (Madan et al., 2005a; Mahajan et al., 2013). Intranasal delivery of recombinant SP-D proteins via nebulisers or inhalers would provide the fastest delivery to the site of action, maximal efficacy up to distal airways and half-life (bypassing the proteolytic degradation by other routes of delivery) as evident from the animal model studies (Madan et al., 2001, 2005b, 2010; Singh et al., 2009). rfhSP-D would significantly and immediately reduce the pathogen load as well as restore the immune homeostasis in both allergic and invasive mycoses. In view of the serious adverse effects of available anti-fungal drugs, and a significant therapeutic efficacy and safety of rfhSP-D reported in murine models of allergic and invasive aspergillosis, rfhSP-D as an adjunct therapy may be a more effective option. However, there are no studies yet that have evaluated rfhSP-D in conjunction with standard therapies such as Amphotericin B/azoles for invasive pulmonary aspergillosis and corticosteroids for allergic pulmonary aspergillosis. Insight into the molecular mechanisms and reproducibility of the preclinical proof-of-concept therapeutic efficacy of rfhSP-D in animal models of fungal infections, strengthen the case for pursuing clinical trials of inhalation formulations of rfhSP-D.

It is important to recognize that there are additional biological functions of SP-D that have been demonstrated already for other diseases. These include: (i) assisting elimination of several viral and bacterial pathogens (Kishore et al., 2005); (ii) enhanced apoptosis of cancer cells (Mahajan et al., 2013) and activated T lymphocytes (Pandit et al., 2016); (iii) attenuation of sepsis-induced pancreatic injury (Liu et al., 2015); (iv) dual role in vascular inflammation and pro-inflammatory disease (Colmorten et al., 2019); and (v) regulation of energy intake and inhibitor of metabolic endotoxemia (Stidsen et al., 2012). This is in addition to its recently discovered involvement in male and female fertility (Kay and Madan, 2016; Rokade et al., 2017). Therefore, it is pertinent to consider that clinical application of SP-D may impact upon more than one facet of health.

AUTHOR CONTRIBUTIONS

TM wrote the first draft of the review. UK provided critical suggestions for the manuscript.

ACKNOWLEDGMENTS

The authors dedicate this article to Dr. Puranam Usha Sarma who mentored their initial research in the area of fungal immunology. TM would like to thank ICMR-National Institute for Research in Reproductive Health, Mumbai for the financial support. Editorial help by Dr Sanjeev Kumar Gupta is gratefully appreciated.

REFERENCES

Aliouat, E. M., Escamilla, R., Cariven, C., Vieu, C., Mullet, C., Dei-Cas, E., et al. (1998). Surfactant changes during experimental pneumocystosis are related to Pneumocystis development. *Eur. Respir. J*. 11, 542–547.

Allen, M. J., Voelker, D. R., and Mason, R. J. (2001). Interactions of surfactant proteins A and D with *Saccharomyces Cerevisiae* and *Aspergillus Fumigatus*. *Infect. Immun*. 69, 2037–2044. doi: 10.1128/IAI.69.4.2037-2044.2001

Atochina, E. N., Beck, J. M., Scanlon, S. T., Preston, A. M., and Beers, M. F. (2001). Pneumocystis carinii pneumonia alters expression and distribution of lung collectins SP-A and SP-D. *J. Lab Clin. Med*. 137, 429–439. doi: 10.1067/mlc.2001.115220

Atochina, E. N., Beers, M. F., Tomer, Y., Scanlon, S. T., Russo, S. J., Panettieri, R. A. Jr, et al. (2003). Attenuated allergic airway hyperresponsiveness in C57BL/6 mice is associated with enhanced surfactant protein (SP)-D production following allergic sensitization. *Respir. Res*. 4, 15. doi: 10.1186/1465-9921-4-15

Awasthi, S., Magee, D. M., and Coalson, J. J. (2004). *Coccidioides Posadasii* infection alters the expression of pulmonary surfactant proteins (SP)-A and SP-D. *Respir. Res*. 5:28. doi: 10.1186/1465-9921-5-28

Barrow, A. D., Palarasah, Y., Bugatti, M., Holehouse, A. S., Byers, D. E., Holtzman, M. J., et al. (2015). OSCAR is a receptor for surfactant protein D that activates TNF-alpha release from human CCR2+ inflammatory monocytes. *J. Immunol*. 194, 3317–3326. doi: 10.4049/jimmunol.1402289

Bongomin, F., Gago, S., Oladele, R. O., and Denning, D. W. (2017). Global and multi-national prevalence of fungal diseases—estimate precision. *J. Fungi.* 3:57. doi: 10.3390/jof3040057

Botas, C., Poulain, F., Akiyama, J., Brown, C., Allen, L., Goerke, J., et al. (1998). Altered surfactant homeostasis and alveolar type II cell morphology in mice lacking surfactant protein D. *Proc. Natl. Acad. Sci. U. S. A* 95, 11869–11874 doi: 10.1073/pnas.95.20.11869

Brown-Augsburger, P. K. L., Hartshorn, D., Chang, K., Rust, C., Fliszar, H. G., and Welgus, E. C. (1996). Crouch. Site-directed mutagenesis of Cys-15 and Cys-20 of pulmonary surfactant protein D. *J. Biol. Chem*. 271, 13724–13730. doi: 10.1074/jbc.271.23.13724

Carreto-Binaghi, L. E., Aliouat, E. M., and Taylor, M. L. (2016). Surfactant proteins, SP-A and SP-D, in respiratory fungal infections: their role in the inflammatory response. *Respir. Res*.17:66. doi: 10.1186/s12931-016-0385-9

Che, C. Y., Jia, W. Y., Xu, Q., Li, N., Hu, L. T., Jiang, N., et al. (2012a). The roles of surfactant protein D during Aspergillus fumigatus infection in human corneal epithelial cells. *Int. J. Ophthalmol*. 5, 13–17. doi: 10.3980/j.issn.2222-3959.2012.01.03

Che, C. Y., Li, X. J., Jia, W. Y., Li, N., Xu, Q., Lin, J., et al. (2012b). Early expression of surfactant proteins D in fusarium solani infected rat cornea. *Int. J. Ophthalmol*. 5, 297–300. doi: 10.3980/j.issn.2222-3959.2012.03.09

Cheng, G., Ueda, T., Numao, T., Kuroki, Y., Nakajima, H., Fukushima, Y., et al. (2000). Increased levels of surfactant protein A and D in bronchoalveolar lavage fluids in patients with bronchial asthma. *Eur. Respir. J*. 16, 831–835. doi: 10.1183/09031936.00.16583100

Colmorten, K. B., Nexoe, A. B., and Sorensen, G. L. (2019). The dual role of surfactant protein-D in vascular inflammation and development of cardiovascular disease. *Front. Immunol.* 10:2264. doi: 10.3389/fimmu.2019.02264

Crouch, E. C. (2000). Surfactant protein-D and pulmonary host defense. *Respir. Res.* 1, 93–108. doi: 10.1186/rr19

Dodagatta-Marri, E., Mitchell, D. A., Pandit, H., Sonawani, A., Murugaiah, V., Idicula-Thomas, S., et al. (2017). Protein-protein interaction between surfactant protein D and DC-SIGN via C-type lectin domain can suppress HIV-1 transfer. *Front. Immunol.* 8:834. doi: 10.3389/fimmu.2017.00834

Erpenbeck, V. J., Ziegert, M., Cavalet-Blanco, D., Martin, C., Baelder, R., Glaab, T., et al. (2006). Surfactant protein D inhibits early airway response in *Aspergillus Fumigatus*-sensitized mice. *Clin. Exp. Allergy*. 36, 930–940. doi: 10.1111/j.1365-2222.2006.02524.x

Fakih, D., Pilecki, B., Schlosser, A., Jepsen, C. S., Thomsen, L. K., Ormhøj, M., et al. (2015). Protective effects of surfactant protein D treatment in 1,3-β-glucan-modulated allergic inflammation. *Am. J. Physiol. Lung Cell Mol. Physiol*. 309, L1333–L1343. doi: 10.1152/ajplung.00090.2015

Fisher, J. H., Larson, J., Cool, C., and Dow, S. W. (2002). Lymphocyte activation in the lungs of SP-D null mice. *Am. J. Respir. Cell Mol. Biol*. 27, 24–33. doi: 10.1165/ajrcmb.27.1.4563

Fukuzawa, T., Ishida, J., Kato, A., Ichinose, T., Ariestanti, D. M., Takahashi, T., et al. (2013). Lung surfactant levels are regulated by Ig-Hepta/GPR116 by monitoring surfactant protein D. *PLoS ONE* 8:e69451. doi: 10.1371/journal.pone.0069451

Gardai, S. J., Xiao, Y. Q., Dickinson, M., Nick, J. A., Voelker, D. R., Greene, K. E., et al. (2003). By binding SIRPalpha or calreticulin/CD91, lung collectins act as dual function surveillance molecules to suppress or enhance inflammation. *Cell* 115, 13–23. doi: 10.1016/S0092-8674(03)00758-X

Ge, M. Q., Kokalari, B., Flayer, C. H., Killingbeck, S. S., Redai, I. G., MacFarlane, A. W. IV., et al. (2016). Cutting edge: role of NK cells and surfactant protein D in dendritic cell lymph node homing: effects of ozone exposure. *J. Immunol*. 196, 553–557. doi: 10.4049/jimmunol.1403042

Geunes-Boyer, S., Beers, M. F., Perfect, J. R., Heitman, J., and Wright, J. R. (2012). Surfactant protein D facilitates *Cryptococcus Neoformans* infection. *Infect. Immun*. 80, 2444–2453. doi: 10.1128/IAI.05613-11

Geunes-Boyer, S., Heitman, J., Wright, J. R., and Steinbach, W. J. (2010). Surfactant protein D binding to *Aspergillus Fumigatus* hyphae is calcineurin-sensitive. *Med. Mycol*. 48, 580–588. doi: 10.3109/13693780903401682

Geunes-Boyer, S., Oliver, T. N., Janbon, G., Lodge, J. K., Heitman, J., Perfect, J. R., et al. (2009). Surfactant protein D increases phagocytosis of hypocapsular *Cryptococcus Neoformans* by murine macrophages and enhances fungal survival. *Infect. Immun*. 77, 2783–2794. doi: 10.1128/IAI.00088-09

Goyal, S., Castrillón-Betancur, J. C., Klaile, E., and Slevogt, H. (2018). The interaction of human pathogenic fungi with C-type lectin receptors. *Front. Immunol*. 9:1261. doi: 10.3389/fimmu.2018.01261

Griese, M., Wiesener, A., Lottspeich, F., von Bredow, C. H. (2003). Limited proteolysis of surfactant protein D and causes a loss of its calcium-dependent lectin functions. *Biochim. Biophys. Acta* 1638, 157–63. doi: 10.1016/S0925-4439(03)00063-2

Haczku, A., Atochina, E. N., Tomer, Y., Chen, H., Scanlon, S. T., Russo, S., et al. (2001). Aspergillus fumigatus-induced allergic airway inflammation alters surfactant homeostasis and lung function in BALB/c mice. *Am. J. Respir. Cell Mol. Biol*. 25, 45–50. doi: 10.1165/ajrcmb.25.1.4391

Hasegawa, Y., Takahashi, M., Ariki, S., Asakawa, D., Tajiri, M., Wada, Y., et al. (2015). Surfactant protein D suppresses lung cancer progression by downregulation of epidermal growth factor signaling. *Oncogene* 34, 838–845. doi: 10.1038/onc.2014.20

Holmer, S. M., Evans, K. S., Asfaw, Y. G., Saini, D., Schell, W. A., Ledford, J. G., et al. (2014). Impact of surfactant protein D, interleukin-5, and eosinophilia on cryptococcosis. *Infect. Immun*. 82, 683–693. doi: 10.1128/IAI.00855-13

Ikegami, M., Na, C. L., Korfhagen, T. R., and Whitsett, J. A. (2005). Surfactant protein D influences surfactant ultrastructure and uptake by alveolar type II cells. *Am. J. Physiol. Lung Cell Mol. Physiol*. 288, L552–L561 doi: 10.1152/ajplung.00142.2004

Ikegami, M., Whitsett, J. A., Jobe, A., Ross, G., Fisher, J., and Korfhagen, T. (2000). Surfactant metabolism in SP-D gene-targeted mice. *Am. J. Physiol. Lung Cell Mol. Physiol*. 279, L468–L476. doi: 10.1152/ajplung.2000.279.3.L468

Jakel, A., Qaseem, A. S., Kishore, U., and Sim, R. B. (2013). Ligands and receptors of lung surfactant proteins SP-A and SP-D. *Front. Biosci.* 18, 1129–1140. doi: 10.2741/4168

Jawed, S., Saeed, M., and Parveen, N. (2015). Respiratory tract infections in diabetic and non-diabetic individuals are linked with serum surfactant protein-D. *J. Pak. Med. Assoc*. 65, 1210–1213.

Kay, S., and Madan, T. (2016). Fertility defects in Surfactant associated protein D knockout female mice: altered ovarian hormone profile. *Mol Immunol*. 71, 87–97. doi: 10.1016/j.molimm.2016.01.002

Kishore, U., Bernal, A. L., Kamran, M. F., Saxena, S., Singh, M., Sarma, P. U., et al. (2005). Surfactant proteins SP-A and SP-D in human health and disease. *Arch Immunol. Ther. Exp*. 53, 399–417.

Kishore, U., Greenhough, T. J., Waters, P., Shrive, A. K., Ghai, R., Kamran, M. F., et al. (2006). Surfactant proteins SP-A and SP-D: structure, function and receptors. *Mol. Immunol*. 43, 1293–1315. doi: 10.1016/j.molimm.2005.08.004

Koopmans, J. G., van der Zee, J. S., Krop, E. J., Lopuhaa, C. E., Jansen, H. M., and Batenburg, J. J. (2004). Serum surfactant protein D is elevated in allergic patients. *Clin. Exp. Allergy* 34, 1827–1833. doi: 10.1111/j.1365-2222.2004.02083.x

Korfhagen, T. R., Sheftelyevich, V., Burhans, M. S., Bruno, M. D., Ross, G. F., Wert, S. E., et al. (1998). Surfactant protein-D regulates surfactant phospholipid homeostasis *in vivo*. *J. Biol. Chem*. 273, 28438–28443 doi: 10.1074/jbc.273.43.28438

Kurimura, Y., Nishitani, C., Ariki, S., Saito, A., Hasegawa, Y., Takahashi, M., et al. (2012). Surfactant protein D inhibits adherence of uropathogenic *Escherichia Coli* to the bladder epithelial cells and the bacterium-induced cytotoxicity: a possible function in urinary tract. *J. Biol. Chem*. 287, 39578–39588. doi: 10.1074/jbc.M112.380287

Kuroki, Y., Shiratori, M., Murata, Y., and Akino, T. (1991). Surfactant protein D (SP-D) counteracts the inhibitory effect of surfactant protein A (SP-A) on phospholipid secretion by alveolar type II cells. Interaction of native SP-D with SP-A. *Biochem. J*. 279 (Pt 1), 115–119. doi: 10.1042/bj2790115

Lekkala, M., LeVine, A. M., Linke, M. J., Crouch, E. C., Linders, B., Brummer, E., et al. (2006). Effect of lung surfactant collectins on bronchoalveolar macrophage interaction with *Blastomyces Dermatitidis*: inhibition of tumor necrosis factor alpha production by surfactant protein D. *Infect. Immun*. 74, 4549–4556. doi: 10.1128/IAI.00243-06

Leth-Larsen, R., Garred, P., Jensenius, H., Meschi, J., Hartshorn, K., Madsen, J., et al. (2005). A common polymorphism in the SFTPD gene influences assembly, function, and concentration of surfactant protein D. *J. Immunol*. 174, 1532–1538. doi: 10.4049/jimmunol.174.3.1532

LeVine, A. M., Elliott, J., Whitsett, J. A., Srikiatkhachorn, A., Crouch, E., DeSilva, N., et al. (2004). Surfactant protein-d enhances phagocytosis and pulmonary clearance of respiratory syncytial virus. *Am. J. Respir. Cell Mol. Biol*. 31, 193–199 doi: 10.1165/rcmb.2003-0107OC

LeVine, A. M., Whitsett, J. A., Gwozdz, J. A., Richardson, T. R., Fisher, J. H., Burhans, M. S., et al. (2000). Distinct effects of surfactant protein A or D deficiency during bacterial infection on the lung. *J. Immunol*. 165, 3934–3940 doi: 10.4049/jimmunol.165.7.3934

LeVine, A. M., Whitsett, J. A., Hartshorn, K. L., Crouch, E. C., and Korfhagen, T. R. (2001). Surfactant protein D enhances clearance of influenza A virus from the lung *in vivo*. *J. Immunol*. 167, 5868–5873 doi: 10.4049/jimmunol.167.10.5868

Liu, C. F., Rivere, M., Huang, H. J., Puzo, G., and Wang, J. Y. (2010). Surfactant protein D inhibits mite-induced alveolar macrophage and dendritic cell activations through TLR signalling and DC-SIGN expression. *Clin. Exp. Allergy* 40, 111–122. doi: 10.1111/j.1365-2222.2009.03367.x

Liu, Z., Shi, Q., Liu, J., Abdel-Razek, O., Xu, Y., Cooney, R. N., et al. (2015). Innate immune molecule surfactant protein D attenuates sepsis-induced acute pancreatic injury through modulating apoptosis and NF-κB-mediated inflammation. *Sci. Rep*. 5:17798. doi: 10.1038/srep17798

López-Cano, C., Lecube, A., García-Ramírez, M., Muñoz, X., Sánchez, E., Seminario, A., et al. (2017). Serum surfactant protein D as a biomarker for measuring lung involvement in obese patients with type 2 diabetes. *J. Clin. Endocrinol. Metab.* 102, 4109–4116. doi: 10.1210/jc.2017-00913

Madan, T., Eggleton, P., Kishore, U., Strong, P., Aggrawal, S. S., Sarma, P. U., et al. (1997a). Binding of pulmonary surfactant proteins A and D to *Aspergillus fumigatus* conidia enhances phagocytosis and killing by

human neutrophils and alveolar macrophages. *Infect. Immun*. 65, 3171–3179. doi: 10.1128/IAI.65.8.3171-3179.1997

Madan, T., Kaur, S., Saxena, S., Singh, M., Kishore, U., Thiel, S., et al. (2005a). Role of collectins in innate immunity against aspergillosis. *Med. Mycol*. 43(Suppl. 1), S155–S163. doi: 10.1080/13693780500088408

Madan, T., Kishore, U., Shah, A., Eggleton, P., Strong, P., Wang, J. Y., et al. (1997b). Lung surfactant proteins A and D can inhibit specific IgE binding to the allergens of *Aspergillus Fumigatus* and block allergen-induced histamine release from human basophils. *Clin. Exp. Immunol*. 110, 241–249. doi: 10.1111/j.1365-2249.1997.tb08323.x

Madan, T., Kishore, U., Singh, M., Strong, P., Clark, H., Hussain, E. M., et al. (2001). Surfactant proteins A and D protect mice against pulmonary hypersensitivity induced by *Aspergillus Fumigatus* antigens and allergens. *J. Clin. Invest*. 107, 467–475. doi: 10.1172/JCI10124

Madan, T., Reid, K. B., Clark, H., Singh, M., Nayak, A., Sarma, P. U., et al. (2010). Susceptibility of mice genetically deficient in SP-A or SP-D gene to invasive pulmonary aspergillosis. *Mol. Immunol*. 47, 1923–1930. doi: 10.1016/j.molimm.2010.02.027

Madan, T., Reid, K. B., Singh, M., Sarma, P. U., and Kishore, U. (2005b). Susceptibility of mice genetically deficient in the surfactant protein (SP)-A or SP-D gene to pulmonary hypersensitivity induced by antigens and allergens of *Aspergillus Fumigatus*. *J. Immunol*. 174, 6943–6954. doi: 10.4049/jimmunol.174.11.6943

Mahajan, L., Pandit, H., Madan, T., Gautam, P., Yadav, A. K., Warke, H., et al. (2013). Human surfactant protein D alters oxidative stress and HMGA1 expression to induce p53 apoptotic pathway in eosinophil leukemic cell line. *PLoS ONE* 8:e85046. doi: 10.1371/journal.pone.0085046

Malloy, J. L., Veldhuizen, R. A., Thibodeaux, B. A., O'Callaghan, R. J., and Wright, J. R. (2005). Pseudomonas aeruginosa protease IV degrades surfactant proteins and inhibits surfactant host defense and biophysical functions. *Am. J. Physiol. Lung Cell Mol. Physiol*. 288, L409–L418 doi: 10.1152/ajplung.00322.2004

McCormack, F. X., Gibbons, R., Ward, S. R., Kuzmenko, A., Wu, H., and Deepe, G. S Jr. (2003). Macrophage-independent fungicidal action of the pulmonary collectins. *J. Biol. Chem*. 278, 36250–36256. doi: 10.1074/jbc.M303086200

Nie, X., Nishitani, C., Yamazoe, M., Ariki, S., Takahashi, M., Shimizu, T., et al. (2008). Pulmonary surfactant protein D binds MD-2 through the carbohydrate recognition domain. *Biochemistry* 47, 12878–12885. doi: 10.1021/bi8010175

Ohya, M., Nishitani, C., Sano, H., Yamada, C., Mitsuzawa, H., Shimizu, T., et al. (2006). Human pulmonary surfactant protein D binds the extracellular domains of Toll-like receptors 2 and 4 through the carbohydrate recognition domain by a mechanism different from its binding to phosphatidylinositol and lipopolysaccharide. *Biochemistry* 45, 8657–8664. doi: 10.1021/bi060176z

Olde Nordkamp, M. J., van Eijk, M., Urbanus, R. T., Bont, L., Haagsman, H. P., and Meyaard, L. (2014). Leukocyte-associated Ig-like receptor-1 is a novel inhibitory receptor for surfactant protein D. *J. Leukoc. Biol*. 96, 105–111. doi: 10.1189/jlb.3AB0213-092RR

Ordonez, S. R., van Eijk, M., Escobar Salazar, N., de Cock, H., Veldhuizen, E. J. A., and Haagsman, H. P. (2019). Antifungal activities of surfactant protein D in an environment closely mimicking the lung lining. *Mol. Immunol*. 105, 260–269. doi: 10.1016/j.molimm.2018.12.003

O'Riordan, D. M., Standing, J. E., Kwon, K. Y., Chang, D., Crouch, E. C., and Limper, A. H. (1995). Surfactant protein D interacts with Pneumocystis carinii and mediates organism adherence to macrophages. *J. Clin. Invest*. 95, 2699–2710. doi: 10.1172/JCI117972

Pandit, H., Madhukaran, S. P., Nayak, A., and Madan, T. (2012). SP-A and SP-D in host defense against fungal infections and allergies. *Front. Biosci.* 4, 651–661. doi: 10.2741/e406

Pandit, H., Thakur, G., Koippallil Gopalakrishnan, A. R., Dodagatta-Marri, E., Patil, A., Kishore, U., et al. (2016). Surfactant protein D induces immune quiescence and apoptosis of mitogen-activated peripheral blood mononuclear cells. *Immunobiology* 221, 310–322. doi: 10.1016/j.imbio.2015.10.004

Persson, A., Chang, D., and Crouch, E. (1990). Surfactant protein D is a divalent cation-dependent carbohydrate-binding protein. *J. Biol. Chem*. 265, 5755–5760.

Postle, A. D., Mander, A., Reid, K. B. M., Wang, J. Y., Wright, S. M., Moustaki, M., et al. (1999). Deficient hydrophilic lung surfactant proteins A and D with normal surfactant phospholipid molecular species in cystic fibrosis. *Am. J. Respir. Cell Mol. Biol*. 20, 90–98. doi: 10.1165/ajrcmb.20.1.3253

Qu, J., He, L., Rong, Z., Pan, J., Chen, X., Morrison, D. C., et al. (2001). Alteration of surfactant proteins A and D in bronchoalveolar lavage fluid of *Pneumocystis* carinii pneumonia. *Chin. Med. J.* 114, 1143–1146.

Rezaei, S., Shamsi, M. M., Mahdavi, M., Jamali, A., Prestes, J., Tibana, R. A., et al. (2017). Endurance exercise training decreased serum levels of surfactant protein D and improved aerobic fitness of obese women with type-2 diabetes. *Diabetol. Metab. Syndr*. 9:74. doi: 10.1186/s13098-017-0273-6

Rokade, S., Kishore, U., and Madan, T. (2017). Surfactant protein D regulates murine testicular immune milieu and sperm functions. *Am. J. Reprod. Immunol*. 77, 1–15. doi: 10.1111/aji.12629

Salazar, F., and Brown, G. D. (2018). Antifungal innate immunity: a perspective from the last 10 years. *J. Innate Immun*. 10, 373–397 doi: 10.1159/000488539

Sano, H., Chiba, H., Iwaki, D., Sohma, H., Voelker, D. R., and Kuroki, Y. (2000). Surfactant proteins A and D bind CD14 by different mechanisms. *J. Biol. Chem*. 275, 22442–22451. doi: 10.1074/jbc.M001107200

Schelenz, S., Malhotra, R., Sim, R. B., Holmskov, U., and Bancroft, G. J. (1995). Binding of host collectins to the pathogenic yeast *Cryptococcus Neoformans*: human surfactant protein D acts as an agglutinin for acapsular yeast cells. *Infect. Immun*. 63, 3360–3366. doi: 10.1128/IAI.63.9.3360-3366.1995

Schob, S., Schicht, M., Sel, S., Stiller, D., Kekulé, A. S., Paulsen, F., et al. (2013). The detection of surfactant proteins A, B, C and D in the human brain and their regulation in cerebral infarction, autoimmune conditions and infections of the CNS. *PLoS ONE* 8:e74412. doi: 10.1371/journal.pone.0074412

Singh, M., Madan, T., Waters, P., Sonar, S., Singh, S. K., Kamran, M. F., et al. (2009). Therapeutic effects of recombinant forms of full-length and truncated human surfactant protein D in a murine model of invasive pulmonary aspergillosis. *Mol. Immunol*. 46, 2363–2369. doi: 10.1016/j.molimm.2009.03.019

Sorensen, G. L. (2018). Surfactant protein D in respiratory and non-respiratory diseases. *Front. Med*. 5:18. doi: 10.3389/fmed.2018.00018

Sorensen, G. L., Madsen, J., Kejling, K., Tornoe, I., Nielsen, O., Townsend, P., et al. (2006). Surfactant protein D is proatherogenic in mice. *Am. J. Physiol. Heart Circ. Physiol*. 290, H2286–H2294. doi: 10.1152/ajpheart.01105.2005

Stidsen, J. V., Khorooshi, R., Rahbek, M. K., Kirketerp-Møller, K. L., Hansen, P. B., Bie, P., et al. (2012). Surfactant protein D deficiency in mice is associated with hyperphagia, altered fat deposition, insulin resistance, and increased basal endotoxemia. *PLoS ONE* 7:e35066. doi: 10.1371/journal.pone.0035066

van de Wetering, J. K., Coenjaerts, F. E., Vaandrager, A. B., van Golde, L. M., and Batenburg, J. J. (2004). Aggregation of *Cryptococcus Neoformans* by surfactant protein D is inhibited by its capsular component glucuronoxylomannan. *Infect. Immun*. 72, 145–153. doi: 10.1128/IAI.72.1.145-153.2004

van Rozendaal, B. A., van Spriel, A. B., van De Winkel, J. G., and Haagsman, H. P. (2000). Role of pulmonary surfactant protein D in innate defense against *Candida Albicans*. *J. Infect. Dis*. 182, 917–922. doi: 10.1086/315799

von Bredow, C., Hartl, D., Schmid, K., Schabaz, F., Brack, E., Reinhardt, D., et al. (2006). Surfactant protein D regulates chemotaxis and degranulation of human eosinophils. *Clin. Exp. Allergy* 36, 1566–1574. doi: 10.1111/j.1365-2222.2006.02598.x

Vuk-Pavlovic, Z., Diaz-Montes, T., Standing, J. E., and Limper, A. H. (1998). Surfactant protein-D binds to cell wall b-glucans. *Am. J. Respir. Crit. Care Med*. 157:A236.

Vuk-Pavlovic, Z., Mo, E. K., Icenhour, C. R., Standing, J. E., Fisher, J. H., and Limper, A. H. (2006). Surfactant protein D enhances pneumocystis infection in immune-suppressed mice. *Am. J. Physiol. Lung Cell. Mol. Physiol*. 290, L442–L449. doi: 10.1152/ajplung.00112.2005

Vuk-Pavlovic, Z., Standing, J. E., Crouch, E. C., and Limper, A. H. (2001). Carbohydrate recognition domain of surfactant protein D mediates interactions with *Pneumocystis* carinii glycoprotein A. *Am. J. Respir. Cell Mol. Biol*. 24, 475–484. doi: 10.1165/ajrcmb.24.4.3504

Wert, S. E., Yoshida, M., LeVine, A. M., Ikegami, M., Jones, T., Ross, G. F., et al. (2000). Increased metalloproteinase activity, oxidant production, and emphysema in surfactant protein D gene-inactivated mice. *Proc Natl Acad Sci U S A* 97, 5972–5977. doi: 10.1073/pnas.100448997

Wojcik, M., Zieleniak, A., Zurawska-Klis, M., Cypryk, K., and Wozniak, L. A. (2016). Increased expression of immune-related genes in leukocytes of patients with diagnosed gestational diabetes mellitus (GDM). *Exp. Biol. Med.* 241, 457–465. doi: 10.1177/1535370215615699

Wong, S. S. W., Rani, M., Dodagatta-Marri, E., Ibrahim-Granet, O., Kishore, U., Bayry, J., et al. (2018). Fungal melanin stimulates surfactant protein D-mediated opsonization of and host immune response to *Aspergillus Fumigatus* spores. *J. Biol. Chem*. 293, 4901–4912. doi: 10.1074/jbc.M117.815852

Wu, X., Zhao, G., Lin, J., Jiang, N., Li, C., Hu, L., et al. (2015). The production mechanism and immunosuppression effect of pulmonary surfactant protein D via toll like receptor 4 signaling pathway in human corneal epithelial cells during *Aspergillus Fumigatus* infection. *Int. Immunopharmacol*. 29, 433–439. doi: 10.1016/j.intimp.2015.10.018

Yamazoe, M., Nishitani, C., Takahashi, M., Katoh, T., Ariki, S., Shimizu, T., et al. (2008). Pulmonary surfactant protein D inhibits lipopolysaccharide (LPS)-induced inflammatory cell responses by altering LPS binding to its receptors. *J. Biol. Chem*. 283, 35878–35888. doi: 10.1074/jbc.M807268200

Yang, Z., Jaeckisch, S. M., and Mitchell, C. G. (2000). Enhanced binding of *Aspergillus Fumigatus* spores to A549 epithelial cells and extracellular matrix proteins by a component from the spore surface and inhibition by rat lung lavage fluid. *Thorax* 55, 579–584. doi: 10.1136/thorax.55.7.579

Conflict of Interest: The authors declare that the research was conducted in the absence of any commercial or financial relationships that could be construed as a potential conflict of interest.

Advantages of publishing in Frontiers

OPEN ACCESS
Articles are free to read for greatest visibility and readership

FAST PUBLICATION
Around 90 days from submission to decision

HIGH QUALITY PEER-REVIEW
Rigorous, collaborative, and constructive peer-review

TRANSPARENT PEER-REVIEW
Editors and reviewers acknowledged by name on published articles

Frontiers
Avenue du Tribunal-Fédéral 34
1005 Lausanne | Switzerland

Visit us: www.frontiersin.org
Contact us: info@frontiersin.org | +41 21 510 17 00

REPRODUCIBILITY OF RESEARCH
Support open data and methods to enhance research reproducibility

DIGITAL PUBLISHING
Articles designed for optimal readership across devices

FOLLOW US
@frontiersin

IMPACT METRICS
Advanced article metrics track visibility across digital media

EXTENSIVE PROMOTION
Marketing and promotion of impactful research

LOOP RESEARCH NETWORK
Our network increases your article's readership